Electronic Theses and Dissertations

Theses, Dissertations, and Major Papers

2019

Evaluating the biogeochemistry and microbial function in the Athabasca Oil Sands region: Understanding natural baselines for reclamation end-points

Thomas Reid
University of Windsor

Follow this and additional works at: https://scholar.uwindsor.ca/etd

Evaluating the biogeochemistry and microbial function in the Athabasca Oil Sands region: Understanding natural baselines for reclamation end-points

By

Thomas Reid

A Dissertation
Submitted to the Faculty of Graduate Studies
through the Great Lakes Institute for Environmental Research
in Partial Fulfillment of the Requirements for
the Degree of Doctor of Philosophy
at the University of Windsor

Windsor, Ontario, Canada

2019

Evaluating the biogeochemistry and microbial function in the Athabasca Oil Sands region: Understanding natural baselines for reclamation end-points

By

Thomas Reid

APPROVED BY:

_____
G. Ferris, External Examiner
University of Toronto

_____
J. Ciborowski
Department of Biological Sciences

_____
S.R. Chaganti
Great Lakes Institute for Environmental Research

_____
S. Mundle
Great Lakes Institute for Environmental Research

_____
C. Weisener, Advisor
Great Lakes Institute for Environmental Research

_____
I.G. Droppo, Co-Advisor
Environment and Climate Change Canada

April 26, 2019

DECLARATION OF CO-AUTHORSHIP / PREVIOUS PUBLICATION

I.   Co-Authorship

I hereby declare that this thesis incorporates material that is result of joint research, as follows:

Chapter 2 of the thesis was co-authored with S.R. Chaganti, I.G. Droppo, and C.G. Weisener, under the supervision of both I.G. Droppo and C.G. Weisener. In all cases, the key ideas, primary contributions, data analysis, interpretation, and writing were performed by the author, and the contribution of co-authors was primarily through the provision of grant funding alongside experimental design. All co-authors also provided feedback for the purpose of editing and refining the manuscript.

Chapter 3 of the thesis was co-authored with S.R. Chaganti, I.G. Droppo, and C.G. Weisener, under the supervision of both I.G. Droppo and C.G. Weisener. In all cases, the key ideas, primary contributions, data analysis, interpretation, and writing were performed by the author, and the contribution of co-authors was primarily through the provision of grant funding alongside experimental design. All co-authors also provided feedback for the purpose of editing and refining the manuscript.

Chapter 4 of the thesis was co-authored with S.R. Chaganti, I.G. Droppo, and C.G. Weisener, under the supervision of both I.G. Droppo and C.G. Weisener. In all cases, the key ideas, primary contributions, data analysis, interpretation, and writing were performed by the author, and the contribution of co-authors was primarily through the provision of grant funding alongside experimental design. All co-authors also provided feedback for the purpose of editing and refining the manuscript.

I am aware of the University of Windsor Senate Policy on Authorship and I certify that I have properly acknowledged the contribution of other researchers to my

thesis, and have obtained written permission from each of the co-author(s) to include the above material(s) in my thesis.

I certify that, with the above qualification, this thesis, and the research to which it refers, is the product of my own work.

II.   Previous Publication

This thesis includes 3 original papers that have been previously published/submitted for publication in peer reviewed journals, as follows:

Thesis Chapter	Publication title/full citation	Publication status*
Chapter [2]	Reid, T., Chaganti, S.R., Droppo, I.G., Weisener, C.G., 2018. Novel insights into freshwater hydrocarbon-rich sediments using metatranscriptomics: Opening the black box. Water Res. 136, 1–11. https://doi.org/10.1016/j.watres.2018.02.039	Published
Chapter [3]	Reid, T., Droppo, I.G., Chaganti, S.R., Weisener, C.G., 2019. Microbial metabolic strategies for overcoming low-oxygen in naturalized freshwater reservoirs surrounding the Athabasca Oil Sands: A proxy for End-Pit Lakes? Sci. Total Environ. 665, 113–124. https://doi.org/10.1016/j.scitotenv.2019.02.032	Published
Chapter [4]	Reid, T., Droppo, I.G., Chaganti, S.R., Weisener, C.G., 2019. Tracking Functional Bacterial Biomarkers in Response to a Gradient of Contaminant Exposure within the Oil Sands River Sediment Continuums	Submitted by mid-May 2019

I certify that I have obtained a written permission from the copyright owner(s) to include the above published material(s) in my thesis. I certify that the above material describes work completed during my registration as a graduate student at the University of Windsor.

III.   General

    I declare that, to the best of my knowledge, my thesis does not infringe upon anyone's copyright nor violate any proprietary rights and that any ideas, techniques, quotations, or any other material from the work of other people included in my thesis, published or otherwise, are fully acknowledged in accordance with the standard referencing practices. Furthermore, to the extent that I have included copyrighted material that surpasses the bounds of fair dealing within the meaning of the Canada Copyright Act, I certify that I have obtained a written permission from the copyright owner(s) to include such material(s) in my thesis.

    I declare that this is a true copy of my thesis, including any final revisions, as approved by my thesis committee and the Graduate Studies office, and that this thesis has not been submitted for a higher degree to any other University or Institution.

ABSTRACT

Understanding the biogeochemical processes governed by the complex metabolic pathways of microbial communities is paramount in understanding overall ecosystem services. Their ability to adapt to the world's harshest environments allows them to thrive in otherwise hostile environments. The Athabasca Oil Sands of Northern Alberta, Canada, constitutes one of the largest oil sands deposits in the world. This uniquely hydrocarbon-rich environment is a diverse and complex ecosystem governed by strong anthropogenic (i.e. industrial mine sites) and natural environmental gradients (i.e. substantial bitumen outcroppings). The economically significant oil sands deposit produces millions of barrels of bitumen daily, with waste materials (i.e. sands, clays, residual bitumen etc.) pumped into large settling basins called tailings ponds. The Government of Alberta requires oil sands operators to return their mine sites to a reclaimed landscape after mining has completed, thus leaving an enormous task of determining appropriate reclamation procedures, target end-points and water quality targets. However, what remains unknown is an understanding of the baseline biogeochemical fingerprint of the natural McMurray Formation (MF) – the geological strata constituting the mineable bitumen ore. Additionally, there has yet to be any studies focusing on the microbial function in the MF, a vital research gap that would provide insight into how the indigenous microbial communities deal with this ubiquitous, natural hydrocarbon presence.

The research comprising the chapters of this dissertation, are the first to reveal the active, in-situ metabolism of the bacterial communities within the MF. Novel metatranscriptomics approaches from in-situ samples are used to characterize the microbial

metabolic processes governing these ecosystems, to better understand what may constitute viable ecosystem reclamation end-points. Functional characterizations are compared to hydrocarbon signatures and redox state of the various study sites. Results indicate a unique microbial consortium with both energy and xenobiotic metabolic pathways tailored to the complex hydrocarbon substrate of the MF. Further, the sensitivity of this metatranscriptomics approach was tested and validated as a means of tracking hydrocarbon exposure down a river continuum. Clusters of closely related co-expressing genes revealed patterns of expression indicative of exposure to the hydrocarbons of the MF, providing interesting methodologies to track pollution exposure in a hydrodynamic context. Finally, a field-scale mesocosm study was used to track the biogeochemical evolution of tailings following a novel detoxification treatment and further compare back to the natural reference sites also studied. Treatments caused the reduction of toxic organics and the promotion of microbial taxa adept at metabolizing complex organics. These cumulative insights into the natural and anthropogenically impacted ecosystems of the Athabasca Oil Sands region provides much needed characterizations of reference/baseline environments from which to guide best management practices and gauge reclamation success.

DEDICATION

I dedicate this dissertation to my wonderful wife, kids, mom, dad, brothers and sisters and all my family and friends for their continued love and support.

ACKNOWLEDGEMENTS

I would like to sincerely thank Dr. Chris Weisener and Dr. Ian Droppo for their expertise, guidance, assistance and mentorship during the course of my PhD research. They have allowed me the freedom and flexibility to pursue my research in what has truly been an exciting adventure of scientific exploration and discovery. Their insights and leadership have sparked in me a true sense of excitement with respect to multidisciplinary research and exploratory science. They have provided me with invaluable knowledge and a skillset that goes beyond the research itself, and for that I am truly grateful!

I would like to thank my committee members, Dr. Subba Rao Chaganti, Dr. Scott Mundle and Dr. Jan Ciborowski for their expertise and guidance along the way. Dr. Chaganti has be a fundamental part of my microbial research, and his insight has made him an invaluable colleague and mentor. Dr. Scott Mundle has exemplified what it is to be an extremely effective researcher with a drive for scientific exploration. Dr. Jan Ciborowski has been a fundamental thread throughout by graduate studies, exemplifying the power of collaboration and what it is to be a truly remarkable researcher and colleague. His breadth of knowledge and expertise has been truly insightful through the years. I would also like to thank Dr. Rick Frank for his expertise, assistance, mentorship and friendship over the years, it has been very much appreciated!

Thank you to my friends and colleagues at GLIER and Earth and Environmental Sciences for the support and encouragement throughout my graduate studies and work as a graduate assistant. Specifically, Mary Lou Scratch, Christine Weisener, Kendra Thompson-Kumar, Sharon Lackie, and Marg Mayer. Thanks to everyone in the Weisener Lab for your lab and field assistance, discussions and laughs along the way, specifically Nick Falk, Danielle VanMensel, Adam Skoyles, and Sara Butler.

Thanks to my Mom and Dad for everything you've taught me through the years, and all of the love, laughs and memories we've shared along the way. Somewhere along the line, probably during one of our many travels, my interest in environmental sciences arose, and I wouldn't have it any other way. Thanks to Bre, Luke and Mikkyla for watching the Discovery Channel with me when we were younger. I love you all!

And finally, I would like to thank my best friend and lovely wife Laura for her love and support over the years. Her patience, love and advice has allowed me to pursue my passion for science and has kept me going throughout. I am truly grateful for her being in my life, and for the future that awaits us. I would also like to thank Wynne and Oryn for keeping me on my toes and reminding me that life's too short to work all the time, let alone sleep. I love you guys!

TABLE OF CONTENTS

LIST OF TABLES

LIST OF FIGURES

CHAPTER 4

CHAPTER 5

LIST OF APPENDICES

LIST OF ABBREVIATIONS/SYMBOLS

DO	Dissolved Oxygen
DE	Differential Expression
EPL	End-Pit Lake
ER	Ells River
FFT	Fluid Fine Tailings
GI	Gamma Irradiation/Irradiated
GP	Groundwater Plume
G+	Gamma treated
G-	Untreated (no gamma irradiation)
H_2S/HS^-	Hydrogen Sulfide
MF	McMurray Formation
MFT	Mature Fine Tailings
NA	Naphthenic Acids
OSPM	Oil sands process-affected material
OSPW	Oil sands process-affected waters
P1A	Pond 1A (Suncor)
PAH	Polycyclic Aromatic Hydrocarbon
PCR	Poplar Creek Reservoir
REDOX	Reduction-oxidation
RL	Ruth Lake
STB	Steepbank River
STP	Pond STP (Suncor)

CHAPTER 1 **INTRODUCTION**

1.1 Research Introduction

Aquatic environments, be it lake, river, wetland or ocean, experience dramatic fluxes of nutrients and compounds through complex hydrodynamic processes, often inducing spatiotemporally varied redox gradients leading to complex ecosystem alteration. The microbial consortia that dominate the primary production in these ecosystems greatly influence the cycling of elements, ecosystem homeostasis and simply its overall health. The compounds are altered by complex processes as they cycle through the environment, and multidisciplinary approaches are needed to unravel their intricacies. Understanding the flow of xenobiotic substances and contaminants into and through various media is an issue of global concern. However, too often we lack a frame of reference against which to adequately assess the effects of major catastrophes, such is often the case in sudden, catastrophic oil spills or tailings breaches where baseline ecosystem characteristics may be scarce. The lack of knowledge about the natural biogeochemical nature of a site is troubling and limits one's ability to identify remediatory and/or reclamation goals after contamination has occurred.

The ability for microbes to thrive and adapt to even the most extreme environments is an impressive example of functional plasticity. Recent advancements in sequencing technologies are providing researchers with greater opportunity to study these unique and diverse organisms in a natural context, allowing for in-situ sampling, preservation and sequencing of environmental samples (Jiang et al. 2016; Rabus et al. 2016). Studies have expanded from single-culture approaches to in-situ studies in the most complex of environments, from deep sea nutrient and hydrocarbon cycling to shallow, freshwater,

riverine sediments (Baker et al. 2013; Li et al. 2014; Reid et al. 2018, 2019). Amplicon studies of single gene segments (targeted primer sequences for specific taxa or microbial groups) and targeted gene expression surveys (specific gene primers) have given rise to shotgun surveys identifying whole-community gene expression from our planet's most diverse ecosystems (Anantharaman et al. 2013; McKay et al. 2017), to our local waste-water treatment facilities (Weisener et al. 2017). What has become evident in recent years, is the immense phenotypic and functional plasticity of these microbes, in that their metabolic capabilities go far beyond what was ever known through conventional culturing approaches (Comte, Fauteux, and Giorgio 2013; Sabater et al. 2016). Microbes live and adapt in harsh environments, and in the process are able to utilize xenobiotic compounds that are typically harmful to other biota. Additionally, advancements with in-situ approaches to sequencing natural microbial communities, has only advanced our ability to understand how microbes can work in a cooperative framework at an interspecies level (Reid et al. 2018; Schink 1997; Sieber, McInerney, and Gunsalus 2012). Microbes are metabolically active in some of the most extreme and potentially thermodynamically constrained systems. Unfortunately, contaminants often spill into natural environments with extensive anthropogenic activity remaining an ongoing occurrence. As such, xenobiotic infiltration into our local and regional ecosystems effects the natural metabolic activities of indigenous microbial communities and therefore remains an extremely important research area to date.

The impacts of xenobiotic substances on natural ecosystem biogeochemistry has been studied for decades. Studies have characterized the effects of everything from sewage effluents, to chronic pollution sources from industrial facilities (Carmona et al. 2009;

Fernández et al. 2009; Pérez-Jiménez, Young, and Kerkhof 2001; Williams et al. 2007).

on the physical and chemical processes of freshwater and marine resources. The effects are fairly well understood at a chemical level, but are understudied in a microbial context, under in-situ conditions. Scientists have been able to understand how aquatic ecosystems are impacted by (often inadvertent) enhancements to oxygen consuming processes, or those that boost nutrient levels to unnatural levels (Rabouille et al. 2003; Sell and Morse 2006; Weisener et al. 2017). However, it remains extremely difficult to understand biogeochemical shifts as they pertain to aquatic sediments, as they are complicated by the complexities of microbe-mineral interactions alongside biofilm governed microbe-microbe cooperation. Northern Alberta, Canada, home to the Athabasca Oil Sands and its extensive mining operations, these studies remain severely lacking, in that there is little to no knowledge on the natural biogeochemical signature of the region, outside the influence of industrial practices. Conventional and routine geochemical testing provides estimates of time trends in concentrations of trace metals, PAH and nutrients. However, these assessments provide little information about how these materials are cycled through this uniquely hydrocarbon-rich ecosystem in terms of microbially mediated metabolic processes.

Microbial degradation of hydrocarbons in natural environments worldwide is a pressing topic, with global mining of fossil fuels and shipment through cross-continental pipelines potentially posing unique environmental risks, not to mention simply the ubiquitous presence of hydrocarbons worldwide. In Alberta, Canada, a unique ecosystem exists as a part of the geologic McMurray Formation (MF), constituting the mineable Athabasca Oil Sands. The MF itself contains surface mineable deposits, with overburdens

less than 75 m, constituting approximately 144 x 10^9 billion barrels of bitumen (Chalaturnyk, Scott, and Özüm 2002), with a production rate of approximately 2.8 bbl/day in 2017 (https://www.alberta.ca/oil-sands-facts-and-statistics.aspx). Caustic hot water extraction procedures break apart the bonds holding the bituminous ore together, separating sands and clays from the target bitumen. Waste tailings, a slurry of water, sands, clays and residual bitumen are pumped into large settling basins called tailings ponds. Generally this tailings slurry is comprised of approximately 55 wt% solids (82 wt% sands; 14 wt% fines < 44 um), and 1 wt% bitumen (Chalaturnyk, Scott, and Özüm 2002). As of 2013, fluid fine tailings volumes totaled approximately 976 Mm^3, with tailings pond infrastructure covering a land area of 220 km^2 (AESRD, 2014). These ponds receive sands, silts, clays and residual hydrocarbons leftover after the bitumen extraction process. Government mandates that these mines and ponds must be reclaimed into a natural landscape following mining activity, thus it is vital to accurately characterize these ponds prior to attempting such reclamation. Recently studies have characterized the biotic and abiotic evolution of different tailings materials (Chen et al. 2013a; Frank et al. 2016b; Frankel et al. 2016; Fru et al. 2013; Reid et al. 2016), utilizing the latest geochemical techniques. These studies have collectively revealed that these ponds are truly unique from one another in a geochemical context. Additionally, studies evaluated the evolution of tailings treated with gamma irradiation (GI) in both a geochemical and molecular framework (Boudens et al. 2016; VanMensel et al. 2017). This GI treatment approach was realized during a study by Chen et al., 2014, where it was utilized to sterilize tailings slurries for chemical analyses. At the same time, it was determined that the GI treatment had broken down the toxic naphthenic acid mixture. This is unique in that other treatment options (i.e. UV or

ozonation) have difficulty penetrating turbid fluids (Boudens et al. 2016). VanMensel et al., 2018, determined that there was a microbial community response from this treatment, boosting the relative abundance of complex organic degraders and increasing the rate biodegradation within the tailings. Additional studies have further outlined the similarities and differences between tailings ponds in a biogeochemical context, attributed to source materials and extraction procedures (Frank et al. 2016a; Mahaffey and Dubé 2016; Xue et al. 2018). Frank et al., 2016 for instance, were able to use high resolution mass spectroscopy to spatially differentiate tailings sources, indicating measurable heterogeneity with respect to the organic compounds within each pond.

However, given the immense volumes of tailings waste materials being produced now and well into the future, effective and efficient reclamation strategies remain an ongoing interest in the region. Current plans are aimed towards the development of end-pit lake systems (EPL) – essentially filling open-pit mines with matured tailings and a mixture of fresh and process-affected waters – though there are no proven end-points from which to judge reclamation success. To effectively and efficiently proceed with reclamation procedures, it is necessary to expand research beyond the focus of the contaminated sites themselves and understand the natural biogeochemistry of the MF, from a baseline reference perspective. In the Athabasca Oil Sands, few studies have truly characterized the surrounding natural environment in a microbial context, particularly with respect to actual metabolic activity. Yergeau et al., 2012, identified the microbial taxa at various natural reference locations proximal to the industrial sites, though left a question mark as to the true metabolic function of the microbes in those environments (Yergeau et al. 2012). This dissertation seeks to fill in this knowledge gap, providing the first ever metatranscriptomics

(i.e. active gene expression) surveys of the MF, identifying dominant metabolic pathways governing the regional biogeochemistry. Research presented within this dissertation identifies dominant energy metabolism and hydrocarbon degradation genes from these hydrocarbon-rich environments in Northern Alberta, Canada. Furthermore, novel in-situ techniques allowed for the collection of suspended materials for tracking hydrocarbon compounds down a river continuum using microbial biomarkers. Finally, research is presented providing insights into the evolution of tailings materials as they progress towards a remediated state. This collection of dissertation chapters outlines these baseline biogeochemical characteristics governing both the natural and polluted environments within the Athabasca Oil Sands region, expanding our understanding of not only the natural ecology of these complex ecosystems, but also the best management practices for mine-closures and remediation guidelines down the road.

1.2 Research Focus

The research incorporated into this dissertation, addresses the biogeochemical processes governing natural, man-made and linking these end points to contaminated tailings ecosystems. The research objectives for Ch.3-5 are the first to address established end-points for microbial communities in the Athabasca Oil Sands region of Alberta, Canada. Establishing these correlations between these tailings ponds (Ch.5) and the adjacent natural environments (Ch.2-4), we can better understand how to proceed with future reclamation procedures, since this research now highlights established microbial end-points for the diverse range of environments within and outside the McMurray Formation.

The primary objective of the cumulative chapters comprising this dissertation is to bridge the knowledge gap between the well-studied tailings environments and the regional natural landscapes as reclamation becomes increasingly important. These natural ecosystems have not been sufficiently studied, and this opportunity provides ideal insight into potential reclamation end-points, indicative of how the indigenous ecology live and evolve in such a unique, hydrocarbon-impacted environment. The primary research objectives and subsequent hypotheses are broken down in the following sections.

1.2.1 Research Hypotheses and Objectives

The first hypothesis to be tested is that the baseline biogeochemical signature of naturally hydrocarbon rich sediments will exhibit a clear signature of metabolic adaptation given the long-term exposure to such unique conditions. To test this hypothesis, RNA is extracted from sediments of the MF for shotgun metatranscriptomics analysis to observe the active function of the bacterial communities. Here, we can characterize the natural, active, in-situ biogeochemical cycles governed by the indigenous microbial consortia.

The second hypothesis to be tested is that the microbial communities will be actively utilizing the hydrocarbons present, as they represent a large, viable carbon source. To test this hypothesis, metatranscriptomics datasets were analyzed for differentially expressed genes related to aromatic and/or alkane hydrocarbon degradation. Further, characterization of genes related to secondary and tertiary breakdown pathways were characterized.

The third hypothesis tested is that the microbial genetic response to the MF may be difficult to decipher early in the river continuum due to lack of exposure time (particularly in

suspended sediment communities), though will be clearly evident as exposure time within the formation increases. Bed sediments will likely show a strong response inside the MF, though a small or potentially insignificant response may be measured in the suspended sediments. To test these hypotheses, again gene expression surveys of both suspended and bed sediments along a river continuum were conducted, to determine if there is a microbial genetic response to the McMurray Formation (i.e. increasing hydrocarbon content moving into, and through the formation). If so, correlation of co-expressing genes in relation to increasing exposure time are characterized to provide robust gene biomarkers for compound tracking under hydrodynamic conditions.

The fourth research hypothesis is that the geochemical signature of tailings materials will trend towards more naturalized systems over the course of the 3-year study, though there will remain distinct differences primarily associated with salinity and elevated naphthenic acid concentrations. This hypothesis will be tested by characterizing the geochemical evolution of oil sands tailings materials from different operators, treated with gamma irradiation to promote reclamation and compare to natural wetland maturation. Over a three-year study period, early reclamation evolution can be observed from a controlled field-scale biogeochemical context.

References

Alberta Environment and Sustainable Resource Development. (2014). Reclamation Information System, 2013. Annual Conservation and Reclamation Report Submissions.

Anantharaman, K., Breier, J. A., Sheik, C. S., & Dick, G. J. (2013). Evidence for hydrogen oxidation and metabolic plasticity in widespread deep-sea sulfur-oxidizing bacteria. Proceedings of the National Academy of Sciences, 110(1), 330–335. https://doi.org/10.1073/pnas.1215340110

Baker, B. J., Sheik, C. S., Taylor, C. a, Jain, S., Bhasi, A., Cavalcoli, J. D., & Dick, G. J. (2013). Community transcriptomic assembly reveals microbes that contribute to deep-sea carbon and nitrogen cycling. The ISME Journal, 7(10), 1962–1973. https://doi.org/10.1038/ismej.2013.85

Boudens, R., Reid, T., VanMensel, D., Sabari Prakasan, M. R., Ciborowski, J. J. H., & Weisener, C. G. (2016). Bio-physicochemical effects of gamma irradiation treatment for naphthenic acids in oil sands fluid fine tailings. Science of the Total Environment, 539, 114–124. https://doi.org/10.1016/j.scitotenv.2015.08.125

Carmona, M., Zamarro, M. T., Blázquez, B., Durante-Rodríguez, G., Juárez, J. F., Valderrama, J. A., … Díaz, E. (2009). Anaerobic catabolism of aromatic compounds: a genetic and genomic view. Microbiology and Molecular Biology Reviews : MMBR, 73(1), 71–133. https://doi.org/10.1128/MMBR.00021-08

Chalaturnyk, R. J., Scott, J. D., & Özüm, B. (2002). Management of oil sands tailings. Petroleum Science and Technology, 20(9–10), 1025–1046. https://doi.org/10.1081/LFT-120003695

Chen, M., Walshe, G., Chi Fru, E., Ciborowski, J. J. H., & Weisener, C. G. (2013). Microcosm assessment of the biogeochemical development of sulfur and oxygen in oil sands fluid fine tailings. Applied Geochemistry, 37(2010), 1–11. https://doi.org/10.1016/j.apgeochem.2013.06.007

Comte, J., Fauteux, L., & Giorgio, P. A. (2013). Links between metabolic plasticity and functional redundancy in freshwater bacterioplankton communities. Frontiers in Microbiology, 4(MAY), 1–11. https://doi.org/10.3389/fmicb.2013.00112

Fernández, M., Duque, E., Pizarro-tobías, P., Dillewijn, P. Van, Wittich, R., & Ramos, J. L. (2009). Brief report Microbial responses to xenobiotic compounds . Identification of genes that allow Pseudomonas putida KT2440 to cope with 2 , 4 , 6-trinitrotoluene, 2, 287–294. https://doi.org/10.1111/j.1751-7915.2009.00085.x

Frank, R. A., Milestone, C. B., Rowland, S. J., Headley, J. V., Kavanagh, R. J., Lengger, S. K., … Hewitt, L. M. (2016a). Assessing spatial and temporal variability of acid-extractable organics in oil sands process-affected waters. Chemosphere, 160, 303–313. https://doi.org/10.1016/j.chemosphere.2016.06.093

Frank, R. A., Milestone, C. B., Rowland, S. J., Headley, J. V., Kavanagh, R. J., Lengger, S. K., … Hewitt, L. M. (2016b). Assessing spatial and temporal variability of acid-

extractable organics in oil sands process-affected waters. Chemosphere, 160, 303–313. https://doi.org/10.1016/j.chemosphere.2016.06.093

Frankel, M. L., Demeter, M. A., Lemire, J. A., & Turner, R. J. (2016). Evaluating the metal tolerance capacity of microbial communities isolated from Alberta oil sands process water. PLoS ONE, 11(2), 1–16. https://doi.org/10.1371/journal.pone.0148682

Fru, E. C., Chen, M., Walshe, G., Penner, T., Weisener, C., Chi Fru, E., … Weisener, C. (2013). Bioreactor studies predict whole microbial population dynamics in oil sands tailings ponds. Applied Microbiology and Biotechnology, 97(7), 3215–3224. https://doi.org/10.1007/s00253-012-4137-6

Jiang, Y., Xiong, X., Danska, J., & Parkinson, J. (2016). Metatranscriptomic analysis of diverse microbial communities reveals core metabolic pathways and microbiome-specific functionality. Microbiome, 1–18. https://doi.org/10.1186/s40168-015-0146-x

Li, M., Jain, S., Baker, B. J., Taylor, C., & Dick, G. J. (2014). Novel hydrocarbon monooxygenase genes in the metatranscriptome of a natural deep-sea hydrocarbon plume. Environmental Microbiology, 16(1), 60–71. https://doi.org/10.1111/1462-2920.12182

Mahaffey, A., & Dubé, M. (2016). Review of the composition and toxicity of oil sands process-affected water. Environmental Reviews, 25(1), 1–18. https://doi.org/10.1139/er-2015-0060

McKay, L. J., Hatzenpichler, R., Inskeep, W. P., & Fields, M. W. (2017). Occurrence and expression of novel methyl-coenzyme M reductase gene (mcrA) variants in hot spring sediments. Scientific Reports, 7(1), 1–12. https://doi.org/10.1038/s41598-017-07354-x

Pérez-Jiménez, J. R., Young, L. Y., & Kerkhof, L. J. (2001). Molecular characterization of sulfate-reducing bacteria in anaerobic hydrocarbon-degrading consortia and pure cultures using the dissimilatory sulfite reductase (dsrAB) genes. FEMS Microbiology Ecology, 35(2), 145–150. https://doi.org/10.1016/S0168-6496(00)00123-9

Rabouille, C., Denis, L., Dedieu, K., Stora, G., Lansard, B., & Grenz, C. (2003). Oxygen demand in coastal marine sediments: Comparing in situ microelectrodes and laboratory core incubations. Journal of Experimental Marine Biology and Ecology, 285–286, 49–69. https://doi.org/10.1016/S0022-0981(02)00519-1

Rabus, R., Boll, M., Heider, J., Meckenstock, R. U., Buckel, W., Einsle, O., … Wilkes, H. (2016). Anaerobic microbial degradation of hydrocarbons: From enzymatic reactions to the environment. Journal of Molecular Microbiology and Biotechnology, 26(1–3), 5–28. https://doi.org/10.1159/000443997

Reid, T., Boudens, R., Ciborowski, J. J. H., & Weisener, C. G. (2016). Physicochemical gradients, diffusive flux, and sediment oxygen demand within oil sands tailings materials from Alberta, Canada. Applied Geochemistry, 75, 90–99. https://doi.org/10.1016/j.apgeochem.2016.10.004

Reid, T., Chaganti, S. R., Droppo, I. G., & Weisener, C. G. (2018). Novel insights into freshwater hydrocarbon-rich sediments using metatranscriptomics: Opening the black box. Water Research, 136, 1–11. https://doi.org/10.1016/j.watres.2018.02.039

Reid, T., Droppo, I. G., Chaganti, S. R., & Weisener, C. G. (2019). Microbial metabolic strategies for overcoming low-oxygen in naturalized freshwater reservoirs surrounding the Athabasca Oil Sands: A proxy for End-Pit Lakes? Science of The Total Environment, 665, 113–124. https://doi.org/10.1016/j.scitotenv.2019.02.032

Sabater, S., Timoner, X., Borrego, C., & Acuña, V. (2016). Stream Biofilm Responses to Flow Intermittency: From Cells to Ecosystems. Frontiers in Environmental Science, 4(March), 1–10. https://doi.org/10.3389/fenvs.2016.00014

Schink, B. (1997). Energetics of syntrophic cooperation in methanogenic degradation. Microbiology and Molecular Biology Reviews : MMBR, 61(2), 262–280. https://doi.org/1092-2172/97/$04.0010

Sell, K. S., & Morse, J. W. (2006). Dissolved $Fe2+$ and $\sum H2S$ Behavior in Sediments Seasonally Overlain by Hypoxic-to-anoxic Waters as Determined by CSV Microelectrodes. Aquatic Geochemistry, 12(2), 179–198. https://doi.org/10.1007/s10498-005-4574-2

Sieber, J. R., McInerney, M. J., & Gunsalus, R. P. (2012). Genomic Insights into Syntrophy: The Paradigm for Anaerobic Metabolic Cooperation. Annual Review of Microbiology, 66(1), 429–452. https://doi.org/10.1146/annurev-micro-090110-102844

VanMensel, D., Chaganti, S. R., Boudens, R., Reid, T., Ciborowski, J., & Weisener, C. (2017). Investigating the Microbial Degradation Potential in Oil Sands Fluid Fine Tailings Using Gamma Irradiation: A Metagenomic Perspective. Microbial Ecology, 74(2), 362–372. https://doi.org/10.1007/s00248-017-0953-7

Weisener, C., Lee, J., Chaganti, S. R., Reid, T., Falk, N., & Drouillard, K. (2017). Investigating sources and sinks of N2O expression from freshwater microbial communities in urban watershed sediments. Chemosphere, 188, 697–705. https://doi.org/10.1016/j.chemosphere.2017.09.036

Williams, A. P., Avery, L. M., Killham, K., & Jones, D. L. (2007). Persistence, dissipation, and activity of Escherichia coli O157:H7 within sand and seawater environments. FEMS Microbiology Ecology, 60(1), 24–32. https://doi.org/10.1111/j.1574-6941.2006.00273.x

Xue, J., Huang, C., Zhang, Y., Liu, Y., & Gamal El-Din, M. (2018). Bioreactors for oil sands process-affected water (OSPW) treatment: A critical review. Science of the Total Environment, 627, 916–933. https://doi.org/10.1016/j.scitotenv.2018.01.292

Yergeau, E., Lawrence, J. R., Sanschagrin, S., Waiser, M. J., Darren, R., Korber, D. R., … Darren, R. (2012). Next-generation sequencing of microbial communities in the athabasca river and its tributaries in relation to oil sands mining activities. Applied and Environmental Microbiology, 78(21), 7626–7637. https://doi.org/10.1128/AEM.02036-12

CHAPTER 2: **NOVEL INSIGHTS INTO FRESHWATER HYDROCARBON-RICH SEDIMENTS USING METATRANSCRIPTOMICS: OPENING THE BLACK BOX**

GRAPHICAL ABSTRACT

2.1 Introduction

Understanding the biogeochemical function within natural aquatic ecosystems is a necessity given the inevitable impacts of climate change and broad ranging anthropogenic stressors. Aquatic ecosystems respond readily to external inputs, altering entire biogeochemical signatures with impacts on ecosystem health, possibly extending throughout the entire food web. Microbes, the dominant driver of chemical cycling, will inevitably alter their function to accommodate nutrient fluxes within their surrounding environment. When subjected to increased levels of hydrocarbons, for example, utilization of these hydrocarbons as an energy source is to their advantage. Given the global ubiquity of hydrocarbons in our aquatic ecosystems, studying environments chronically exposed to *naturally* occurring hydrocarbon sources (i.e. bitumen, coal deposits etc.) can provide great insight into how microbes function in these complex environments. Several studies have characterized microbial activity in hydrocarbon-rich, marine spill-sites, legacy contaminant sediments, alongside natural hydrothermal vents (Boufadel and Michel 2008; Bragg et al. 1994; Kappell et al. 2014; Kimes et al. 2014; Mason et al. 2012; Pritchard et al. 1992; Reid et al. 2018; Zhang, Lo, and Yan 2015). However, microbial dynamics in association with freshwater hydrocarbon-rich environments is still poorly studied.

In Northern Alberta, Canada, the McMurray formation is a bituminous sand layer constituting the Athabasca Oil Sands. Rivers cut through this formation, providing a major conduit of hydrocarbon expression into the natural environment (Figure 1). Erosion, transportation and deposition of the bitumen has a profound effect on the natural chemistry and overall health of these ecosystems. These unique, natural hydrocarbon outcrops provide an interesting environment from which to compare natural microbial metabolism in the

presence of hydrocarbons, between regional outcrop sites. If the microbes in these ecosystems are naturally metabolizing these complex compounds, and their metabolic pathways can be characterized, then reclamation efforts within the industrial oil sands mining areas can utilize these baseline characterizations for optimizing reclamation strategies. Furthermore, this environment gives a unique opportunity to study biodegradation in a freshwater, boreal setting, unlike the many marine-based studies in recent years. Until now, studies in this region have stopped at taxonomic assessments alongside geochemical surveys (Yergeau et al. 2012). This can be attributed to not only logistical difficulties accessing these sites, but also molecular difficulties in attempting to extract viable messenger RNA (that which shows active gene transcription) from such complex sediments.

The McMurray Formation, is characterized by a complex hydrocarbon mixture of both unsubstituted and substituted species, dominated by sulfur and nitrogen compounds. Aromatic hydrocarbons, chlorinated hydrocarbons and linear and chained alkanes are widely studied due to their persistence in the environment, and their complexity in terms of the breadth of variation between chemical structures (Dabestani and Lvanov, Ilia N. 1999). Polycyclic aromatic hydrocarbons (PAHs) are most difficult to degrade (as opposed to linear alkanes) due to their complex ringed structure, and are found both naturally in these hydrocarbon-rich environments, as well as in industrially influenced sites (Dabestani and Lvanov, Ilia N. 1999; Haritash and Kaushik 2009). The atmospheric release can also contribute to the spatial distribution of PAHs because of the combustion of various compounds from industrial processes, including automotive emissions (Ravindra, Sokhi, and Van Grieken 2008). Natural contributions can also occur as a result of the many forest fires in the area (Ravindra, Sokhi, and Van Grieken 2008).

In the natural environment, the native microbial consortia will utilize these complex molecules in their energy metabolism, as they are a readily available carbon source. However, many studies involve potentially biased cultured microbial consortia, thus studying environments containing naturally occurring hydrocarbon outcrops is a unique opportunity for an unbiased functional analysis (Ghazali et al. 2004; Jaekel et al. 2015). Furthermore, in a natural freshwater setting, it could be that microbial community development has evolved to metabolize certain groups of hydrocarbons, though this remains poorly understood. Identifying novel degradation pathways under various redox conditions in natural reference systems could provide insight into the potential for enhanced microbial reclamation strategies in existing contaminate environments, where bioremediation is a potential option.

The importance of characterizing actual microbial gene expression in the natural environment should not be overlooked, as conventional taxonomic assessments and subsequent inferences are becoming a risky venture. High-throughput sequencing has further emphasized the vastly complex microbial phylogenetic tree, with ongoing studies proving this complexity is only growing (Hug et al. 2016; Long et al. 2016; Lynch and Neufeld 2015; Pace 1997). Microbial species that differ by only fractions of a percent in terms of their genetic code make the quest for taxonomic identification and subsequent functional *inferences* a shot-in-the-dark in some cases (Hanage, Fraser, and Spratt 2006; Konstantinidis and Tiedje 2005; Rosselli et al. 2016). Recent studies identifying microbes with single genes (or perhaps closely related homologs) being responsible for multiple processes has further emphasized the need for microbial characterization on an expression and activity level (Chistoserdova, Vorholt, and Lidstrom 2005). This study investigates the dominant

hydrocarbon signatures and in-situ microbial function within 3 major freshwater tributaries of the Lower Athabasca River which cut through the McMurray Formation, including a unique groundwater bitumen seep. Functional processes relating to energy metabolism and hydrocarbon degradation at these sites will be discussed, with inferences as to how these findings can be utilized in actual contaminant environments for improving aquatic resource management.

In the context of this dissertation, this chapter seeks to unravel the natural microbial metabolism governing the MF as outline in RO1 and RH1, revealing how the unique hydrocarbon-rich strata impact the energy and degradation metabolic processes of the indigenous microbial community. Insights gathered here can begin to unravel how this unique landscape shapes the natural biogeochemical signature of the region, providing insight into reclamation end-points for the oil sands tailings systems. These natural baseline signatures are unique to the MF and the Athabasca Oil Sands region, providing much needed insight into the complex geochemical and microbiology of this hydrocarbon hotspot.

2.2 Methodology

2.2.1 Sampling Site Descriptions

In situ sampling sites (Figure 1) were chosen at natural locations known to contain bitumen outcrops, outside direct mining sites. The site named "groundwater plume" (GP) appeared the most (visually) untouched, though historical chemical data (Table 1 (AEMERA 2016)) suggests the highest polycyclic aromatic hydrocarbon (PAH) concentrations compared to the other two sites. In 1974-1975, Syncrude Canada Ltd. performed a baseline study of Ruth Lake and Poplar Creek before the commencement of hydrocarbon extraction from "Lease No. 17", since Beaver Creek had to be diverted from the mining area.

Obviously, this was before to advanced sequencing technologies, so baseline measurements consisted of fairly standard chemical measurements, and benthic flora and fauna (Syncrude 1975; Wasmund et al. 2009). This site is truly a unique groundwater plume system, included here as a novel baseline environment. Steepbank River (STB) is closest to the mining activity in terms of proximity, and contained large volumes of bitumen outcropping on the riverbank. STB water also was high in PAH content and overall humic substances. Environment and Climate Change Canada has several long-term monitoring studies recording water quality data from the chosen sample sites. Finally, Ells River (ER) sample site is located north of industrial mining sites, though still had a large amount of bitumen outcropping from the riverbank. Historical data suggested that that ER has relatively low PAH levels (both parent and substituted) relative to GP, but only slightly less than STB.

2.2.2 Sediment Sample Collection

In situ sample collection and preservation took place on September 2, 2015, at the 3 sites explained in the previous section (Figure 1). Sediment samples from the river banks at each site were taken in sterile, RNase and DNase free, 5 mL cryogenic vials and immediately flash frozen in liquid nitrogen within the Molecular Dimensions Dry Shipper (CX100). Riverbed sediments were collected in duplicate at the river's edge, directly below the hydrocarbon outcrops, consisting of surface sediments down to approximately 1-2 cm depth. Samples remained in liquid nitrogen until returning to the lab in which they were stored at -80 $^\circ$C until extractions were performed.

2.2.3 PAH Analyses

Samples for polycyclic aromatic hydrocarbon (PAH) analysis were sent for analysis at the Pacific Yukon Laboratory for Environmental Testing at Environment and Climate

Change Canada (ECCC). Dichloromethane (DCM) extractions were performed on bulk solids samples after deuterated surrogate standards were added. Following shaking and centrifugation, extracts were analyzed using gas chromatography/tandem triple quadrupole mass spectrometry (GC/MS/MS) (Agilent Technologies Inc., Santa Clara, CA. USA). Two standard calibration curves were used (high $0.01 – 2$ µg/mL; and low $0.1 – 10$ ng/mL) for quantification in multiple reaction monitoring mode (MRM), in accordance with PAH and substituted PAH concentrations. To cover the range of C1 – C4 carbon substitutions, an appropriate range of retention times was used to integrate the substituted PAH homolog groups and calculations based on authentic substituted PAH standard response factors. Isomer pairs are reported in cases where compounds could not be isolated on the MS, given equal masses (e.g. C1-Phenanthrene/Anthracene). Data is publicly accessible via the Canada-Alberta Oil Sands Environmental Monitoring data portal (http://donnees.ec.gc.ca/data/). The practical limit of quantification was 0.02 µg/g and 0.04 µg/g for unsubstituted and substituted PAHs respectively. The limit of detection was 0.01 µg/g and 0.02 µg/g dry weight solids for unsubstituted and substituted PAHs respectively.

3.2.4 Sediment RNA Isolation and Quality Control

RNA was extracted from each sediment sample with the MoBio PowerSoil Total RNA Isolation Kit (MO-BIO Laboratories, Inc., CA) with slightly modified protocols concerning manufacturer guidelines. Samples were slowly thawed in their cryogenic vials on ice, and immediately added to extraction tubes in a still semi-frozen state as to minimize RNA degradation. All reagents and instruments (extraction tubes, pipet tips, strippettes etc.) were kept chilled on ice before and during use when feasible. Further, 5 g of sediment was added to each extraction tube, and subsequent reagent additions were adjusted for this

additional volume. The precipitation of RNA was performed for 24 h at -20 ℃ to increase

RNA yield. Following final centrifugation, the pellet was dissolved in 30 µL RNase-free

water to concentrate the extracted RNA further. Aliquots of extracted RNA isolations were

kept at -80 ℃ until quality control and sequencing was performed.

2.2.5 RNA Library Construction and Sequencing

RNA extractions were sent for transcriptome analysis on the Illumina HiSeq 2000 at

the Genome Quebec Innovation Center at McGill University in Montreal, Quebec, Canada.

Extracted RNA was analyzed in house to assure sufficient quality for sequencing on the

Illumina HiSeq 2000.   Samples with RNA Integrity Numbers (RIN) over 7 and

concentrations of at least 100 ng/ul were sent off for analysis, with additional QC checks

performed at Genome Quebec prior to sequencing. Depletion of rRNA was also performed

before sequencing using the Illumina Ribo-Zero rRNA Removal Kit for Bacteria, enhancing

mRNA quantity in each sample for improved functional assignments. Duplicate samples

were sequenced to ensure sample accuracy.

2.2.6 Bioinformatic Analysis

Paired end-reads obtained from Illumina HiSeq were uploaded to the MG-RAST

(Meta Genome Rapid Annotation using Subsystem Technology, v3.1) server at the Argonne

National Library (http://metagenomics.anl.gov/) (Meyer et al. 2008). This automated

bioanalysis pipeline is used for the analysis of large shotgun metagenomic datasets, targeted

amplicons, and metatranscriptome RNA-seq datasets. Functional assignments using KEGG

orthology within MGRAST assigned over 500 000 annotations for each of the Ells River

(ER) and Steepbank (STB) samples, with over 1.5 million assigned to the groundwater plume

(GP). Quality scores (Phred) were set at Q=30, to remove low-quality reads, and subsequent

similarity thresholds set to 60% for gene expression functional annotations. Phylogenetic associations of residual 16S rRNA sequences were also annotated within MG-RAST, annotated to the RDP Database at a 60% minimum sequence identity. All reads were analyzed and compared within the MG-RAST analysis platform, before exportation of read data for further normalization and data mining. Functional read annotations for presented figures and tables were assigned using the KO (Kegg Orthology) database. Gene expression pathways were explored/visualized using the KEGG mapper. Reads assigned to recognized functional groups were normalized within each sample to rpoC (DNA-directed RNA polymerase subunit beta') (Berdygulova et al. 2011; Colston et al. 2014; Nieto et al. 2009; Rivers et al. 2016). Duplicates for each sample were averaged for accuracy and then compared between sample sites.

Analysis of functional hits was broken down into two categories for this publication: energy metabolism and alkane/hydrocarbon biodegradation and metabolism. Results present these level 3 functional annotations providing insight into where dominant expression was observed. Functional assignments within these dominant categories are further interpreted and plotted within Aabel 3 graphical software to present visual comparisons between specific genes corresponding to active transcripts.

2.3 Results and Discussion

2.3.1 Unsubstituted/Substituted PAH Concentrations

PAH concentrations are included for the ER and STB sites, measured during sample acquisition for this research (Table 2). Samples could not be attained for site GP. High concentrations of C1-C4 substituted hydrocarbons we recorded for both ER and STB, which is characteristic of the bituminous sands found in the McMurray Formation. Especially

dominant are C4-Dibenzothiophene, C2-C3-Phenanthrene/Anthracenes, C1-C4-Fluoranthene/Pyrene and C1-C4-Benzo[a]anthracene/Chrysene. The consistently lower PAH expression in STB (total PAHs ~26% that of ER) suggests a possible mechanism of biodegradation controlling the PAH signature here compared to ER. Overall, ER has the higher total PAH content, though interestingly, consistently measured lower parent PAH concentrations than STB. This suggests that many of the PAHs in these sites are in fact a result of diagenetic processes and are not a result of combustion sources. The PAH characteristics measured in these sites closely match previous studies and reflect the chemical characteristics of the bitumen deposit present at these outcrop sites. Historic water PAH measurements at GP indicate high concentrations there, inviting future studies to characterize this novel location as well. From here on in, the Ells River sample site is referred to as "ER", the groundwater plume on Poplar Creek as "GP" and the Steepbank River sample as "STB".

2.3.2 Sequencing Statistics & Functional Assignments

Sequencing stats are outlined in Appendix A (Table S1) for all sample sites. Briefly, the Illumina HiSeq 2000 sequencing resulted in over 67 million, 53 million and 29 million sequence counts for ER, GP and STB respectively. Identified functional categories (for use in gene expression results to follow) all exceeded 500 000 reads for all three sites. Hereafter, expression levels, where expressed in text and figures, are expressed as a percentage of the rpoC gene as noted previously.

2.3.3 Differential Gene Expression

2.3.3.1 Energy Metabolism

Gene expression data derived from the MG-RAST pipeline, utilizing the KEGG annotations, and KO database annotations were normalized to the rpoC gene encoding the DNA-directed RNA polymerase enzyme, to allow normalized comparisons between sites. Initial characterizations of dominant level 3 functional assignments were compared for the three sampling locations (Appendix A, Figure S1). Dominant transcripts are evident in level 3 categories of methane metabolism [ko00680], carbon fixation [ko00720], nitrogen metabolism [ko00910], and sulfur metabolism [ko00920]. The most highly expressed transcripts were annotated to carbon fixation, where GP transcripts dominated, followed by similar transcripts expressed for both nitrogen and sulfur metabolism regardless of location. Visualization of specific functional annotations (Figure 2) reveal the differential expression for methane, carbon fixation, nitrogen and sulfur metabolisms concerning specific enzymatic pathways.

2.3.3.1.1 Nitrogen

Dominant transcripts related to nitrogen metabolism were observed in all sample sites (Figure 2 & Figure 3), indicating strong linkages between the degradation of hydrocarbons and denitrification processes. Nitrogen is often associated with aromatic petroleum hydrocarbons via increase in carbon-nitrogen bonding, making the cleaving of these bonds extremely difficult (Scott et al. 2014). Results shown indicate a higher expression of nitrogen metabolism genes in sites known to contain correspondingly high concentrations of hydrocarbons (in this case GP), relating to other studies observing similar characteristics in oil rich environments (Scott et al. 2014). Historical water quality data (Table 1) indicates

GP contains the highest concentrations of PAHs, which appear to correlate with denitrification transcripts of *napA, nirB, norB, and nosZ*. Sediment PAH data (Table 2) indicates similar PAH concentrations between ER and STB, aside from c2, c3 and c4-substituted homologs, correlating to more similar dentrification transcript abundance as noted in Figure 3. Metabolic expressions observed in nitrate reduction and denitrification environments suggest that these reference sites are influenced by excess carbon input, regulating primary metabolisms of organics and nutrients with symbiotic biodegradation of hydrocarbons (Scott et al. 2014) showed a shift towards denitrification processes in contaminated environments, where nitrate appeared to be consumed, with increasing concentrations of nitrite and nitric oxide. Further, here we observe nitrogen metabolism, in general, is more highly expressed across all sites compared to sulfur metabolism, correlating with previous studies indicating the preferential use of nitrate as electron acceptors in BTEX degradation pathways. In the presence of more complex BTEX compounds, sulfate reduction was out-competed by nitrate reduction processes as well (Dou et al. 2008).

2.3.3.1.2 Sulfur

A differential expression relating to sulfur transcripts can be observed between all sites in Figure 2. Sulfate-adenyltransferase and several associated subunits (*cysND, met3/SAT*) indicate the activity of both assimilatory and dissimilatory sulfate reduction. Intermediate pathways including genes encoding APS to PAPS to sulfide (assimilatory) and APS straight to sulfide (dissimilatory) are also expressed. Assimilatory sulfide production as a result of *sir* gene expression indicates the highest sulfide production in the GP, followed closely by ER then STB (17.68%; 17.00%; 15.20% respectively). This is perhaps correlated to the higher c3- and c4-dibenzothiophene measured in ER compared to STB (Table 2). This

sulfide pathway may be scavenging sulfur from the dibenzothiophenes within the environment. Regarding dissimilatory sulfide production, *dsrAB* expression indicates high expression in STB (7.4%), followed by ER (6.1%) then GP (4.1%) in this case. Overall gene expression indicates more highly expressed dissimilatory reduction activity, following previous studies identifying SRB communities thriving in hydrocarbon rich environments, actively reducing a variety of BTEX compounds (Kleikemper et al. 2002). Interestingly, these authors observed visible iron sulfide deposition in the riverine sediments adjacent to the outcrops samples, supporting the aforementioned gene expression results. Further, it has been noted that sulfur metabolism (specifically sulfate reduction) often works in cooperation with carbon fixation cycles and alkane consumption, as thioautotrophic bacteria in extreme environments, such as deep ocean hydrothermal vents, are capable of using reduced sulfur compounds for energy (Bose et al. 2013; Mattes et al. 2013). These deep-sea vents, like these hydrocarbon-rich environments in this study, are subject to steep chemical gradients and redox pockets due to the rich nutrient fluxes throughout the systems. It is also interesting to note that annotations of the *dsrAB* genes are also related to nitrotoluene degradation enzyme production (see 2.3.3.2). The high concentration of dibenzothiophene measured at both ER and STB suggest that perhaps these sulfur related transcripts imply an active degradation of this dominant organosulfur compound. These "extreme environment" characteristics could be the cause of these complex intermediate pathways, working in cooperation with several other processes in a unique symbiotic relationship. Interestingly, the expression (from high to low) of *aprAB* and *dsrAB* follows STB>ER>GP, which roughly correlates to the inverse ranking of measured total hydrocarbon concentrations (i.e. GP contains highest total hydrocarbons followed by STB and ER according to historical records). This possible

suppression of both enzymes constituting dissimilatory sulfate reduction perhaps indicates an inhibitory effect because of elevated hydrocarbon levels. This supports the previously outlined characterization that nitrate reduction will preferentially out-compete sulfate reduction as the provided electron acceptor in the degradation of various BTEX components.

2.3.3.1.3 Methane

The *mcrA* gene encoding methyl-coenzyme M reductase, which is associated with the final stage of methanogenesis, was most dominant in STB (4.28%), followed by GP (3.42%) and then ER (2.37%). Related to *mcrA*, the expression of *mcrBCD*, as well as the expression of several subunits of *mtr* genes encoding tetrahydromethanopterin S-methyltransferase, further provide an indication of methane production within all sites; though in these cases GP presents the highest expression levels. Expression of hydrogenase and acetyl-CoA pathways, as well as pathways indicating methylamine utilization, indicates that acetoclastic, hydrogenotrophic and methylotrophic methanogenesis is occurring through extensive electron transport systems. The utilization of not only acetate but also methylated compounds, CO_2 and H_2 for methane production is indicative of the diverse nature of the microbial population sampled in this study. This is further corroborated by the extensive abundance of unclassified organisms identified in the taxonomy derived from the RNAseq dataset (Figure 4). The occurrence of the methylotrophic methanogenic activity specifically is interesting given hydrogenotrophic methane production tends to dominate in most systems (Vanwonterghem et al. 2016). Utilization of hydrogen for methane production relieves the buildup of H_2 resulting from prior degradation processes and further boosts ongoing biodegradation. The presence of *Methanosarcina* at these same sites (aside from the previously unstudied GP) in the study by Yergeau et al., (2012) directly correlates to these

findings (Yergeau et al. 2012). *Methanosarcina* are capable of producing methane from not only acetate but CO_2 and H_2 as well. Further, *Methanosarcina* are tolerant to environmental changes which may inhibit CH_4 production from acetate, or otherwise hinder growth under varying physicochemical conditions (Ali Shah et al. 2014).

Highly expressed *hdrA* (heterodisulfide reductase, subunit A) encoding the reduction of heterodisulfide was evident across all sites, correlating to intracellular transport associated with methane metabolism. *HdrA* utilizes F_{420}-non-reducing hydrogenase (*mvhADG* and *mvhB*) to complete the H_2-dependent reduction of heterodisulfide to ferredoxin. In the case of *hdr* expression, sites were ranked STB>ER>GP in order from highest to lowest expression levels (32.12%, 29.29%, 22.05% respectively). The *Hdr* expression has also been linked to oxidizing sulfides, though perhaps, more importantly, facilitating reverse methanogenesis: methane oxidation under anaerobic conditions (Wang et al. 2014). Here, taxonomy data identified a relatively high abundance of active potential methanotrophs, alongside potential methanotrophs that are were identified as not only unclassified Archaea but also Bacteria (Figure 4). Expression of *mcrA*, *mtrABCDEFGH,* and *dsrAB* also have the potential for facilitating anaerobic oxidation of methane (AOM) within the sediment alongside the traditional characterization of methane production and sulfate reduction respectively (Nercessian et al. 2005; Timmers et al. 2017). Studies characterizing various methanotrophic archaea have indicated the ability of these genes to function in reverse, to oxidize methane in the absence of oxygen (Biddle et al. 2012). This novel process of AOM was reported in several studies, both in laboratory settings and in the field (Dhillon et al. 2003; Hallam, Putnam, and F 2004; He et al. 2015; Lloyd, Lapham, and Teske 2006; Nunoura et al. 2006; Thomsen 2001). Two recent studies have also observed anaerobic oxidation of methane

within microcosm oil sands tailings systems (Boudens et al. 2016; Reid et al. 2016) indicating that perhaps these natural sites exhibit some functional similarities to those tailings ponds in the region. The dominant cycling of nitrogen across all sites, and the sulfate reduction transcripts observed further indicate possible electron acceptors for this oxidation process, though perhaps in association with bacteria (Zhu et al. 2016). *Methylomonas* (a genus of the family Methylococcaceae, and class of Gammaproteobacteria) is able to cooperatively couple nitrate reduction with methane oxidation, though is reported to be an aerobic methane oxidizing bacteria (MOB) (Kits, Klotz, and Stein 2015; Milucka et al. 2015; Zhu et al. 2016). However, no reads encoding monooxygenases were observed, indicating that the sample locations were operating under limited oxygen conditions at the time of sampling. Though counterintuitive, this finding is the same as those in other studies, where aerobic-MOB can in fact thrive in anoxic conditions, and actively oxidize methane despite their *obligate aerobe* designation (Blees et al. 2014; Bowman 2006; Milucka et al. 2015). The sequestering of methane within the sediments is a beneficial process limiting the expression of harmful greenhouse gas from these hydrocarbon-rich environments, though the complexity that is methane oxidation within steep redox gradient environments continues to provide ample research opportunity. The use of biomarker genes once primarily accepted as purely responsible for methanogenic activity (i.e. *mcr*) should be used with caution, given the now commonly accepted notion that these same genes could be responsible for reverse methanogenesis as well (Timmers et al. 2017). Novel strains of bacteria capable of oxidizing methane (i.e. *Methylomonas*) indicate the importance of augmenting taxonomy assessments with more in-depth functional analyses, as taxonomic inferences can be misguided. Finally, the presence of these types of genes able to function in both methanogenic and

methanotrophic conditions indicates the need for further characterization of the AOM/aerobic-MOB process involving the culturing of pure strains, which has so far remained an unsuccessful venture (Timmers et al. 2017). The authors believe the study of microbial function within an environment, and the correlative syntrophic relations revealed through these advanced molecular approaches is becoming the new paradigm for microbial ecology and biogeochemical studies in general.

2.3.3.2 Biodegradation of Alkanes and Hydrocarbons

The direct influence of the McMurray formation to the ER, STB and GP reference sites, suggests that the microbial consortia is likely benefiting from the array of hydrocarbon compounds measured at these sites. Associated with level 3 functional categories (Appendix A, Figure S2) indicating various hydrocarbon constituent degradation pathways, the most highly expressed biodegradations regions for all 3 sites include nitrotoluene degradation [ko00633] and chlorocyclohexane and chlorobenzene degradation [ko00361]. For the noted highly expressed nitrotoluene degradation pathways (Figure 5), expression of the genes *nemA* and *nfnB/nfsB* (encoding N-ethylmaleimide reductase and nitroreductase/dihydropteridine reductase respectively) show the capability of the microbial consortia to degrade a wide array of nitroalkanes and nitroaromatics (Valle et al. 2012). Their ability to naturally degrade these compounds is advantageous given that these compounds tend to be a result of hydrocarbon combustion, and are present along with fossil fuels (Ju and Parales 2010). Degradation of these lower complexity aromatics suggests further degradation of more complex molecules given appropriate redox and nutrient substrates. Further, the highly expressed chlorocyclohexanes and chlorobenzene degradation pathways (Figure 5) indicate degradation of chlorinated hydrocarbons, as a result of an accumulation

of chlorinated aromatics within these sites (Kappell et al. 2014). The most dominant transcripts expressed were largely carboxymethylenebutenolidase (EC 3.1.1.45) followed by dehalogenases and mono- and di-oxygenases. These enzymes are associated with the degradation of halogenated compounds such as chlorohexenes, chlorobenzenes and fluorinated BTEX compounds. These mono- and di-oxygenase, as well as dehalogenase enzymatic functions, are most highly expressed at GP, indicating the diversity of this site both in energy metabolism and xenobiotic degradation capabilities. On the other hand, ER and STB exhibited a higher expression of nitrotoluene degradation compared to GP, suggesting, not surprisingly, that these two sites are more closely related than the unique plume site located on Poplar Creek. It should also be taken into consideration that complex interactions between the various PAH compounds and the surrounding particulate grains within the sediment can affect the bioavailability of the PAH for degradation. Though not studied here, these varying sorption affects could provide reasoning for the seemingly selective degradation of certain families of PAHs.

Further interpretation of the gene expression data indicates further evidence for aromatic compound degradation. Within the level 3 category of Benzoate Degradation [ko00362] several key genes are notably expressed, including *badA* (benzoate-CoA ligase), *badBCDEFGHI* (benzoyl-CoA reductases), *pcaB,C,D,F,H,I,J* (intermediate stages of benzene ring degradation), as well as *pobA* (p-hydroxybenzoate 3-monooxygenase). Of interest is the expression of *pobA* which has previously been indicated as being the initial oxidation of aromatic compounds, leading to further degradation by the aforementioned *pca* genes (Jiménez et al. 2002). The highest expression of *pobA* directly correlates to the overall higher biodegradation related transcripts observed at the GP site. These expressed benzoate

33

degradation genes indicate that benzene rings are being selectively cleaved via enzymatic activity, and further broken down through subsequent degradation pathways. The fact that the benzoyl-CoA is expressed, indicates that a range of aromatic compound have been degraded by various tertiary processes, all of which narrow to the benzoyl-CoA pathways, which are then degraded further through subsequent central pathways. Expression of *oah*, a homolog of the *bamA* gene (a ring-opening hydrolase), indicates that the natural microbial consortia are breaking benzene rings naturally. The array of genes suggesting natural biodegradation of hydrocarbons, alongside the syntrophic nature of the energy metabolism, provides insight into the complexity of the in-situ degradation processes. Unlike controlled lab studies, these pathways are quite intricate, involving a mixed consortium of microbes all working syntrophically towards a degraded end-product.

Reads annotated to fatty acid metabolism indicate highly expressed *fadE* genes (acyl-CoA dehydrogenase) as well as the presence of the important *alkB* (alkane monooxygenase), which implies the degradation of medium (C5-C22) chain alkanes is also occurring across all sites, but most highly expressed within the GP site at 3.8%. Additionally, *alkB* has been suggested in several papers to be a biomarker gene indicating hydrocarbon levels within an environment (Smith et al. 2013; Wasmund et al. 2009). In the case of these three sample sites, the differentially expressed *alkB* directly appears to correlate in the ranking with unsubstituted PAH concentrations between ER and STB (Table 2), supporting the use of this gene as a biomarker here. Furthermore, a study by Nie et al. 2014 also suggested gene copies of *alkB* were identified in several key bacterial phyla and classes of Proteobacteria (Nie et al. 2014). The enrichment of *alkB* in Alpha- Beta- and Gammaproteobacteria, alongside Actinobacteria and Bacteroidetes correlate with taxonomic abundances observed here

(Figure 4), alongside those described in Yergeau et al. (2012). These results strongly support the notion that the expression of *alkB* could indeed be a novel bioindicator gene to systematically survey an environment for active hydrocarbon degradation, and should be studied further in targeted, freshwater functional studies. However, given the high concentrations of select substituted PAHs in this environment, and the syntrophy of microbial metabolism observed, future work should also attempt to correlate a broader range of biomarkers to these observed PAH compounds. Additionally, more intricate characterizations (i.e. RNA-SIP) of various hydrocarbon degradation pathways would establish novel *in situ* metabolic capabilities of the native microbial community concerning specific substrates (i.e. naphthalene, dibenzothiophene, anthracene, etc.).

2.4 Conclusions

In this study, high throughput sequencing of environmental mRNA (metatranscriptomics) was used to gain further insight into these hydrocarbon rich environments. Results provide insight into the microbial communities responsible for hydrocarbon degradation in syntrophic association with methane, sulfate and nitrate reduction within several Athabasca River tributaries. The abundance of alkane degradation transcripts and mono- and di-oxygenases at all sites suggest considerable natural degradation of small to medium chained hydrocarbons. The high expression of sulfate and nitrate reduction transcripts, alongside cooperative methanogenic/methanotrophic activity, all promote this notion of multiple mechanisms facilitating the degradation of hydrocarbons and the oxidation of methane within these unique sediments. The current study allowed us to examine the variation within the natural hydrocarbon rich environments and to identify the functional biomarkers for the active microbial community involved in degradation. Further,

35

our analysis revealed novel lineages of microbe's potentially involved in hydrocarbon degradation, alongside sulfur, nitrate and methane metabolism. The current study could provide insight into how contaminated sites may behave given the sudden presence of a similarly complex hydrocarbon mixture.

These results and conclusion begin to provide much needed baseline characteristics of the MF, allowing researchers to look to the future of reclamation studies and understand how a "natural" MF ecosystem is likely to behave. This clearly complex biogeochemical signature has revealed a syntrophic cooperation of microbial metabolism that are in face metabolizing available hydrocarbons in the substrate. Understanding the MF baseline (obviously unique given its naturally hydrocarbon-rich sediments), needs to be followed up by further studies within different environmental contexts. Given the push for end-pit lake development down the road, there is a need to understand how deeper, freshwater lakes or reservoirs are governed by sediment microbial processes. This would allow researchers to understand how varying redox environments (i.e. oxic vs suboxic vs anoxic) contribute to the modification of standard microbial metabolic capabilities in-situ.

Conflicts of Interest
The authors declare no conflict of interest.

Figures & Tables
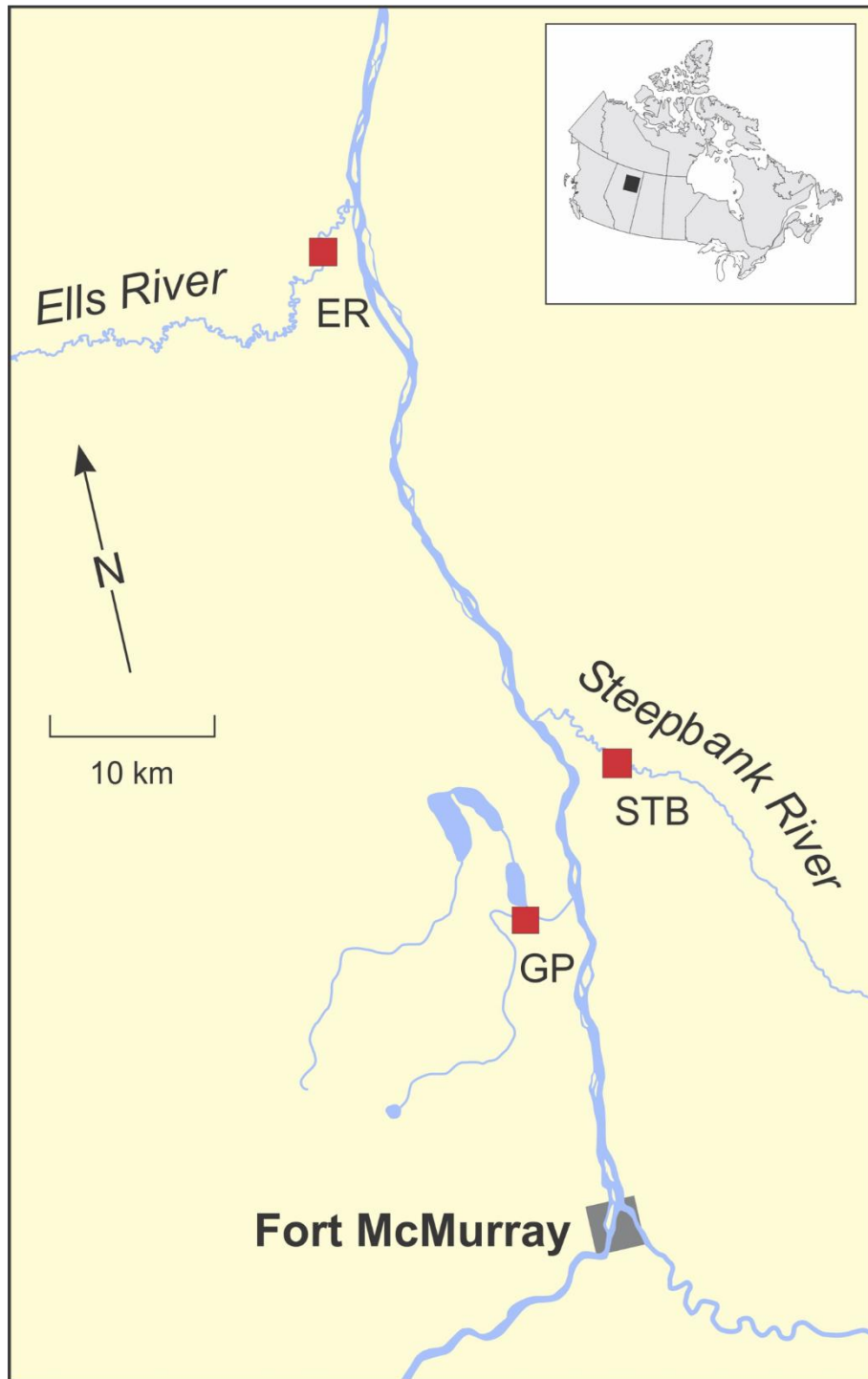
Figure 1: Sample collection locations along the Athabasca River tributaries. ER refers Ells River; GP is the groundwater plume on Poplar Creek; and STB is Steepbank River.
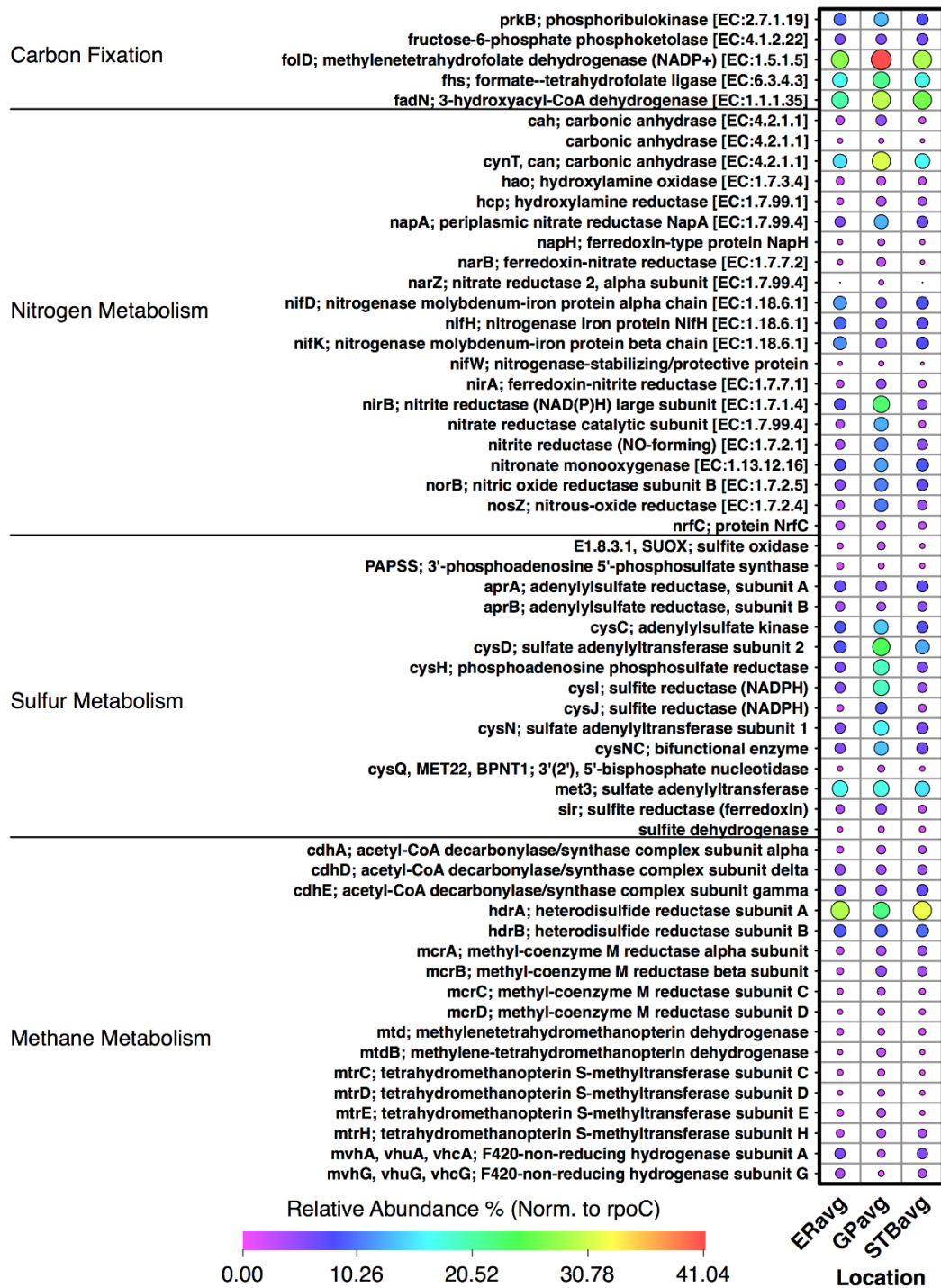
Figure 2: Functional annotations assigned to transcripts relating to methane, carbon fixation, sulfur and nitrogen metabolism. Ball plots are scaled and colorized to relative abundance % normalized to rpoC.
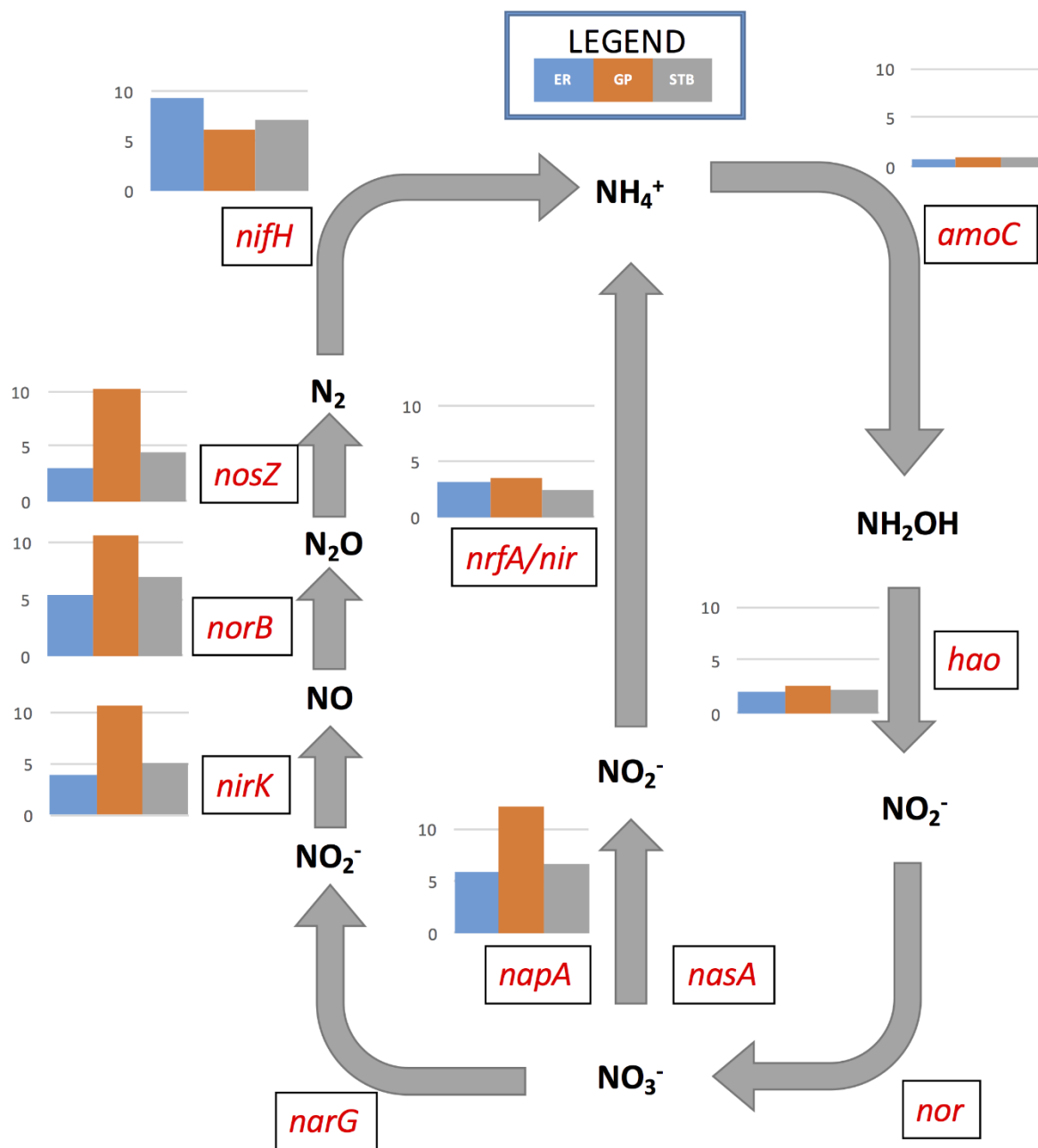
Figure 3: Nitrogen metabolic pathways of denitrification and nitrogen fixation expressed within the 3 sample locations. Differential expression between locations are expressed as bar plots next to gene expressed. From left to right on the x-axis: ER, GP, STB.

Dominant Taxa

STB
GP
ER
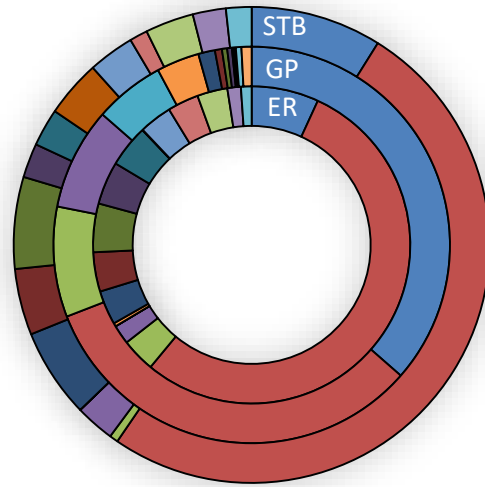
- Bacillus
- unclassified (derived from Bacteria)
- Escherichia
- unclassified (derived from Gammaproteobacteria)
- unclassified (derived from Methylococcaceae)
- Oscillatoria
- unclassified (derived from Archaea)
- Methanosaeta
- unclassified (derived from Deltaproteobacteria)
- Synechococcus
- unclassified (derived from Betaproteobacteria)
- Nodularia
- Candidatus Nitrososphaera
- Nitrosopumilus
- Thermococcus
- Planctomyces
- Methanosarcina
- Methylomonas

Figure 4: Top abundant taxonomy derived from RNAseq data, using the RDP database.
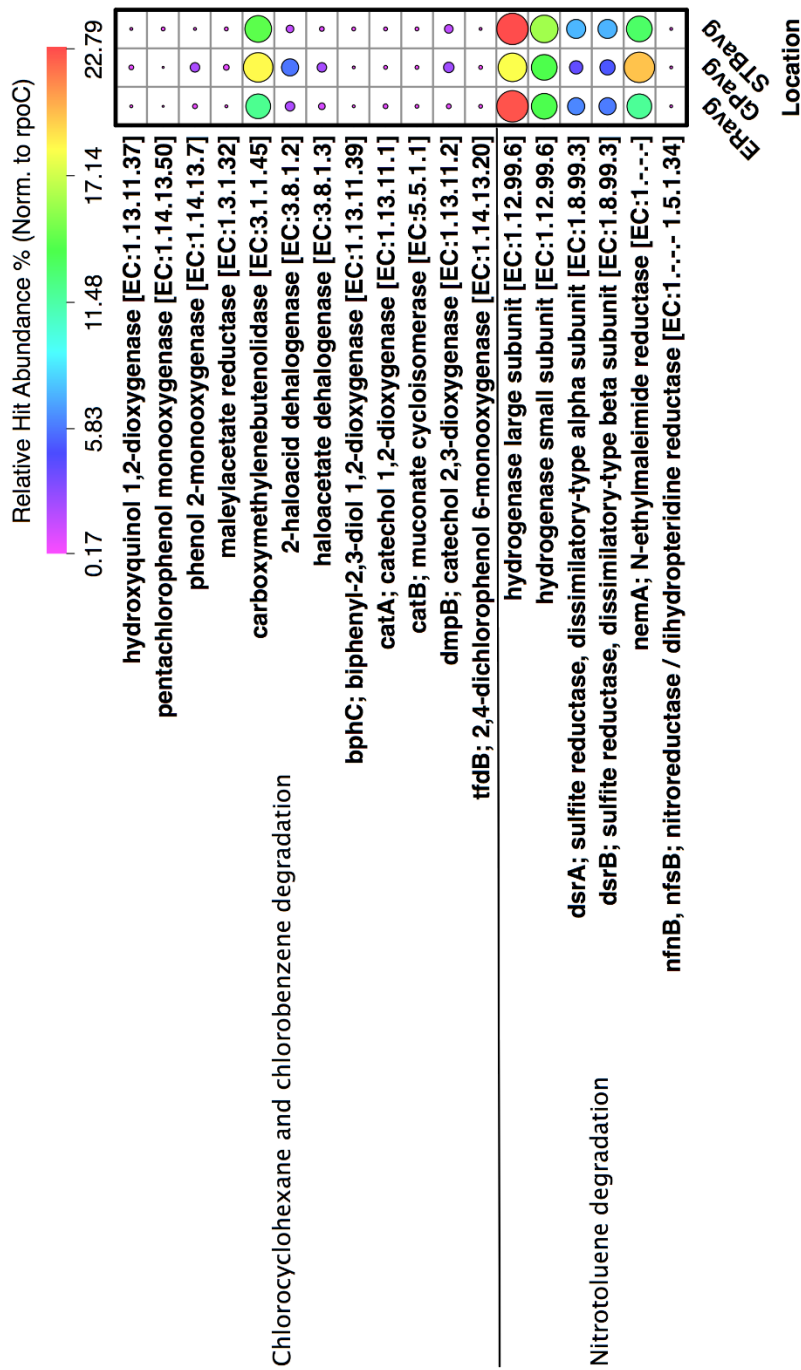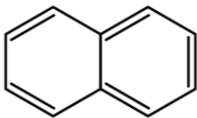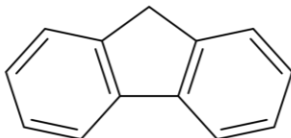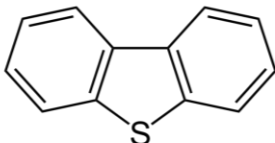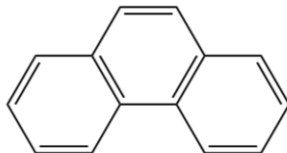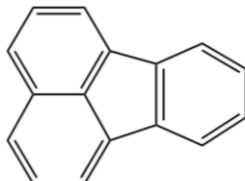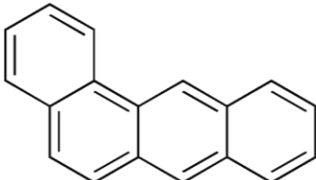
Figure 5: Functional annotations assigned to transcripts relating to chlorocyclohexane and chlorobenzene, as well as nitrotoluene biodegradation. Ball plots are scaled and colorized to relative abundance % normalized to rpoC.

Table 1: Historical chemical data for each sampled site (AEMERA 2016)

		Ells River	Groundwater Plume	Steepbank River
Latitude		57.280433	56.911013	56.998641
Longitude		-111.704749	-111.482391	-111.403359
Historic Sample Date		Fall 2015	Fall 2015	Fall 2015
pH		8.07	8.1	8.28
Total Suspended Solids (mg/L)		2.7	23	1.3
Conductivity (uS/cm)		230	1000	240
DOC (mg/L)		12	25	23
Naphthenic Acids (mg/L)		0.24	1.91	0.16
Polycyclic Aromatic Hydrocarbon (PAHs) (ng/L)	**Naphthalene**	<13.55	<13.55	<13.55
	Total dibenzothiophenes	9.4	88.8	41.4
	Total PAHs	133.9	369	178.4
	Total Parent PAHs	22.7	37	23.8
	Total Alkylated PAHs	111.2	332	154.6
Sulphate (mg/L)		21	36	5.1
Sulphide (mg/L)		-	0.0054	0.007
Dissolved Iron (mg/L)		-	0.594	0.492

Table 2: PAH concentrations for the Ells River and Steepbank River sampling sites. Unsubstituted and substituted PAH concentrations are presented alongside their chemical structure.

PAH/Alkylated PAH	Ells River [ng/g]	Steepbank River [ng/g]	
Naphthalene	12.8	18.1	
c1-Naphthalene	514.3	112.3	
c2-Naphthalene	4538.1	981.0	
c3-Naphthalene	5776.2	1569.6	
c4-Naphthalene	2254.0	3489.3	
Fluorene	11.9	19.4	
c1-Fluorene	8092.2	2292.7	
c2-Fluorene	15166.4	4586.9	
c3-Fluorene	30355.0	7619.5	
c4-Fluorene	12945.9	3932.1	
Dibenzothiophene	189.2	194.2	
c1-Dibenzothiophene	52.4	39.7	
c2-Dibenzothiophene	7833.6	2445.3	
c3-Dibenzothiophene	38524.1	7833.4	
c4-Dibenzothiophene	375231.6	88761.3	
Phenanthrene	123.4	96.4	
Anthracene	58.9	95.7	
c1-Phenanthrene/Anthracene	46.0	37.6	
c2-Phenanthrene/Anthracene	25293.2	6405.0	
c3-Phenanthrene/Anthracene	25666.8	5274.8	
c4-Phenanthrene/Anthracene	151.3	117.6	
Fluoranthene	181.3	241.3	
Pyrene	883.6	1213.4	
c1-Fluoranthene	19755.4	5380.2	
c2-Fluoranthene/Pyrene	54640.8	14187.9	
c3-Fluoranthene/Pyrene	594243.5	142509.5	
c4-Fluoranthene/Pyrene	658186.5	164122.3	
Benzo(a)anthracene	142.1	162.7	
Triphenylene	1333.9	2225.9	
Chrysene	1383.2	1747.5	
c1-Benzo[a]anthracene/chrysene	10382.7	17326.0	
c2-Benzo[a]anthracene/chrysene	84565.2	22132.2	
c3-Benzo[a]anthracene/chrysene	95603.7	23917.2	
c4-Benzo[a]anthracene/chrysene	36280.9	8134.9	
Total PAHs	2110420.214	539222.966	

References

AEMERA. (2016). Final 2015 Program Report April 2016 Alberta Environmental
Monitoring , Evaluation and Reporting Agency (AEMERA) JOINT OIL SANDS
MONITORING PLAN 2015 Final Program Report.

Ali Shah, F., Mahmood, Q., Maroof Shah, M., Pervez, A., & Ahmad Asad, S. (2014).
Microbial ecology of anaerobic digesters: The key players of anaerobiosis. The
Scientific World Journal, 2014. https://doi.org/10.1155/2014/183752

Berdygulova, Z., Westblade, L. F., Florens, L., Koonin, E. V., Chait, B. T., Ramanculov,
E., … Minakhin, L. (2011). Temporal regulation of gene expression of the thermus
thermophilus bacteriophage P23-45. Journal of Molecular Biology, 405(1), 125–142.
https://doi.org/10.1016/j.jmb.2010.10.049

Biddle, J. F., Cardman, Z., Mendlovitz, H., Albert, D. B., Lloyd, K. G., Boetius, A., &
Teske, A. (2012). Anaerobic oxidation of methane at different temperature regimes in
Guaymas Basin hydrothermal sediments. The ISME Journal, 6(5), 1018–1031.
https://doi.org/10.1038/ismej.2011.164

Blees, J., Niemann, H., Wenk, C. B., Zopfi, J., Schubert, C. J., Kirf, M. K., … Lehmann,
M. F. (2014). Micro-aerobic bacterial methane oxidation in the chemocline and
anoxic water column of deep south-Alpine Lake Lugano (Switzerland). Limnology
and Oceanography, 59(2), 311–324. https://doi.org/10.4319/lo.2014.59.2.0311

Bose, A., Rogers, D. R., Adams, M. M., Joye, S. B., & Girguis, P. R. (2013).
Geomicrobiological linkages between short-chain alkane consumption and sulfate

reduction rates in seep sediments. Frontiers in Microbiology, 4(DEC), 1–13. https://doi.org/10.3389/fmicb.2013.00386

Boudens, R., Reid, T., VanMensel, D., Sabari Prakasan, M. R., Ciborowski, J. J. H., & Weisener, C. G. (2016). Bio-physicochemical effects of gamma irradiation treatment for naphthenic acids in oil sands fluid fine tailings. Science of the Total Environment, 539, 114–124. https://doi.org/10.1016/j.scitotenv.2015.08.125

Boufadel, M. C., & Michel, J. (2008). Pilot studies of bioremediation of the Exxon Valdez oil in Prince William Sound Beaches. MPB, 113(1–2), 156–164. https://doi.org/10.1016/j.marpolbul.2016.08.086

Bowman, J. (2006). The Methanotrophs — The Families Methylococcaceae and Methylocystaceae. The Prokaryotes, 5, 266–289. https://doi.org/10.1007/0-387-30745-1

Bragg, J. R., Prince, R. C., Harner, E. J., & Atlas, R. M. (1994). Effectiveness of bioremediation for the Exxon Valdez oil spill. Nature, 368, 413–418.

Chistoserdova, L., Vorholt, J. A., & Lidstrom, M. E. (2005). A genomic view of methane oxidation by aerobic bacteria and anaerobic archaea. Genome Biology, 6(2), 1–6.

Colston, S. M., Fullmer, M. S., Beka, L., Lamy, B., Peter Gogarten, J., & Graf, J. (2014). Bioinformatic genome comparisons for taxonomic and phylogenetic assignments using aeromonas as a test case. MBio, 5(6), 1–13. https://doi.org/10.1128/mBio.02136-14

Dabestani, R., & Lvanov, Ilia N. (1999). A Compilation of Physical, Spectroscopic and Photophysical Properties of Polycyclic Aromatic Hydrocarbons. Photochemistry and Photobiology, 70(1), 10–34. https://doi.org/10.1562/0031-8655(1999)070<0010:IRACOP>2.3.CO;2

Dhillon, A., Teske, A., Dillon, J., Stahl, D. a, & Sogin, M. L. (2003). Molecular Characterization of Sulfate-Reducing Bacteria in the Guaymas Basin Molecular Characterization of Sulfate-Reducing Bacteria in the Guaymas Basin †. Applied and Environmental Microbiology, 69(5), 2765. https://doi.org/10.1128/AEM.69.5.2765

Dou, J., Liu, X., Hu, Z., & Deng, D. (2008). Anaerobic BTEX biodegradation linked to nitrate and sulfate reduction. Journal of Hazardous Materials, 151(2–3), 720–729. https://doi.org/10.1016/j.jhazmat.2007.06.043

Ghazali, F. M., Rahman, R. N. Z. A., Salleh, A. B., & Basri, M. (2004). Biodegradation of hydrocarbons in soil by microbial consortium. International Biodeterioration and Biodegradation, 54(1), 61–67. https://doi.org/10.1016/j.ibiod.2004.02.002

Hallam, S. J., Putnam, N., & F, C. M. P. (2004). Reverse Methanogenesis: Testing the Hypothesis with Environmental Genomics. Science (New York, NY), 305(September), 7. https://doi.org/10.1126/science.1100025

Hanage, W. P., Fraser, C., & Spratt, B. G. (2006). Sequences , sequence clusters and bacterial species, (October), 1917–1927. https://doi.org/10.1098/rstb.2006.1917

Haritash, A. K., & Kaushik, C. P. (2009). Biodegradation aspects of Polycyclic Aromatic

    Hydrocarbons (PAHs): A review. Journal of Hazardous Materials, 169(1–3), 1–15.

    https://doi.org/10.1016/j.jhazmat.2009.03.137

He, Z., Geng, S., Shen, L., Lou, L., Zheng, P., Xu, X., & Hu, B. (2015). The short- and

    long-term effects of environmental conditions on anaerobic methane oxidation

    coupled to nitrite reduction. Water Research, 68, 554–562.

    https://doi.org/10.1016/j.watres.2014.09.055

Hug, L. A., Baker, B. J., Anantharaman, K., Brown, C. T., Probst, A. J., Castelle, C. J., …

    Banfield, J. F. (2016). A new view of the tree of life. Nature Microbiology, 1(5),

    16048. https://doi.org/10.1038/nmicrobiol.2016.48

Jaekel, U., Zedelius, J., Wilkes, H., & Musat, F. (2015). Anaerobic degradation of

    cyclohexane by sulfate-reducing bacteria from hydrocarbon-contaminated marine

    sediments. Frontiers in Microbiology, 6(FEB), 1–11.

    https://doi.org/10.3389/fmicb.2015.00116

Jiménez, J. I., Miñambres, B., García, J. L., & Díaz, E. (2002). Genomic analysis of the

    aromatic catabolic pathways from Pseudomonas putida KT2440. Environmental

    Microbiology, 4(12), 824–841. https://doi.org/10.1046/j.1462-2920.2002.00370.x

Ju, K.-S., & Parales, R. E. (2010). Nitroaromatic compounds, from synthesis to

    biodegradation. Microbiology and Molecular Biology Reviews : MMBR, 74(2), 250–

    272. https://doi.org/10.1128/MMBR.00006-10

Kappell, A. D., Wei, Y., Newton, R. J., van Nostrand, J. D., Zhou, J., McLellan, S. L., & Hristova, K. R. (2014). The polycyclic aromatic hydrocarbon degradation potential of Gulf of Mexico native coastal microbial communities after the Deepwater Horizon oil spill. Frontiers in Microbiology, 5(MAY), 1–13. https://doi.org/10.3389/fmicb.2014.00205

Kimes, N. E., Callaghan, A. V., Suflita, J. M., & Morris, P. J. (2014). Microbial transformation of the Deepwater Horizon oil spillâ€"past, present, and future perspectives. Frontiers in Microbiology, 5(NOV), 1–11. https://doi.org/10.3389/fmicb.2014.00603

Kits, K. D., Klotz, M. G., & Stein, L. Y. (2015). Methane oxidation coupled to nitrate reduction under hypoxia by the Gammaproteobacterium Methylomonas denitrificans, sp. nov. type strain FJG1. Environmental Microbiology, 17(9), 3219–3232. https://doi.org/10.1111/1462-2920.12772

Kleikemper, J., Schroth, M. H., Sigler, W. V., Schmucki, M., Bernasconi, S. M., & Zeyer, J. (2002). Activity and diversity of sulfate-reducing bacteria in a petroleum hydrocarbon-contaminated aquifer. Applied and Environmental Microbiology, 68(4), 1516–1523. https://doi.org/10.1128/AEM.68.4.1516-1523.2002

Konstantinidis, K. T., & Tiedje, J. M. (2005). Genomic insights that advance the species definition for prokaryotes, 102(7), 2567–2572.

Lloyd, K. G., Lapham, L., & Teske, A. (2006). An anaerobic methane-oxidizing community of ANME-1b archaea in hypersaline gulf of Mexico sediments. Applied

and Environmental Microbiology, 72(11), 7218–7230.

https://doi.org/10.1128/AEM.00886-06

Long, P. E., Williams, K. H., Hubbard, S. S., & Ban, J. F. (2016). Microbial Metagenomics

Reveals Climate-Relevant Subsurface Biogeochemical Processes, 24(8), 600–610.

Lynch, M. D. J., & Neufeld, J. D. (2015). Ecology and exploration of the rare biosphere.

Nat Rev Micro, 13(4), 217–229. Retrieved from

http://dx.doi.org/10.1038/nrmicro3400

Mason, O. U., Hazen, T. C., Borglin, S., Chain, P. S. G., Dubinsky, E. A., Fortney, J. L., …

Jansson, J. K. (2012). Metagenome, metatranscriptome and single-cell sequencing

reveal microbial response to Deepwater Horizon oil spill. ISME Journal, 6(9), 1715–

1727. https://doi.org/10.1038/ismej.2012.59

Mattes, T. E., Nunn, B. L., Marshall, K. T., Proskurowski, G., Kelley, D. S., Kawka, O. E.,

… Morris, R. M. (2013). Sulfur oxidizers dominate carbon fixation at a

biogeochemical hot spot in the dark ocean. The ISME Journal, 7(10), 2349–2360.

https://doi.org/10.1038/ismej.2013.113

Meyer, F., Paarmann, D., D'Souza, M., Olson, R., Glass, E., Kubal, M., … Edwards, R.

(2008). The metagenomics RAST server – a public resource for the automatic

phylogenetic and functional analysis of metagenomes. BMC Bioinformatics, 9(1),

386. https://doi.org/10.1186/1471-2105-9-386

Milucka, J., Kirf, M., Lu, L., Krupke, A., Lam, P., Littmann, S., … Schubert, C. J. (2015). Methane oxidation coupled to oxygenic photosynthesis in anoxic waters. The ISME Journal, 9(9), 1991–2002. https://doi.org/10.1038/ismej.2015.12

Nercessian, O., Bienvenu, N., Moreira, D., Prieur, D., & Jeanthon, C. (2005). Diversity of functional genes of methanogens, methanotrophs and sulfate reducers in deep-sea hydrothermal environments. Environmental Microbiology, 7(1), 118–132. https://doi.org/10.1111/j.1462-2920.2004.00672.x

Nie, Y., Chi, C.-Q., Fang, H., Liang, J.-L., Lu, S.-L., Lai, G.-L., … Wu, X.-L. (2014). Diverse alkane hydroxylase genes in microorganisms and environments. Scientific Reports, 4, 4968. https://doi.org/10.1038/srep04968

Nieto, P. a, Covarrubias, P. C., Jedlicki, E., Holmes, D. S., & Quatrini, R. (2009). Selection and evaluation of reference genes for improved interrogation of microbial transcriptomes: case study with the extremophile Acidithiobacillus ferrooxidans. BMC Molecular Biology, 10, 63. https://doi.org/10.1186/1471-2199-10-63

Nunoura, T., Oida, H., Toki, T., Ashi, J., Takai, K., & Horikoshi, K. (2006). Quantification of mcrA by quantitative fluorescent PCR in sediments from methane seep of the Nankai Trough. FEMS Microbiology Ecology, 57(1), 149–157. https://doi.org/10.1111/j.1574-6941.2006.00101.x

Pace, N. R. (1997). A molecular view of microbial diversity and the biosphere. Science (New York, N.Y.), 276(5313), 734–740. https://doi.org/10.1126/science.276.5313.734

Pritchard, P. H., Mueller, J. G., Rogers, J. C., Kremer, F. V., & Glaser, J. A. (1992). Oil

spill bioremediation: experiences, lessons and results from the Exxon Valdez oil spill

in Alaska. Biodegradation, 3(2–3), 315–335. https://doi.org/10.1007/BF00129091

Ravindra, K., Sokhi, R., & Van Grieken, R. (2008). Atmospheric polycyclic aromatic

hydrocarbons: Source attribution, emission factors and regulation. Atmospheric

Environment, 42(13), 2895–2921. https://doi.org/10.1016/j.atmosenv.2007.12.010

Reid, T., Boudens, R., Ciborowski, J. J. H., & Weisener, C. G. (2016). Physicochemical

gradients, diffusive flux, and sediment oxygen demand within oil sands tailings

materials from Alberta, Canada. Applied Geochemistry, 75, 90–99.

https://doi.org/10.1016/j.apgeochem.2016.10.004

Reid, T., Chaganti, S. R., Droppo, I. G., & Weisener, C. G. (2018). Novel insights into

freshwater hydrocarbon-rich sediments using metatranscriptomics: Opening the black

box. Water Research, 136, 1–11. https://doi.org/10.1016/j.watres.2018.02.039

Rivers, A. R., Burns, A. S., Chan, L.-K., & Moran, M. A. (2016). Experimental

Identification of Small Non-Coding RNAs in the Model Marine Bacterium Ruegeria

pomeroyi DSS-3. Frontiers in Microbiology, 7(March).

https://doi.org/10.3389/fmicb.2016.00380

Rosselli, R., Romoli, O., Vitulo, N., Vezzi, A., Campanaro, S., de Pascale, F., … Squartini,

A. (2016). Direct 16S rRNA-seq from bacterial communities: a PCR-independent

approach to simultaneously assess microbial diversity and functional activity

potential of each taxon. Scientific Reports, 6, 12.

Scott, N. M., Hess, M., Bouskill, N. J., Mason, O. U., Jansson, J. K., & Gilbert, J. A. (2014). The microbial nitrogen cycling potential is impacted by polyaromatic hydrocarbon pollution of marine sediments. Frontiers in Microbiology, 5(MAR), 1–8. https://doi.org/10.3389/fmicb.2014.00108

Smith, C. B., Tolar, B. B., Hollibaugh, J. T., & King, G. M. (2013). Alkane hydroxylase gene (alkB) phylotype composition and diversity in northern Gulf of Mexico bacterioplankton. Frontiers in Microbiology, 4(DEC), 1–8. https://doi.org/10.3389/fmicb.2013.00370

Syncrude, L. C. (1975). Baseline environmental studies of Ruth Lake and Poplar Creek. Edmonton, Alberta.

Thomsen, T. (2001). Biogeochemical and molecular signatures of anaerobic methane oxidation in a marine sediment. Applied and Environmental …, 67(4), 1646–1656. https://doi.org/10.1128/AEM.67.4.1646

Timmers, P. H. A., Welte, C. U., Koehorst, J. J., Plugge, C. M., Jetten, M. S. M., & Stams, A. J. M. (2017). Reverse Methanogenesis and Respiration in Methanotrophic Archaea. Archaea, 2017(Figure 1). https://doi.org/10.1155/2017/1654237

Valle, A., Le Borgne, S., Bolívar, J., Cabrera, G., & Cantero, D. (2012). Study of the role played by NfsA, NfsB nitroreductase and NemA flavin reductase from Escherichia coli in the conversion of ethyl 2-(2???- nitrophenoxy)acetate to 4-hydroxy-(2H)-1,4-benzoxazin-3(4H)-one (D-DIBOA), a benzohydroxamic acid with interesting bi. Applied Microbiology and Biotechnology, 94(1), 163–171. https://doi.org/10.1007/s00253-011-3787-0

Vanwonterghem, I., Evans, P. N., Parks, D. H., Jensen, P. D., Woodcroft, B. J. 5,

    Hugenholtz, P., & Tyson, G. W. (2016). Methylotrophic methanogenesis discovered

    in the novel archaeal phylum. Submitted for Publication in Nature, (October), 1–9.

    https://doi.org/10.1038/nmicrobiol.2016.170

Wang, F.-P., Zhang, Y., Chen, Y., He, Y., Qi, J., Hinrichs, K.-U., … Boon, N. (2014).

    Methanotrophic archaea possessing diverging methane-oxidizing and electron-

    transporting pathways. Isme J, 8(5), 1069–1078.

    https://doi.org/10.1038/ismej.2013.212

Wasmund, K., Burns, K. A., Kurtbo, D. I., & Bourne, D. G. (2009). Novel Alkane

    Hydroxylase Gene (alkB) Diversity in Sediments Associated with Hydrocarbon

    Seeps in the Timor Sea , Australia ▢, 75(23), 7391–7398.

    https://doi.org/10.1128/AEM.01370-09

Yergeau, E., Lawrence, J. R., Sanschagrin, S., Waiser, M. J., Darren, R., Korber, D. R., …

    Darren, R. (2012). Next-generation sequencing of microbial communities in the

    athabasca river and its tributaries in relation to oil sands mining activities. Applied

    and Environmental Microbiology, 78(21), 7626–7637.

    https://doi.org/10.1128/AEM.02036-12

Zhang, Z., Lo, I. M. C., & Yan, D. Y. S. (2015). An integrated bioremediation process for

    petroleum hydrocarbons removal and odor mitigation from contaminated marine

    sediment. Water Research, 83, 21–30. https://doi.org/10.1016/j.watres.2015.06.022

Zhu, J., Wang, Q., Yuan, M., Tan, G.-Y. A., Sun, F., Wang, C., … Lee, P.-H. (2016).

    Microbiology and potential applications of aerobic methane oxidation coupled to

denitrification (AME-D) process: A review. Water Research, 90, 203–215.

https://doi.org/10.1016/j.watres.2015.12.020

CHAPTER 3: **MICROBIAL METABOLIC STRATEGIES FOR OVERCOMING LOW-OXYGEN IN NATURALIZED FRESHWATER RESERVOIRS SURROUNDING THE ATHABASCA OIL SANDS: A PROXY FOR END-PIT LAKES?**

GRAPHICAL ABSTRACT
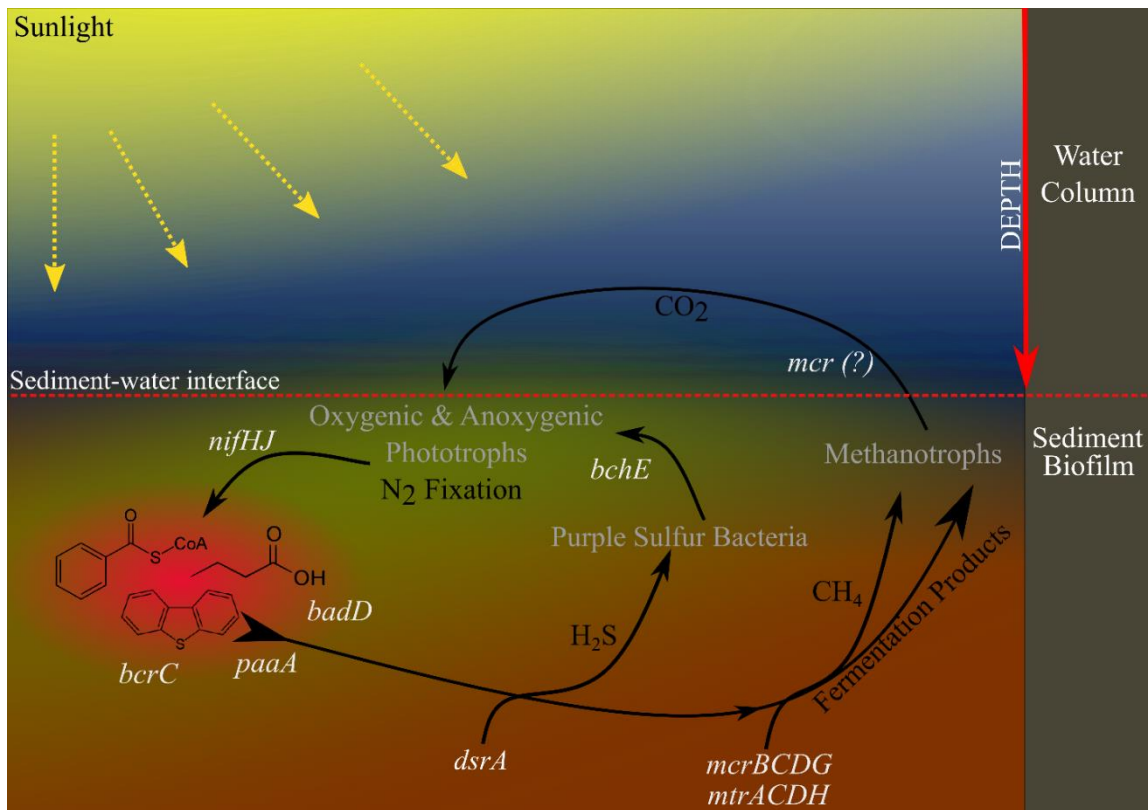
3.1 Introduction

Microorganisms are the most diverse group of organisms on the planet, therefore the need to understand both diversity and metabolic capabilities in a range of environments is vital in characterizing their roles for shaping their surroundings (Cowan et al. 2015; Foght and Fedorak 2015; Hua et al. 2015). Increasing our comprehension of microbial influences on ecosystem dynamics is crucial for not only understanding biodiversity itself, but is also extremely useful in the fields of bioengineering and bioremediation where these diverse microorganisms are considered workhorses in degrading, transforming or sequestering a range of contaminants (Callaghan 2013; DiLoreto et al. 2016; Jin et al. 2012; Scott et al. 2014; VanMensel et al. 2017). Advancements in microbial genomics has allowed researchers to piece together not only microbial energy metabolism, but also identify novel biodegradation pathways by which microbes take complex reactants to a more reduced, bioavailable product (An et al. 2013; Embree et al. 2014; Haritash and Kaushik 2009; Reid et al. 2018). Certain polycyclic aromatic hydrocarbons (PAHs), for example, have been degraded by microbes under both controlled laboratory and select *in-situ* research (Reid et al. 2018). Further, many marine-based studies to date have shown the ability of complex natural microbial populations to metabolize hydrocarbon compounds, though there remains little research characterizing these metabolic capabilities for inland, freshwater ecosystems (Kappell et al. 2014; Mason et al. 2012; Reid et al. 2018; Scott et al. 2014). Additionally, despite being theoretically preferred in oxygen-rich environments, research has revealed several unique and effective biodegradation pathways are utilized by microbes under sub-oxic (i.e. extremely low dissolved oxygen; sometimes coexisting with sulfides) conditions (Haritash and Kaushik 2009). Though many of these pathways have yet to be characterized, several studies have begun to shed light on how co-metabolic activity and syntrophy between

microbial groups is facilitating their ability to overcome thermodynamic hurdles in low-oxygen environments (Dolfing, Larter, and Head 2008; Morris et al. 2013; Pernthaler et al. 2008). Many of these degradation pathways culminate in the production of byproducts such as methane, which can have significant impacts on global greenhouse gas emissions.

In-situ, shotgun genomic approaches allow for whole population, unbiased characterizations, where targeted gene approaches and culturing studies can fall short in understanding the whole picture. These advancements are helping researchers understand how human impacts such as point-source and chronic pollution and even climate change are altering "natural" microbial diversity in various environments (Kimes et al. 2014; Reid et al. 2018; Weisener et al. 2017). Studies have revealed the plasticity of microbial function in response to contaminant presence, though there is generally a lack of studies simply characterizing microbial diversity and metabolic dynamics in naturally extreme environments (i.e. near hydrocarbon deposits; acidic springs; arctic tundra etc.) (Anantharaman et al. 2013; Brochier-Armanet and Moreira 2015; Comte, Fauteux, and Giorgio 2013). It is these studies that could prove vital in the future, when large scale bioremediation efforts seek to determine an appropriate baseline reference, or target end-point from which to gauge bioremediation success. This is perhaps of no greater relevance than in northern Alberta, Canada, where one of the world's largest bitumen (i.e. oil) reserves is actively being mined (Reid et al., 2016). In this unique geographic region, where bitumen naturally outcrops to the surface, there are also millions of liters of mining process-affected waters sitting in settling basins called tailings ponds. The large amount of bitumen extracted from the oil sands in the region creates large volumes of these process-affected materials (i.e. waste products), including water, sands, silts and clays, alongside a host of residual

hydrocarbons and other contaminants. Government mandates that oil companies must perform reclamation practices once mining has ceased, and therefore much research is focused on identifying possible detoxification and reclamation strategies (Boudens et al. 2016; CEMA 2012; Dhadli et al. 2012; Warren et al. 2016). End-Pit Lakes (EPLs) are one of the strategies being studied for the eventual remediation and reclamation of mines in the Athabasca Oil Sands region (CEMA 2012). Given such diversity in the contaminant footprint in the region, it is imperative to understand the cumulative effects of multiple stressors on the natural environment (Lima and Wrona 2019).

EPLs are large lake basins created in the remnants of open-pit mines, filled with a mixture of both processed mine waters and natural waters from the local rivers and tributaries (CEMA 2012). Mimicking any natural lake system, these EPLs will be subject to not only depth, light, and oxygen variation, but also a host external and internal environmental stimulus. Recently, research has revealed the collective impact freshwater basins such as lakes, reservoirs and wetlands, have on global biogeochemical cycles, therefore forecasting the fate of future EPLs should be a vital area of research moving forward (Battin et al. 2009; Cole et al. 2007; Rooney, Bayley, and Schindler 2012; Trimmer et al. 2015). Early research on the first EPL (Base Mine Lake) - in the Athabasca Oil Sands region, has revealed similarities and differences to tailings environments, specifically noting increased nitrification activity (Risacher et al. 2018). What remains poorly defined and understood is the long-term fate of these EPLs, considering that their inevitably rich hydrocarbon footprint will influence their development towards an otherwise "normal" lake ecosystem biogeochemical signature. Additionally, there is still a poor understanding of how oil sands mining contributes to the contaminant signature in the surrounding natural landscape

(Hodson 2013; Kelly et al. 2009; Reid et al. 2018; Rooney, Bayley, and Schindler 2012). Within this context natural or man-made "analogues" are required. In northern Alberta, there are two man-made reservoirs that serve this purpose. They were created to divert water around mining operations, which could act as perfect simulation or end-point for matured EPLs. These reservoirs are created amidst the overburden of the same geologic formation from which the bitumen is extracted, therefore contain a natural hydrocarbon signature, largely void of additional anthropogenic input. These reservoirs are the closest representation of what a future EPLs will behave like, though remain unstudied in this context. The structural and functional diversity of the microbes studied here provide not only unbiased insight into the future biogeochemical characteristics of EPLs, but in a broader context, furthers our understanding of boreal, freshwater, meso- to oligotrophic lakes.

In this paper we collected a series of sediment cores in different redox conditions in two freshwater lakes/reservoirs within the Oil Sands footprint of Northern Alberta, Canada. Alongside measurements of PAH concentrations and accompanying physicochemical measurements, metatranscriptomics analyses were performed on the bed sediments to determine the *in-situ* biodegradation and general metabolic capabilities of the indigenous microbes. Metataxonomics analysis was also performed to gain insight into which microbes were associated with the metabolic processes observed through the gene expression analyses. Results aim to answer questions of how the indigenous microbial population deals with multiple stressors and varying environmental redox conditions.

In the context of this dissertation, this chapter seeks to unravel the varied biogeochemical signature of deep freshwater reservoirs, acting as proxies to matured end-pit lakes in the future. This is the first time these deep reservoirs have been studied in this

context, providing much needed insight into how varied oxygen and redox conditions impact the holistic biogeochemical processes governing the bed sediments on the MF.

3.2 Methods

3.2.1 Study Systems and Location

Ruth Lake (RL) and Poplar Creek Reservoir (PCR) are located in northern Alberta, Canada, adjacent to the Athabasca Oil Sands industrial sites (Figure 1). Both water bodies are located on primarily organic lacustrine deposits, overlying glacial fluvial sediments, straddling the Clearwater and McMurray Formations (the Clearwater Formation overlies the McMurray Formation - the geologic formation constituting the minable bitumen of the Athabasca Oil Sands). These reservoirs were created in 1975, to divert water around industrial mining operations and are not directly influenced by any industrial process. Categorized as a moderately eutrophic, shallow, littoral lake, RL empties via a small stream channel into PCR (Syncrude 1975). PCR is a slightly deeper reservoir, with its northern section exhibiting similar characteristics to RL, though reaches 10-15 m depth at the south end of the reservoir. Sampling sites were chosen along a roughly north-to-south transect through the centers of each basin, to get thorough limnological characterizations of each. Sample locations where sediment cores were collected for PAH analysis and DNA/RNA analysis are shown in Figure 1, accessed via float-helicopter. A single set of RL cores were used as representative samples for the entire lake given its relatively homogenous limnological profile and logistical difficulties acquiring viable sediments given the abundance of wood debris littering the lake bed. $PCR_{Shallow}$ and PCR_{Deep} were used to characterize oxic (north) and sub-oxic (south) regions prominent within this reservoir.

3.2.2 In Situ Coring/Sediment Sampling

Using a gravity-assisted coring device, replicate sediment cores were collected at the aforementioned sample locations. Core tubes were 67 mm diameter, approximately 1000 mm in length. Samples for 16S rRNA amplicon targeted sequencing and RNAseq (metatranscriptomics) were scooped into individual, sterile 5 ml cryotubes from the top 1-2 cm of the cored sediment, and subsequently flash frozen in a liquid nitrogen filled dewar (Molecular Dimensions CX-100 Dry Shipper). Samples were preserved in the liquid nitrogen until returning to the lab at which point they were stored at -80 °C until extractions were performed. Preservation and storage at -80 °C is the preferred technique to maintain DNA/RNA yield and integrity, especially with respect to lake bed sediments high in organic and humic compounds (Rissanen et al. 2010). All DNA/RNA samples were collected in duplicate for accuracy. Additionally, bulk sediment samples were taken in amber jars for PAH analysis at Environment and Climate Change Canada. PAH concentrations were analyzed according to protocols explained in Reid et al., (2018). Physicochemical parameters were measured using the YSI Exo 2 Sonde to measure depth, dissolved oxygen, temperature, conductivity, pH and ORP at the top and bottom of the water columns at the North and South sites of each lake/reservoir.

3.2.3 Sediment DNA/RNA Extractions

Total DNA extractions were carried out in duplicate using the MoBio Powersoil Total DNA Isolation Kits (now Qiagen DNeasy Powersoil Kit). Sediments were extracted according to manufacturer protocols. To explore the V5/V6 region of 16S rRNA gene, extracted DNA was amplified and purified according to Reid et al. (Reid et al. 2016a). Briefly, dual polymerase chain reactions (PCR) were performed to initially amplify the

V5/V6 region, followed by a second barcoding PCR to uniquely identify samples for pooling and sequencing on the Ion Torrent PGM platform (Life Technologies, Carlsbad, California) at the Great Lakes Institute for Environmental Research at the University of Windsor (Windsor, Ontario, Canada). Quality and concentrations of pooled DNA libraries were analyzed on the Agilent 2100 Bioanalyzer prior to sequencing.

Total RNA extractions were performed using the MoBio Powersoil Total RNA Isolation Kits (MoBio Laboratories; Carlsbad, California) per slightly modified protocols. Initial sediment quantity for extraction was bumped to 5 g to increase overall RNA yield. All reagents and samples were kept on ice throughout extraction to maintain RNA integrity and minimize degradation throughout the extraction. Quality and concentrations were analyzed on the Agilent 2100 Bioanalyzer, where concentrations exceeded 100 ng/µL, and quality scores exceeded RIN # of 7.5. Samples of sufficient quality and concentration were sent in duplicate to Genome Quebec Innovation Center at McGill University in Montreal, Quebec, Canada. There, samples were again checked to ensure they met quality control standards, and rRNA-depletion (Illumina Ribo-Zero rRNA Removal Kit, bacterial and yeast) was performed to enhance the mRNA concentration. Samples were then sequenced on the Illumina HiSeq 4000 Nextgen sequencer.

3.2.4 16S Community Structure Analysis

Microbial taxonomy was determined for augmentation of the metatranscriptomics dataset, providing information as to *which* microbes were likely associated with observed gene expression. Raw sequences were processed through the MacQiime (v.1.9.1) pipeline (www.qiime.org), an open-source bioinformatics pipeline for 16S sequences (Caporaso et al. 2010). Sequence files were filtered and sequences with a Phred score below 20 were omitted.

Sequences were then clustered into operational taxonomic units (OTUs), omitting singletons and doubletons, at a similarity threshold of 97% using the uclust algorithm. Chimeras were removed using the usearch61 algorithm with MacQiime. Taxonomy was assigned to representative OTU sequences for each cluster, using the default GreenGenes database, at a 90% confidence threshold. Relative abundances (% of reads per sample) were calculated in order to gain an understanding of the dominant taxa and those proportionally different between sample sites.

3.2.5 Metatranscriptomics Data Processing and Differential Expression Analysis

Raw paired-end RNAseq files were downloaded from the Genome Quebec server to be processed utilizing the Metatrans Pipeline (Martinez et al. 2016) for 16s rRNA taxonomic and functional gene expression analyses. Briefly, filtering, sorting and both functional and taxonomic annotations are performed within Metatrans, running under Linux (Ubuntu 14.04 LTS). Filtering of raw reads was performed using the FastQC (v0.10.1) tool, where Kraken (v13.274) then processed those acceptable reads from the FastQC report. SortMeRNA (v1.9) is then used to isolate potential mRNA reads from rRNA/tRNA reads, utilizing the Silva (v115) database. Taxonomic annotations were annotated to residual rRNA reads utilizing USEARCH (v5.2.236) and the GreenGenes (v13.5) database. Functional annotations are then generated following merging of paired-end reads using Fastq-join (v1.1.2). FragGeneScan (v1.17) then performed an additional QC step, removing undesired sequences (ie. non-coding regions), configured to work with short reads associated with the Illumina sequencing platform. To reduce computational time, CD-HIT (v4.6) was used to cluster similar predicted genes with a similarity threshold of $>= 95$ %. Functional annotations were then assigned using the M5nr database (provided by the MG-RAST server). EggNOG (v4)

clusters of orthologous groups (COGs) were assigned to these gene clusters. The DESeq2 package was used to normalize reads between samples, alongside performing differential expression analyses. Briefly, DESeq2 utilizes negative-binomial generalized linear models to estimate the logarithmic fold changes and dispersal of sequence expression from the mean between two datasets. Significantly different expression is reported when $p<0.05$ (Love, Huber, and Anders 2014).

3.3 Results and Discussion

3.3.1 Geochemistry

The PAH signature observed at all sites is indicative of the heavy oil/bitumen deposit of the McMurray Formation (Table 1). PAH distributions were plotted to determine origin, and general trends with respect to substituted and unsubstituted compounds within each PAH family (Figure 2). The approximate normal distribution of benz[a]anthracene/chrysene and naphthalene families of PAHs is indicative of petrogenic origin (oil products). Compared to the other PAH compounds measured, benzopyrene and benzo(a)pyrene/perylene were especially low in concentration across all sites (<0.05 µg/g for all sites). Compared to all other sites, there was a strong depletion of certain PAHs in PCR_{Deep}, particularly in the phenanthrene/anthracene and fluoranthene/pyrene families of compounds. On the other hand, RL measured consistently higher concentrations overall compared to PCR, with C3-dibenzothiophene and C2-naphthalene particularly high in RL (2.18 µg/g and 1.55 µg/g respectively). Additionally, $PCR_{Shallow}$ and Mid exhibited relatively high concentrations of C5-fluoranthene/pyrene (1.40 µg/g) and C3-phenanthrene/anthracene (2.11 µg/g). Selective depletion of certain substituted PAHs is likely indicative of both weathering and microbial degradation. An interesting observation is the depletion of sulfur containing

66

dibenzothiophene and phenanthrene in PCR$_{Deep}$, where it would appear as though microbial sulfate reduction may be promoting the degradation of these families of PAHs (see Figure 2). Increased sorption of specific compound structures to soil and sediment particles may the limiting factor in the accessibility of the higher concentration PAHs to microbial degradation.

Metals analysis indicates a considerably higher concentration overall in RL compared to any site in PCR (Table 1). Total recoverable iron averaged 390 µg/L in RL, compared to 194.5 µg/L in PCR, while total recoverable aluminum was unexpectedly high in RL at 51.6 µg/L and only 16-17 µg/L at both PCR sites. Additionally, RL contains a higher dissolved organic carbon (DOC) signature compared to both PCR sites, though this is reversed with respect to dissolved inorganic carbon (DIC) measurements. The higher inorganic content within PCR$_{Deep}$ specifically may indicate higher CO_2 content and/or carbonates within this zone of the reservoir. The higher organic carbon signature in RL is related to the substantial amount of decaying organic matter present and readily observed during sampling, attributed to the fact that the lake was formed over an existing forested area. Additionally, this may partially explain the higher iron and aluminum concentrations, both known to have an affinity to bind with organic carbon (Wagai et al. 2013). The nutrient content measured in both RL and PCR$_{Shallow}$ and PCR$_{Deep}$ are lower than oil sands tailings environments, likely given the absence of concentrated hydrocarbon compounds as a result of water recycling. However, this provides useful context from which to compare the evolution of EPLs under the context of limited nutrients.

Given the noted depth of PCR$_{Deep}$, a water column profile was measured to observe oxygen and temperature fluctuation with depth (Appendix B, Figure S1). Dissolved oxygen (DO) profiles indicate the presence of a thermocline at approximately 5-7 m depth. Though

saturated oxygen conditions exist in the upper 4 m of the water column, concentrations at and slightly above the sediment are reduced to below approximately 0.5 mg/L. Further, where the other sampling locations measured consistent water column temperatures down to the sediment-water interface (Table 2), PCR_{Deep} saw a strong reduction through the water column. Surface temperature were between 15 and 16 $^{\circ}$C, but quickly declined, with temperatures between 7 and 8 $^{\circ}$C at the sediment-water interface. The depth and noted thermocline of PCR_{Deep} provide perhaps the most realistic representation of an EPL, where DO depletion is a likely attribute nearing the sediment-water interface. The shallow nature of both RL and $PCR_{Shallow}$ are unlikely to represent EPLs, therefore may serve as less of a surrogate for a matured EPL compared to PCR_{Deep}.

3.3.2 Metatranscriptomics & Metataxonomics

Metatranscriptomics and metataxonomic data consisted of 3 sets of duplicate samples from the 2 reservoirs as outlined earlier. In total, the RNAseq dataset consisted of a total of 166.4 million reads, averaging 27.7 million per sample. The average Phred quality score for each sample was 39. Metataxonomic data consisted of a total of 332,887 sequences with an average of 36,987 sequences per sample after filtering. Metatranscriptomics sequence data was also deposited in GenBank (Sequence Read Archive) and is available under the BioProject (PRJNA517747). 16S rRNA sequence data was deposited in GenBank (Sequence Read Archive) and is available under the BioProject (PRJNA517751).

3.3.2.1 Catabolic Diversity & PAH Biodegradation

Exploration of the metatranscriptomics dataset indicates a functional diversity likely governed by this oxygen availability. Though the shallower, oxygen-rich locations exhibited similar expression, the limited oxygen influx to the sediment in PCR_{Deep} appeared to

drastically change its functional attributes. Differential expression (DE) analysis confirmed this hypothesis, revealing an 11.11 % significant difference between overall expression between PCR_{Deep} and RL, the most variation observed between all sites. Additionally, it should be noted that many of those genes differentially expressed between PCR_{Deep} and RL also correspond to comparisons between PCR_{Deep} and $PCR_{Shallow}$. In correlation to the measured depletion of DO at PCR_{Deep}, alongside the noted differential expression results, RL was used as a representative baseline for an "oxygen-rich" reservoir, from which PCR_{Deep} could then be analyzed to observe variation in expression based on a "sub-oxic" signature. Additionally, as noted previously, PCR_{Deep} may serve as the most appropriate surrogate for a matured EPL given its geochemical and limnological characteristics. Apparent in the differential expression data (Figure 3 and Figure S2) were several specific microbial mechanisms implemented in response to the unique conditions of PCR_{Deep} – carbohydrate transport/metabolism, transcription, cell motility and cofactor/coenzyme expression. Increased expression of carbohydrate transport and metabolism is likely evidence towards the notion of increased biodegradation at PCR_{Deep}, where hydrocarbons have been broken down to simpler carbohydrate structures. Additionally, these carbohydrates are likely partially attributed to the energy stores resulting from the phototrophic activity discussed below. Further the observed increase in transcription expression at PCR_{Deep} is also indicative of the diversity of metabolic mechanisms observed in this study, providing the necessary proteins for efficient cellular metabolism. Most interesting perhaps is the high chemotaxis expression, indicating an active microbial response to gradients in environmental stimuli, driven by cellular motility. In fact, some of the most highly DE transcripts observed here is a methyl-accepting chemotaxis protein (MCP), in addition to other significantly higher

expressed chemotaxis proteins (*cheABCDXY*) ($p < 0.05$). These chemotaxis or motility mechanisms allow microbes to syntrophically inhabit zones of high nutrient density, playing a role biofilm formation and degradation of xenobiotics (Lux and Shi 2004; Stocker and Seymour 2012). Interestingly, several lab-based studies have correlated increased chemotaxis expression with aromatic compound utilization (Ortega-Calvo et al. 2003), alongside observed high chemotaxis as a result of the Deep-Water Horizon oil spill in the Gulf of Mexico (Luu et al. 2015; Mason et al. 2012). Chemotaxis, mechanistically driven by chemical cues, can therefore also control the flux of key elements such as hydrogen, oxygen, nitrogen and sulfur within the environment, relating to the expression observed here (Figure 4). These mechanisms support strong microbe-microbe interactions, in a mutualistic cooperation. Strong chemical gradients provide evidence towards the presence of micro-redox environments of enhanced biodegradation. This type of redox zonation was also observed in raw tailings studies, while observing their temporal evolution within tailings pond environments themselves (Boudens et al. 2016; Reid et al. 2016; VanMensel et al. 2017).

In addition to chemotaxis, a diverse coenzyme transport and functional metabolism was observed to be 2x and 2.6x times highly expressed under sub-oxic conditions of PCR_{Deep} compared to RL and $PCR_{Shallow}$ respectively. This is clearly advantageous under depleted oxygen conditions, where metabolism is limited due to available thermodynamic energy. It is likely that the observed highly expressed photosynthetic and methanogenic genes (*mcr*) are responsible for most of this increased coenzyme expression (see Section 2.2.3), alongside several coenzyme A (CoA) genes facilitating some alternate core pathways of hydrocarbon degradation. Benzoyl-CoA reductase (*bcrC/badD*), a classic aromatic degradation central

pathway (Fuchs, Boll, and Heider 2011; Harwood et al. 1999), is highly expressed across all sites, though most highly expressed in PCR$_{Deep}$ followed by RL then PCR$_{Shallow}$. Additionally, another significantly ($p<0.05$) overexpressed central pathway in PCR$_{Deep}$ compared to RL is *paaA* (phenylacetyl-CoA epoxidase) (Figure 5). This is especially interesting in that *paaA* bridges the gap between strictly aerobic and strictly anaerobic degradation pathways, in essence avoiding limitations of each. Grishin and Cygler (2015) reported that this pathway is able to proceed despite fluctuating oxygen conditions, which would otherwise act as a metabolic inhibitor (Grishin and Cygler 2015). *PaaA* uses both aerobic (oxygen) and anaerobic mechanisms (coenzyme A) to complete the epoxidase reaction, and has been reported to be present in at least 16% of bacterial species sequenced (Teufel et al. 2010). The use of CoA is intriguing as it may be a mechanism to keep degradation products within the cell of the organism, alongside making an otherwise small, inaccessible hydrophobic molecule more accessible to the microbe (Grishin and Cygler 2015). This CoA derivative of both the benzoyl and phenylacetyl pathways are readily accessed via facultative organisms, making this mechanism potentially more efficient than simple oxygenase reactions whereby only strict aerobes govern its success. Additionally, these metal cofactors could explain the metal concentrations discussed earlier. If the metals and organic carbon in RL are in fact bound, they become inaccessible to enzymatic microbial breakdown. Therefore, the observation of metal cofactor utilization in PCR$_{Deep}$ would correspond to more available iron at this site, allowing for these biodegradation mechanisms to proceed.

It is interesting to note that there's no *significantly* differentially expressed genes with known annotations directly to hydrocarbon degradation, aromatic or otherwise, aside from

the noted *paaA* expression. However, given the elevated expression of the central pathways of *bcrC/badD* and *paaA*, transcript abundances suggest hydrocarbon degradation is influential, and likely a significant central metabolic function at all sites sampled. This baseline expression is not surprising in this region of Northern Alberta, given the broad availability of these natural hydrocarbons as a nutrient source for these indigenous microbes. Upon construction of EPLs, these results suggest that given sufficient time for the indigenous microbial population to equilibrate, these reclamation environments may well see continued degradation of hydrocarbon compounds well into the future. Further, the apparent enhancement of the functional diversity with PCR$_{Deep}$ and no indication of biodegradation suppression despite reducing conditions, is favorable for future EPLs, where there will inevitably be both oxic and anoxic zones. Maintaining efficient primary productivity and biodegradation potential throughout the ecosystem is vital for long-term success of these reclaimed environments.

3.3.2.2 Phototrophic Metabolism

To gain an understanding of the overall energy metabolism governing the sites on RL and PCR, transcripts annotated to energy metabolism were compared to phylogenetic associations through 16S rRNA gene sequencing (see Figure 6). These taxonomic associations support and correlate to the gene expression data presented here. Initially apparent is the abundance of phototrophic organisms present across all sites, with the exception of Cyanobacterial reads only observed in PCR$_{Deep}$. This location, the deepest sampled (~12-13 m), contained both *Synechococcus* and *Dolichospermum*, both freshwater algal species. *Synechococcus* is an organism capable of thriving in cold, freshwater lakes and rivers, comprising a large majority of the biomass constituting phototrophic organisms as

observed in this study (Vincent 2009). *Synechococcus* is particularly adept at acquiring light in low-light environments where other species may suffer, and maintains a metabolic advantage in its high surface-area-to-volume ratio compared to some other species (Vincent 2009). These characteristics make this microbe especially suitable for an environment such as PCR_{Deep} (i.e. deep, mesotrophic lake). A relatively high abundance of other phototrophic organisms (Chlorobi, Chloroflexi, *Cyanobacteria* spp., green and purple sulfur bacteria) in both systems indicate that these organisms may have a crucial role in the biogeochemistry at the sediment-water interface. Several studies have indicated the importance of Cyanobacteria in biofilms, particularly where complex organics are present, actively succumbing to microbial degradation (Benthien et al. 2004; Chronopoulou et al. 2013). Differential gene expression analyses further support this finding of cooperative microbial metabolism was actively taking place, particularly in syntrophy with phototrophic activity. The abundance of Chloroflexi (phylum consisting of anoxic phototrophs, and halorespirers) in RL, but also highly abundant in $PCR_{Shallow}$ and PCR_{Deep} indicates a potential dependence on the organics produced by this phototrophic community yet may also provide evidence of degradation of chlorinated compounds. The sulfur bacteria, such as Caldiserica (40x more abundant in PCR_{Deep} vs $PCR_{Shallow}$) utilize these organics, alongside sulfides produced by anaerobic sulfur reducers (H_2S) for their metabolic requirements. Interestingly, this anoxygenic photosynthetic pathway utilizes an array of cofactors to produce ATP. This too correlates to the increase cofactor and coenzyme expression noted earlier (Figure 3).

This photosynthetic activity is evident within the gene expression data, with significant overexpression in PCR_{Deep}. A ferredoxin protochlorophyllide (*bciB*) is approx. 6x higher expressed in PCR_{Deep} compared to RL (log2(FC) = 2.5589; $p<0.05$) responsible for

the biosynthesis of chlorophyll in phototrophs, particularly green and purple sulfur bacteria (i.e. Chlorobiaceae, certain families within the Chloroflexi phylum etc.). Bacteriochlorophyll (*bch*), constituting anoxygenic photosynthesis is also highly expressed in all sites, but is particularly high in RL where it is approximately 2x higher (though oxic in the water column, the high organic content in RL would undoubtedly result in highly reduced sediment, hence the observation of this anoxygenic photosynthesis here). However, given high relative expression of *bch* in all sites, this is obviously a highly active process in both the sediments of RL and PCR. *BchE* (anaerobic magnesium-protoporphyrin IX monomethyl ester cyclase) is the most highly expressed of the bacteriochlorophylls and is responsible for far-red visible light absorption from 720 – 750 nm wavelengths. Absorption of far-red visible light is to be expected in these environments, since red light is able to penetrate to the depths studied in this study, whereas only blue light to extend to extremely deep depths such as the deep ocean. Interestingly, chlorophyll d (*chlD*) was the highest oxygenic photosynthetic transcript measured, with $PCR_{Shallow}$ containing 2x higher expression than PCR_{Deep}, and RL containing approximately 3x that of PCR_{Deep}. Both RL and $PCR_{Shallow}$ have more available oxygen at the sediment-water interface than PCR_{Deep}, thus this higher expression of oxygenic photosynthesis is not surprising. The combination of results from both 16S amplicon sequencing and metatranscriptomics are significant in that clearly phototrophic activity is extremely active in these reservoirs. Interestingly, a recent study on the only EPL (Base Mine Lake) measured enhanced primary productivity, indicating the importance of oxygen flux in these reclaimed ecosystems (Risacher et al. 2018). Transcript expression is indicating the presence of a heterotrophic, functionally diverse biofilm or mat, likely consisting of an oxygenic upper layer, followed by an anoxygenic phototrophic layer, followed by sub-oxic

or anoxic lower chemotrophic layers (Roeselers, Loosdrecht, and Muyzer 2008). Proximity within this biofilm or mat structure is likely inducing strong redox and physicochemical gradients, facilitating the high gene transcription, chemotaxis and nutrient flux observed in this study. Further, the presence of sulfur reducing bacteria producing sulfide gas (*dsrA* significantly higher expressed in $PCR_{Shallow}$ and PCR_{Deep} compared to RL; $p<0.05$) provides a possible mechanism by which photosynthesis proceeds in the low-light, low-oxygen environment of PCR_{Deep}. Both inhibitory and enhancing effects of H_2S on photosynthesis depending on conditions have been reported (Klatt et al. 2015). Briefly, a low light, sulfidic zone can promote an enhancement of oxygenic photosynthesis following dark conditions, which is likely what is being observed here (Klatt et al. 2015). These results suggest a complex interplay between available light and sulfide concentrations is governing the balance between oxygenic and anoxygenic photosynthesis, hence directly affecting subsequent biodegradation processes.

3.3.2.3 Chemotrophic Biodegradation

These observed phototrophic functions are likely contributing to the enhancement of hydrocarbon degradation through the supply of nutrients to chemotrophic organisms. Nitrogen-fixation, often associated with cyanobacterial mats, can be a key supplier of such nutrients to facilitate degradation processes. Transcripts associated with nitrogen fixation (*nifH*) alongside glutamine synthase, that which facilitates ammonia uptake, are highly expressed in PCR_{Deep} though not statistically different (2x higher than RL; 4x higher than $PCR_{Shallow}$). Interestingly, another nitrogenase gene, *nifJ*, is significantly higher expressed in PCR_{Deep} than RL (P=0.028), also responsible for the shuttling of electrons, particularly from iron-containing proteins. The presence of oxygen however can inhibit this function, therefore

increasing the plausibility of microredox zonation, allowing for the continuation of both oxygenic and anoxygenic processes to proceed in close proximity. If biofilm formation is actively occurring, it may be to control the flux of oxygen through chemotaxis mechanisms, allowing for these oxygen dependent reactions to proceed. Interestingly, a novel oxidoreductase gene *(ssuD)* was significantly overexpressed in PCR$_{Deep}$ as well. *SsuD* is a flavin-dependent oxidoreductase and is also suggested to be part of a luciferase family of genes constituting bioluminescence. Given that luminescence itself would not be advantageous in this environment, this gene has been suggested to act as a detoxification mechanism, possibly as an antioxidant in this environment (Eichhorn, Van Der Ploeg, and Leisinger 1999). However, given its high abundance in PCR$_{Deep}$, bioluminescent assays could provide as useful measure of biodegradation success but would require further controlled study to validate this notion. This antioxidant behavior could be reducing the toxicity of oxygen radical end-products as a result of the biodegradation processes. This too could explain how anaerobic processes are proceeding despite the presence of oxygen (though minimal). The relatively high abundance of *Synechococcus* affirms this notion, as it is known to both create biofilm mats, and fix nitrogen in both freshwater and marine environments (Bharti, Velmourougane, and Prasanna 2017). The enhancement in nitrogen fixation as a result of phototrophic activity is likely increasing the ability of associated heterotrophs (i.e. Deltaproteobacteria) to metabolize the hydrocarbons, alongside stimulating respiratory pathways such as nitrate and sulfate reduction. This may provide reasoning for the apparent lack of hydrocarbon reduction under aerobic conditions. The aerobic degradation processes would be reliant on nutrient availability, of which there is very little. Under anaerobic conditions however, the nitrogen-fixation observed may be providing the

necessary nutrients for such degradation to proceed. Additionally, studies have shown that methanogenic growth requires less nutrients than aerobic microbes, further corroborating these findings (Head, Gray, and Larter 2014).

Aside from the unexpected phototrophic activity at such depths, a highly abundant Deltaproteobacteria community was evident in the deeper PCR_{Deep} site. This is indicative of a highly diverse and extreme environment, supporting observations by Acosta-Gonzalez et al., 2013, who found dominant Deltaproteobacteria in deeper oil-polluted sediments following the Prestige Oil Spill off the coast of Spain (Acosta-González, Rosselló-Móra, and Marqués 2013). RL and $PCR_{Shallow}$ exhibited similar dominant taxa, though at much lower numbers. Differential gene expression analyses support these observations, indicating highly expressed nitrogen and sulfur reduction processes, alongside methanogenesis at PCR_{Deep} compared to RL. A general sulfite and nitrite reductase transcript revealed a $\log_2(FC)$ ($\log_2$ fold change) of 2.55. Dissimilatory sulfate reductase (*dsrA*) was significantly higher expressed in PCR_{Deep} with a $\log_2(FC)$ of 1.42. Methanogenic activity (*mcrBCDG* and *mtrACDH*) revealed consistently higher expression in PCR_{Deep} with $\log_2(FC)$ ranging from 1.18-2.68 ($p<0.05$). This complex REDOX interplay particularly between oxygen, ammonia and methane was also observed in Base Mine Lake, where researchers tracked the concentrations of ammonia and methane into the hypolimnion, clearly indicating their importance in these dynamic ecosystems (Risacher et al. 2018). It should also be noted that anaerobic methane oxidation (AMO) is likely active here, though remains a poorly understood process overall. It has been suggested that *mcr* genes can act in reverse, oxidizing methane instead of producing it. Given the complex syntrophy observed, and in correlation

with findings of similar studies, it would not be surprising to have a considerable amount of AMO ongoing (Reid et al. 2018).

3.3.2.4 Syntrophic Cooperation

The presence of *Syntrophus* in PCR$_{Deep}$ (18x more abundant than RL; 2x more abundant than PCR$_{Shallow}$) alongside genes indicative of cooperative metabolic activity, indicates fermentative processes are also likely ongoing in association with the methanogenic community. The methanogenic organisms are likely metabolizing the H$_2$, CO$_2$ and fermentation end-products such as fatty acids. The higher abundance of methanogenic transcripts, alongside a noted abundance of *Methanospirillum* in PCR$_{Deep}$ supports another study where the presence of this methanogenic genus was indicative of an environment reliant on syntrophy (Gunsalus et al. 2016). Particularly, *Methanospirillum* has been shown to work syntrophically with a variety of degraders, one of which is *Syntrophus* (Jackson et al. 1999; Mountfort et al. 1984). *Syntrophus* can also metabolize benzoate in isolated cultures (utilizing the Benzoyl-CoA reductase gene that is expressed most highly in PCR$_{Deep}$) but can do so in a more energetically favorable manner in syntrophy with hydrogen utilizing organisms such as SRBs and methanogens. This is particularly advantageous within the thermodynamically limiting conditions of PCR$_{Deep}$, where diversified metabolic efficiency can be maintained without suppression of core cellular functions. These results were observed in pure cultures and co-cultures in a lab setting, showing the thermodynamic advantage of benzoate reduction and fermentation compared to typical oxidation pathways (Elshahed and McInerney 2001). Interestingly, another microbial study observed *Syntrophus* in matured oil sands tailings material also within a laboratory study (VanMensel et al. 2017). Nonetheless, this suggests that the syntrophic metabolic capabilities of *Syntrophus* is a key

player in not only raw tailings environments but may also play a key role in reclaimed EPLs as well.

3.3.3 Implications for EPL Reclamation Success

The significance of the phototrophic/chemotrophic syntrophy observed, alongside the presence of Syntrophus in this environment should not be overlooked. Given its role in benzoate removal under anoxic conditions, this genus is clearly a vital ecosystem player, where hydrocarbon removal (largely derived of polycyclic aromatic compounds) is an extremely pertinent issue. Benzoyl-CoA reductase is a dominant central pathway for the degradation of a variety of aromatic and xenobiotic compounds, and its dominance across all sites studied here indicates that the native microbial consortia has likely evolved to thrive in this hydrocarbon impacted environment. The apparent initiation of these degradation processes by phototrophic activity despite the deeper water column depth within PCRDeep, is especially interesting. Studies examining sediment redox environments seem to ignore phototrophic activity or are otherwise unable to accurately reproduce in-situ conditions in a laboratory setting. However, given in-situ observations derived here, this photosynthetic syntrophy clearly has a significant impact on the biogeochemistry of these reservoirs and will likely play an important role in future EPLs. The cooperative metabolism observed here may also be dictating the selective nature of the observed PAH depletion. Further, the origin of the measured PAHs (petrogenic vs. pyrogenic) (Figure 2) alongside binding mechanisms with metals or other compounds may dictate bioavailability of compounds degraded through microbial activity.

The observations made here are promising with respect to EPL establishment moving forward, alongside oil spill reclamation in other freshwater environments. The apparent

79

plasticity of the functional pathways attributed to the photosynthesis observed, would likely be indicative of mature EPLs, once environmental equilibrium could be reached. Reclaimed environments would contain a host of indigenous microbes suited to life in hydrocarbon-rich substrates, likely allowing ongoing biodegradation of toxic hydrocarbons to persist long into the future. However, given the dominance of photosynthetic activity promoting the observed biodegradation processes, light penetration to the sediment and nutrient (i.e. nitrogen) availability appear to be limiting factors. Variables such as water column turbidity and depth would inherently shape the nature of phototrophic activity and should be taken into account before assuming the processes observed here will inherently dominate in future EPLs. However, photosynthesis can also occur outside of the visible light spectrum (i.e. infrared), thus these limitations may not be so easily defined without further study. Dissolved oxygen and sulfide gas concentrations appear to also dictate the nature of photosynthetic activity (oxygenic vs. anoxygenic), though these gases, alongside methane, appear to also be controlled by the complex syntrophy of metabolism at play. This would also control nutrient availability, perhaps dictating whether biodegradation could in fact persist or not. These observations may in fact differ from an immature EPL, where such an equilibrium may not yet exist, and the functional attributes may be more indicative of current tailings ponds pre-reclamation. These findings however support EPL reclamation as being an efficient and sustainable option well into the future, once these cyanobacterial and other phototrophic communities can establish. The identification of these photosynthetic pathways and the mere presence of this group of microbes also provides a unique direction from which to approach defining water quality objectives. Though not a new perspective in bioremediation studies, oil sands mine reclamation could use this cyanobacterial signature as a biomarker for

reclamation success and overall water quality. Studies of tailings ponds suggest a suppression or overall absence of these phototrophs, though results from this study and others suggest an emergence of this phylum during reclamation events. Examining ratios of certain phototrophs (i.e. Chlorobi, Chloroflexi etc.) to chemotrophs (i.e. Deltaproteobacteria) for example, could provide a quantitative index indicative of reclamation progress and success. This type of index could greatly improve our understanding of reclamation success, providing answers to the ongoing issue of determining water quality standards. This could also hold true for gene biomarkers, where identification of some of the photosynthetic processes observed here may be indicative of a successfully reclaimed environment.

3.4 Conclusions

The microbial function and biogeochemical signatures observed in this study provide the first unbiased glimpse into the microbial ecology and metabolic processes that one day may be attributed to large, reclaimed freshwater lakes in the region, in the footprint of the McMurray Formation. Representing analogues to future EPLs, these results give insight into how natural landscapes behave in this region and provide biogeochemical targets for current and future reclamation projects. These types of holistic studies are invaluable in determining the true geochemical and microbial signature governing such systems, without inadvertently introducing biases from lab-based experiments, or more targeted molecular approaches. Results observed here indicate a complex syntrophy of microbial metabolism at play, beginning with oxygenic and anoxygenic phototrophy, down to methanogenesis and subsequently methanotrophy. This evidence of syntrophic cooperation is perhaps an ideal marker from which to compare waste ponds as they progress towards a remediated state. Augmentation of the RNAseq dataset with stable isotope probing can further increase our

holistic understanding of the functional microbial characteristics in such unique environments. Aside from implications for EPL establishment and hydrocarbon degradation, this study provides fundamental insight into mechanisms of microbial metabolism in other natural and anthropogenically impacted freshwater ecosystems, limited by depth, temperature, DO and sunlight exposure. Future studies should continue to characterize the biogeochemical processes governing bed sediments and begin to understand how microbes affect suspended sediment loads, as they are eroded, transported and deposited under varying hydrodynamic conditions. The complexity of the syntrophic interactions observed here, significantly advances our understanding as to how these microbes maintain such metabolic efficiency at depth, under these oxygen-limited conditions so often associated with larger boreal lake ecosystems.

Author Contributions Statement
T.R, I.G.D, S.R.C. and C.G.W all contributed to the writing and editing of the manuscript. All figures were produced by T.R. All authors reviewed the manuscript.

Competing Interests
The authors declare no competing interests.

Figures and Tables
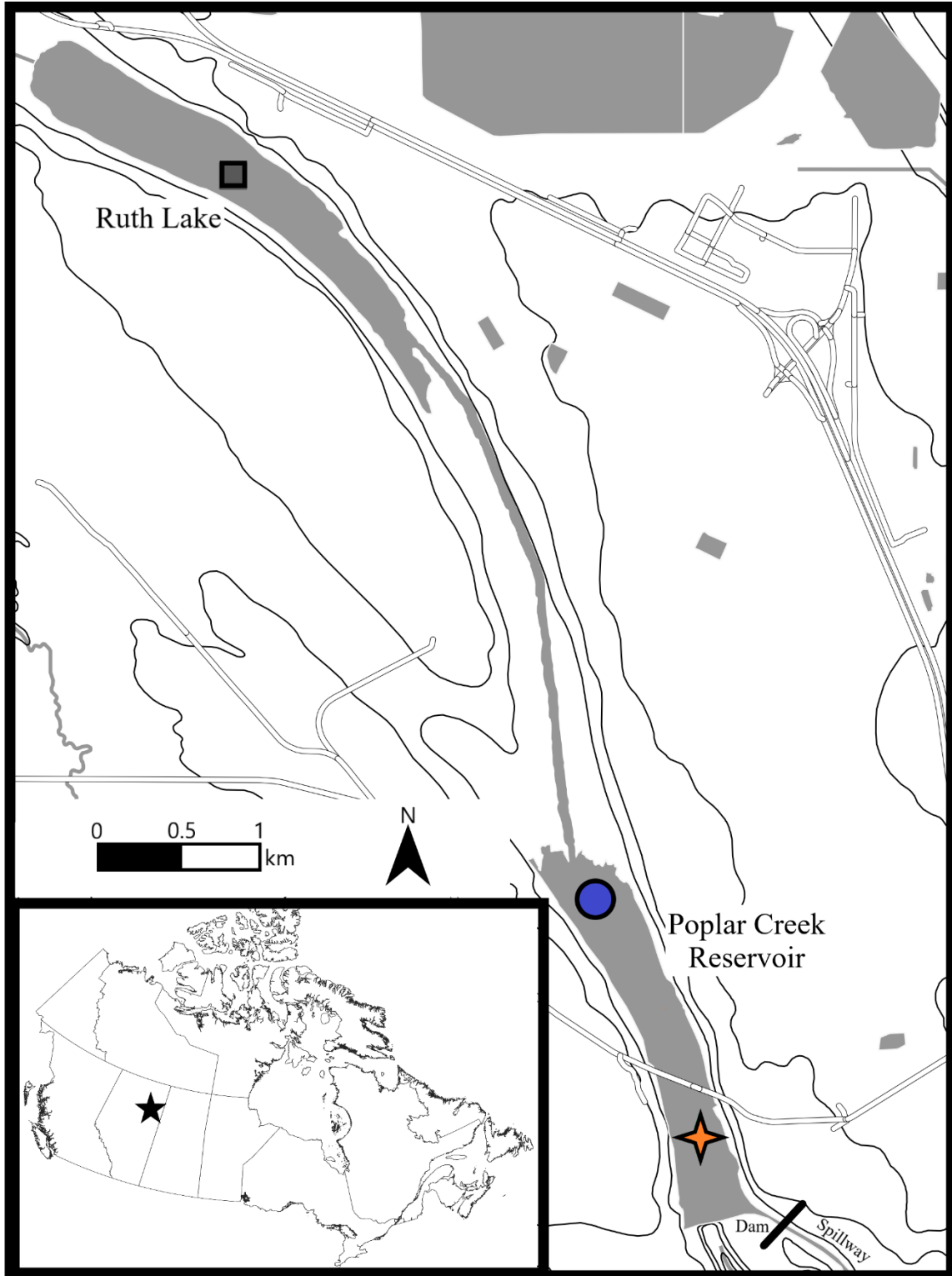
FIGURE 1 Map of Ruth Lake (North) and Poplar Creek Reservoir (South) located north of Fort McMurray, Alberta, Canada. Sampling locations marked as colored dots on each lake, including RL (grey square), and PCR$_{Shallow}$ (blue circle), and PCR$_{Deep}$ (orange star).
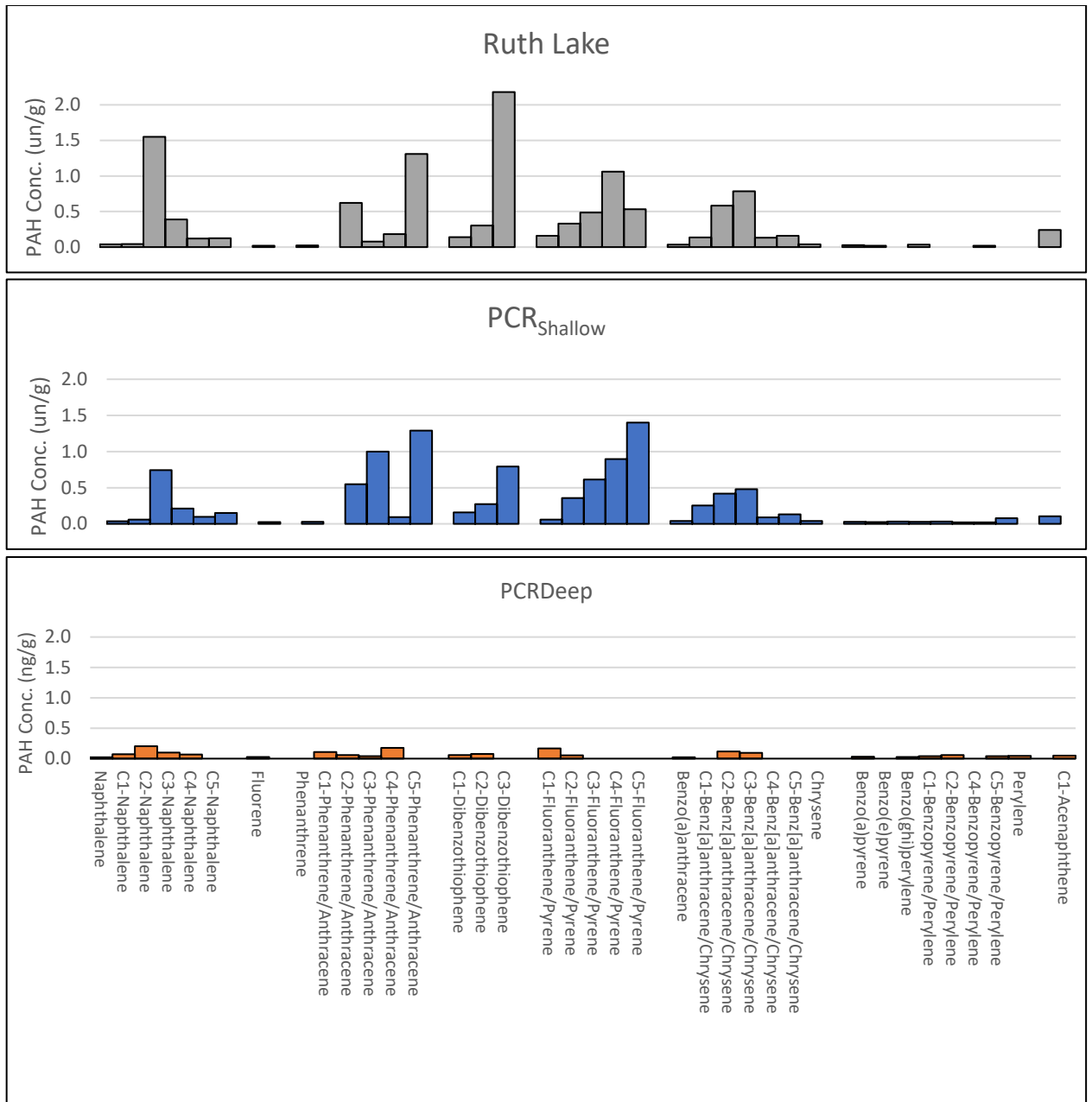
FIGURE 2 PAH distributions by family. Colors correspond to sample sites as detailed in Figure 1. Bell shaped distributions indicating petrogenic origin; depletion towards C4-C5 compounds indicating pyrogenic origin.

FIGURE 3 Doughnut plot comparing dominant expressed functional COG Categories between sampling sites. Values are normalized for comparison within DESeq2. Values represent normalized hits averaged from RNAseq replicate samples. Outer: PCR$_{Deep}$; Middle: PCR$_{Shallow}$; Inner: RL.
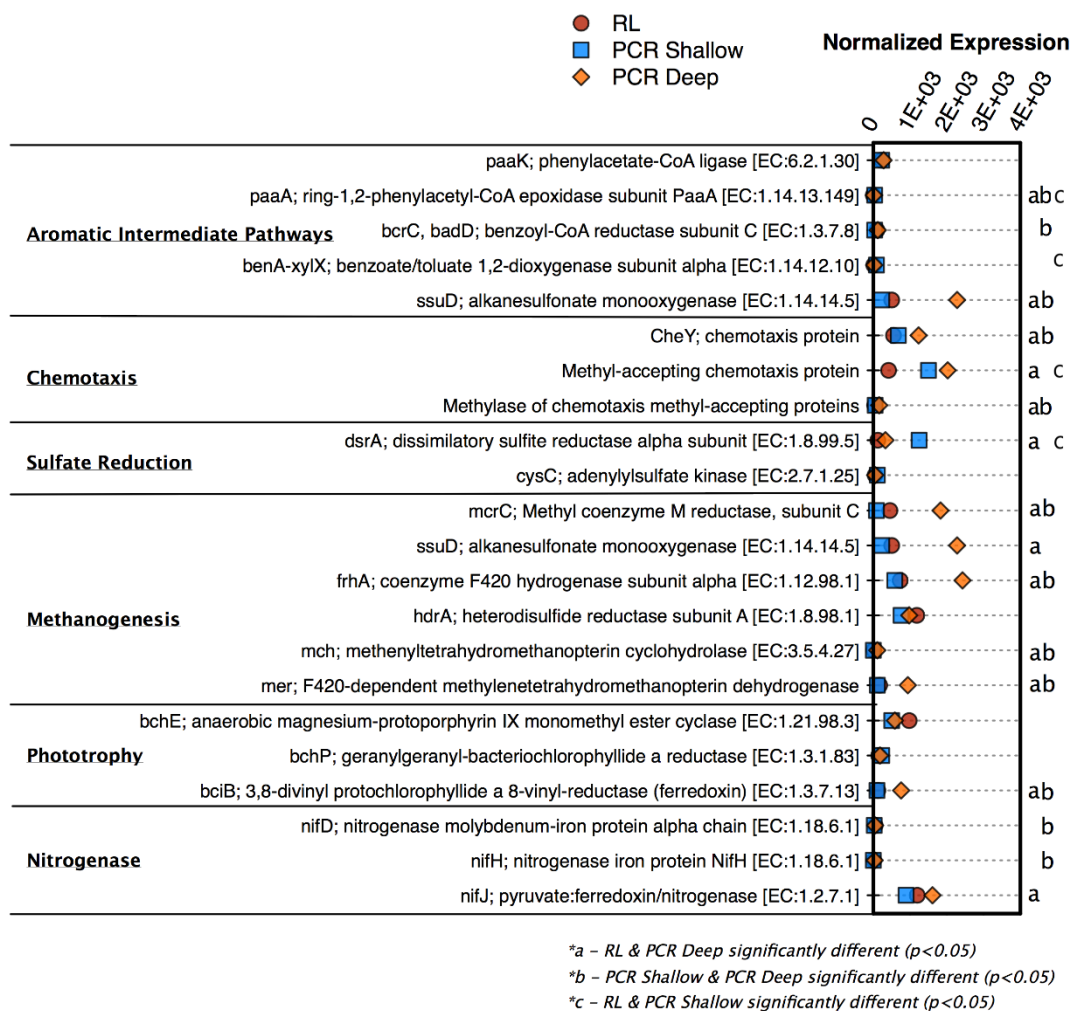
FIGURE 4 Selected normalized gene expression data outlining dominant processes revealed in the differential expression analysis, associated with aromatic degradation, chemotaxis, sulfate reduction, methanogenesis, phototrophic activity, nitrogenases. For complete list of differentially expressed genes see Appendix B.
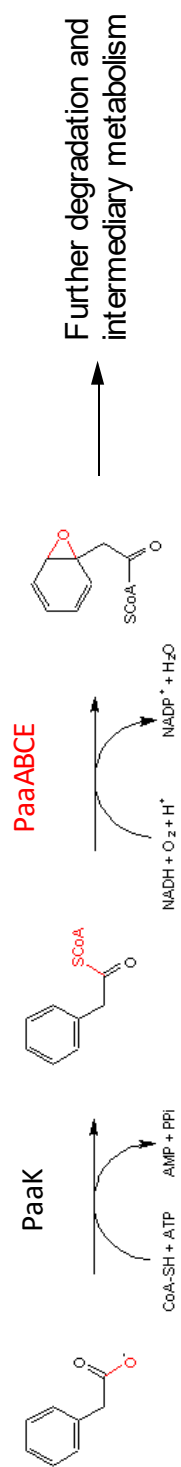
FIGURE 5 Phenylacetate degradation pathway with noted expression of *PaaABCE* and *PaaK* in the reservoirs

88
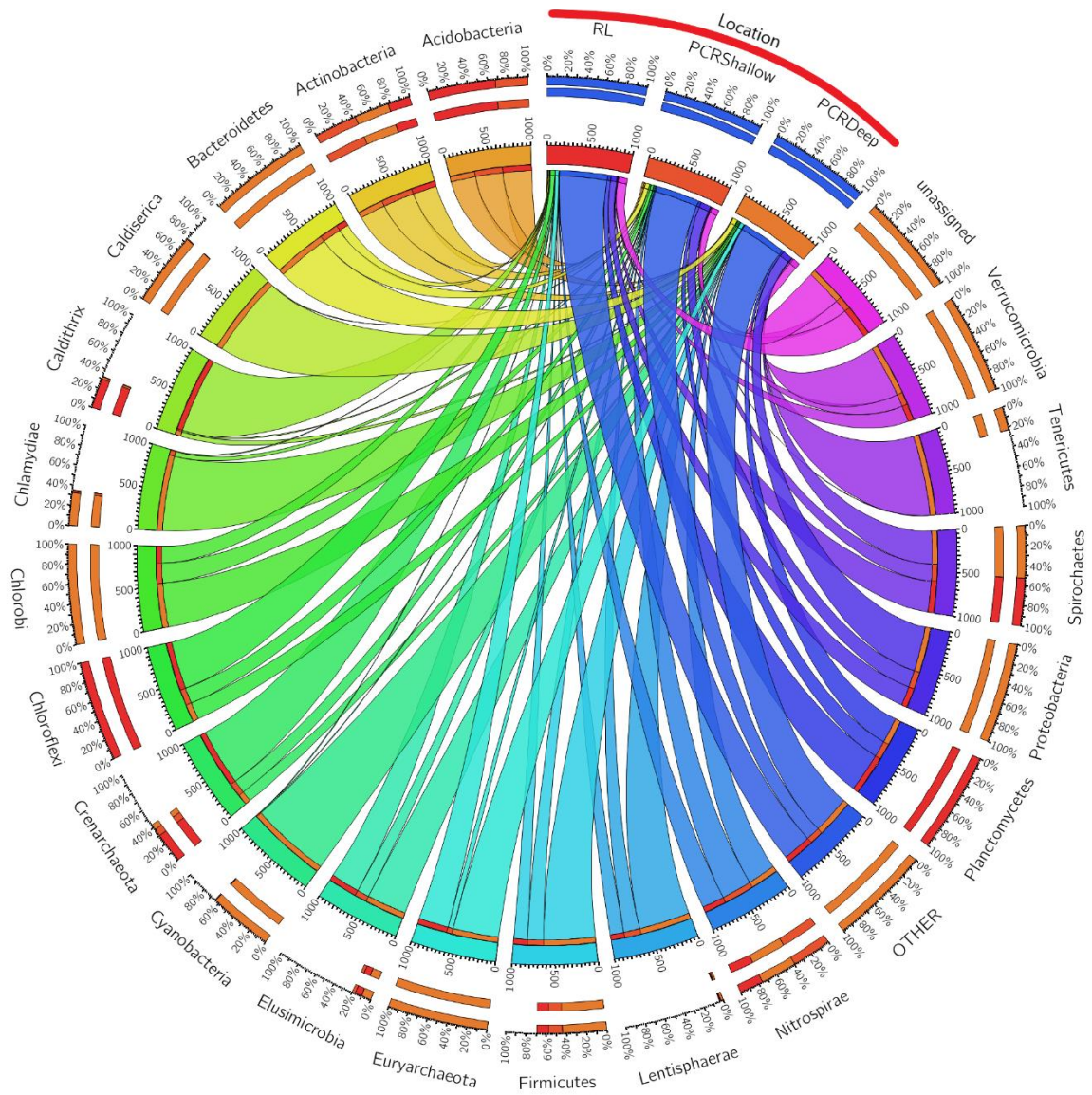
FIGURE 6 Normalized taxonomic read abundances of major phyla identified by 16S rRNA amplicon sequencing, plotted using Circos software (Krzywinski et al. 2009).

Table 1 Geochemical characteristics of both Poplar Creek Reservoir and Ruth Lake, showing average (n=2) Total Metals and Nutrient concentrations.

		Sample Site		
		RL	$PCR_{Shallow}$	PCR_{Deep}
Total Metals [µg/L]	Aluminum, Total Recoverable	51.6	16.7	17.3
	Boron, Total Recoverable	186.0	193.0	190.0
	Iron, Total Recoverable	503.0	202.0	194.5
	Barium, Total Recoverable	36.2	43.7	43.6
	Lithium, Total Recoverable	21.4	24.1	24.0
	Manganese, Total Recoverable	109.0	85.4	85.1
	Strontium, Total Recoverable	165.0	185.0	184.5
	Calcium, Total Recoverable	27600.0	34600.0	34500.0
	Magnesium, Total Recoverable	10900.0	12100.0	12050.0
	Potassium, Total Recoverable	2470.0	2080.0	2070.0
	Sodium, Total Recoverable	37600.0	42600.0	42950.0
Nutrients [mg/L]	Carbon, Dissolved Inorganic	34.6	41.3	44.0
	Carbon, Dissolved Organic	28.2	20.4	22.2
	Total Nitrogen	1.4	1.1	1.0
	Total Phosphorus	0.0	0.0	0.0

Table 2 Water column measurements of DO (dissolved oxygen), Temperature, Conductivity, pH and ORP (oxidation-reduction potential). Measurements were taken at the surface and just above the sediment-water interface

Location	Depth (m)	DO (mg/L)	Temp [ºC]	Cond. (uS/cm)	pH	ORP (mV)
RL	0.065	9.40	13.6	275	7.93	210
	0.961	6.51	13.8	422	7.23	144
PCR$_{Shallow}$	0.123	7.89	14.6	331	7.58	268
	2.136	6.79	14.4	331	7.60	272
PCR$_{Deep}$	0.25	7.98	15.1	335	7.76	220
	12.38	1.35	7.31	314	7.09	18.1

References

Acosta-González, A., Rosselló-Móra, R., & Marqués, S. (2013). Characterization of the anaerobic microbial community in oil-polluted subtidal sediments: aromatic biodegradation potential after the Prestige oil spill. Environmental Microbiology, 15(1), 77–92. https://doi.org/10.1111/j.1462-2920.2012.02782.x

An, D., Brown, D., Chatterjee, I., Dong, X., Ramos-Padron, E., Wilson, S., … Voordouw, G. (2013). Microbial community and potential functional gene diversity involved in anaerobic hydrocarbon degradation and methanogenesis in an oil sands tailings pond. Genome, 56(10), 612–618. https://doi.org/10.1139/gen-2013-0083

Anantharaman, K., Breier, J. A., Sheik, C. S., & Dick, G. J. (2013). Evidence for hydrogen oxidation and metabolic plasticity in widespread deep-sea sulfur-oxidizing bacteria. Proceedings of the National Academy of Sciences, 110(1), 330–335. https://doi.org/10.1073/pnas.1215340110

Battin, T. J., Luyssaert, S., Kaplan, L. A., Aufdenkampe, A. K., Richter, A., & Tranvik, L. J. (2009). The boundless carbon cycle. Nature Geoscience, 2(9), 598–600. https://doi.org/10.1038/ngeo618

Benthien, M., Wieland, A., de Oteyza, T. G., Grimalt, J. O., & Kühl, M. (2004). Oil-contamination effects on a hypersaline microbial mat community (Camargue, France) as studied with microsensors and geochemical analysis. Ophelia, 58(3), 135–150. https://doi.org/10.1080/00785236.2004.10410221

Bharti, A., Velmourougane, K., & Prasanna, R. (2017). Phototrophic biofilms: diversity, ecology and applications. Journal of Applied Phycology, 29(6), 2729–2744. https://doi.org/10.1007/s10811-017-1172-9

Boudens, R., Reid, T., VanMensel, D., Sabari Prakasan, M. R., Ciborowski, J. J. H., & Weisener, C. G. (2016). Bio-physicochemical effects of gamma irradiation treatment for naphthenic acids in oil sands fluid fine tailings. Science of the Total Environment, 539, 114–124. https://doi.org/10.1016/j.scitotenv.2015.08.125

Brochier-Armanet, C., & Moreira, D. (2015). Environmental Microbiology: Fundamentals and Applications. (J.-C. Bertrand, P. Caumette, P. Lebaron, R. Matheron, P. Normand, & T. Sime-Ngando, Eds.), Environmental Microbiology: Fundamentals and Applications. Dordrecht: Springer Netherlands. https://doi.org/10.1007/978-94-017-9118-2

Callaghan, A. V. (2013). Metabolomic investigations of anaerobic hydrocarbon-impacted environments. Current Opinion in Biotechnology, 24(3), 506–515. https://doi.org/10.1016/j.copbio.2012.08.012

Caporaso, J. G., Kuczynski, J., Stombaugh, J., Bittinger, K., Bushman, F. D., Costello, E. K., … Knight, R. (2010). QIIME allows analysis of high-throughput community sequencing data. Nature Methods, 7, 335. Retrieved from https://doi.org/10.1038/nmeth.f.303

CEMA. (2012). End Pit Lakes Guidance Document, 1–436.

Chronopoulou, P.-M., Fahy, A., Coulon, F., Païssé, S., Goñi-Urriza, M., Peperzak, L., … McGenity, T. J. (2013). Impact of a simulated oil spill on benthic phototrophs and nitrogen-fixing bacteria in mudflat mesocosms. Environmental Microbiology, 15(1), 242–252. https://doi.org/10.1111/j.1462-2920.2012.02864.x

Cole, J. J., Prairie, Y. T., Caraco, N. F., McDowell, W. H., Tranvik, L. J., Striegl, R. G., … Melack, J. (2007). Plumbing the Global Carbon Cycle: Integrating Inland Waters into the Terrestrial Carbon Budget. Ecosystems, 10(1), 172–185. https://doi.org/10.1007/s10021-006-9013-8

Comte, J., Fauteux, L., & Giorgio, P. A. (2013). Links between metabolic plasticity and functional redundancy in freshwater bacterioplankton communities. Frontiers in Microbiology, 4(MAY), 1–11. https://doi.org/10.3389/fmicb.2013.00112

Cowan, D., Ramond, J., Makhalanyane, T., & De Maayer, P. (2015). Metagenomics of extreme environments. Current Opinion in Microbiology, 25, 97–102. https://doi.org/10.1016/j.mib.2015.05.005

Dhadli, N., Fair, A., Hyndman, A., Langer, A., McEachern, P., Nadeau, S., … Sission, R. (2012). Technical Guide for Fluid Fine Tailings Management. Oil Sands Tailings Consortium.

DiLoreto, Z. A., Weber, P. A., Olds, W., Pope, J., Trumm, D., Chaganti, S. R., … Weisener, C. G. (2016). Novel cost effective full scale mussel shell bioreactors for metal removal and acid neutralization. Journal of Environmental Management, 183, 601–612. https://doi.org/10.1016/j.jenvman.2016.09.023

Dolfing, J., Larter, S. R., & Head, I. M. (2008). Thermodynamic constraints on methanogenic crude oil biodegradation. The ISME Journal, 2(4), 442–452. https://doi.org/10.1038/ismej.2007.111

Eichhorn, E., Van Der Ploeg, J. R., & Leisinger, T. (1999). Characterization of a two-component alkanesulfonate monooxygenase from Escherichia coli. Journal of Biological Chemistry, 274(38), 26639–26646. https://doi.org/10.1074/jbc.274.38.26639

Elshahed, M. S., & McInerney, M. J. (2001). Benzoate Fermentation by the Anaerobic Bacterium Syntrophus aciditrophicus in the Absence of Hydrogen-Using Microorganisms. Applied and Environmental Microbiology, 67(12), 5520–5525. https://doi.org/10.1128/AEM.67.12.5520-5525.2001

Embree, M., Nagarajan, H., Movahedi, N., Chitsaz, H., & Zengler, K. (2014). Single-cell genome and metatranscriptome sequencing reveal metabolic interactions of an alkane-degrading methanogenic community. The ISME Journal, 8(4), 757–767. https://doi.org/10.1038/ismej.2013.187

Foght, J. M., & Fedorak, P. (2015). Microbial metagenomics of oil sands tailings ponds: small bugs, big data. Genome, 58(November), 507–510. https://doi.org/10.1139/gen-2015-0146

Fuchs, G., Boll, M., & Heider, J. (2011). Microbial degradation of aromatic compounds — from one strategy to four. Nature Reviews Microbiology, 9(11), 803–816. https://doi.org/10.1038/nrmicro2652

Grishin, A., & Cygler, M. (2015). Structural Organization of Enzymes of the Phenylacetate
Catabolic Hybrid Pathway. Biology, 4(2), 424–442.
https://doi.org/10.3390/biology4020424

Gunsalus, R. P., Cook, L. E., Crable, B., Rohlin, L., McDonald, E., Mouttaki, H., …
McInerney, M. J. (2016). Complete genome sequence of Methanospirillum hungatei
type strain JF1. Standards in Genomic Sciences, 11(1), 2.
https://doi.org/10.1186/s40793-015-0124-8

Haritash, A. K., & Kaushik, C. P. (2009). Biodegradation aspects of Polycyclic Aromatic
Hydrocarbons (PAHs): A review. Journal of Hazardous Materials, 169(1–3), 1–15.
https://doi.org/10.1016/j.jhazmat.2009.03.137

Harwood, C., Burchhardt, G., Herrmann, H., & Fuchs, G. (1999). Anaerobic metabolism of
aromatic compounds via the benzoyl-CoA pathway. FEMS Microbiology Reviews, 22,
439–458. https://doi.org/10.1128/IAI.01312-09

Head, I. M., Gray, N. D., & Larter, S. R. (2014). Life in the slow lane; biogeochemistry of
biodegraded petroleum containing reservoirs and implications for energy recovery and
carbon management. Frontiers in Microbiology, 5(OCT), 1–23.
https://doi.org/10.3389/fmicb.2014.00566

Hodson, P. V. (2013). History of environmental contamination by oil sands extraction.
Proceedings of the National Academy of Sciences, 110(5), 1569–1570.
https://doi.org/10.1073/pnas.1221660110

Hua, Z. S., Han, Y. J., Chen, L. X., Liu, J., Hu, M., Li, S. J., … Shu, W. S. (2015). Ecological roles of dominant and rare prokaryotes in acid mine drainage revealed by metagenomics and metatranscriptomics. ISME Journal, 9(6), 1280–1294. https://doi.org/10.1038/ismej.2014.212

Jackson, B. E., Bhupathiraju, V. K., Tanner, R. S., Woese, C. R., & McInerney, M. J. (1999). Syntrophus aciditrophicus sp. nov., a new anaerobic bacterium that degrades fatty acids and benzoate in syntrophic association with hydrogen-using microorganisms. Archives of Microbiology, 171(2), 107–114. https://doi.org/10.1007/s002030050685

Jin, R.-C., Yang, G.-F., Yu, J.-J., & Zheng, P. (2012). The inhibition of the Anammox process: A review. Chemical Engineering Journal, 197, 67–79. https://doi.org/10.1016/j.cej.2012.05.014

Kappell, A. D., Wei, Y., Newton, R. J., van Nostrand, J. D., Zhou, J., McLellan, S. L., & Hristova, K. R. (2014). The polycyclic aromatic hydrocarbon degradation potential of Gulf of Mexico native coastal microbial communities after the Deepwater Horizon oil spill. Frontiers in Microbiology, 5(MAY), 1–13. https://doi.org/10.3389/fmicb.2014.00205

Kelly, E. N., Short, J. W., Schindler, D. W., Hodson, P. V., Ma, M., Kwan, A. K., & Fortin, B. L. (2009). Oil sands development contributes polycyclic aromatic compounds to the Athabasca River and its tributaries. Proceedings of the National Academy of Sciences, 106(52), 22346–22351. https://doi.org/10.1073/pnas.0912050106

Kimes, N. E., Callaghan, A. V., Suflita, J. M., & Morris, P. J. (2014). Microbial transformation of the Deepwater Horizon oil spillâ€"past, present, and future

perspectives. Frontiers in Microbiology, 5(NOV), 1–11. https://doi.org/10.3389/fmicb.2014.00603

Klatt, J. M., Haas, S., Yilmaz, P., de Beer, D., & Polerecky, L. (2015). Hydrogen sulfide can inhibit and enhance oxygenic photosynthesis in a cyanobacterium from sulfidic springs. Environmental Microbiology, 17(9), 3301–3313. https://doi.org/10.1111/1462-2920.12791

Lima, A. C., & Wrona, F. J. (2019). Multiple threats and stressors to the Athabasca River Basin: What do we know so far? Science of The Total Environment, 649, 640–651. https://doi.org/10.1016/j.scitotenv.2018.08.285

Love, M. I., Huber, W., & Anders, S. (2014). Moderated estimation of fold change and dispersion for RNA-seq data with DESeq2. Genome Biology, 15(12), 1–21. https://doi.org/10.1186/s13059-014-0550-8

Luu, R. A., Kootstra, J. D., Nesteryuk, V., Brunton, C. N., Parales, J. V., Ditty, J. L., & Parales, R. E. (2015). Integration of chemotaxis, transport and catabolism in P seudomonas putida and identification of the aromatic acid chemoreceptor PcaY. Molecular Microbiology, 96(1), 134–147. https://doi.org/10.1111/mmi.12929

Lux, R., & Shi, W. (2004). Chemotaxis-guided movements in bacteria. Critical Reviews in Oral Biology & Medicine, 15(5), 207–220. https://doi.org/10.1177/154411130401500404

Martinez, X., Pozuelo, M., Pascal, V., Campos, D., Gut, I., Gut, M., … Manichanh, C. (2016). MetaTrans: an open-source pipeline for metatranscriptomics. Scientific Reports, 6(1), 26447. https://doi.org/10.1038/srep26447

Mason, O. U., Hazen, T. C., Borglin, S., Chain, P. S. G., Dubinsky, E. A., Fortney, J. L., … Jansson, J. K. (2012). Metagenome, metatranscriptome and single-cell sequencing reveal microbial response to Deepwater Horizon oil spill. ISME Journal, 6(9), 1715–1727. https://doi.org/10.1038/ismej.2012.59

Morris, B. E. L., Henneberger, R., Huber, H., & Moissl-Eichinger, C. (2013). Microbial syntrophy: Interaction for the common good. FEMS Microbiology Reviews, 37(3), 384–406. https://doi.org/10.1111/1574-6976.12019

Mountfort, D. O., Brulla, W. J., Krumholz, L. R., & Bryant, M. P. (1984). Syntrophus buswellii gen. nov., sp. nov.: a Benzoate Catabolizer from Methanogenic Ecosystems. International Journal of Systematic Bacteriology, 34(2), 216–217. https://doi.org/10.1099/00207713-34-2-216

Ortega-Calvo, J. J., Marchenko, A. I., Vorobyov, A. V., & Borovick, R. V. (2003). Chemotaxis in polycyclic aromatic hydrocarbon-degrading bacteria isolated from coal-tar- and oil-polluted rhizospheres. FEMS Microbiology Ecology, 44(3), 373–381. https://doi.org/10.1016/S0168-6496(03)00092-8

Pernthaler, A., Dekas, A. E., Brown, C. T., Goffredi, S. K., Embaye, T., & Orphan, V. J. (2008). Diverse syntrophic partnerships from deep-sea methane vents revealed by direct cell capture and metagenomics. Proceedings of the National Academy of Sciences, 105(19), 7052–7057. https://doi.org/10.1073/pnas.0711303105

Reid, T., Boudens, R., Ciborowski, J. J. H., & Weisener, C. G. (2016). Physicochemical gradients, diffusive flux, and sediment oxygen demand within oil sands tailings materials from Alberta, Canada. Applied Geochemistry, 75, 90–99. https://doi.org/10.1016/j.apgeochem.2016.10.004

Reid, T., Chaganti, S. R., Droppo, I. G., & Weisener, C. G. (2018). Novel insights into freshwater hydrocarbon-rich sediments using metatranscriptomics: Opening the black box. Water Research, 136, 1–11. https://doi.org/10.1016/j.watres.2018.02.039

Reid, T., VanMensel, D., Droppo, I. G. G., & Weisener, C. G. G. (2016). The symbiotic relationship of sediment and biofilm dynamics at the sediment water interface of oil sands industrial tailings ponds. Water Research, 100, 337–347. https://doi.org/10.1016/j.watres.2016.05.025

Risacher, F. F., Morris, P. K., Arriaga, D., Goad, C., Nelson, T. C., Slater, G. F., & Warren, L. A. (2018). The interplay of methane and ammonia as key oxygen consuming constituents in early stage development of Base Mine Lake, the first demonstration oil sands pit lake. Applied Geochemistry, 93(August 2017), 49–59. https://doi.org/10.1016/j.apgeochem.2018.03.013

Rissanen, A. J., Kurhela, E., Aho, T., Oittinen, T., & Tiirola, M. (2010). Storage of environmental samples for guaranteeing nucleic acid yields for molecular microbiological studies. Applied Microbiology and Biotechnology, 88(4), 977–984. https://doi.org/10.1007/s00253-010-2838-2

Roeselers, G., Loosdrecht, M. C. M. Van, & Muyzer, G. (2008). Phototrophic biofilms and their potential applications. Journal of Applied Phycology, 20(3), 227–235. https://doi.org/10.1007/s10811-007-9223-2

Rooney, R. C., Bayley, S. E., & Schindler, D. W. (2012). Oil sands mining and reclamation cause massive loss of peatland and stored carbon. Proceedings of the National Academy of Sciences, 109(13), 4933–4937. https://doi.org/10.1073/pnas.1117693108

Scott, N. M., Hess, M., Bouskill, N. J., Mason, O. U., Jansson, J. K., & Gilbert, J. A. (2014). The microbial nitrogen cycling potential is impacted by polyaromatic hydrocarbon pollution of marine sediments. Frontiers in Microbiology, 5(MAR), 1–8. https://doi.org/10.3389/fmicb.2014.00108

Stocker, R., & Seymour, J. R. (2012). Ecology and Physics of Bacterial Chemotaxis in the Ocean. Microbiology and Molecular Biology Reviews, 76(4), 792–812. https://doi.org/10.1128/MMBR.00029-12

Syncrude, L. C. (1975). Baseline environmental studies of Ruth Lake and Poplar Creek. Edmonton, Alberta.

Teufel, R., Mascaraque, V., Ismail, W., Voss, M., Perera, J., Eisenreich, W., … Fuchs, G. (2010). Bacterial phenylalanine and phenylacetate catabolic pathway revealed. Proceedings of the National Academy of Sciences, 107(32), 14390–14395. https://doi.org/10.1073/pnas.1005399107

Trimmer, M., Shelley, F. C., Purdy, K. J., Maanoja, S. T., Chronopoulou, P.-M., & Grey, J. (2015). Riverbed methanotrophy sustained by high carbon conversion efficiency. The ISME Journal, 9(10), 2304–2314. https://doi.org/10.1038/ismej.2015.98

VanMensel, D., Chaganti, S. R., Boudens, R., Reid, T., Ciborowski, J., & Weisener, C. (2017). Investigating the Microbial Degradation Potential in Oil Sands Fluid Fine Tailings Using Gamma Irradiation: A Metagenomic Perspective. Microbial Ecology, 74(2), 362–372. https://doi.org/10.1007/s00248-017-0953-7

Vincent, W. F. (2009). Protists, Bacteria and Fungi: Planktonic and Attached. In Encyclopedia of Inland Waters, Volume 1 (pp. 226–232).

Wagai, R., Mayer, L. M., Kitayama, K., & Shirato, Y. (2013). Association of organic matter with iron and aluminum across a range of soils determined via selective dissolution techniques coupled with dissolved nitrogen analysis. Biogeochemistry, 112(1–3), 95–109. https://doi.org/10.1007/s10533-011-9652-5

Warren, L. A., Kendra, K. E., Brady, A. L., & Slater, G. F. (2016). Sulfur Biogeochemistry of an Oil Sands Composite Tailings Deposit. Frontiers in Microbiology, 6(February), 1–14. https://doi.org/10.3389/fmicb.2015.01533

Weisener, C., Lee, J., Chaganti, S. R., Reid, T., Falk, N., & Drouillard, K. (2017). Investigating sources and sinks of N2O expression from freshwater microbial communities in urban watershed sediments. Chemosphere, 188, 697–705. https://doi.org/10.1016/j.chemosphere.2017.09.036

CHAPTER 4: **TRACKING FUNCTIONAL BACTERIAL BIOMARKERS IN RESPONSE TO A GRADIENT OF CONTAMINANT EXPOSURE WITHIN THE OIL SANDS RIVER SEDIMENT CONTINUUMS**

GRAPHICAL ABSTRACT
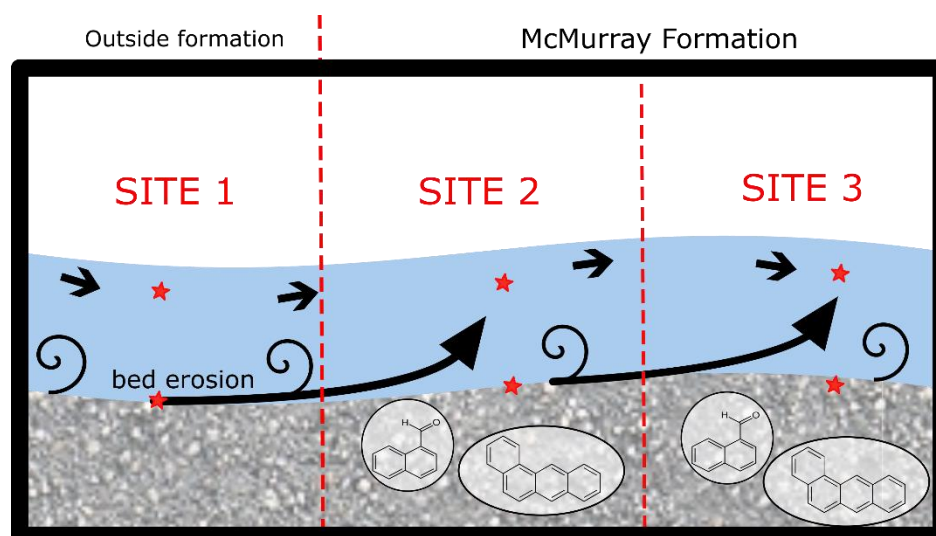
★ Sample Locations

4.1 Introduction

While water quality and ecological changes within the lower Athabasca River (LAR) are often perceived to be resultant from industrial oil sand deposit exploitation, the differentiation of industrial versus natural contributions of hydrocarbons is a complex and, yet, unresolved issue. Additionally, there has yet to be definitive studies identifying fundamental biogeochemical shifts attributed to this natural polycyclic aromatic hydrocarbon (PAH) signature. No proven fingerprinting method to achieve the above has been proven or accredited to date (Culp et al., 2018). Further, Culp et al. (2018) and Kirk et al. (2018) have suggested that while there is significant data on particulate atmospheric deposition, there is no information or model that can project the proportion of surface washoff that enters a river course. As such, Droppo et al. (2018) suggests that most of the PAHs that are transported within the rivers of the LAR are derived from hillslope and channel erosion of the McMurray formation (MF) (the geologic formation that defines the minable oil sands deposit), and not from direct or atmospheric anthropogenic inputs.

Regardless of PAH source, a substantive knowledge gap in relation to how the microbial consortium, 1) is influenced by the high hydrocarbon content of the sediments (suspended and bed), and 2) on how the microbes influence the contaminant speciation of the PAHs. Both of these synonymous biochemical processes will inevitably alter the biogeochemical footprints with concomitant impacts on the natural ecology. While most studies of contaminants and microbial impacts in rivers have been studied only on the bed sediment community structure (e.g. biofilms – Yergeau et al. 2012), few studies have characterized the dynamics of bitumen containing suspended sediment (SS) within rivers of the LAR. Droppo et al. (2018) did observe temporal and spatial trends in SS loads and PAH

signatures with distance downstream for the Ells and Steepbank (STB) rivers using passive SS samplers. They however did not investigate any microbial influence relative to these spacial and temporal trends. Recent studies have begun to unravel the natural microbial structure within bed sediments in the region (Reid et al., 2019; Reid et al., 2018; Yergeau et al., 2012), though there remains a lack of understanding with respect to the true microbial function within the entire region, including both SS and bed sediments. Further, there are, to our knowledge, no studies that provide potential gene biomarkers which reveal statistically differing expression patterns as a direct result to increasing hydrocarbon exposure of the MF.

Tracking contaminants is clearly not a new area of research. For years, scientists have studied contaminant sites such as those of the Exxon Valdez oil spill and the Deep-Water Horizon disaster. In most studies tracking contaminant distribution, conventional geochemical testing in association with taxonomic surveys, only provides researchers a glimpse into the effects these contaminants have on the natural ecology. What has been missing is how the primary producers, such as the diverse microbial communities found in all lakes, rivers and streams, deal with the stressors resulting from the exposure to various compounds. Shifts in the functional attributes of microbial communities are direct and primary biological responses, that can induce ecosystem-wide alteration. What is too often the case is that contaminant sites are only studied after contamination has occurred, leaving a knowledge gap as to the true baseline character of the ecosystem prior to xenobiotic exposure.

This study uses metatranscriptomics analyses to determine the efficiency of shotgun gene expression surveys for tracking the microbial response to increasing hydrocarbon exposure in SS and bed sediments through the river continuum of the Steepbank River (STB)

of the LAR (Alberta, Canada). A control location upstream of the natural hydrocarbon deposit (MF) provide our reference site within the same river continuum, void of any hydrocarbon signature. This research aims to provide 1) insight into the natural genetic response of microbes to increasing hydrocarbon exposure, and 2) provide potential gene biomarkers that reveal statistically differing expression patterns as a direct result to increasing hydrocarbon exposure. This has strong implications worldwide, where gene expression surveys of aquatic microbial communities could be ideal tools in tracking contaminant exposure, be it legacy or otherwise.

This chapter brings clarity and insight into the baseline characteristics of the MF, and how they relate to external ecosystems, outside of the MF. Results and conclusions gained here, will provide a better understanding of how the MF itself shapes the biogeochemical signature within various aquatic ecosystems, allowing direct comparison to sites outside of the hydrocarbon influence. Herein we assess the baseline conditions representative of the MF itself, as they relate to baseline conditions outside of the MF.

4.2 Methods

4.2.1 Sampling Site Descriptions

Sampling sites were collected on the Steepbank River (STB) at three sites representing a gradient of PAH concentrations from upstream to downstream (Figure 1). The middle to lower reaches of STB cuts through the MF, the ore deposit constituting the Athabasca Oil Sands. The upstream site was located within the Clearwater Formation (CF) and as such contained marginal to no bitumen. Sample sites from upstream to downstream are therefore designated CF-Low, MF-Med, and MF-High. All samples are presumed to represent the natural PAH characteristics of the STB given there are legislated no direct

discharges from industrial properties. If there were an input, it can only be from atmospheric deposition which will be highly diluted by the volume of water in the rivers and the primary source of particle load being from the channel itself (Droppo et al. 2018).

The STB flows from the east, with an elevation change from 625 to 320 m at the confluence with the Athabasca River (Figure 1). MF is composed of minable bitumen-rich deposits combined with fine- to coarse-grained sand interbedded with lesser amounts of silt and clay (Musial et al. 2012; Haug et al. 2014). STB has a mean annual flow of 4.8 m^3 s^{-1} and is considered a groundwater dominated river with an average of 50 % of flow derived from groundwater (Gibson and Birks, 2016).

4.2.2 Sediment Collection

Sediments were collected from both the river beds and suspended particulates. Bed sediments were collected in triplicate into sterile 5 ml cryotubes, and flash frozen in liquid nitrogen in the field for nucleic acid extractions. Bulk sediments were collected into 500 ml HDPE Nalgene Bottles with no headspace and kept frozen until analysis.

SS were collected by a portable continuous-flow centrifugation (Alfa-Laval model WSB 103B). Water was pumped (4 L min^{-1}) to the centrifuge by a 5C-MD March submersible pump located in the middle of the river at mid depth. Recovery of SS was greater than 90% (% recovery = outflow TSS/inflow TSS). Sediment collected in the centrifuge bowl was immediately removed and placed in 5 ml cryotubes and flash frozen as above. Total PAH data from each sampling location was obtained from the Regional Aquatics Monitoring Program (RAMP) database (www.ramp-alberta.org).

4.2.3 SEM Analysis

Bulk bed sediments were analyzed by Scanning Electron Microscopy (SEM), to understand particle distribution and evidence for hydrocarbon signatures. Specifically, the Environmental Scanning Electron Microscope (FEI Quanta200F, Eindhoven, Netherlands) was used at the Great Lakes Institute for Environmental Research (GLIER), University of Windsor (Windsor, ON, Canada). Here, analyses were performed at high vacuum (20 kV) with a theoretical spot size of 2.6 nm. Grain inspections and size distributions were performed using both secondary electron (SE) and backscattered electron (BSE) detectors. Elemental composition analysis was performed with the EDAX® SiLi detector (EDAX, Mahwah, New Jersey, USA).

4.2.4 DNA/RNA Extractions & Library Preparation

Total DNA extractions were carried out in duplicate using the MoBio Powersoil Total DNA Isolation Kits (now Qiagen DNeasy Powersoil Kit). Sediments were extracted according to manufacturer protocols. To explore the V5/V6 region of 16S rRNA gene, extracted DNA was amplified and purified according to Reid et al. (Reid et al. 2016a). Briefly, dual polymerase chain reactions (PCR) were performed to initially amplify the V5/V6 region, followed by a second barcoding PCR to uniquely identify samples for pooling and sequencing on the Ion Torrent PGM platform (Life Technologies, Carlsbad, California) at the Great Lakes Institute for Environmental Research at the University of Windsor (Windsor, Ontario, Canada). Quality and concentrations of pooled DNA libraries were analyzed on the Agilent 2100 Bioanalyzer prior to sequencing.

Total RNA extractions were performed using the MoBio Powersoil Total RNA Isolation Kits (MoBio Laboratories; Carlsbad, California) per slightly modified protocols.

Initial sediment quantity for extraction was bumped to 5 g to increase overall RNA yield. All reagents and samples were kept on ice throughout extraction to maintain RNA integrity and minimize degradation throughout the extraction. Quality and concentrations were analyzed on the Agilent 2100 Bioanalyzer, where concentrations exceeded 100 ng/µL, and quality scores exceeded RIN # of 7.5. Samples of sufficient quality and concentration were sent in duplicate to Genome Quebec Innovation Center at McGill University in Montreal, Quebec, Canada. There, samples were again checked to ensure they met quality control standards, and rRNA-depletion (Illumina Ribo-Zero rRNA Removal Kit, bacterial and yeast) was performed to enhance the mRNA concentration. Samples were then sequenced on the Illumina HiSeq 4000 Nextgen sequencer.

4.2.5 16S Community Structure Analysis

Microbial taxonomy was determined for augmentation of the metatranscriptomics dataset, providing information as to which microbes were likely associated with observed gene expression. Raw sequences were processed through the MacQiime (v.1.9.1) pipeline (www.qiime.org), an open-source bioinformatics pipeline for 16S sequences (Caporaso et al. 2010). Sequence files were filtered and sequences with a Phred score below 20 were omitted. Sequences were then clustered into operational taxonomic units (OTUs), omitting singletons and doubletons, at a similarity threshold of 97% using the uclust algorithm. Chimeras were removed using the usearch61 algorithm with MacQiime. Taxonomy was assigned to representative OTU sequences for each cluster, using the default GreenGenes database, at a 90% confidence threshold. Relative abundances (% of reads per sample) were calculated in order to gain an understanding of the dominant taxa and those proportionally different between sample sites.

4.2.6 Metatranscriptomics Data Processing and Differential Expression Analysis

All raw metatranscriptomics sequence data was processed through the MG-RAST (MetaGenomics Rapid Annotation using Subsystem Technology) pipeline (Meyer et al. 2008). This automated pipeline was designed for the analysis of high-throughput sequencing datasets, proving both functional and phylogenetic summaries. Raw paired-end sequence files were submitted, where pairing, quality filtering, and the annotation of functional genes was performed. A Phred quality score of >30 was applied to submitted raw sequence files. Transcripts were annotated to the KO (Kegg Orthology) database. Visualizations for gene expression correlations were performed using the START app, a web-based RNAseq analysis and visualization resource (Nelson et al. 2017). Raw expression values were normalized to counts per million using the limma package (Linear Models for Microarray and RNA-seq Data) of R/Bioconductor, within the START application. Gene expression boxplots are expressed as logCPM values, and p-values are provided where statistical significance is noted. Mean-variance modelling at the observation level (voom) was utilized for the log counts per million (logCPM) determination. Expression heatmaps were created through Heatmapper, a free online server for the creation of heatmaps and other visualization tools (Babicki et al. 2016).

4.3 Results and Discussion

4.3.1 Physicochemical Characteristics of SS and Bed Sediments

Spatial trends of PAH concentrations in the suspended and bed sediments of the STB, were measured at the 3 sample sites. PAH concentrations (Figure 2) indicate a generally increasing load of PAH moving downstream from CL-Low (upstream) to MF-High (downstream). Overall, there is a significant increase in total PAH as exposure increases

through the MF, with concentrations totaling 34.8, 118.3 and 425.5 ng/L at CF-Low, MF-Med and MF-High respectively. These findings correlate with those of Droppo et al., (2018), who also observed increases in PAH loadings in the SS moving through the formation in the STB. Interestingly, the highest concentration PAHs were alkylated compounds, specifically C2, C3, C4-Dibenzothiphenes, C2, C3, C4-Phenanthrenes/Anthracenes, C2-Fluoranthenes/Pyrenes and C4-Napthalenes. These alkyl homologs are indicative of the MF and have been used as indicators of the bitumen deposit in various other studies, as they can reveal minute variations within the deposit (Droppo et al. 2018).

Scanning Electron Microscopy also revealed similar trends of increasing hydrocarbon concentrations within the bed sediment. Figure 3 reveals the interstitial hydrocarbon content of the bed sediments, where increasing carbon content correlates to the observed bituminous compounds within the interstitial sediment grains. RAMAN spectroscopy partially confirmed the bitumen content within MF-High, revealing peaks potentially indicative of the aromatic hydrocarbons with the MF bitumen (Appendix C). The presence of bitumen in the interstitial pore spaces of several prepared SEM slides portrays the truly ubiquitous presence of the PAHs in the sediments of the MF. Additionally, visual analysis on the SEM appeared to show a decreasing trend in particle size distribution from CF-Low to MF-High. Sediment particles appeared to be well sorted upstream of the MF,

It is interesting to note that CF-Low does in fact contain some measurable PAHs despite being outside of the McMurray Formation (though no bitumen was observable under the SEM). However, this could be attributed to natural PAHs resulting from combustion of organics such as wood or grasses, or perhaps some other anthropogenic influence (e.g., atmospheric deposition). This is especially relevant in this region, where a large forest fire

swept through a year earlier and would have inevitably introduced a PAH signature to the natural landscape. However, this type of PAH is indicative of pyrogenic origin, and thus is chemically different than the PAH signature of the MF. Droppo et al., 2018 indicated that there was a correlation between wood/grass/coal burning and low flow events, which may be what we are observing here. Nonetheless, there was no visible evidence of bitumen derived from that from the MF within the sediments observed under the SEM. These chemical characterizations of increasing PAH loads within the SS and the associated microscopy results reveal considerable hydrocarbon content, that is not only highly concentrated in the bed sediments but is readily eroded and transported through the water column and downstream. These hydrocarbon signatures in both the water and sediment compartment provides an idea opportunity to characterize how the microbial community is dealing with such a unique hydrodynamic sediment regime under varying PAH exposures.

4.3.2 Microbial Community Structure & Functional Dynamics

4.3.2.1 Sequencing Summaries and Statistics

The metataxonomic analysis consisted of a total of 12 single-end sequence files, averaging 88,995 raw sequences per sample. The metatranscriptomics dataset also consisted of 12 paired-end sequence files, with over 39 million reads per sample, averaging 46,549,109 sequences each, with Phred quality scores all >30. Sequence files will be submitted to the NCBI Sequence Read Archive (SRA) upon manuscript publication.

4.3.2.2 Microbial Community Structure (16S Amplicon)

Metataxonomic analyses were performed in order to understand how the exposure of MF hydrocarbons may have altered the taxonomic distribution at each site. Figures 4 & 5 clearly illustrate a shift in the microbial structure between the SS and bed sediments. Most

prominent is the dominance of Proteobacteria in both the SS and bed sediments, constituting approximately 61, 59 and 66 % of the community within the SS and only about 41, 43, and 47 % in the bed sediments of CF-Low, MF-Med and MF-High respectively. In general, SS is more abundant in Actinobacteria, Cyanobacteria and Proteobacteria compared to their bed counterparts at each respective site. Bed sediments showed similar trends in community structure as previous studies, showing more abundant Acidobacteria, Bacteroidetes, Chlorobi, Chloroflexi, Firmicutes, Plantomycetes, Spirochaetes and Verrumicrobia, representing a diverse microbial assemblage, capable of thriving in this unique environment (Yergeau et al. 2012). Acidobacteria, though remaining poorly understood, are a diverse range of organisms ubiquitous in soils and sediments (Naether et al. 2012). Of note is the family Holophagaceae, containing genera capable of aromatic compound degradation, and Geothrix, and anaerobic chemoorganotroph generally utilizing Fe(III) as its electron acceptor. Bacteroidetes also comprise a diverse range of organisms and was second in abundance overall behind the Proteobacteria. One of the most dominant families of Bacteroidetes was Cytophagaceae. Within this family, a novel genus Dyadobacter is known to degrade xenobiotic compounds in tar-contaminated soils (Willumsen et al. 2005). Dyadobacter was most observed here to be most abundant in the SS at MF-Med, though these were at relatively low abundances overall. Still, the overall high abundance of Cytophagaceae suggests that there may be other genera of similar metabolic capabilities responsible for degradation of similarly complex carbon compounds. Chlorobi contains organisms that are both anaerobic photoautotrophs alongside obligate heterotrophs, and was also found in man-made reservoirs in the region (Reid et al. 2019). It's presence in the bed sediments indicates a response to sulfide production deeper within the sediments, perhaps

also acting as a detoxifier in it's oxidation of sulfides. Chloroflexi are also anoxygenic phototrophic bacteria, though some are also able to utilize halogenated compounds as electron acceptors in their respiratory process. Notable taxonomic families observed include Anaerolinaceae and Dehalococcoidaceae. Anaerolinaceae has been found to closely affiliate with methanogenic activity, with the ability to activate the breakdown of long-chain n-alkanes (B. Liang et al. 2016). Dehalococcoidaceae is an organohalide-respiring organism, known to utilize H_2 as its electron donor. This is significant as it may suggest a means by which to reduce the build-up of H_2 as a result of methanogenic biodegradation processes, allowing for these processes to proceed. Clostridium *spp.* within the Firmicutes phylum has been shown to also closely associate with methanogens, and has been shown to be highly abundant in oil cultures and toluene-degrading methanogenic cultures (Fowler, Toth, and Gieg 2016). However, it was also noted that they may *only* be involved in the subsequent breakdown of hydrocarbons after initial activation has taken place (Fowler, Toth, and Gieg 2016). The remaining phyla observed, Plantomycetes, Spirochaetes and Verrumicrobia all represent diverse groups of organisms, many of which are commonly found in both soils and marine and freshwater environments worldwide.

It is interesting to note that there was an increased abundance of the Proteobacteria and Cyanobacteria within the SS. Within the Cyanobacteria phylum, particularly dominant was the family of Nostocaceae, known for its nitrogen-fixation abilities. Reid et al., 2019 also observed the presence of these organisms in deeper freshwater reservoirs (Chapter 3), suggesting that there is a significant phototrophic influence on the biogeochemistry of this region. The presence of Nostocaceae could be suggestive of a syntrophic cooperation with aquatic plants, who would benefit from the production of ammonia. Additionally, the

production of ammonia could be utilized by other chemoheterotrophs in the breakdown of organics such as the PAHs of the MF. The increased abundance of Cyanobacteria is expected in the SS, where ample sunlight is present alongside ample nutrients derived from some of the breakdown processes within the water column or bed sediments. The increased abundance of Proteobacteria however was somewhat unexpected, where Betaproteobacteria were largely responsible for this increase. Betaproteobacteria was the most dominant class overall, second only to the Alphaproteobacteria (Figure 5). The prominence of these classes of organisms could be linked to their highly diverse metabolic abilities, making them particularly efficient in adapting to the hydrocarbon gradient of the MF (Dworkin et al. 2006). The Betaproteobacteria family of Comamonadaceae was most dominant in all of the SS samples. Comamonadaceae, is an extremely diverse family of organisms, harboring genera capable of wide-ranging phenotypic abilities. Noted abilities of Comamonadaceae and other families of Betaproteobacteria to degrade a variety of petroleum contaminants makes the presence of this organism extremely relevant in the context of this unique hydrocarbon gradient present within the STB (Mukherjee et al. 2017; Zedelius et al. 2011). Additionally, Betaproteobacteria contain organisms with the ability to oxidize ammonia (Stein and Klotz 2016), part of the nitrification pathway, perhaps resulting from PAH breakdown within the STB. Perhaps the greatest noted increase from CF-Low to MF-Med was in the abundance of Spirobacillales, an order of Deltaproteobacteria. Spirobacillales is a known degrader of toxins produced by certain cyanobacteria (Lezcano et al. 2017), providing a potentially interesting correlation to the depletion of Cyanobacteria noted here also . This may be evidence towards the notion of PAH inhibition of photosynthetic activity as noted in other studies (Marwood et al. 1999). However, this heightened abundance could just be

attributed to the increased abundance of complex organics, which could also be utilized by Spirobacillales (Lezcano et al. 2017).

Moving downstream from the CF to MF, there are clearly changes in the microbial community structure, though subtle from upper taxonomic classifications (aside from the Betaproteobacteria). Principal Coordinate Analyses (PCoA) of all operational taxonomic units (OTUs) was implemented in order to better understand community structure variation between sample sites. Initially evident is a clear separation of SS from the bed sediments (Figure 6). Coordinate 1 represents over 50 % of the variation, while coordinate 2 represents approximately 21 %. CF-Low SS and bed sediments appear to be the most unique of all the other sites, and is the only site showing relatively similar SS and bed sediment communities. This is likely attributed to its upstream situation above the MF, where it has not yet been influenced by the significant hydrocarbon signature of MF. It is interesting to observe the divergent nature of both the SS and bed sediments from the CF-Low "control" site, indicating increasing differences in the community structure not only between sites, but also within sites SS and bed samples. MF-Med SS and bed sediments are most divergent from the CF-Low sites, perhaps representative of its sudden hydrocarbon signature moving into the MF. It is extremely interesting that MF-High is taxonomically more closely related to CF-Low, especially given its geographically the most distant sampling site and exhibits the highest PAH signature overall. However, what this may be suggesting is that by MF-High, given enough exposure time within the MF, the microbial community has adapted or equilibrated to the altered environmental stimuli of the MF. The microbial community at MF-Med may be under a drastic state of flux or adaptation, which is perhaps inducing rapid alteration to the DNA signature, resulting in the heightened variation at the OTU level. Nonetheless, this

data suggests that the use of PCoA and similarity indicies (Bray-Curtis in this case) do not positively correlate biogeochemical variation attributed to the stepwise increase in PAHs of the MF.

4.3.2.3 Suspended Sediment Microbial Function

The dramatic increase in PAH content moving downstream through MF-Med and MF-High is however reflected in the microbial gene expression data and can be seen in Figures 7 & 8. In the SS samples, there is a dramatic suppression of several *energy metabolism* genes, including nitrogen fixation, nitrite reductase and assimilatory sulphate reductase. Additionally, there is significant suppression of photosynthetic genes responsible for both the coloring of cyanobacteria (*cpcEF* genes for Phycocyanobilin lyase (logFC > -2.06; p<0.05)) and the photosystem I and II systems (*psa* and *psb*) found in phototrophic organisms (LogFC < -1; p<0.05). This suggests a fundamental shift in natural metabolic character of the microbes, including the phototrophic communities residing within the water column. This suppression of genes specific to cyanobacteria and their photosynthetic functions correlate to the decrease in cyanobacterial abundance noted within the 16S rRNA amplicon data, alongside other studies which revealed photosynthetic inhibition due to PAH presence (Marwood et al. 1999). However, there is a significant increase in the expression of *bchQR* genes, responsible for the photosynthetic function of green sulfur bacteria (anoxygenic phototrophs). Relying on sulfides as an electron source, this may indicate a shift towards a more sulfide-rich system moving towards MF-High. Dissimilatory sulfate reductase genes (dsrAB; aprAB) and methanogenesis genes (mcr and mtr) showed relatively consistent expression within the SS through to MF-High. Interestingly, methane oxidation transcripts (mxaF, methanol dehydrogenase) show signficantly increasing expression (logFC

= 0.774; p<0.05) moving downstream, with some of the overall highest expression noted in the SS. Interestingly, the expression of amoAB showed a gradual increase in expression moving downstream as well, which has been shown to be correlated to hydrocarbon exposure and metabolism (Dolan et al. 2010; Urakawa et al. 2019). This too may correlate to the highly abundant Betaproteobacteria, some of which harbor these same genes for ammonia oxidation. These iterative expression changes correlating to the stepwise increase in hydrocarbon content indicates that even the microbial community within the SS in the water column (which likely has lower cellular density than in the bed) is experiencing significant alteration to their upstream metabolic signature. The increased expression of methanotrophic genes indicate that perhaps the microbial population is adapting to the changes in hydrocarbon content, whereby enhanced methanogenic activity from below (see 3.2.4) is being offset by the equilizing function of the methanotrophs in the overlying water. Further, the fact that many of the significantly differentially expressed genes belong to the broader categories of environmental information processing and cellular processes indicates that the microbial communities travelling on or with the SS are experiencing dramatic changes in their core cellular functionality, not just their energy metabolism alone.

Further, dominant trends where observed in the expression of known *biodegradation* genes within the SS. Remarkably, there were significantly increasing trends from CF-Low through MF-Med to MF-High of several known hydrocarbon degradation genes, including (but not imited to) alkane monooxygenase (*alkB*), benzoyl-CoA reductase (*badDEFG*), nitronate monooxygenase (NMO), and hydroxybenzoate monooxygenase (*pobA*) (logFC > 0.15; p<0.05). There was also a spike in the expression of Benzylsuccinate-CoA (*bbsB*) at both MF-Med and MF-High compared to CF-Low (logFC > 2), though this was not

significantly expressed (p = 0.268). The expression of *alkB* may correlate to the highly abundant Alpha-, Beta- and Gammaproteobacteria classes, alongside Actinobacteria, who all contain closely related homolog genes for alkane-degradation. The magnitude of these fold changes are low, though this is somewhat expected given that what we are observing are small communities of microbes in transit within the water column. There is likely little in the way of redundancy in their functional abilities beyond necessary cell survival, so even small changes observed here may be relatively drastic in terms of their overall functional characteristic. The signficant increase in gene expressions noted here indicate that the microbial community suspended in the water column are directly responding to the hydrocarbon influence of the MF altering their natural energy metabolisms to adjust towards a seemingly increased biodegradation capacity within the MF. This abundance and specificity of the significantly different transcripts within SS, are potential targets from which to evaluate genes for the purpose of hydrocarbon compound tracking in other freshwater environments.

4.3.2.4 Bed Sediment Microbial Function

Similar to the SS analyses, bed sediment community functions shifted significantly in response to the MFs hydrocarbon influence. Interestingly, the absolute magnitude of expressions from within the bed sediments was generally significantly higher than that of the SS (aside from methanotrophy), likely related to the increased cell density within the sediments. The above is also evidenced in the magnitude of change exhibited by the noted genes mentioned. Here, similar trends in the expression of specific *energy* metabolism pathways were observed, though almost all indicate suppression. Dissimilatory and assimilatory nitrate reductase and assimilatory sulfate reductase both reveled signs of

suppression in both MF-Med and MF-High. By MF-High however, dissimilatory nitrate reductase appeared to recover to levels even higher than CF-Low. This would imply a shift in the general nitrogen cycle moving into the MF, noted by the increased dissimilatory nitrate reduction genes. Ammonium Monooxygenase (*amoABC*), dissimilatory sulfate reductase (*dsrAB* and *aprAB*) and methanogenesis (*mcr* and *mtr*) genes saw sharp increased in expression at MF-Med, then a slight decline by MF-High. Here it is again interesting to see in increase in another dissimilatory pathway as noted earlier, and may be evidence towards some sort of energy conservation strategy in response to an overall metabolism signature shift towards biodegradation. The differential expression analyses between MF-Med and CF-Low, revealed several *mtr* and *mcr* subunits as the most highly overexpressed in MF-Med (logFC > 2; $p<0.05$), clearly a response to the increase PAH exposure.

Known *biodegradation* genes within bed sediments also exhibited a clear response to MF exposure, here showing a generally increasing expression moving from upstream to downstream. Alkane monooxygenase (*alkB*), benzoyl-CoA reductase (*badDEFG*), nitronate monooxygenase (NMO), and benzoylsuccinyl-CoA dehydrogenase (*bbsBD*) all exhibited increasing expression moving downstream towards MF-High. Specifically, significant overexpression of *alkB*, *badDEFG*, and *bbsBD* was observed between MF-High and CF-Low (logFC > 1; $p<0.05$). These elevated expression levels further support a specific genetic response to increasing exposure to elevated hydrocarbon levels, indicating their potential as PAH biomarkers further downstream. It is interesting to note that some of these biodegradation expression signatures appeared to be expressed earlier in the bed sediments than in the SS, again possibly due to of the lag time needed for sediments to become suspended in the water column (from surface washoff or channel erosion).

4.3.2.5 Identifying Contaminant Gradients and their impacts on Microbial Metabolic Expression

The breadth of data obtained through shotgun metatranscriptomics surveys is immense, therefore it can be difficult to effectively, efficiently and accurately correlate trends in gene expression patterns. However, in observing metabolic signatures via expression heatmap and computing average linkage clustering for both genes and sample locations, it becomes quite evident that there are contrasting functional characteristics between SS and bed sediments, alongside those between the CF and MF. Additionally, associating trends in co-expression gene clusters provides a more robust means of inferring a genetic response to the increase hydrocarbon exposure moving downstream. What is immediately interesting is that CF-Low bed sediments more closely associate with the SS of all other sites compared to the other bed sites. This is likely attributed to the fact that this site acts as a control and is the only to be outside of the MF influence. This also suggests that the presence of the MF hydrocarbons alone causes a dramatic increase in expressional diversity.

The dramatic shifts in the metabolic signatures of both the SS and bed sediments can be seen in the differential expression scatterplots of Figure 7. Here, shifts in specific gene expression depending on sample location are evident in the amount of deviation from the overall expressional mean. Bed sediments in general, as mentioned previously, generally indicate higher expression magnitudes compared to the SS. Although, there are clearly specific genes and clusters of genes that reveal increased expression at CF-Low and in the SS. The suppression of the *sir* gene for assimilatory sulphate reduction alongside an increase in the genes for dissimilatory sulphate reduction (*dsrAB; aprAB*) indicates a shift from energy consuming to energy producing activity (similar to the noted shift in nitrogen metabolism). This shift of assimilating these sulfur compounds towards the production of

sulfides, could be the energy source for the anoxygenic phototrophs mentioned earlier. This noted abundance of phototrophic sulfur bacteria and sulfur cycling genes here, alongside adjacent freshwater reservoirs in the region, provides insight into their apparent significance in the region (Reid et al. 2019). It has been observed that anoxygenic phototrophs will actually dominate in oligotrophic systems, and actually exceeds primary production rates of oxygenic phototrophs by a large margin. The dense microbial mats that likely inhabit these sediments, containing micro-redox zones of both sulfate and sulfide has been suggested to act as an almost closed system, limiting the reduction of oxygen. In some systems, the oxidation of sulfides within these bed sediments has been up to 100 %, resulting from the dense communities residing within layered biofilms (Dworkin et al. 2006). This therefore explains the relatively little sulfur metabolism observed within the water column, compared to the bed sediments.

The increased expression of both methanogenic and methane-oxidizing transcripts suggests a shift towards a biodegradation dominated metabolic signature of these sites. What is interesting is the closely co-expressed nature of several of the methanogenic transcripts (*mcr* and *mtr*) with biodegradation genes (*benB*; *bbsBD*). In fact, the most significantly over-expressed genes at MF-Med was the *mcrCD* and *mtrC* genes, both responsible for iterative steps of the larger methanogenic pathway. The *mcr* gene and its various subunits are well known methanogenic markers, and are known indicators of biodegradation activity as noted in many a study (McKay et al. 2017; Reid et al. 2018, 2019; Vigneron et al. 2017). The *mtr* gene, a membrane bound methyltransferase, is also responsible for methane production, though is perhaps the less studied of the two. Responsible for the extrusion of a sodium ion from the cell, *mtr* subunits provide the necessary cellular chemiosmotic gradients for final

steps of the methanogenic pathway. This is also an energy conservation mechanism, perhaps allowing for the continuation of these processes under potentially limited thermodynamic constraints. This dependence on this cellular sodium pump could also suggest a broader salinity impact on the expression of the methanogenic pathways observed here. Other studies have indicated the impacts of NaCl on methanogenesis, though in different environmental contexts (Patricia J. et al. 2007). If valid, a genetic response related to salinity gradients in the environment could be an ideal marker for industrial oil sands inputs, given their highly saline nature (Volik et al. 2017; Warren et al. 2016). Though all methanogenic pathways lead to CH_4, the mechanism and phylogenetic diversity of the organisms that lead to this point are quite diverse. This provides an interesting future direction from which to move towards an increased specificity of methanogenic biomarkers depending on the compound of interest. This too could be extended to other gene groups and subunits, where specific environmental stimuli could induce slightly altered expressional patterns potentially useful for source tracking research.

Tracking other nutrient gradients (i.e. carbon, nitrates and phosphorus) would likely induce a similar alteration to the characteristics of the in-situ microbial metabolism as observed here. Shifts in basic physico-chemical parameters such as DO, salinity and conductivity can and will induce a genetic response that could be elucidated through these same shotgun gene expression surveys. The induced response from any environmental stimuli causes what is in essence a cooperative response by groups of microbes, and never an isolated incident (as seen here). Integrating genomics techniques such as these, where clusters of co-expressed genes can be traced alongside conventional chemical tracer approaches is the next step in characterizing the impact of compounds as they move through

our surrounding environments. The ability to genetically determine how target substances effect the natural microbiology of a system provides researchers with a more holistic understanding of the bio-transformations and/or biodegradation trends associated with the given compound of interest.

4.4 Conclusions

A major challenge facing mining companies and environmental scientists globally is trying to evaluate the extent to which anthropogenic practices are affecting the surrounding natural environment, with insights here providing intriguing avenues from which to begin unravelling these complex problems. This is the first study of its kind to explicitly characterize the natural microbial community function in reference to a true baseline, reference-site, upstream of the McMurray Formation and its ubiquitous hydrocarbon-rich strata. Additionally, these are the first results to identify microbial gene expression trends in a compound tracking context, whereby functional trends are directly correlated to the environmental hydrocarbon gradient measured in both the SS and bed sediments. These results, along with the PAH characteristics, provides powerful insight into not only the McMurray Formation's impact on both the SS and bed sediment biogeochemistry, but also on the prospect of microbial functional biomarkers for tracking hydrocarbon exposures in other dynamic aquatic ecosystems.

Results clearly show that the complexities of specific gene subunits can and do provide significant insight into the fundamental metabolic preferences within a given ecosystem. There are fundamental differences in expression pathways between SS and bed sediments, and as such, future studies characterizing river continuums should be aware of these differences in designing their research approach. Alterations are clearly observed for

not only genes responsible for metabolizing these hydrocarbons (*alkB*, *badB, bbsBD etc.*), but also the fundamental energy metabolism processes governing this ecosystem's microbial communities. Shifts from assimilatory to dissimilatory reduction processes give interesting insight into fundamental shifts in the flow of energy through these systems and reveal how widely ecosystems can be impacted biologically.

These advancements in contaminant biogeochemical studies, exemplified here, provide avenues from which to explore bioassay surveys, isolating specific gene combinations clusters for the purpose of targeting and tracking specific compound exposure. There is a need to further our understanding of how entire microbial communities behave in the presence of contaminants, moving beyond single microbe studies to understand entire community dynamics. The very nature of microbial plasticity allows them to be extremely effective and efficient in their metabolic capabilities when in the presence of other microbes and any given environmental stimuli. By harnessing and unravelling their complex genetic response, these novel tools shown here have great potential moving forward for unravelling the movement of compounds through hydrodynamic environments worldwide.

Figures
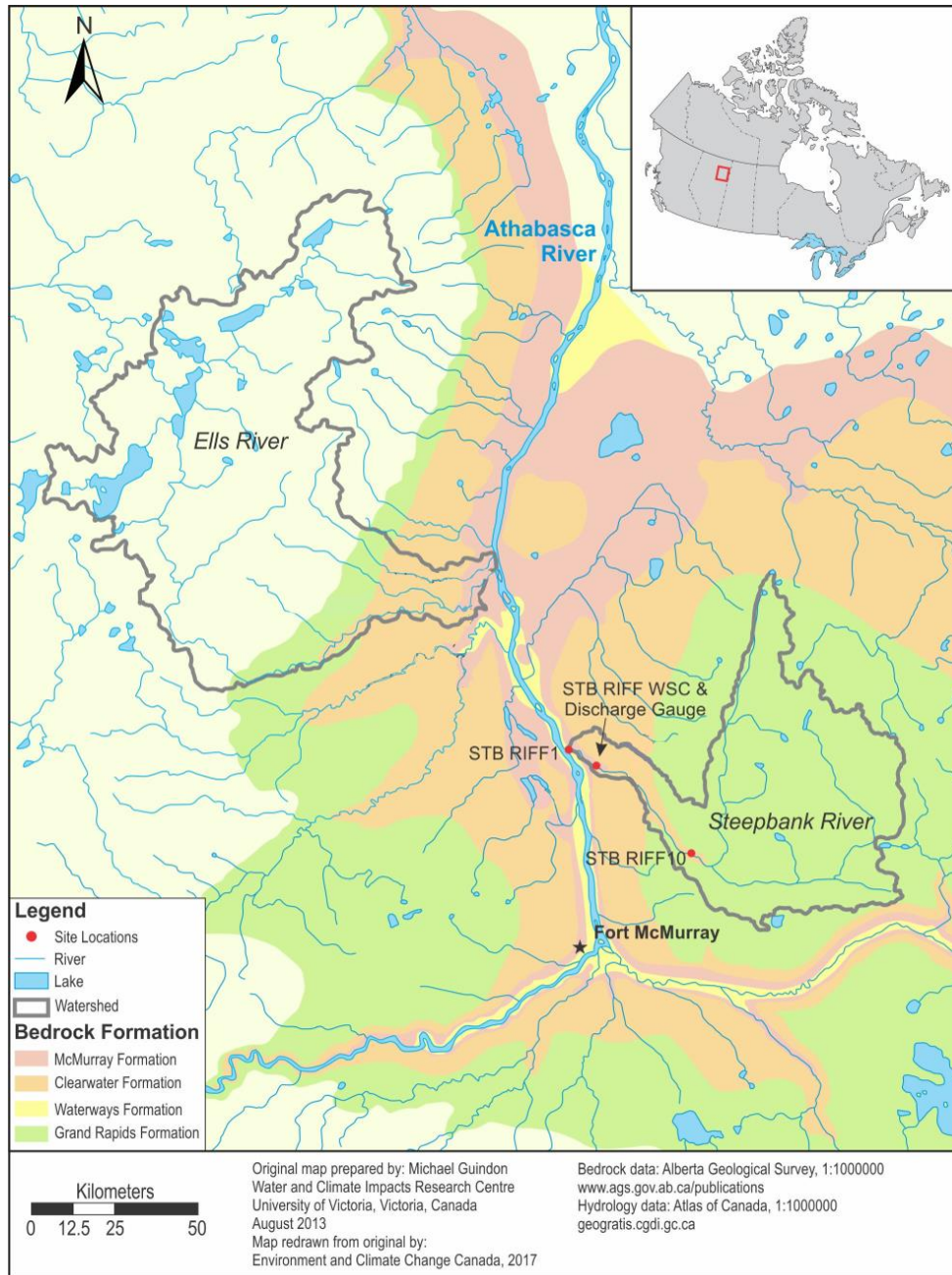
Figure 1: Map of Fort McMurray Region, bedrock formations constituting the bitumen deposit (McMurray Formation) and sampling sites along the Steepbank River. (CF-Low: Riff10; MF-Med: WSC; MF-High: Riff1)
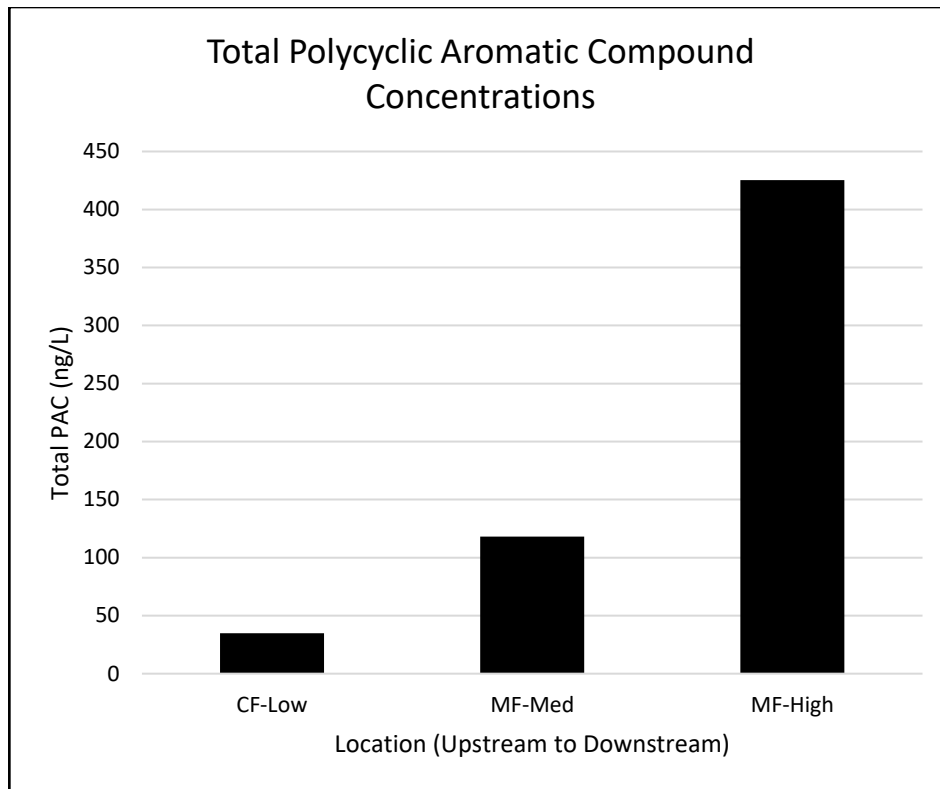
Figure 2: Total PAH loads in the SS of the STB River at each respective sampling site (www.ramp-alberta.org)
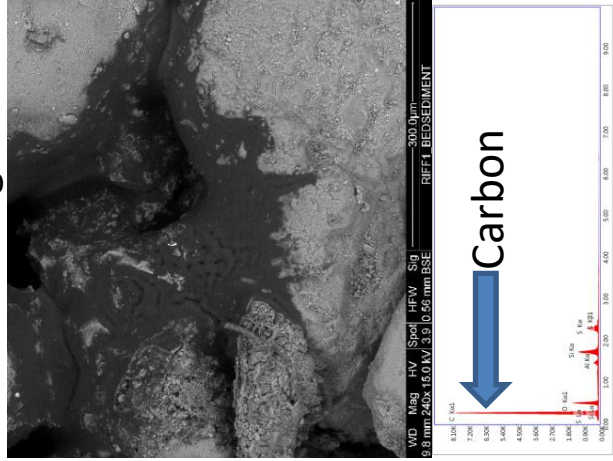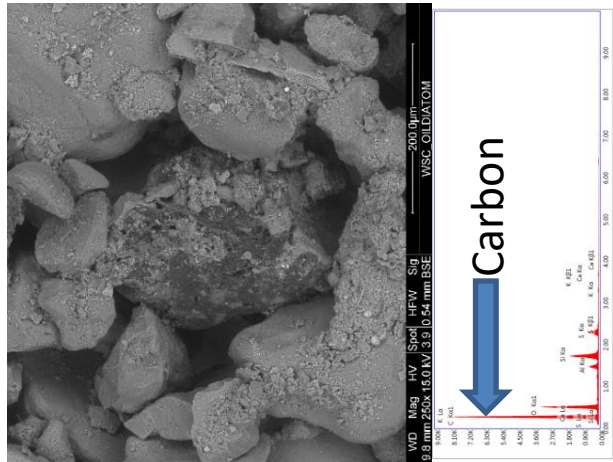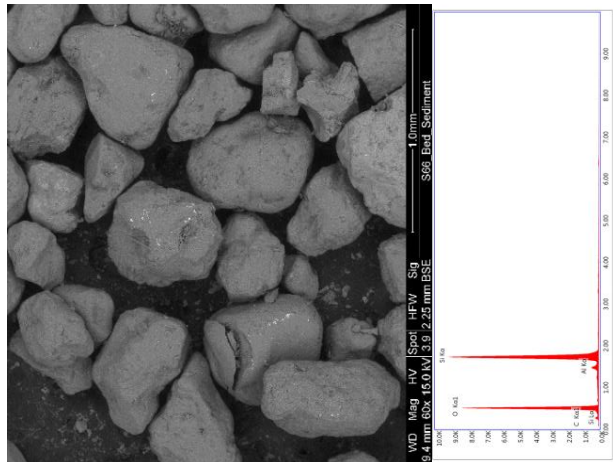
Figure 3: Scanning Electron Microscope images revealing hydrocarbon content in bed sediments of CF-Low (Left), MF-Med (Middle), and MF-High (Right). Associated EDAX analysis histograms reveal correspondingly high peaks of carbon indicative of a hydrocarbon signature. Note, the interstitial black seen in CF-Low (left) is the carbon backing tape on the SEM stub.
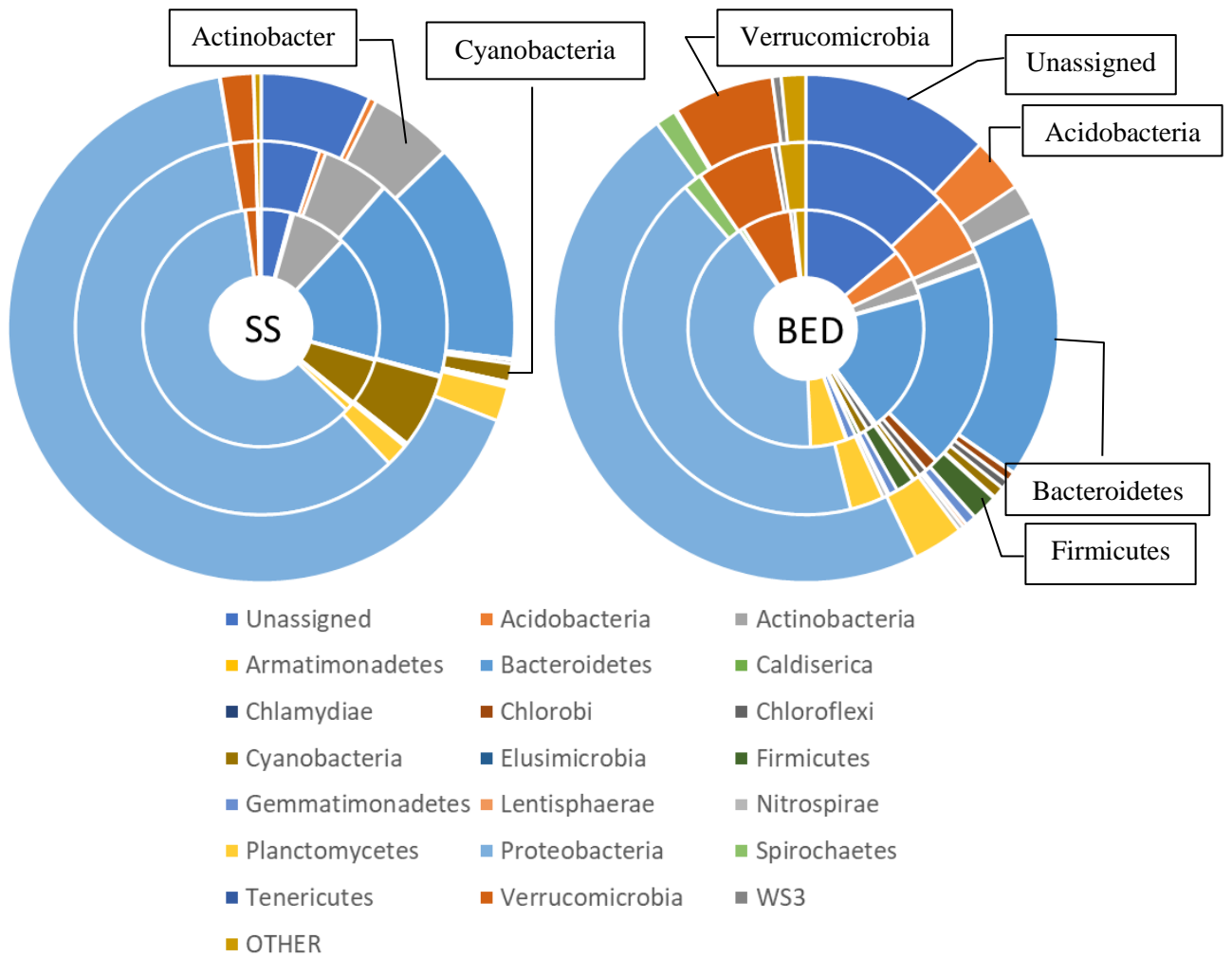
Figure 4: Phylum level normalized abundances (DESeq2) for SS (left) and bed sediments (right). Inner data series represents CF-Low; Middle series MF-Med; Outer series MF-High.
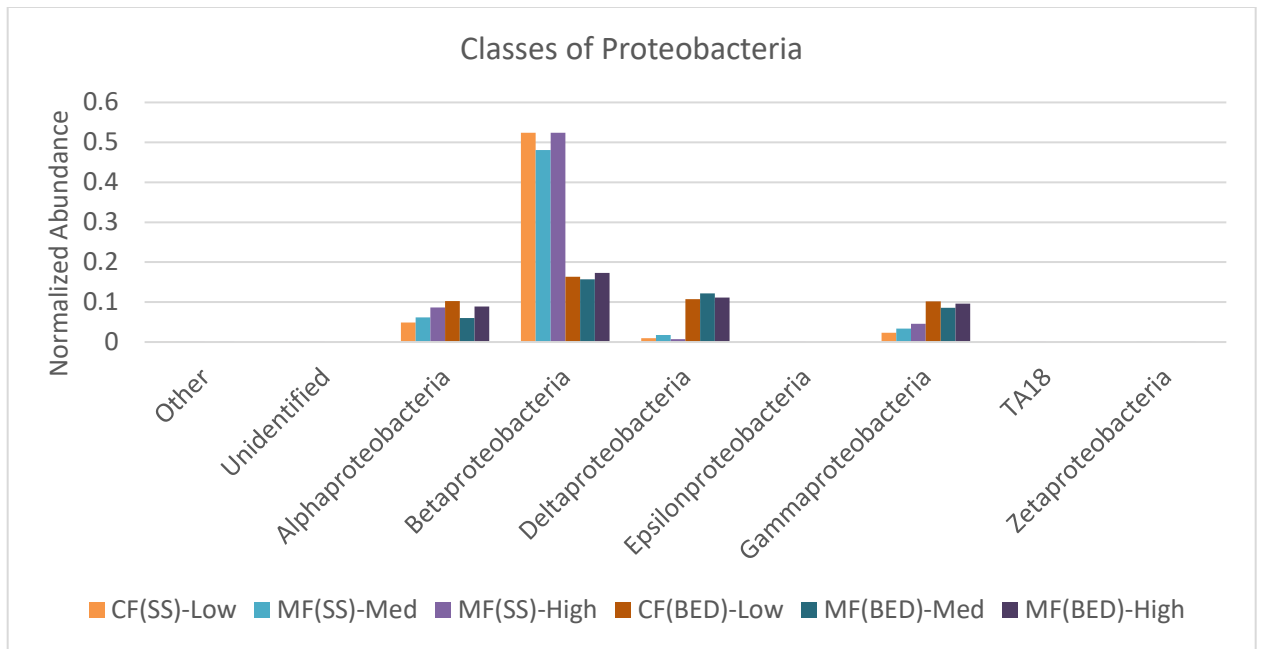
Figure 5: Distribution of Proteobacteria classes within the SS and bed sediments of the STB
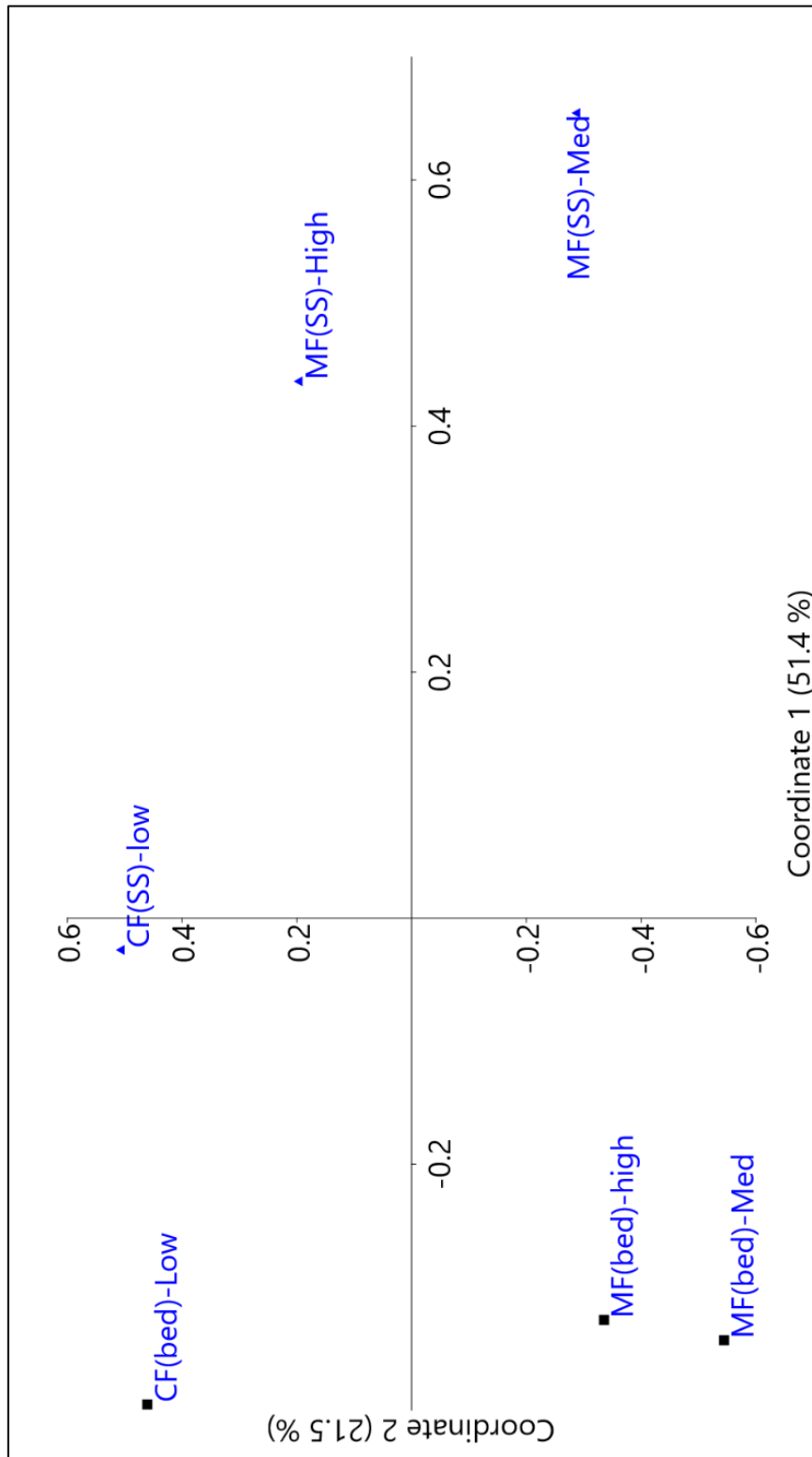
Figure 6: PCoA of Bray-Curtis similarity index of OTUs from both the bed and SS of CF-Low, MF-Med and MF-High
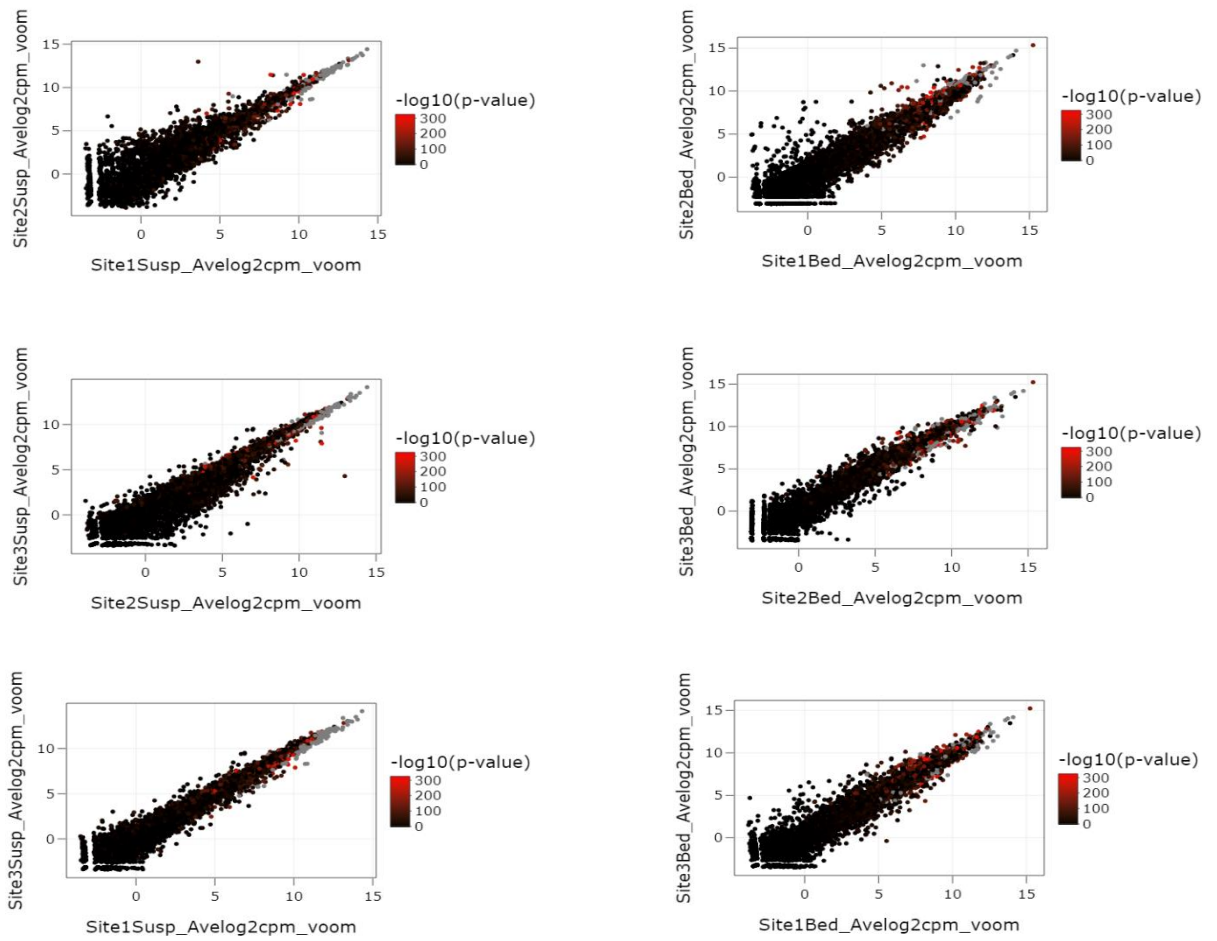
Figure 7: Scatter plots of gene expression fold changes between SS samples (left column) and bed samples (right column). Differential expression is evident especially in WSC, where there is a higher abundance of a diversified increase in expression (Note: Site 1: CF-Low; Site 2: MF-Med; Site 3: MF-High).
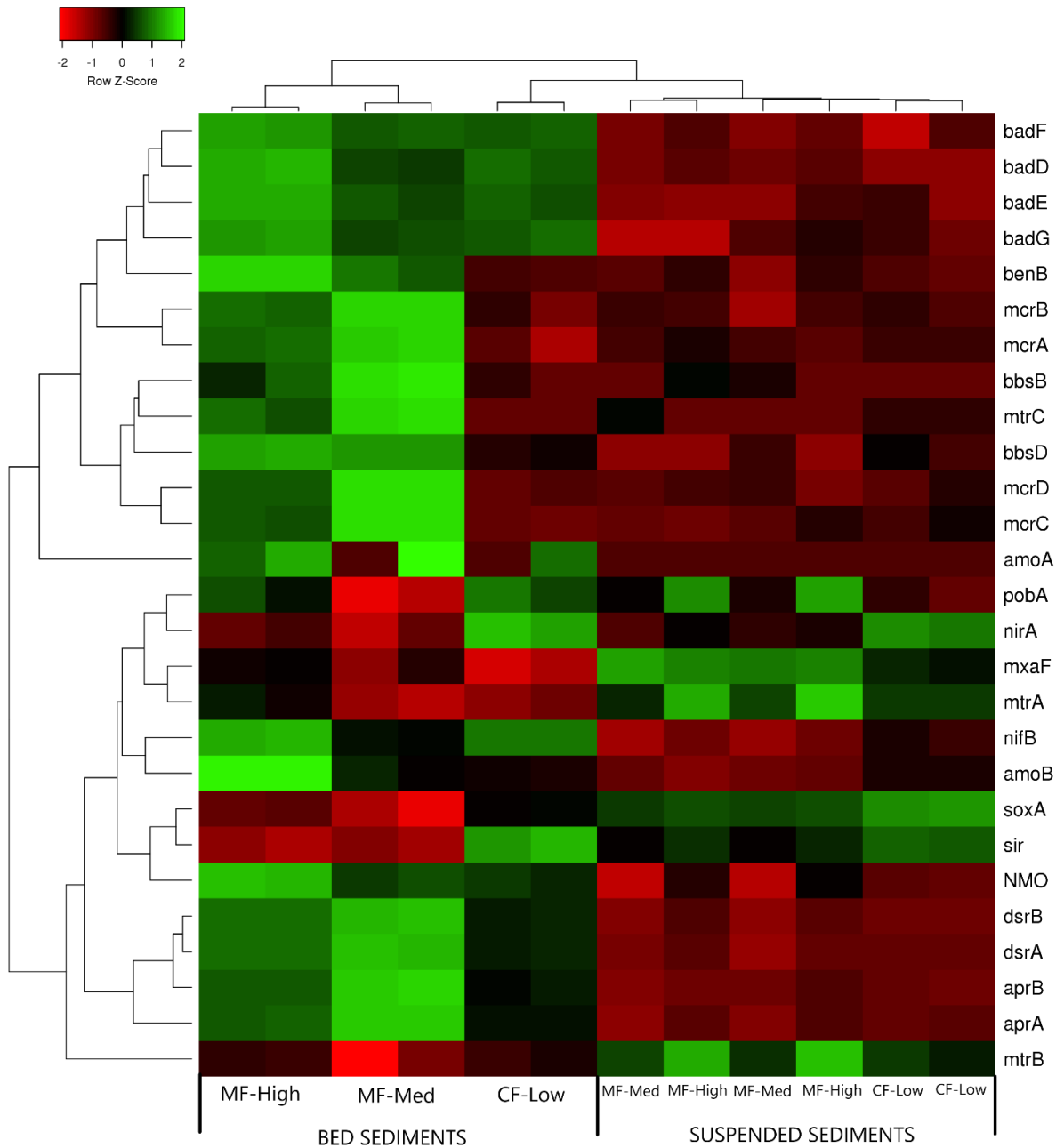
Figure 8: Expression heatmap with dendrograms from both genes and sample locations. Average linkage clustering was performed to identify clusters of genes that closely relate in terms of their expressional shifts down the STB River. Additionally, linkage clustering reveals spatial linkages between sample sites, as well as SS vs bed sediment locations.

References

Babicki, S., Arndt, D., Marcu, A., Liang, Y., Grant, J. R., Maciejewski, A., & Wishart, D. S. (2016). Heatmapper : web-enabled heat mapping for all, 44(May), 147–153. https://doi.org/10.1093/nar/gkw419

Caporaso, J. G., Kuczynski, J., Stombaugh, J., Bittinger, K., Bushman, F. D., Costello, E. K., … Knight, R. (2010). QIIME allows analysis of high-throughput community sequencing data. Nature Methods, 7, 335. Retrieved from https://doi.org/10.1038/nmeth.f.303

Culp JM, Droppo IG, di Cenzo P, Alexander-Trusiak A, Baird DJ, Beltaos S, Bickerton B, Bonsal B, Chambers PA, Dibike Y, Glozier NE, Kirk J, Levesque L, McMaster M, Muir D, Parrott J, Peters DL, Pippy K, Roy J (2018) Synthesis Report for the Water Component, Canada-Alberta Joint Oil Sands Monitoring: Key Findings and Recommendations. Oil Sands Monitoring Program Technical Series No. 1.1, 46 p. ISBN ISBN 978-1-4601-4025-3.

Dolan, M. E., Arp, D. J., Gvakharia, B., Sayavedra-Soto, L. A., & Bottomley, P. J. (2010). Nitrification and degradation of halogenated hydrocarbons—a tenuous balance for ammonia-oxidizing bacteria. Applied Microbiology and Biotechnology, 86(2), 435–444. https://doi.org/10.1007/s00253-010-2454-1

Droppo, I. G., di Cenzo, P., Power, J., Jaskot, C., Chambers, P. A., Alexander, A. C., … Muir, D. (2018). Temporal and spatial trends in riverine suspended sediment and associated polycyclic aromatic compounds (PAC) within the Athabasca oil sands

region. Science of the Total Environment, 626, 1382–1393. https://doi.org/10.1016/j.scitotenv.2018.01.105

Dworkin, M., Falkow, S., Rosenberg, E., Schleifer, K.-H., & Stackebrandt, E. (2006). The Prokaryotes 3rd - A handbook on the Biology of Bacteria - Ecophysiology and Biochemistry - Volume 2. The Prokaryotes. https://doi.org/10.1007/0-387-30742-7

Fowler, S. J., Toth, C. R. A., & Gieg, L. M. (2016). Community structure in methanogenic enrichments provides insight into syntrophic interactions in hydrocarbon-impacted environments. Frontiers in Microbiology, 7(APR), 1–13. https://doi.org/10.3389/fmicb.2016.00562

Gibson, J.J., Birks, S.J., 2016 Isotope-based partitioning of streamflow in the oil sands region, northern Alberta: Towards a monitoring strategy for assessing flow sources and water quality controls. J. Hydrol.: Reg. Stud. 5, 131-148.

Lezcano, M. Á., Velázquez, D., Quesada, A., & El-Shehawy, R. (2017). Diversity and temporal shifts of the bacterial community associated with a toxic cyanobacterial bloom: An interplay between microcystin producers and degraders. Water Research, 125, 52–61. https://doi.org/10.1016/j.watres.2017.08.025

Liang, B., Wang, L.-Y., Zhou, Z., Mbadinga, S. M., Zhou, L., Liu, J.-F., … Mu, B.-Z. (2016). High Frequency of Thermodesulfovibrio spp. and Anaerolineaceae in Association with Methanoculleus spp. in a Long-Term Incubation of n-Alkanes-Degrading Methanogenic Enrichment Culture. Frontiers in Microbiology, 7(September), 1–13. https://doi.org/10.3389/fmicb.2016.01431

Marwood, C. A., Smith, R. E. H., Solomon, K. R., Charlton, M. N., & Greenberg, B. M. (1999). Intact and Photomodified Polycyclic Aromatic Hydrocarbons Inhibit Photosynthesis in Natural Assemblages of Lake Erie Phytoplankton Exposed to Solar Radiation. Ecotoxicology and Environmental Safety, 44(3), 322–327. https://doi.org/10.1006/eesa.1999.1840

McKay, L. J., Hatzenpichler, R., Inskeep, W. P., & Fields, M. W. (2017). Occurrence and expression of novel methyl-coenzyme M reductase gene (mcrA) variants in hot spring sediments. Scientific Reports, 7(1), 1–12. https://doi.org/10.1038/s41598-017-07354-x

Meyer, F., Paarmann, D., D'Souza, M., Olson, R., Glass, E., Kubal, M., … Edwards, R. (2008). The metagenomics RAST server – a public resource for the automatic phylogenetic and functional analysis of metagenomes. BMC Bioinformatics, 9(1), 386. https://doi.org/10.1186/1471-2105-9-386

Naether, A., Foesel, B. U., Naegele, V., Wüst, P. K., Weinert, J., Bonkowski, M., … Friedrich, M. W. (2012). Environmental factors affect acidobacterial communities below the subgroup level in grassland and forest soils. Applied and Environmental Microbiology, 78(20), 7398–7406. https://doi.org/10.1128/AEM.01325-12

Nelson, J. W., Sklenar, J., Barnes, A. P., & Minnier, J. (2017). The START App : a web-based RNAseq analysis and visualization resource. Bioinformatics, 33(October 2016), 447–449. https://doi.org/10.1093/bioinformatics/btw624

Patricia J., W., Steven T., P., Anna M., M., & Klaus, N. (2007). Salinity constraints on subsurface archaeal diversity and methanogenesis in sedimentary rock rich in organic matter. Applied and Environmental Microbiology, 37(13), 4171–4179. https://doi.org/10.1128/AEM.02810-06

Reid, T., Chaganti, S. R., Droppo, I. G., & Weisener, C. G. (2018). Novel insights into freshwater hydrocarbon-rich sediments using metatranscriptomics: Opening the black box. Water Research, 136, 1–11. https://doi.org/10.1016/j.watres.2018.02.039

Reid, T., Droppo, I. G., Chaganti, S. R., & Weisener, C. G. (2019). Microbial metabolic strategies for overcoming low-oxygen in naturalized freshwater reservoirs surrounding the Athabasca Oil Sands: A proxy for End-Pit Lakes? Science of The Total Environment, 665, 113–124. https://doi.org/10.1016/j.scitotenv.2019.02.032

Reid, T., VanMensel, D., Droppo, I. G. G., & Weisener, C. G. G. (2016). The symbiotic relationship of sediment and biofilm dynamics at the sediment water interface of oil sands industrial tailings ponds. Water Research, 100, 337–347. https://doi.org/10.1016/j.watres.2016.05.025

Stein, L. Y., & Klotz, M. G. (2016). The nitrogen cycle. Current Biology : CB, 26(3), R94-8. https://doi.org/10.1016/j.cub.2015.12.021

Urakawa, H., Rajan, S., Feeney, M. E., Sobecky, P. A., & Mortazavi, B. (2019). Ecological response of nitrification to oil spills and its impact on the nitrogen cycle. Environmental Microbiology, 21(1), 18–33. https://doi.org/10.1111/1462-2920.14391

Vigneron, A., Bishop, A., Alsop, E. B., Hull, K., Rhodes, I., Hendricks, R., … Tsesmetzis, N. (2017). Microbial and isotopic evidence for methane cycling in hydrocarbon-containing groundwater from the Pennsylvania region. Frontiers in Microbiology, 8(APR), 1–12. https://doi.org/10.3389/fmicb.2017.00593

Volik, O., Petrone, R. M., Wells, C. M., & Price, J. S. (2017). Impact of Salinity, Hydrology and Vegetation on Long-Term Carbon Accumulation in a Saline Boreal Peatland and its Implication for Peatland Reclamation in the Athabasca Oil Sands Region. Wetlands, 1–10. https://doi.org/10.1007/s13157-017-0974-5

Warren, L. A., Kendra, K. E., Brady, A. L., & Slater, G. F. (2016). Sulfur Biogeochemistry of an Oil Sands Composite Tailings Deposit. Frontiers in Microbiology, 6(February), 1–14. https://doi.org/10.3389/fmicb.2015.01533

Willumsen, P. A., Johansen, J. E., Karlson, U., & Hansen, B. M. (2005). Isolation and taxonomic affiliation of N-heterocyclic aromatic hydrocarbon-transforming bacteria. Applied Microbiology and Biotechnology, 67(3), 420–428. https://doi.org/10.1007/s00253-004-1799-8

Yergeau, E., Lawrence, J. R., Sanschagrin, S., Waiser, M. J., Darren, R., Korber, D. R., … Darren, R. (2012). Next-generation sequencing of microbial communities in the athabasca river and its tributaries in relation to oil sands mining activities. Applied and Environmental Microbiology, 78(21), 7626–7637. https://doi.org/10.1128/AEM.02036-12

Zedelius, J., Rabus, R., Grundmann, O., Werner, I., Brodkorb, D., Schreiber, F., … Widdel, F. (2011). Alkane degradation under anoxic conditions by a nitrate-reducing bacterium with possible involvement of the electron acceptor in substrate activation. Environmental Microbiology Reports, 3(1), 125–135. https://doi.org/10.1111/j.1758-2229.2010.00198.x

CHAPTER 5: **EVALUATING GAMMA IRRADIATION TREATMENTS FOR THE**

PROMOTION OF EARLY TAILINGS RECLAMATION

5.1 Introduction

The hot-water extraction of bitumen from the Athabasca Oil Sands results in a tremendous accumulation of fluid fine tailings (FFT), containing sands, clays and residual bitumen. As the extraction process proceeds, companies recycle the oil sands process affected waters (OSPW) to limit freshwater consumption. This recycling however, causes an accumulation of salts, solvents and other contaminants, leaving the FFT saline, alkaline and toxic to many organisms. The FFT is pumped into large settling basins, often exhibiting unique characteristics depending on ore substrate, extraction procedure and simply the operator (i.e. company extracting the bitumen). As particulates settle out of the water column, the resulting cap water, in some instances, is removed and recycled into the extraction process once again. Given the immense scale of the mining operations, the management of these tailings basins remains an ongoing concern, alongside determining efficient and sustainable means by which to clean up these environments.

Over the past several years, studies have characterized active tailings ponds in the region. Though harboring variations in their chemical and biological signatures, their overall biogeochemical signature remains constant, with highly saline and alkaline waters, overlying fine particulates and matured fine tailings (MFT), governed by a diverse chemotrophic and methanogenic microbial community. The highly reducing nature of tailings environments (i.e. high sediment oxygen demand) creates high sulfide and methane zones, characterized previously in several other studies. However, recently methanotrophic organisms have been shown to consume methane, thus the concern over high methane production may not be as pressing as previously thought. Additionally, high sulfide production is another issue of concern, though studies have also shown that this is not always the case, as HS can be quickly sequestered through FeS mineralization below the sediment-water interface. Despite these

lingering questions regarding their geochemical nature, these ponds are destined for reclamation, though there remains ambiguity as to what this reclamation end-point will be or behave like in a biogeochemical context.

Given the scale and extent of current tailings pond basins, alongside the obviously continued extraction of bitumen into the future, there is immense need to find suitable ways to deal with these waste materials, with the end-goal of full landscape reclamation. The complex ionic composition, alongside the unique microbial consortia residing within them require unique treatment options to either promote or speed up reclamation time-lines. One constituent of the tailings material that has garnered much attention in the literature are compounds called naphthenic acids. These complex compounds are a group of carboxylic acids ranging from 120 to >700 amu, of both linear and cyclic structure. Their breadth of diversity creates an analytical nightmare, making individual compounds extremely hard to characterize. NA today generally refer to any carboxylic acid found in petroleum systems. Treatment technologies such as ozonation, ultraviolet (UV) radiation and microbially driven bioreactors have attempted to treat tailings to degrade these toxic organic acids, though remain relatively inadequate. The turbid nature of the tailing's slurry restricts the penetration of ozone and UV, therefore fail to fully penetrate and treat the entire tailings slurry. Further, given the immense volumes of particulate tailings wastes (i.e. sands, clays and residual bitumen), treatment of just OSPW is an inadequate treatment option moving forward.

In 2013, Chen et al., began using gamma irradiation (GI) as a sterilization procedure for laboratory scale tailings evolution studies. Measuring the NA signature before and after sterilization revealed that the GI treatment reduced the NA signature by upwards of 96% in both the OSPW and FFT. Boudens et al., 2016, then compared the evolution of two tailings

materials, both treated and untreated with GI, again seeing a significant depletion of the parent NA signature after treatment. VanMensel et al., 2017, during a sister study, examined the microbial consortia after GI and re-inoculation of the original microbial community, and determined that the GI treatment appeared to promote the chemotrophic community largely responsible for biodegradation of organics. However, given the relatively controlled laboratory experimentation, and constrain to a year-long-study, a scaled-up study is needed to truly verify the efficacy of this GI treatment. There remains doubt as to the long-term outcome of such treatment, and how it is promoting reclamation in a biogeochemical context.

This study seeks to expand on and validate the findings of both Boudens et al., 2016, and VanMensel et al., 2017, in a field-based, mesocosm experiment north of Fort McMurray, Alberta. Several different tailings sources, alongside natural wetland controls, both treated and untreated, are compared over a three-year field-based study, in a long-term assessment of their evolution/maturation. In addition, this chapter allows for the confirmation of correlations between natural environments as discussed in the previous chapters. A holistic comparison of both GI treated, and untreated tailings seeks to compare reclamation timelines over a longer, 3-year observation period. Results hope to provide insight into how GI treatment may promote a more rapidly remediated ecosystem compared to untreated materials, and the potential for sediment amendments (combining tailings with natural sediments) to speed-up reclamation timelines.

5.2 Methods

5.2.1 Experimental Setup

Oil sands process affected material (OSPM) (constituting both OSPW and FFT) was sourced in the summer of 2014 from two ponds belonging to Suncor's mining operation (P1A

and STP), alongside material from both Syncrude and Shell. These tailings ponds ranged from approximately a decade old to nearly 50 years of age, representing varying levels of pond maturity. Half of the tailings material was GI according to protocols explained prior (Boudens et al., 2016; Reid et al., 2016). Further, natural wetland sediments were collected from regional wetlands of varying geochemical character (i.e. salinity, conductivity etc.), in order to compare evolution and amendments combining both tailings and natural sediments for reclamation purposes. The breakdown of all mesocosm systems is found in Table 1.

Experimental mesocosms were initiated in October 2014, consisting of 16 litres of sediment, 20 litres of water, equating to approximately 10 cm of sediment depth, 15 cm of overlying water. The mesocosms were 68 L Rubbermaid Roughneck totes, arranged at random on the Experimental Trenches location on the Suncor lease site. Mesocosms, with a surface area of approximately $0.25 \ m^2$, were left open to atmospheric influence, allowing for natural inoculation mimicking regional atmospheric effects. As outlined in table 1, tailings sediments were amended/inoculated with 10% equal proportion of all other sediments and waters (both tailings and wetlands), in attempt to mimic conditions of EPL establishment, where similar blending of sediments would take place. Mesocosm water levels were carefully monitored to maintain adequate overlying water levels.

5.2.2 Geochemical Monitoring/Sampling

Bulk water and sediment samples were collected at time 0, 9 months, 11 months, 22 months and 31 months from the onset of the experiment in October 2014. Approximately 250 ml were sent to the Syncrude Research Laboratory in Edmonton, Alberta for each timepoint for chemical analysis (metals, anions, alkalinity, NAs). Elemental analytes measured are listed in Table 2, with the remainder of the geochemical data in Appendix D.

146

Further, a subset of samples was analyzed for NA concentration by gravimetric analysis. Additionally, yearly microsensor measurements measured the dissolved oxygen and hydrogen sulfide gradients and redox potential across the interface of each tailings mesocosm, and a subset of the wetland mesocosms, where plant debris did not inhibit safe manipulation of the microsensors. Microsensor measurements were performed using the H2S, DO, and REDOX sensors from Unisense A/S (Aarhus, Denmark), according to (Boudens et al., 2016; Reid et al., 2016) and slightly modified manufacturer protocols.

5.2.3 Microbial Community Sampling and Extraction

Sediments were collected from central locations within each mesocosm by coring with sterile, modified pipettors, with the conical tip removed. Sediments were placed into sterile 5 ml cryotubes, and flash frozen on site in liquid nitrogen. Samples remained frozen in liquid nitrogen until returning to the lab, where they were stored at -80 $^{\circ}$C until extractions were performed.

DNA was extracted from the collected samples using the MOBIO Power Soil DNA Extraction Kit (MOBIO Laboratories, Carlsbad, CA, USA), followed by amplicon targeting (PCR1) V5/V6 primers (Table 3) to explore the 16S rRNA region of each sample. Reactions were performed in 25 μL volumes containing 1 μL of template DNA, 10 mM of both forward and reverse primers, a final concentration of 10 mM for all four deoxynucleoside triphosphates, 2.5 mM of MgCl2, 0.3 μM DMSO, 1 mg/mL bovine serum albumin (BSA), and 1X buffer solution. DNAase-, and RNAase-sterile H2O was then added until the desired volume is reached. The PCR1 thermocycle was set according to the following: initial denaturation for 5 min at 95 °C followed by 34 cycles of 15 s at 94 °C, 15 s at 48 (bacteria), and 30 s at 72 °C, and a final extension of 1 min at 72 °C. AMPure bead purification was

then used according to the manufacturer's protocol for the pooling and purification of the three amplicon products. A second PCR was then performed for barcoding each of the samples (PCR2), using a unique barcode for each sample as the forward primer and a universal reverse primer referred to as UniB-P1 (Table 3). This second PCR used the same parameters as PCR1, though with only a total of 7 cycles. These PCR2 products were pooled accordingly (based on gel electrophoresis band intensity for normalization purposes) and cleaned once again with the AMPure bead purification protocol. These condensed samples were subjected to a slow gel electrophoresis using TAE buffer and the desired product was obtained via Qiagen Gel Extraction kit following the manufacturer's instructions. Agilent 2100 Bioanalyzer was utilized for DNA concentration and purity determination. The samples were diluted to 25 ng/μL and combined in preparation for the Ion Torrent Personal Genome Machine (Life Technologies).

5.2.4 16S rRNA Amplicon Sequencing Bioinformatics

After sequencing, sequence files were run through the Qiime (v1.9.1) pipeline (Caporaso et al. 2010). Raw read files were quality filtered, demultiplexed, clustered into representative OTUs, and analysed for diversity and statistical analyses. Specifically, sequence reads were cutoff using a phred quality score of 20. Further, sequences were removed if under 100 bp, and above 500 bp. OTUs were clustered using the UCLUST algorithm within Qiime at a 97% similarity threshold. Taxonomy was assigned at an 80% match cutoff.

5.3 Results and Discussion

5.3.1 Water Chemistry

Geochemical characterization of water samples for all samples indicated dominant divergent groupings for both wetland and tailings sediments, especially early on in the study (Figure 1). Drivers of this difference were largely attributed to the high salinity, heightened alkalinity, lower particle size distributions and elevated NA concentrations with the tailings systems. Visualizing these comparisons with Principal Components Analysis (PCA) reveals how dominant these groupings are, and the true dominance of several of the geochemical parameters measured, in driving these changes. There are clearly correlations between this and other studies with respect to the heightened salinity and NA concentrations measured here (Boudens et al., 2016; Reid et al., 2016a). There is no doubt that these are perhaps two of the most significant aspects of the tailings ecosystems impacting the reclamation potential into the future.

The subsequent sampling times at 9, 11, 22 and 31 months revealed interesting trends in the overall geochemical signature of the tailings systems alongside the wetland counterparts. There appeared to be a stepwise decrease in overall dissimilarity between all systems moving towards the 31-month time-point (Figure 2). The variability observed at time 0 on the PCA quickly shrank to relatively small clusters by the end of the study period, representing a natural tendency for the tailings to trend towards a more natural biogeochemical nature over time. What is most intriguing, is that regardless of the G+ or G- nature of the tailings systems, all systems showed similar trends towards a more closely related geochemical signature nearing the 3-year mark. This may suggest a gradual decline in the dewatering effects of the consolidating FFT, therefore limiting the natural variation in geochemical signatures between ponds. The progression of these tailings ecosystems towards

149

juvenile EPLs in recent research have suggested this decrease in dewatering and gradual increase in oxygen concentrations are indeed the primary dynamics driving this initial change (Risacher et al. 2018).

5.3.2 Naphthenic Acid Concentrations

Total NA concentrations of OSPW were measured in each tailings system to understand its temporal breakdown with and without GI treatment (Figure 3). Treating tailings and wetlands as larger respective groups, it is clear that the GI treatment, as noted in previous studies, significantly reduces the overall concentrations by ≥ 50 % in all source materials (Boudens et al., 2016; Chen et al., 2013). Individual concentrations of NA per system are provided in Appendix D, table D-3. At time 0, G- tailings sources measured between 57 and 69 ppm of NA, while G+ tailings measured between 5 and 29 ppm. Syncrude and STP material showed the greatest response to the GI treatment in terms of NA reduction, measuring over a 90% reduction, while P1A was reduced by approximately 50%. Though still a significant reduction, P1A has been shown in previous studies to respond less to the GI treatment than other systems, perhaps due to the recalcitrant nature of the NA compounds within it (Boudens et al. 2016). P1A is the oldest of these tailings sources, therefore it would be assumed that the more readily degraded NAs would already be broken down, leaving only those more recalcitrant compounds resistant to degradation processes. These results appear to closely follow those of Boudens et al., 2016, who noted similar reduction percentages between STP and P1A. This replication of results appears to enforce that this GI treatment for the reduction of toxicity as attributed to the NAs is actually extremely effective and efficient in not only semi-controlled laboratory studies, but also field-scale mesocosms.

There is no refuting the effectiveness of this treatment in the reduction of NAs, as shown in both this and prior laboratory studies (Boudens et al. 2016).

Residual breakdown for the subsequent 31-months was also observed, both for G+ and G- systems. However, it should be noted that this residual breakdown cannot be attributed to a single causal process. It could be assumed however, that either a) UV penetration into these open-air systems caused further breakdown over time, and/or b) the constituent microbial community could have been slowly metabolizing these compounds during the course of this study. Both processes are highly likely, as they have been noted to be effective at breaking down NAs. Regardless, the decreasing trend in the G+ systems was not well defined, with an R^2 value of only 0.076. On the other hand, though the G- treatments exhibited heightened NA concentrations at time 0, these concentrations appeared to quickly decline over the course of the 32-week study. It is interesting to note that by time 32, or the completion of this study, the concentrations of both the G+ and G- systems were indistinguishable. This would indicate that in these field mesocosms, there was considerable natural breakdown of the NAs over the course of 32 weeks. Given recent studies suggesting that microbes can break down some of these compounds, alongside those that affirm UV breakdown, it would be reasonable to assume that both processes were present in these systems.

The converging trends in the concentrations of NAs within both the G+ and G- mesocosms provides interesting insight into the reclamation timelines governing these complex tailings. First, it is interesting to note that there was effectively little residual breakdown of NAs following G+ treatment. This would presumably be attributed to the complex and robust nature of the remaining NAs, and their highly resilient nature to bio-or

151

UV-degradation. On the other hand, the relatively sharp and defined decrease in concentrations of the G- systems indicates that there was considerable natural degradation of NAs over time. It would be interesting and advantageous to study how these concentration decreases are affected in larger, deeper systems, where sunlight would not penetrate as effectively as these mesocosms. This would limit the possibility of UV degradation if this is in fact what is responsible for some of the natural degradation observed over these 32 months of study. This may be the only study to date, as far as we are aware, that provides effective results on the degradation of NAs over time, not reliant on commercial surrogates or laboratory incubations proven to be unreliable.

5.3.3 Sediment Characterization

Sediments were sub-sampled at the initiation of the experiment, to gain an understanding of the fundamental differences between tailings source, G+ vs G- treatment and tailings vs natural wetland sediments. Analyses present interesting correlations between all tailing's sediments, whereby their geochemical and physical characteristics are all largely represented by high NaCl content, the presence of NAs, and general alkalinity (Figure 4). It appeared as though the Na and Cl content were particularly significant drivers in this signature, more so than any other parameter measured. In an inland, boreal setting, this is particularly relevant, where this saline condition is significantly different from the natural freshwater systems in the region. The highly saline nature within these tailings ecosystems can fundamentally alter the natural biogeochemistry compared to their natural baseline counterparts, thus representing a significant hurdle in the reclamation process.

Analysis of grain size distribution (Figure 5) also revealed that the tailings materials contained more variable, and proportionally higher amounts of small grained particulates –

152

silts and clays – responsible for long settling times evident in many tailings ponds, particularly STP. These small particles provide ample surface area for cellular fixation, thus have been shown to contain ample microbial biomass. However, these same particulates make clean and efficient nucleic acid extraction extremely difficult. The charged nature of these clay particles cause them to preferentially co-precipitate with nucleic acids. Overall, the presence of these fine-grained clays and silts has been a long-time issue within these tailings ecosystems, given their tendency to remain suspended within the water column. It is this increased turbidity that presents another major reclamation hurdle, and one which has been studied quite extensively recently, in attempt to speed up the consolidation process (J. Liang et al. 2014; Siddique et al. 2014).

5.3.4 Physico-chemical Gradient Analysis
5.3.4.1 Temporal Dissolved Oxygen Dynamics

Unlike previous laboratory studies, these open-air mesocosms more closely mimic the natural environments of these various tailings and wetland ecosystems. Therefore, there was a consistent influx of oxygen into the overlying water columns, offsetting the oxygen consumed within the sediments. This ample influx of atmospheric oxygen likely contributed to the fact that no tailings sediments experienced complete water column depletion of DO, with the lowest water column concentrations at the 9-month sampling period measuring approximately 150 µmol/L in STP Sterile G+ and Syncrude G+ (though the latter increased in oxygen closer to the sediment interface) (Figure 6). These results appear to closely match those observed by both Boudens et al. (2016) and Reid et al. (2016), noting no fully depleted DO concentrations in those studies. Only the Golden G+ and G- systems experienced any sort of dramatic consumption of DO, ranging from only 45 – 70 µmol/L of DO at this time

point, perhaps relating to relatively increased concentrations of both PO4 and SO4 in these sediments, causing an enhancement to oxygen consuming processes. The fairly hypoxic conditions of the Golden G- and G+ systems indicates a highly reducing environment, with significant sediment oxygen demand (SOD).

Comparing G-, Sterile G+, Inoc G+ and G+ tailings systems, there appeared to be no clear correlation in hierarchy of DO concentrations across their respective sediment-water interfaces. Similar findings were found in a sister study, whereby no significant differences in water column DO and calculated net ecosystem productivity (Dings-Avery, 2018). However, both Syncrude and P1A showed increased water column concentrations in the Sterile G+ and Inoc G+ systems, while STP revealed the inverse, where G- and G+ were the highest DO concentrations in the water. This may be attributed to the relative age of these respective tailings sediments, where STP is generally considered a younger sediment, as opposed to those of P1A and Syncrude which are more matured and consolidated. The fact that the G- and G+ of Syncrude and P1A induced an enhancement in the SOD at this time point suggests that the inoculum mixture had a direct effect on the oxygen dynamics across the interface. This mixture of both wetland and other tailings clearly provided another organic nutrient source, which induced a slightly more rapid oxygen consumption, alongside the untreated (G-) tailings of Syncrude and P1A.

By the 22-month sampling period, DO trends appeared to be relatively similar with a few exceptions (Figure 7). P1A measured the highest water column DO concentrations in G+, G+ sterile and G- mesocosms, whereas the lowest were in the G- Sterile and G+ inoc systems. P1A also measured the highest concentrations of all of the tailings mesocosms, followed by STP, Syncrude, then Shell. Syncrude G+ sterile measured very low DO

154

concentrations indicative of hypoxic conditions, interestingly only somewhat lower than the corresponding G- Sterile mesocosm. This would suggest an oxygen consuming process largely governing the Syncrude G+ and G- sterile mesocosms as this point in time. Here it would appear as though amending the Syncrude FFT with natural wetland inoculum may actually be beneficial, maintaining a suitable concentration of DO within the water column. Examination of the DO profiles within the various wetland mesocosms show the same sort of variability discovered at the 9-month sampling period. There was a similar trend in the slopes of oxygen consumption, though Saline G+ and Muskeg G+ both measured the lowest cap-water concentrations of only approximately 160 – 180 µmol/L. The remainder of the wetland mescocosms showed relatively higher concentrations of DO in the overlying water column, all of which exceeded 250 µmol/L.

The summer of 2017 was the final sampling period for the field-mesocosm experiment. Concentrations observed were consistent with those from the 22-month sampling dates, with overlying water concentrations measuring from 180 – 250 µmol/L (Figure 8). As such, there is a consistent concentration of DO within the tailings systems vertically down to the sediment-water interface, suggestive of the likelihood of maintaining a suitable environment for aerobic organisms into the future. Considering that these measurements represent a static, closed mesocosm system, and are not designed from a dynamic perspective (i.e. open to wind and wave action), one would expect that these DO measurements would increase due to potential atmospheric mixing within a dynamic regime.

5.3.4.2 Hydrogen Sulfide

At the initial sampling period in the summer of 2015, marking the first summer since initiation of the field mesocosms, hydrogen sulfide (total H_2S & HS^-) production appeared

minimal with a few exceptions (Figure 9). It should be noted that the hydrogen sulfide sensor is light sensitive, therefore the heightened concentrations in the overlying water column are attributed to light interference. Further, alkaline conditions dictate that the majority of the sulfide present in all systems is in the form of HS^-. Both Syncrude and STP sediments all exhibited lower HS^- production, but P1A measured up to approximately 50-60 µmol/L in G-, sterile G+ and inoc G+ systems. This correlates with previous lab studies where similar, albeit consistently lower concentrations were measured there (likely attributed to the small-scale, controlled lab conditions) (Boudens et al. 2016; Reid et al. 2016). Wetland sediments all exhibited similar trends, peaking at approximately 60 µmol/L, except for both Golden G- and G+ where 1750 – 2000 µmol/L of HS^- were measured approximately 10 mm below the interface. These were extremely high values, and surprising given the relatively low concentrations measured in all other systems, though appear to correlate to other natural systems indicative of high production zones (Brüchert et al. 2003; Kuwabara et al. 1999).

The 2016 sampling period showed slightly different trends with respect to the HS^- dynamics across the sediment-water interface (Figure 10). It was clear that after 22 months of incubation in the field, there were heightened concentrations of HS^-, in specific treatment totes. First, P1A measured generally under 100 µmol/L in G-, G- sterile, and G+ mesocosms, though between 500 and 750 µmol/L at 40 mm depth in the G+ inoc and G+ sterile systems. This in an interesting observation given that the G+ mesocosm measured no increased HS^- production. This would suggest that the inoculum used after GI treatment may be extremely influential in the sulfide dynamics within these systems as they progress towards matured, remediated states. Clearly the mixed inoculum and strict tailings inoculum of these two totes were enough to stimulate a relatively active community of sulfur reducing microbes.

The Syncrude FFT systems also measured varied trends with respect to the HS^- gradients below the sediment-water interface. The highest measured system was the G+ mesocosm at up to 1250 µmol/L. This was followed by the G+ inoc and then the G- mesocosms measuring from approximately 375 – 650 µmol/L. Again, it is evident that by 22 months of incubation, there has been a clear onset of strong sulfide activity within select mesocosms. It should be noted however, that these concentrations do remain quite low within the overlying water column, suggestive of oxidizing processes at the interface, controlling the release of HS^- from the sediments. It is also interesting to note that for the Syncrude FFT, the G+ treatment appears to show the highest production of HS^-, again indicative of a response to the mixed inoculum. It would be reasonable to assume that since this mixed inoculum contained ample wetland materials, this would essentially be supply a host of valuable nutrients to the microbial community.

The remaining tailings systems, Shell and STP showed minimal signs of sulfide production compared to the other systems. The Shell G+ mesocosm measured only up to approximately 115 µmol/L approximately 10 mm below the interface, with STP measuring 130 µmol/L approximately 1.5 cm below. With respect to all tailings mesocosms, there appears to be a stimulation of sulfide production at the depth, though maintains a consistent concentration across the sediment-water interface.

Wetland sulfide measurements again revealed significant production of sulfides from the Golden G+ mesocosm, though very little in the Golden G- system unlike the first sample period. This could suggest a depletion of sulfide activity after that first year of incubation. What is more surprising is the extremely high concentrations measured in the High Sulphate wetland systems of both G- and G+. In this case, there is clearly a highly active sulfur

reduction process actively producing sulfides within the sediments. There is no distinguishable difference between the G- and G+ treatments, though both quickly reduce to near negligible concentrations once entering the oxic overlying water columns. These extremely high concentrations of sulfide are likely indicative of the 300 – 400 mg/L of sulfate measured, providing a increased sulfate pool compared to other systems. Further, it could be that it is this sediment, as part of the larger inoculum mixture, that is creating a spike in sulfide activity in the tailings systems mentioned earlier.

The final sampling period in 2017 marked the completion of the 32-month field mesocosm study. Again, only Syncrude and P1A measured any significant concentrations of HS$^-$. In these cases, Syncrude G-, G+ and G+ inoc measured up to approximately 336 µmol/L, 2000 µmol/L and 960 µmol/L, respectively, while P1A G+ sterile and G+ inoc measured up to approximately 585 µmol/L and 377 µmol/L but at a depth of approximately 50 mm below the interface. These concentrations are relatively consistent with the previous summer sampling date with respect to both Syncrude and P1A, with Syncrude showing slightly higher concentrations at 32-months. The remainder of the tailings and wetland systems measured minimal concentrations of HS$^-$ in comparison. The High Sulfate sediments were not measured due to sensor issues at this sampling time. It can be assumed however, that there would likely be a significant sulfide presence like the previous sampling period. Overall it is clear that there are specific systems exhibit varied sulfide characteristics likely governed by their underlying sulfate concentrations and available carbon substrates. Both tailings and wetland systems show a heterogeneity in this respect and should be noted when considering reclamation options. It is already known that these tailings environments are unique to operator and host ore, and as such, blanket reclamation approaches may not be a

reliable method of tailings remediation, especially when taking into consideration sulfide activity.

5.3.5 Microbial Community Structure

Since the onset of the tailing's ponds within the region, there have been efforts to effectively extract viable genetic material for the purpose of unravelling the in-situ gene *functions* of the diverse microbial consortia. However, this remains an extremely challenging endeavor due to an array of inhibitors present (i.e. high clay concentrations, hydrocarbons, salinity, humics to name a few), thus we present a brief overview of the microbial taxonomic structure at the onset of this mesocosm experiment. These results are further compared to the numerous other taxonomic surveys conducted in these tailings environments. For a comprehensive review and discussion on the microbes governing these systems, these authors turn the reader towards several excellent papers identifying the diverse organisms present in these systems, studied both in-situ and in laboratory microcosms assessments (Foght and Fedorak 2015; Reid et al. 2016b; VanMensel et al. 2017; Yu et al. 2018).

At the onset of these experiments, the microbial community composition was very similar to previous tailings studies, containing a host of microbial taxa known to inhabit these extreme ecosystems. Proteobacteria dominated the sediments, as was observed by VanMensel et al. (2017), followed by Actinobacteria, Bacteroidetes and Firmicutes (Figure 12). The elevated abundances of Proteobacteria in a relative sense compared to other phyla is not expected, as it is the most abundant and diverse phyla, with a near ubiquitous presence in soils, sediments and waters. On a comparative level, G+ tailings again showed similar increased abundances as discovered by VanMensel et al. (2017), noting increases in organisms responsible for both hydrocarbon, sulfur and metals cycling. What is interesting

to note is that the organisms most enhanced the G+ treatments consisted of Beta, Delta and Gammaproteobacteria, though the overall abundance of Proteobacteria reduced slightly compared to other phyla. G+ treatment appears to also be responsible for increased abundances of Bacteroidetes and Firmicutes, particularly the families of *Flavobacteriaceae* and *Clostridiaceae* respectively, perhaps resulting in the noted decline overall in Proteobacteria. *Comamonadaceae* families (Betaproteobacteria) appeared to be the most affected by the GI treatment, with notable increases in the G+ vs G- systems overall. This facultative anaerobe has been observed in many other tailings studies and is noted for its diverse functional abilities. As noted in VanMensel et al. (2017) and further observed here, the increased Bacteroidetes abundance appears to be a direct result of the GI treatment, promoting this specific taxon increase, noted for their abilities to degrade complex organics.

Overall, these taxonomic assessments appear to corroborate these studies previously identifying microbial organisms within these tailings environments and surrounding natural landscapes (VanMensel et al. 2017; Wilson et al. 2016; Yergeau et al. 2012). It is interesting to compare these taxonomic variations with the significant geochemical differences, as one would perhaps expect to see greater variation in the microbiology as a result. The resilience of the core microbiome observed within these and other studies suggests that there may be more functional plasticity associated with the observed taxa, that taxonomic assessments alone fail to unravel. As such, there must be careful consideration in the analysis of taxonomic analyses, given that our theoretical understanding of the functional abilities of specific microbes are rapidly shifting. Advancements in high-throughput sequencing technologies have allowed researchers to observed the diverse functional plasticity and cooperative metabolic networks governing natural systems, revealing just how complex the

microbial world truly is. It is now understood and observed in many regions (see Ch. 3-5), that the notion of a taxonomic unit, is perhaps more representative of a shuttle for transferring functional genes between species. The close proximity in which microbes operate creates an ideal opportunity for horizontal gene transfer, thus our theoretical approach to understanding, say for example, sulfate reducing bacteria, goes well beyond the simple function of reducing sulfate. We now understand these microbes can be involved in an array of redox processes all the way up and down the redox ladder as we know it. Additionally, we now know that these microbes are capable of novel degradation pathways for an array of compounds. Therefore, we must caution ourselves when we try to associate too many processes based on identity alone. Though this identity is certainly valid, it is the theoretical understanding of *what* that microbe does is what is perhaps limited. Ongoing studies both in the laboratory and in-situ are helping microbial ecologists to slowly but surely unravel this complex microscopic world.

5.3.6 Insights into Temporal Reclamation of Tailings

This 3-year study provided interesting insight into the natural evolution of not only tailings sediments, but also natural wetland sediments collected from the region. Particularly evident was the quite significant difference in the physico-chemical gradients and geochemical characteristics measured between tailings and wetland sediments. The abundance of organics within the wetland sediments, and likely diversified microbial consortia resulted in several mesocosms expressing significant concentrations of sulfide from within the sediments. If sediment amendments are to be used as a reclamation aid, their own biogeochemical attributes could cause inadvertent metabolic effects, potentially increasing greenhouse gas or other toxic gas emissions long-term. It would vital in this case

to have a thorough characterization of these amendments prior to mixing, therefore much research is still needed to characterize these natural wetland sites at a biogeochemical level.

The dynamics of the DO concentrations across the sediment-water interface provided interesting insight into a semi-naturalized mesocosm's oxygen demand over the course of 32-months. What is clear is that the GI treatment generally does not appear to either positively or negatively affect the consumption of oxygen within the sediments, despite a perceived increase in taxa responsible for biodegradation processes. Given lack of replicates at given time points, it is hard to make inferences overall with respect to the treatment conditions best able to maintain the most or least DO within the overlying water columns. Further, without a strong influence of wind and water disturbances, these concentrations should be considered as minimal endpoints. One would likely observe higher influx of DO within these water columns if experiencing disturbances from wind/wave action. Additionally, deeper water columns would inevitably experience seasonal turnover that could induce elevated upward diffusion of compounds from below the sediment-water interface. Furthermore, there is an inevitable temperature variable within these mesocosm totes, as they receive direct sunlight exposure daily. This would inevitably induce significant diurnal temperature fluctuations that would be unlike those within deeper reservoirs, pond or lake environments.

The long-term spatial-temporal variations in HS^- concentrations between source materials provides interesting insight into the heterogeneity of these tailings environments. Similar results to past studies were observed early on, though shifted slightly as the study progressed. Most notably, elevated concentrations were observed in P1A G+ sterile and G+ inoc, and Syncrude G+ and G+ inoc. Additionally, High Sulphate (G+ and G-) and Golden

G+ wetland systems measured extremely high concentrations in the second summer of sampling. These heightened HS⁻ concentrations of P1A were also observed in prior lab studies, perhaps resulting from its maturity and feasible substrate for sulfidic activity (Reid et al. 2016). This temporal change noted between seasons indicates that the sulfide dynamics measured short-term may be inadequate to accurately predict dynamics long-term. The maturation of these sediments over the course of these three years appeared to provide more time for HS production, though this could be attributed to the establishment of the sulfidic zone as observed in other tailings systems (Chen et al. 2013b; Fru et al. 2013). Though there have been shown to be sequestration of sulfides within sulfidic redox zones of these tailings materials (Chen et al. 2013b; Reid et al. 2016), alteration to the natural biogeochemical cycles and the associated sulfide oxidation that takes place should be avoided so as to not inadvertently create a hot spot for HS production out of these sediments. There is a potential to inadvertently cause increased HS production as a result of increased nutrients stemming from the amending of mixed sediments.

Overall these trends in the phyisco-chemical gradients of DO and HS, alongside the water and sediment geochemistry appear to correlate with other studies characterizing the early evolution of a juvenile EPL (Risacher et al. 2018). Their observations of the persistence of an oxygenated water column alongside notable sulfide concentrations provide a direct correlation to geochemical signature of a tailings pond preceding EPL establishment. It would be expected, that exposed to the dynamics of wind and wave action, alongside the open-system of a true EPL, that water column DO would likely continue to increase, assisted by the onset of photosynthetic activity (Risacher et al. 2018). Studies of the natural environments surround these tailings ponds provide evidence for extensive photosynthetic

activity (Reid et al. 2019), which is further corroborated by the visual observation of photosynthetic biofilms suggestion of the onset of photosynthetic activity in these mesocosms after 22-months.

5.4 Conclusions

This is the first study to characterize the long-term evolution of tailings utilizing novel GI treatment in augmentation with sediment amendments from natural wetland sources, for better understanding best management practices for sustainable landscape reclamation. The evolution of these tailings environments is a dynamic process, revealing temporal shifts in oxygen and sulfide dynamics within the sediments and across the sediment-water interface. In comparison to natural reference systems, lack of available organics would suggest that the production of sulfides within strict tailings systems is relatively little compared to some of the wetland counterparts. Extremely high concentrations of sulfides within some of the organic rich wetlands and high sulfate systems would suggest that caution must be taken if proceeding with reclamation utilizing mixtures of tailings and wetland sediments, given potential inadvertent release of toxic gaseous compounds. The relatively consistent DO concentrations maintained within the cap water of the tailings systems generally indicates that under open atmospheric conditions such as those within northern Alberta, Canada, there is enough influx of oxygen into the overlying water column to offset the sediment oxygen demand of most tailings treatment systems. In this case, it may be beneficial to proceed with amendments of tailings/natural sediments, so as to provide the necessary microbial inoculum to offset any increased SOD resultant from tailings alone. Further interpretation of microbial community structure results will help to identify long-term trends in the community structure over the course of 3-years. Decreases in NA

concentrations over time reveal that there is a natural degradation over the course of 32-months, allowing for untreated sediments to rival those treated with GI only after approximately 3 years. This suggests that the GI treatment is clearly effective at immediately degrading NAs (especially in Syncrude, Shell and STP OSPW), though given enough incubation time, natural UV or bio-degradation will inevitably lead to similar NA concentrations between G+ and G- systems. Clearly the progression of these various tailings systems towards reclamation is a complex task, though insights here provide interesting insight into the possibility for both natural and man-made influence on this progression towards a remediated state. The long-term effects of salinity appear to drive the differentiation between natural and tailings systems and should require future studies to tease out the true effects of salinity alone on the ecology of these systems. Further interpretation of results and discussion surrounding the spatial and temporal relationships of these results will provide additional insight into the holistic biogeochemical evolution of these various mesocosm systems. Results presented here, alongside previous studies, are confirm my final hypothesis, showing that GI treatment is extremely effective at breaking down NAs as a rapid treatment/detoxification procedure. This treatment, alongside specific natural sediment amendments and a lag time to allow further ecosystem equalization, could provide the necessary conditions to allow for an efficient and sustainable reclamation to EPLs or reclaimed wetland environments.

Figures and Tables
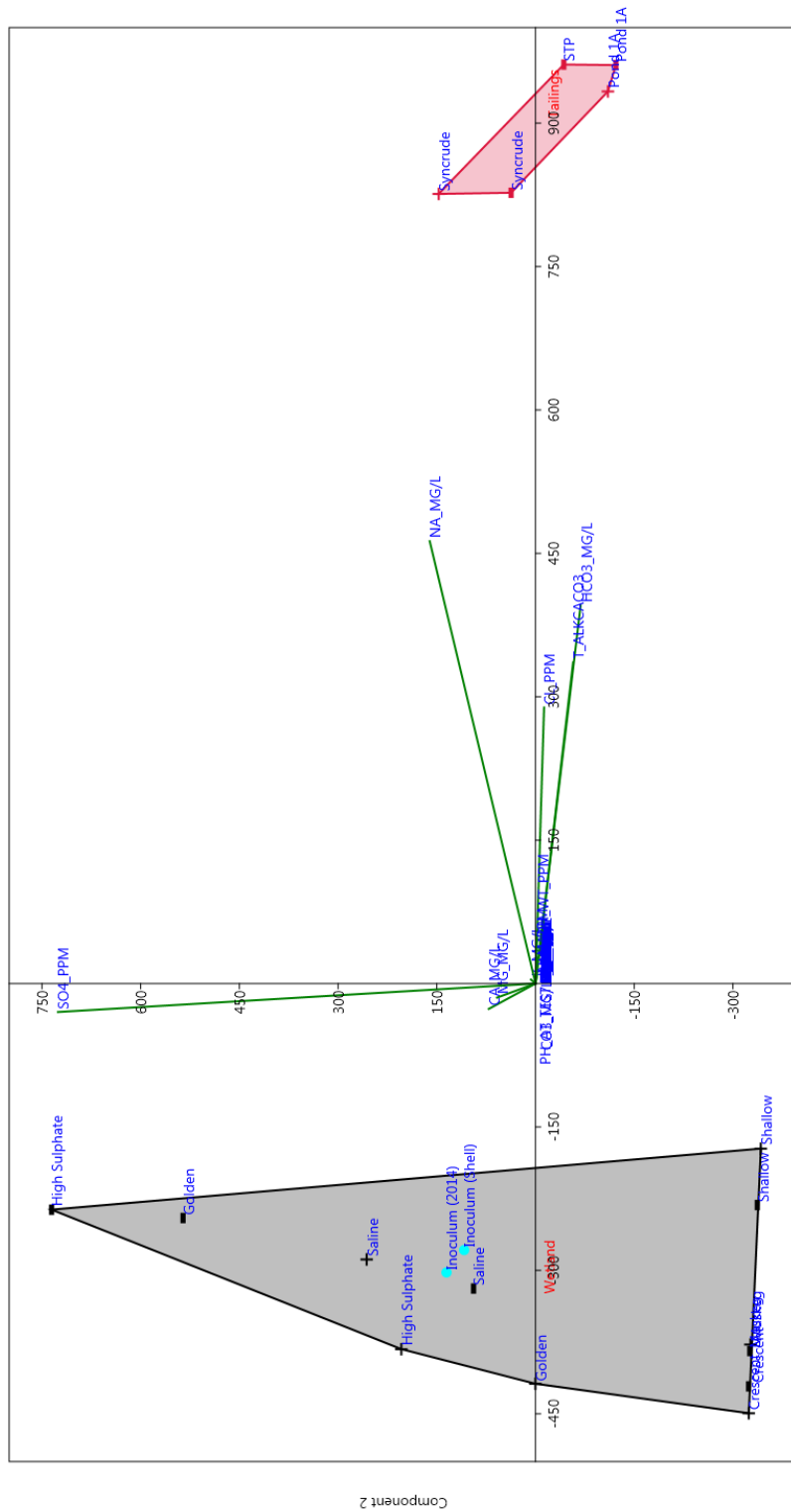
FIGURE 1 Principal Component Analysis (PCA) revealing dominant geochemical drivers differentiating the water chemistry of the natural wetlands from the tailings
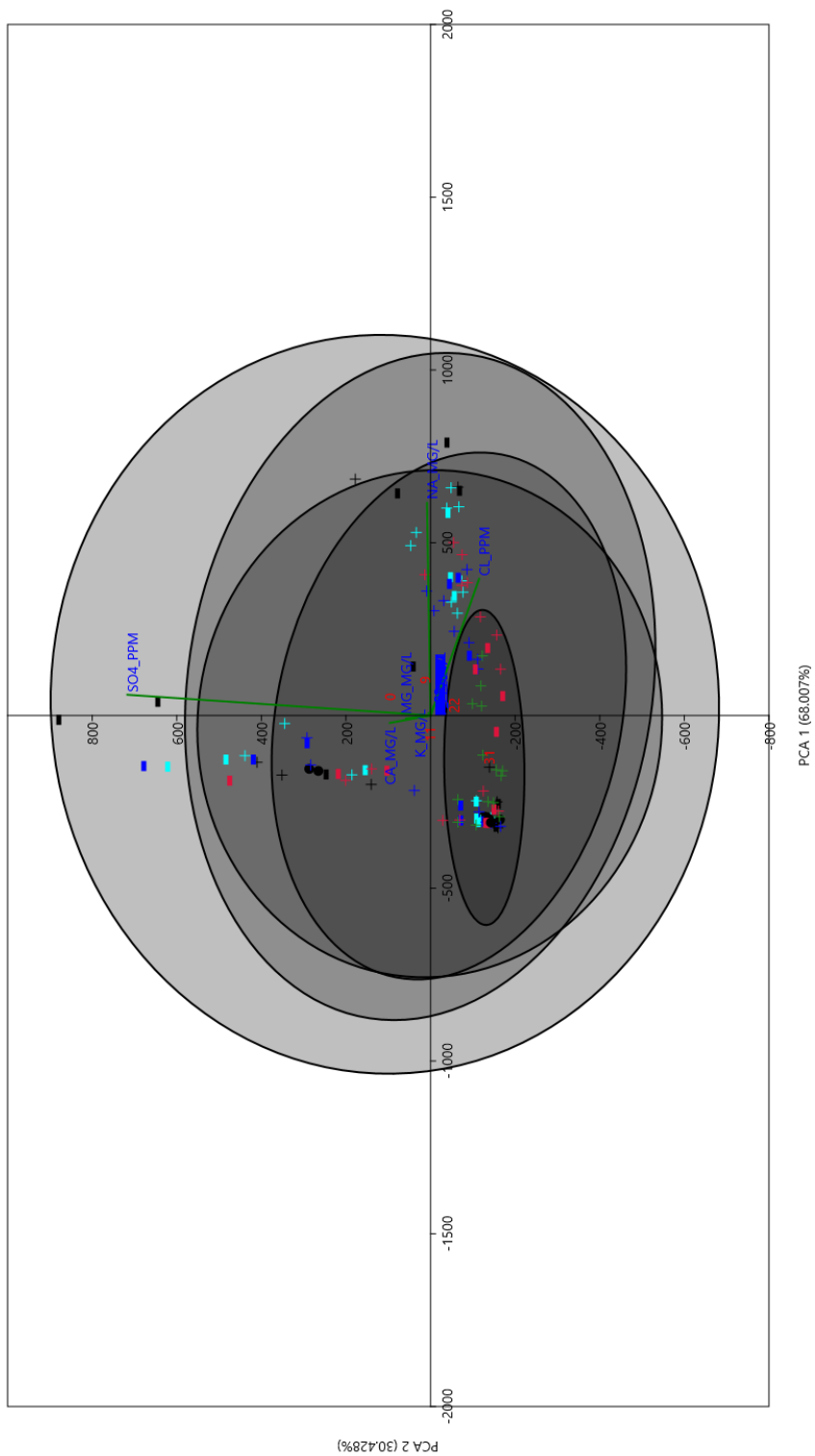
FIGURE 2 PCA plot revealing temporal trends over 32-months in the geochemical progression of the tailings and wetland systems. There is an increasing commonality between G- and G+ systems over the course of the study, noted by the shrinking and darkening of the temporal ellipses.

168
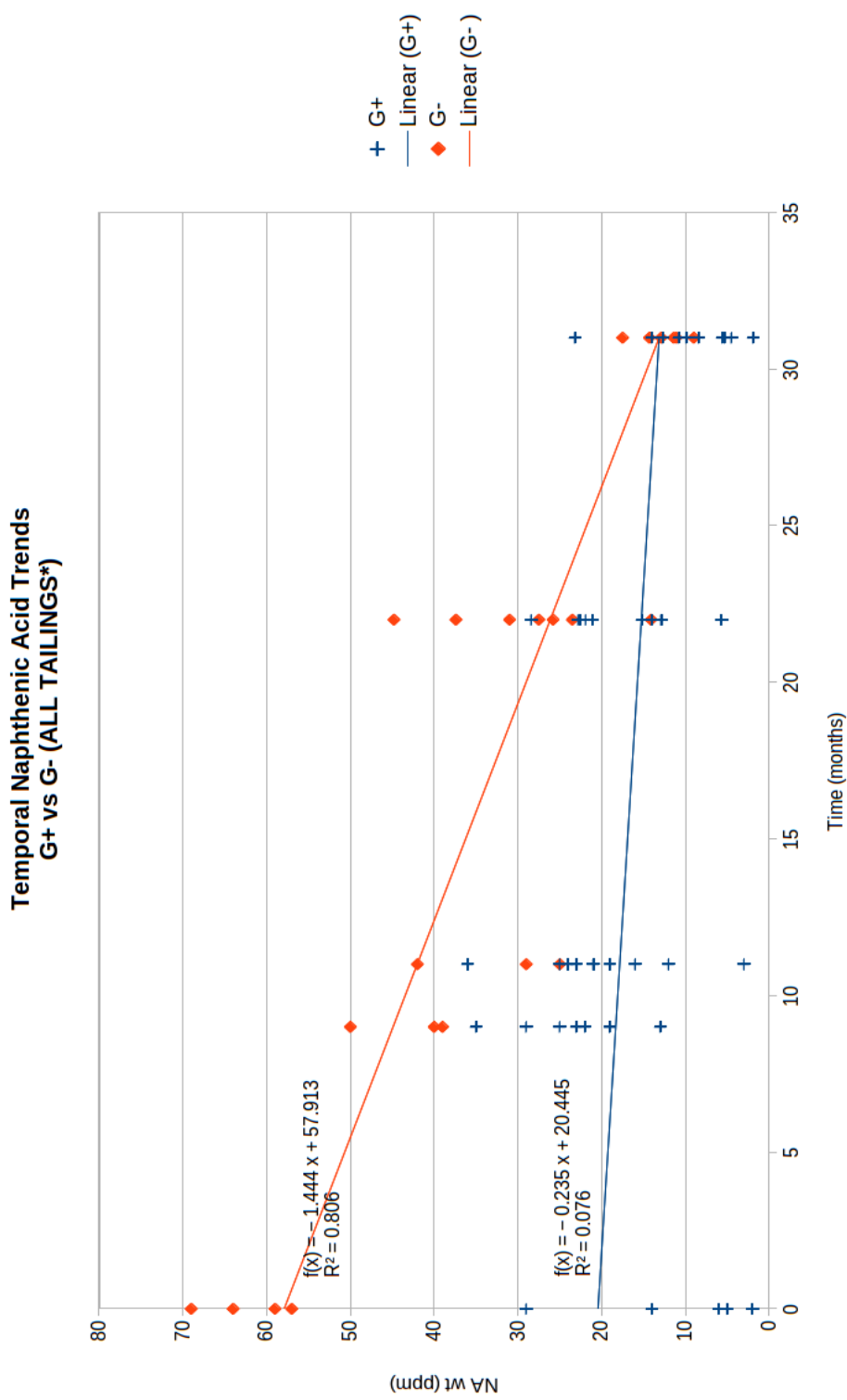
FIGURE 3 Distribution of naphthenic acid concentrations between G+ (blue) and G- (red) treatments over the course of the 32-week study period.
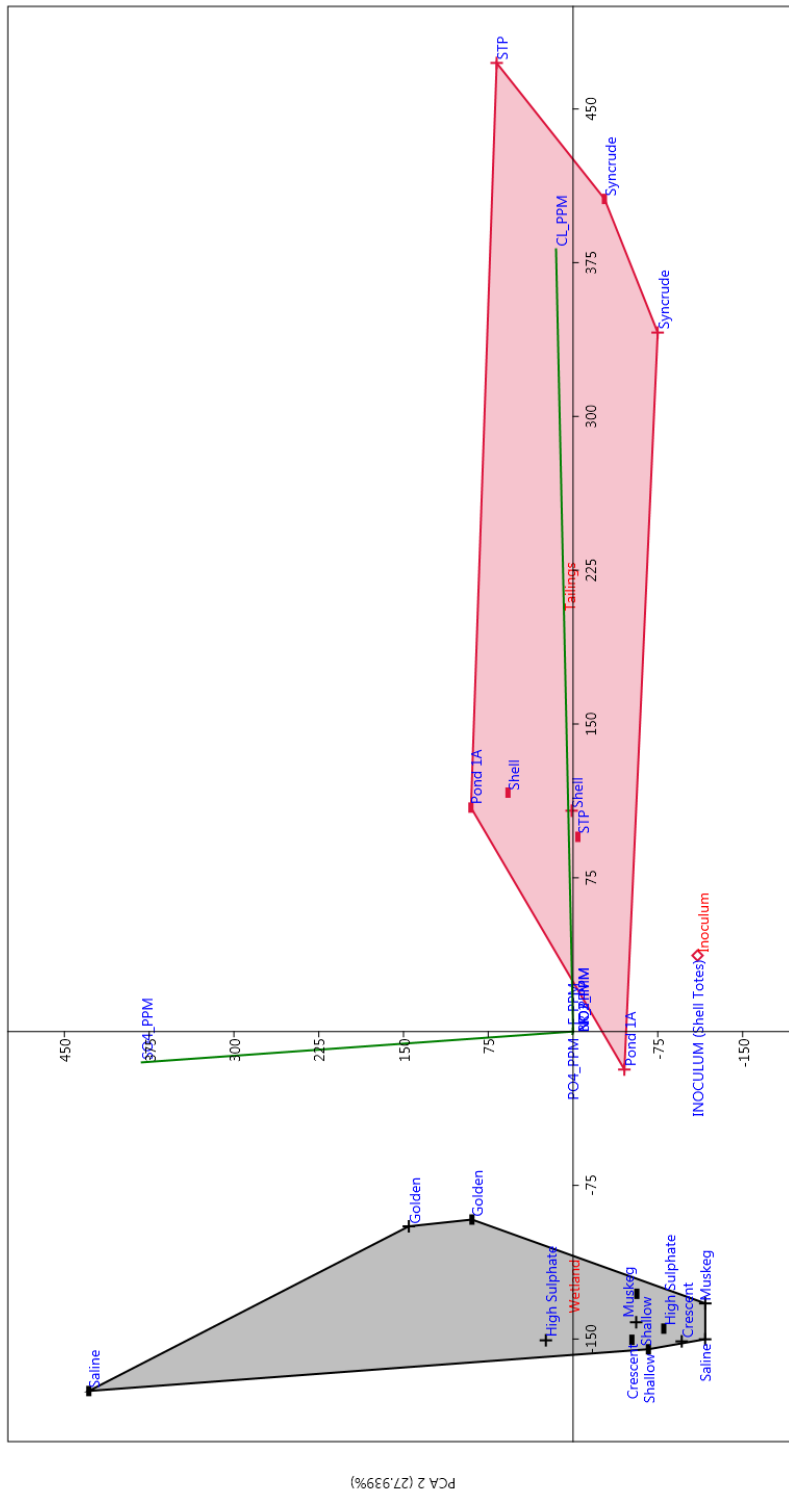
FIGURE 4 PCA plot presenting the geochemical variation between sediments of natural wetlands and tailings systems
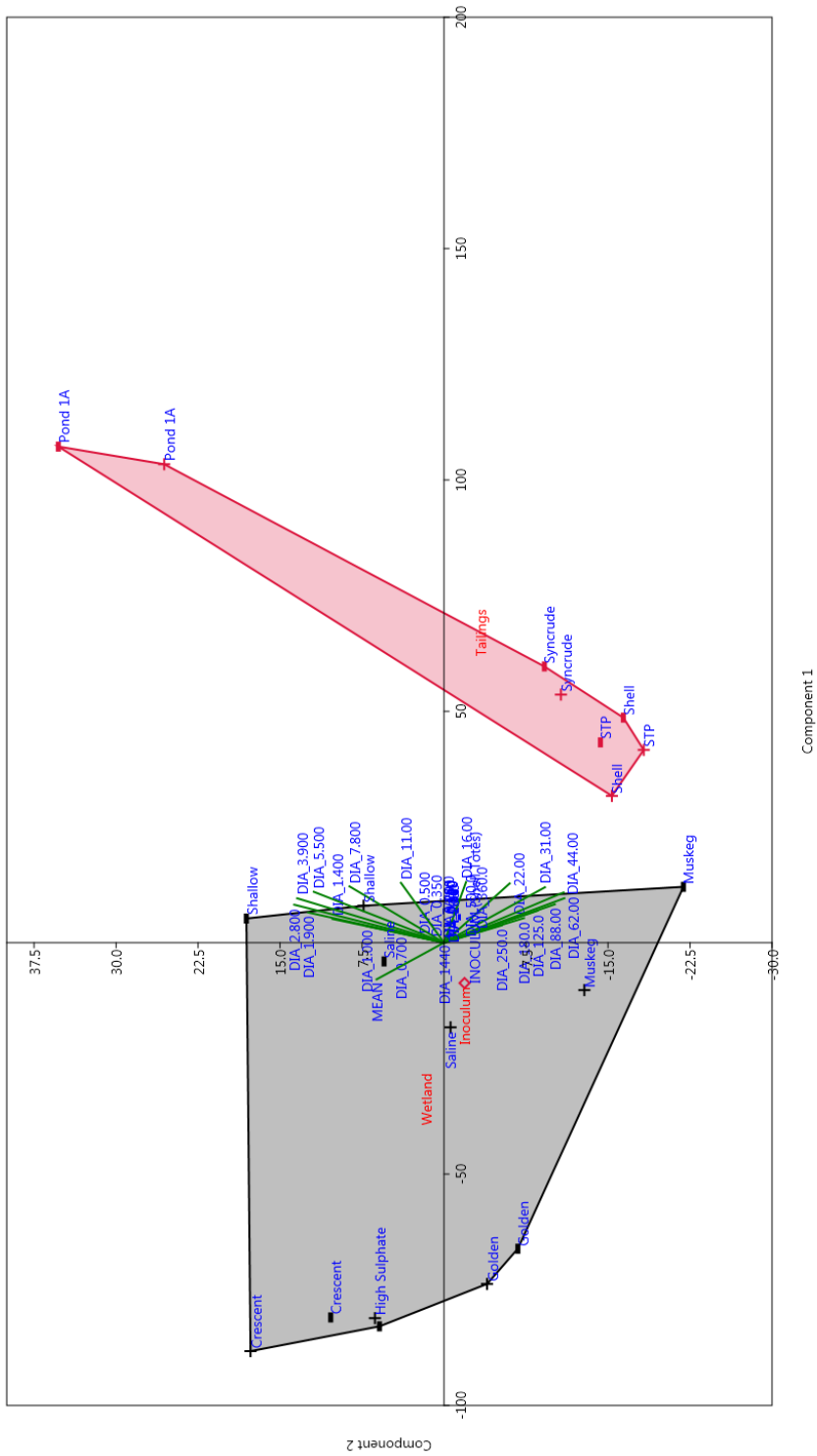
FIGURE 5 PCA plot of the grain size distribution between wetland sediments and tailings sediments.

Syncrude Dissolved Oxygen Gradients (9-months)

P1A Dissolved Oxygen Gradients (9-months)

STP Dissolved Oxygen Gradients (9-months)
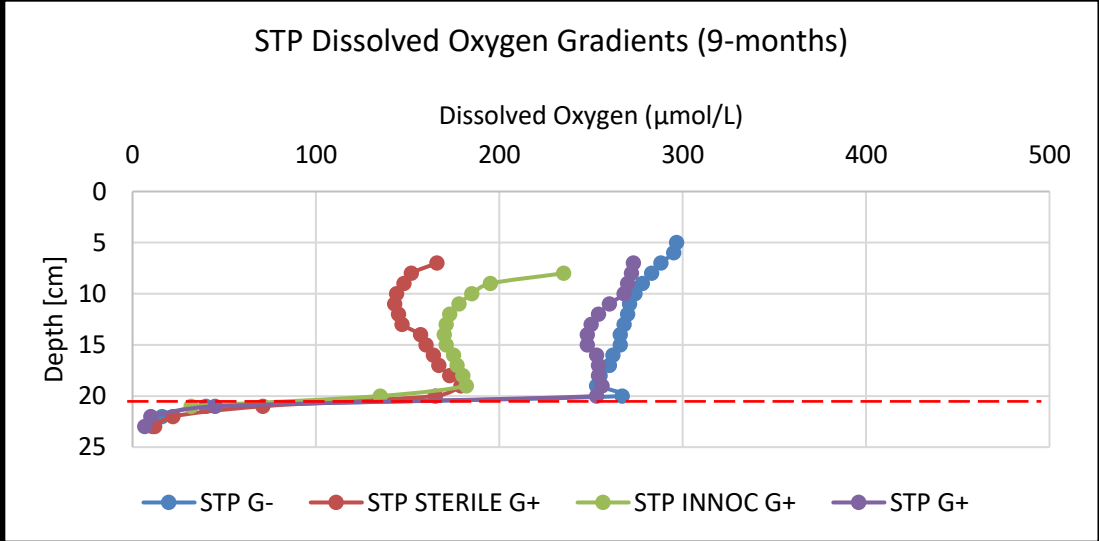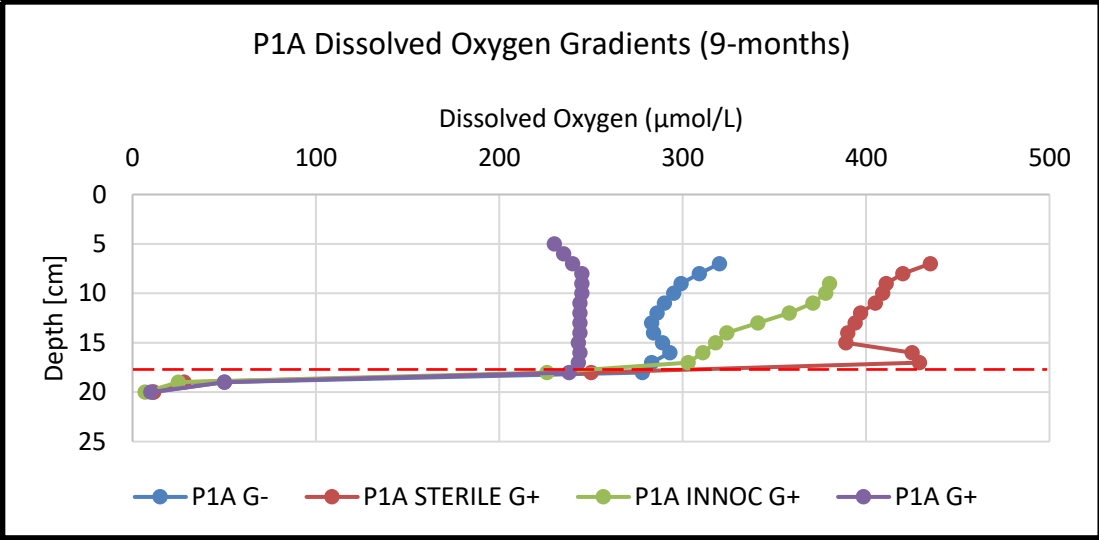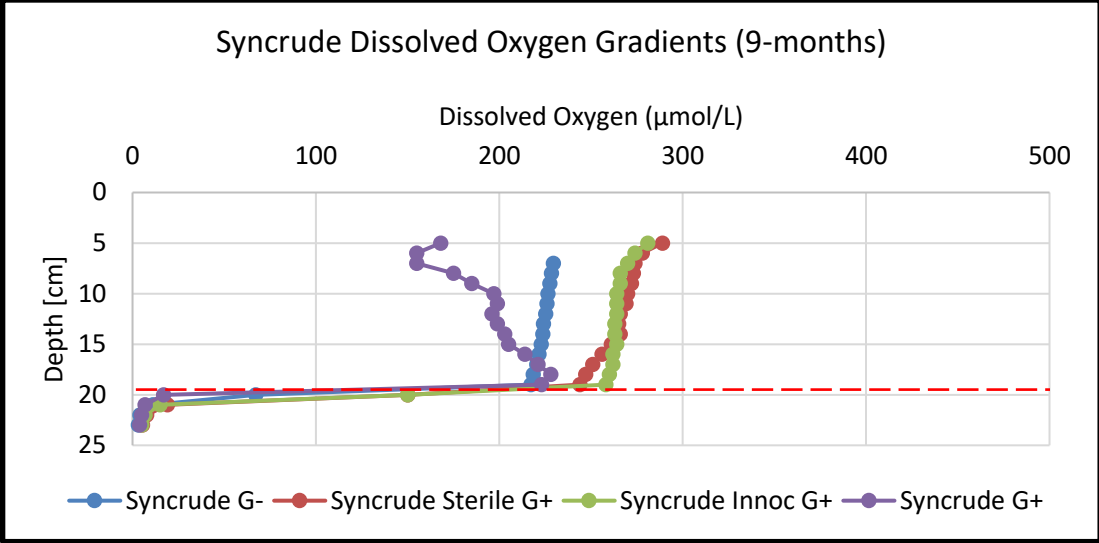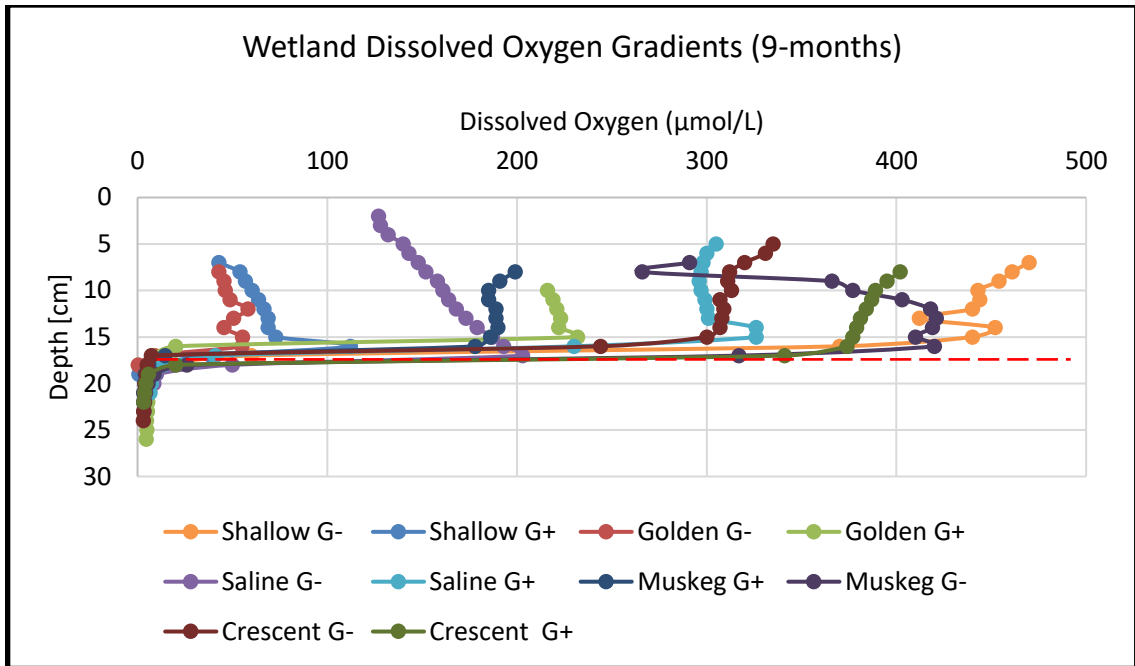
FIGURE 6 Dissolved Oxygen gradients at the 9-month sampling period. Sediment-water interface noted with red dashed line.

Syncrude DO Gradients (22-months)

P1A DO Gradients (22-months)

Shell DO Gradients (11-months)

174
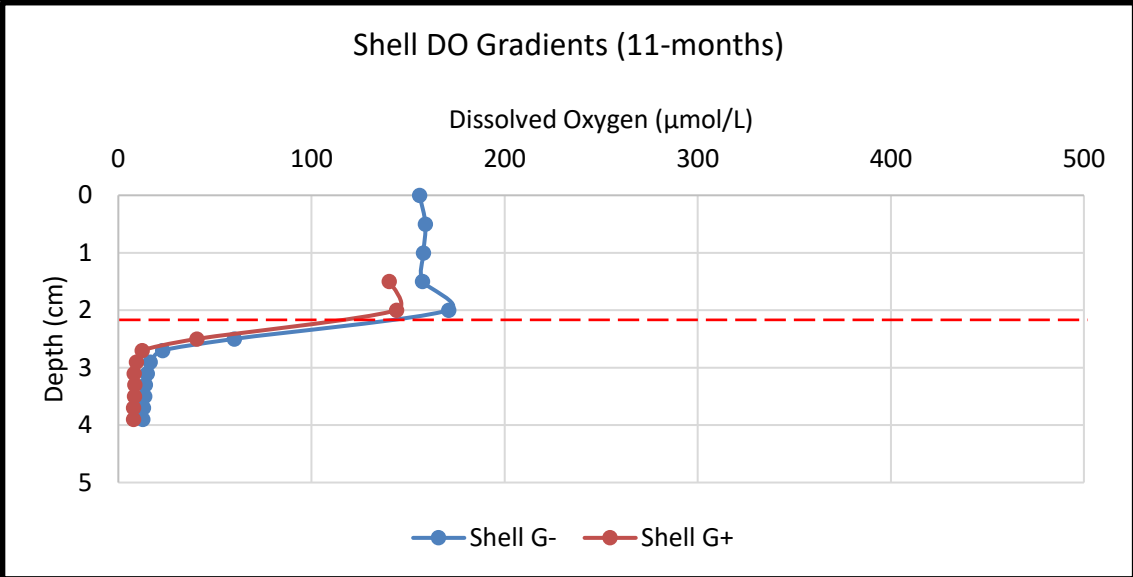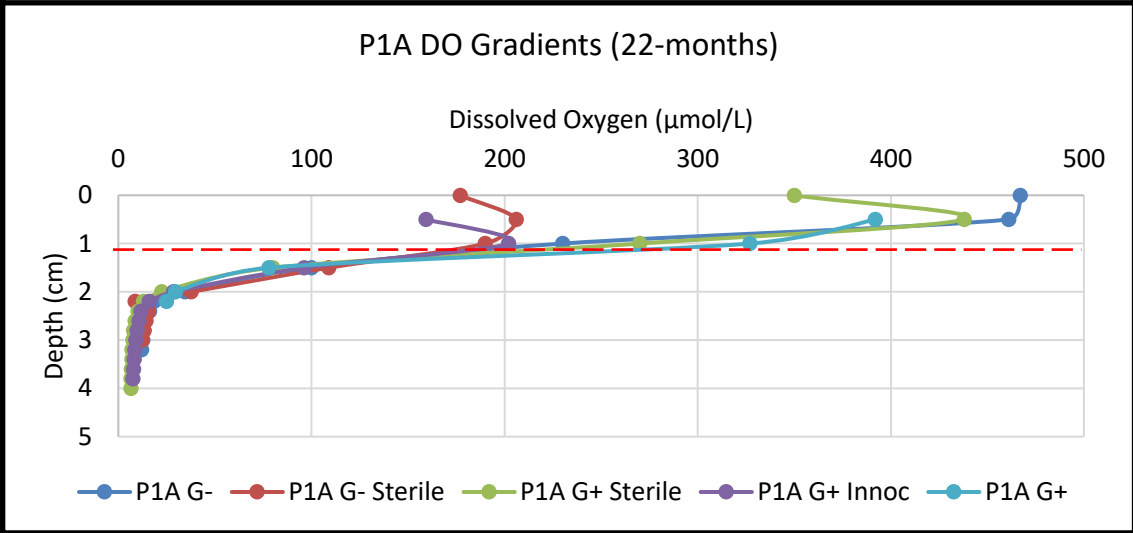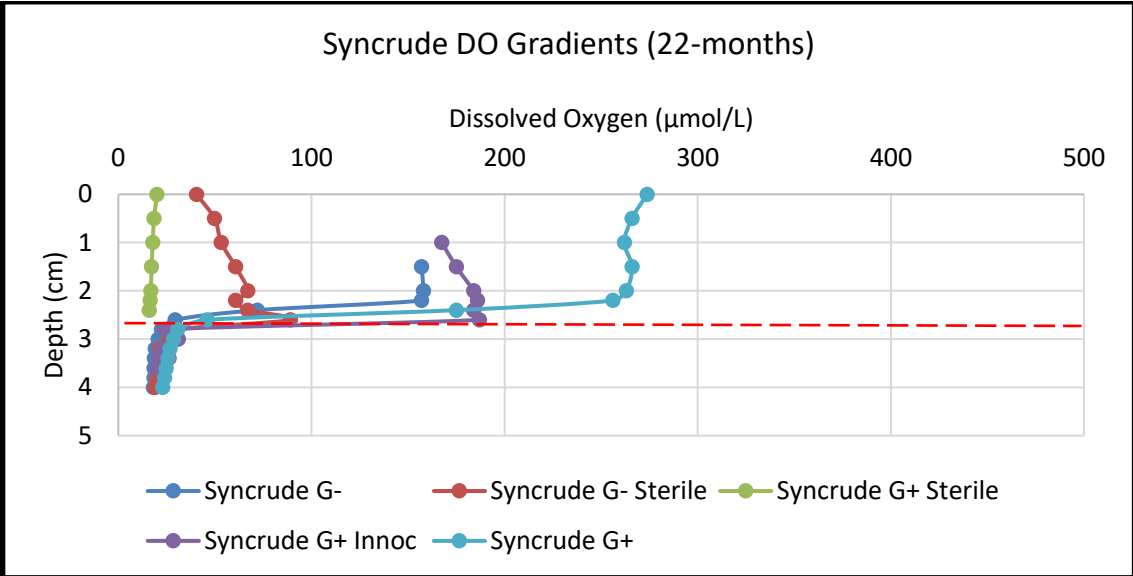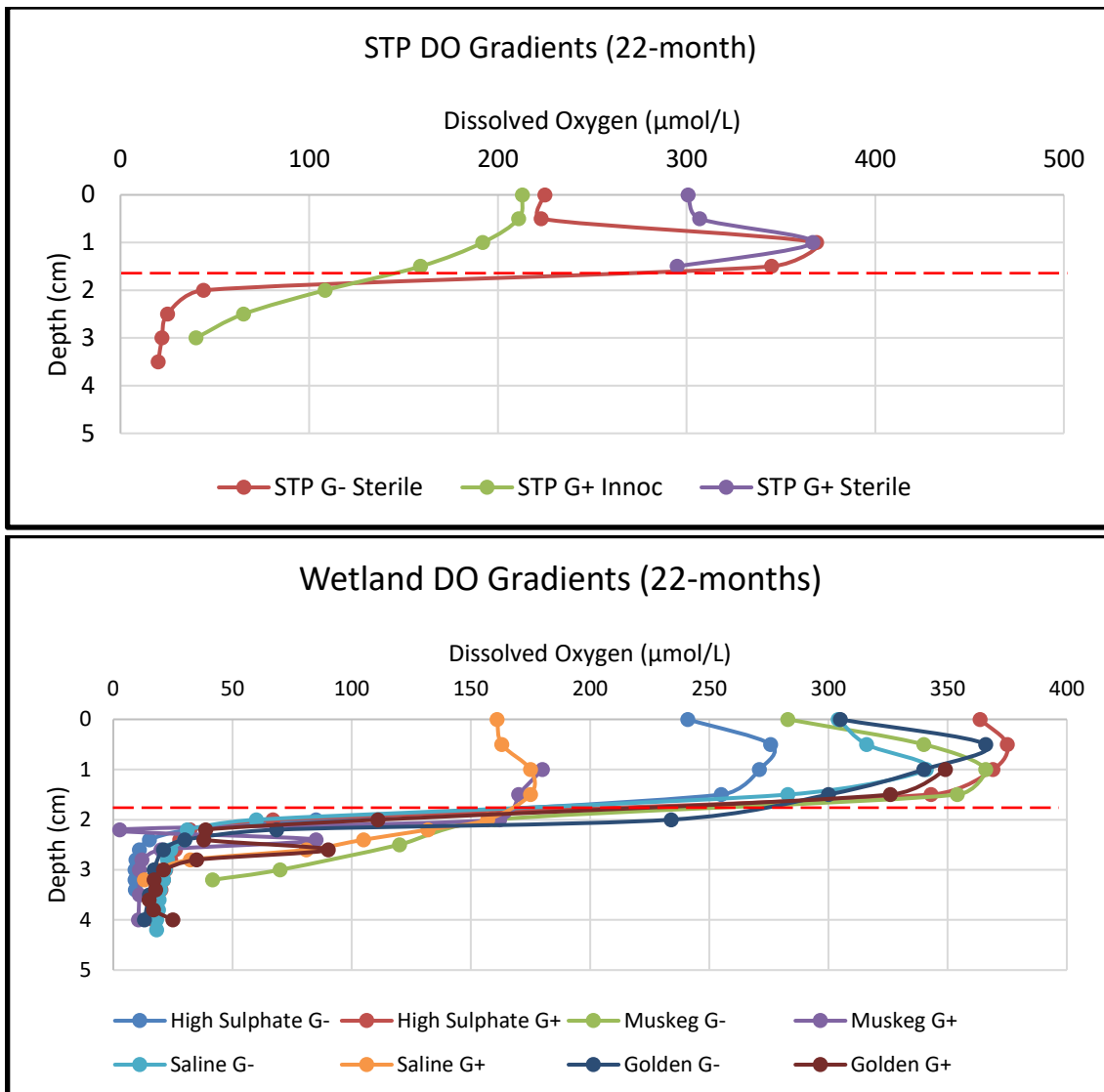
FIGURE 7 Dissolved oxygen gradients at the 22-month sampling period. Sediment-water interface noted with red dashed line.

P1A DO Gradients (32-months)

STP DO Gradients (32-months)

Syncrude DO Gradients (32-months)
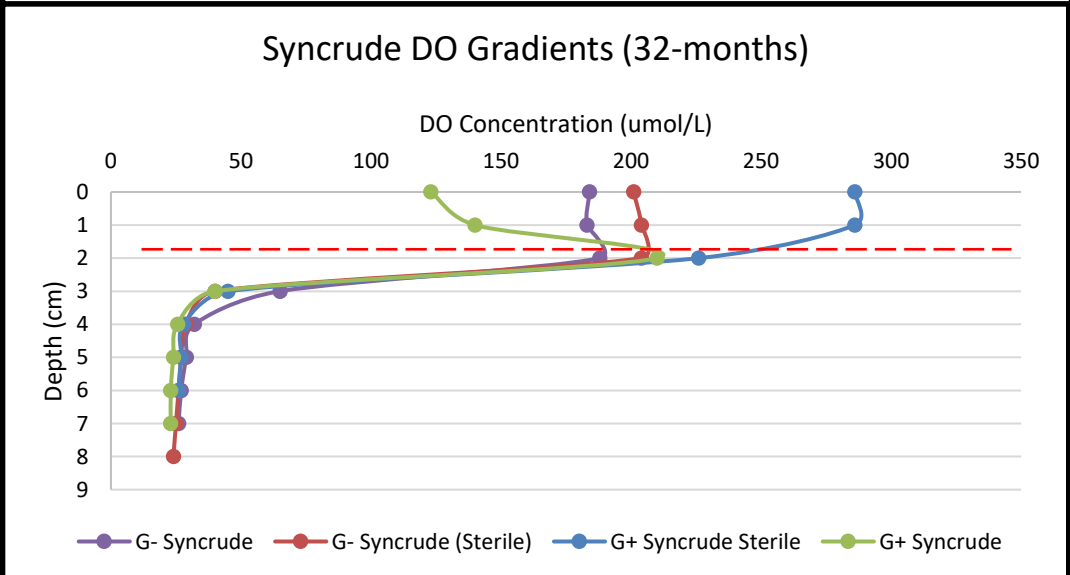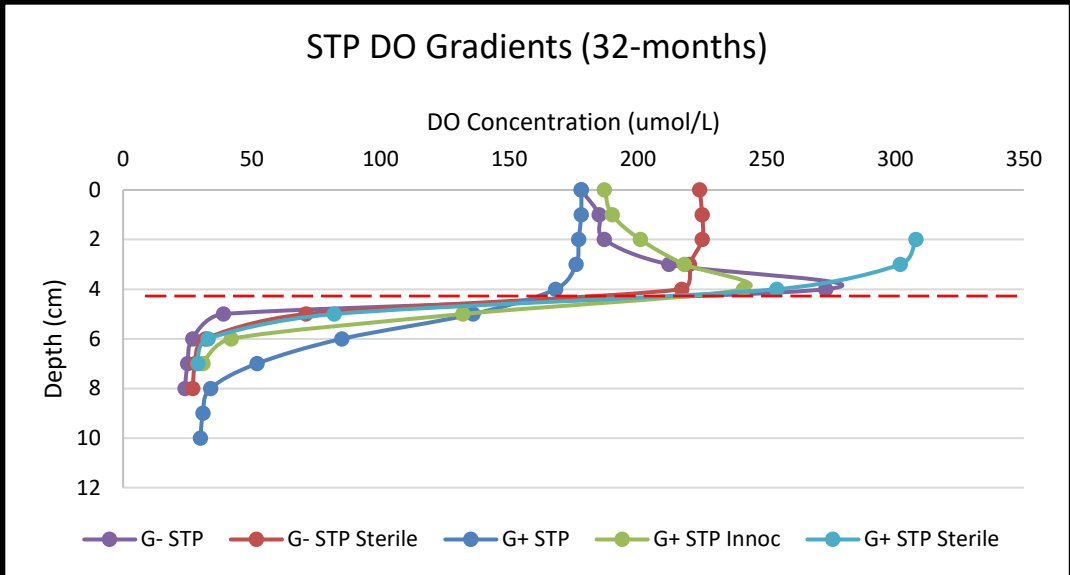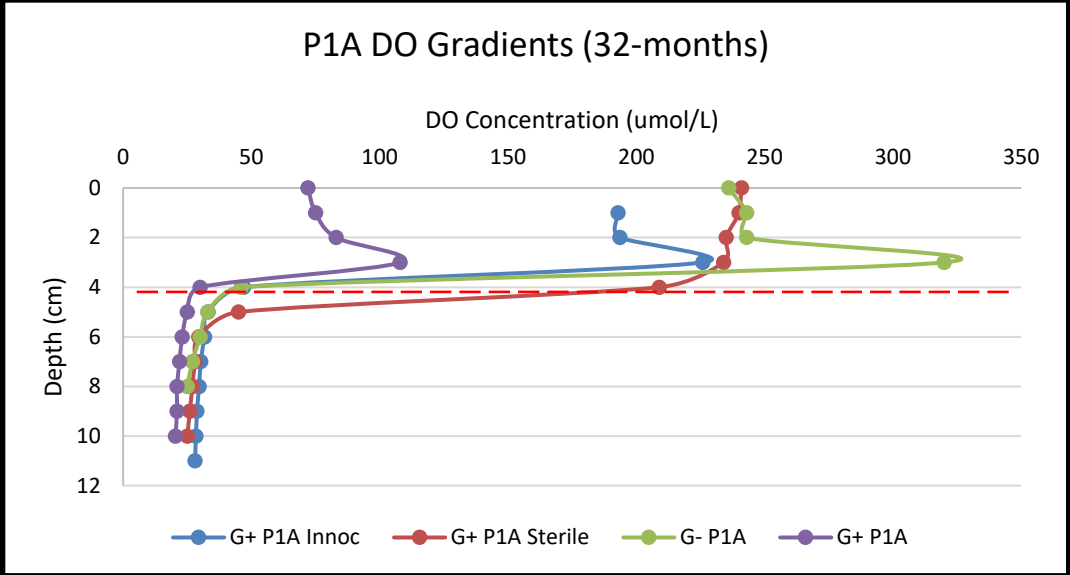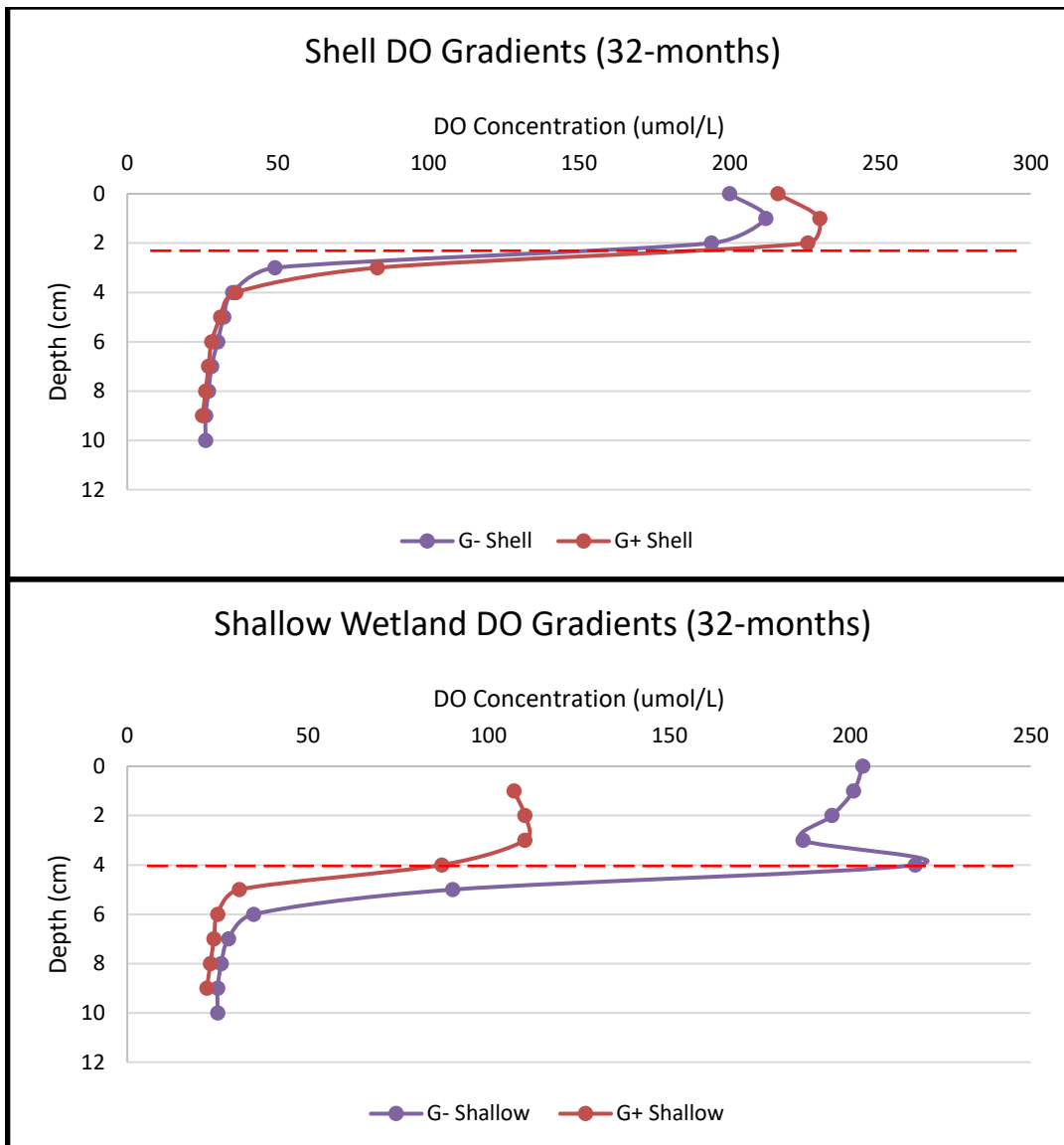
FIGURE 8 Dissolved oxygen gradients at the 32-month sampling period. Sediment-water interface noted with red dashed line.

Syncrude Hydrogen Sulfide Gradients

P1A Hydrogen Sulfide Gradients

STP Hydrogen Sulfide Gradients
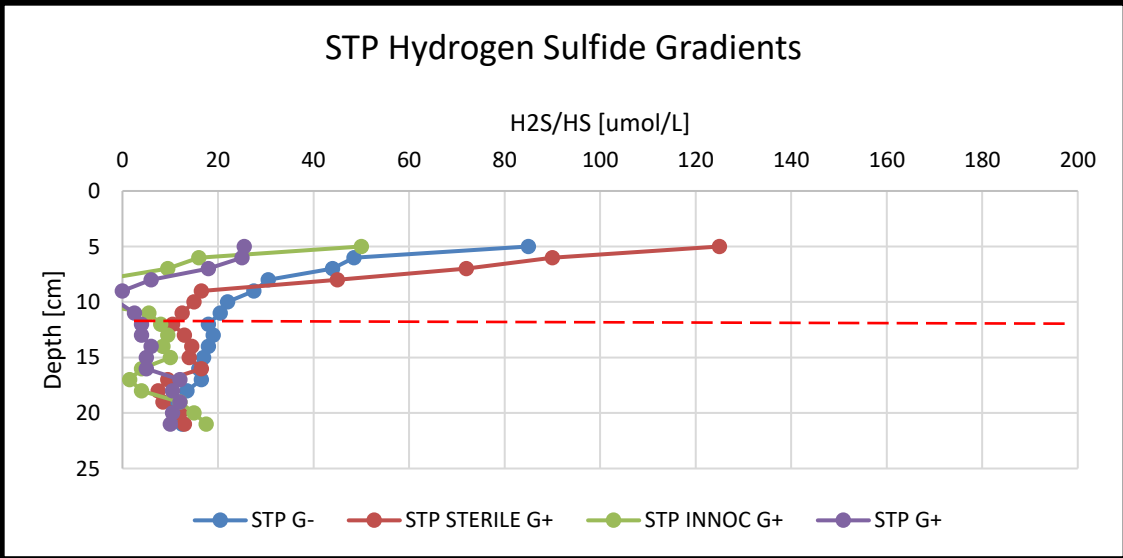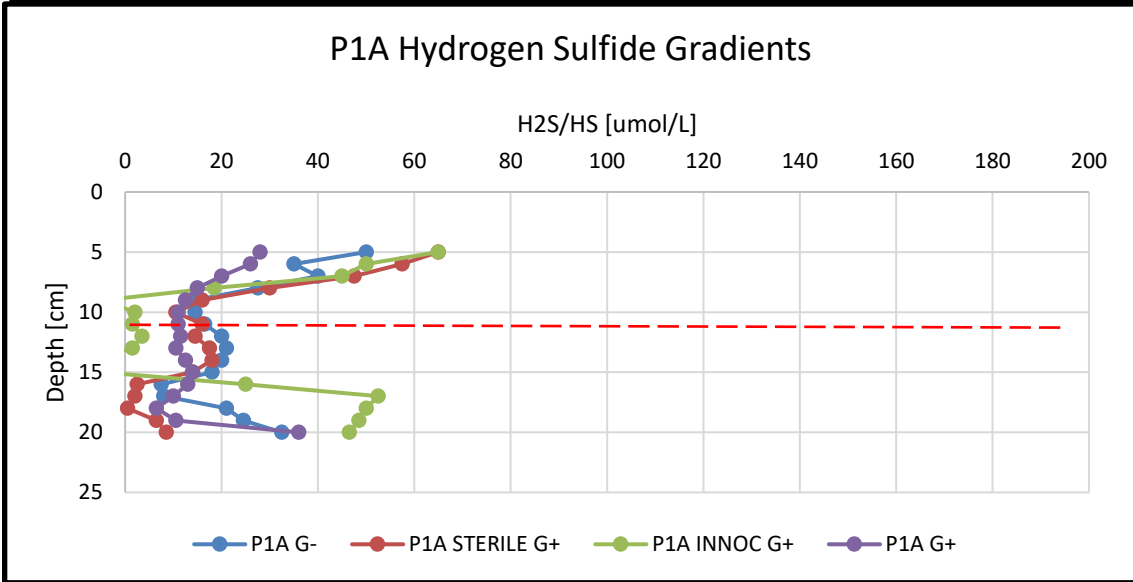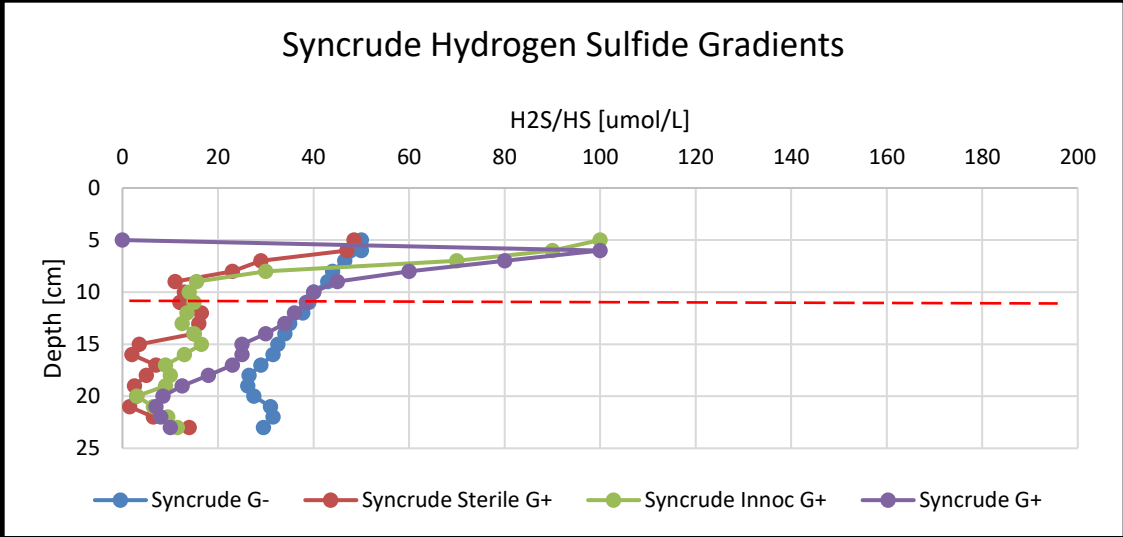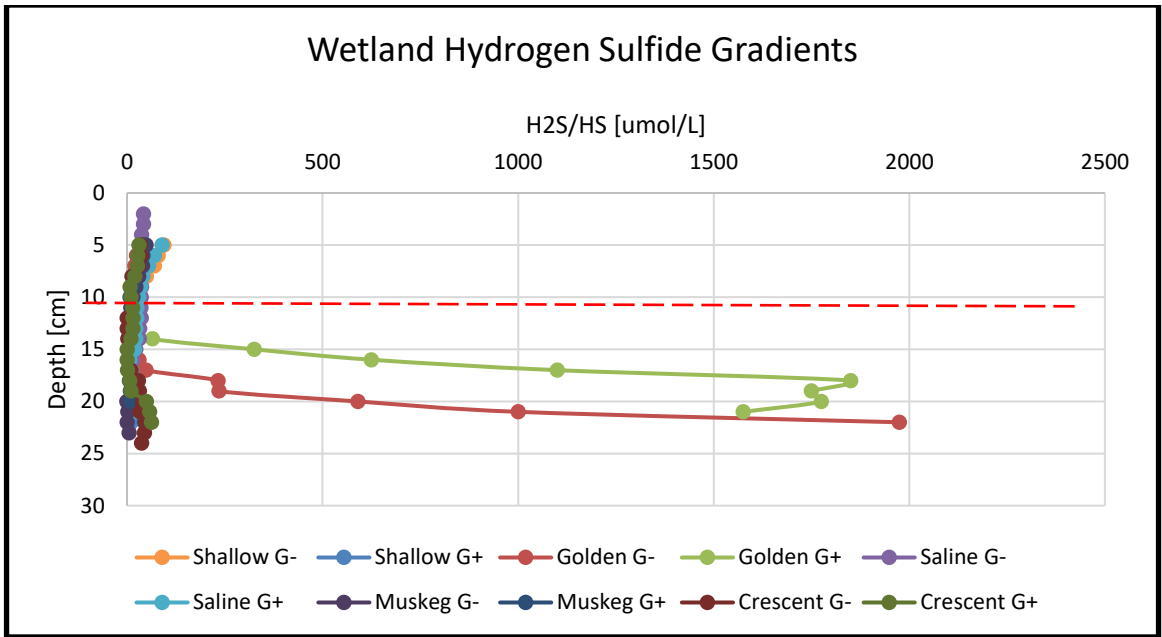
FIGURE 9 Hydrogen Sulfide gradients measured at the 9-month sampling period. Sediment-water interface noted with red dashed line.

P1A Hydrogen Sulfide Gradients (22 months)

Shell Hydrogen Sulfide Gradients (**Time 11 Months)

Syncrude Hydrogen Sulfide Gradients (22 months)
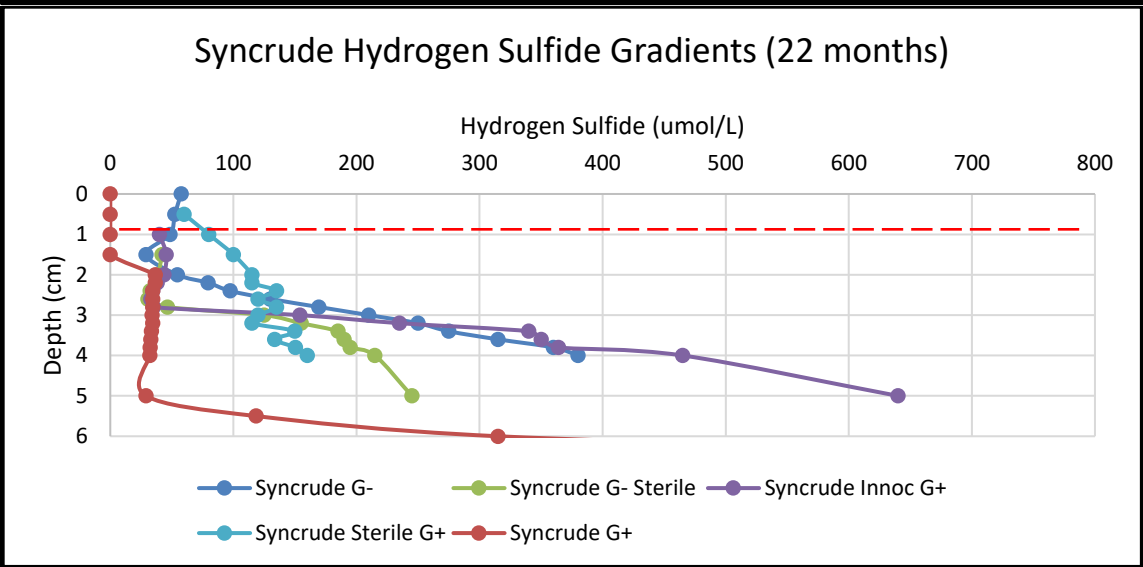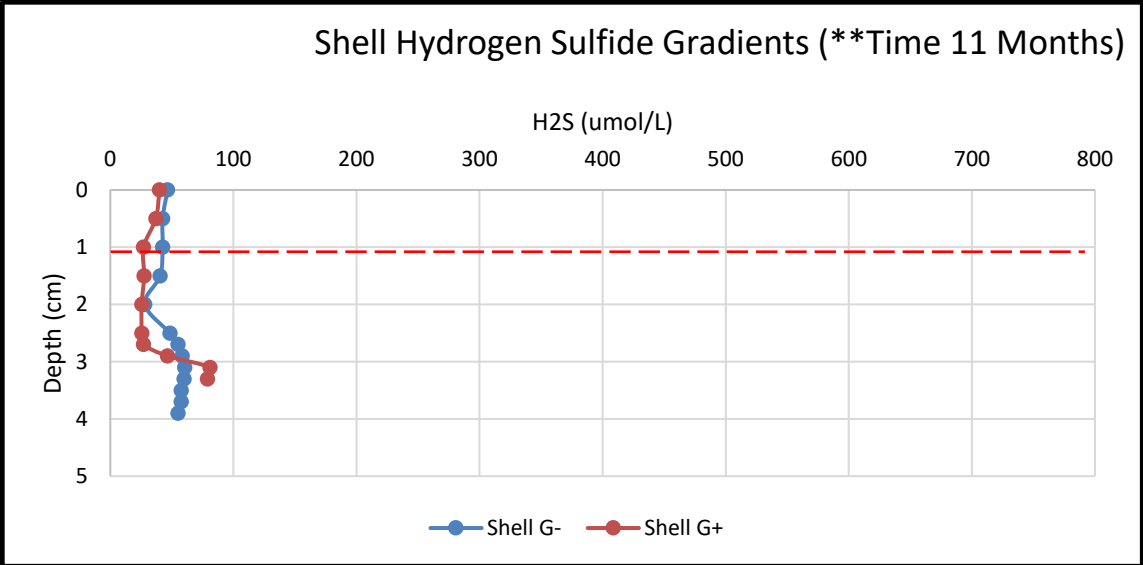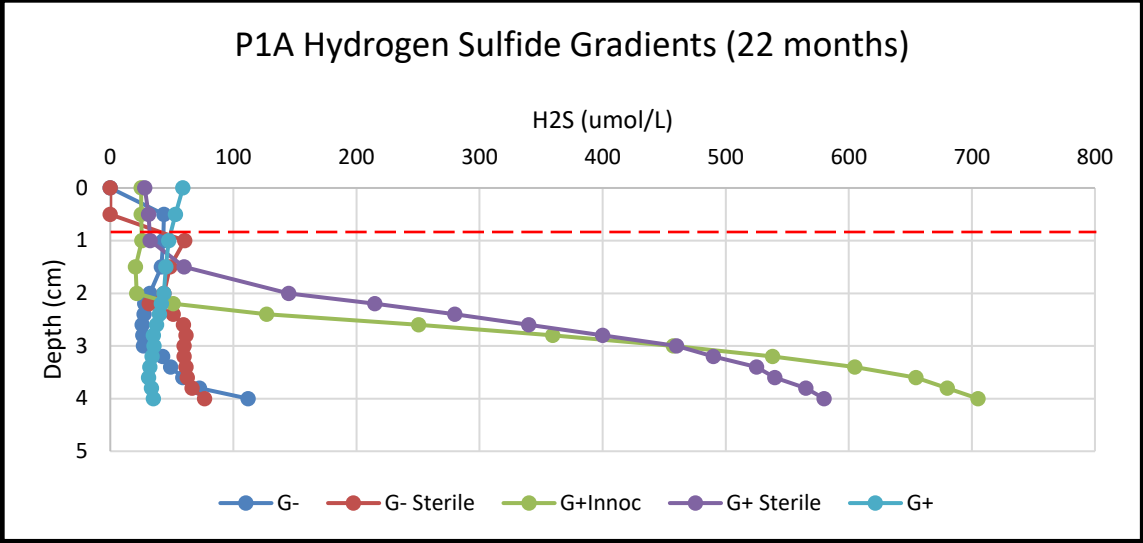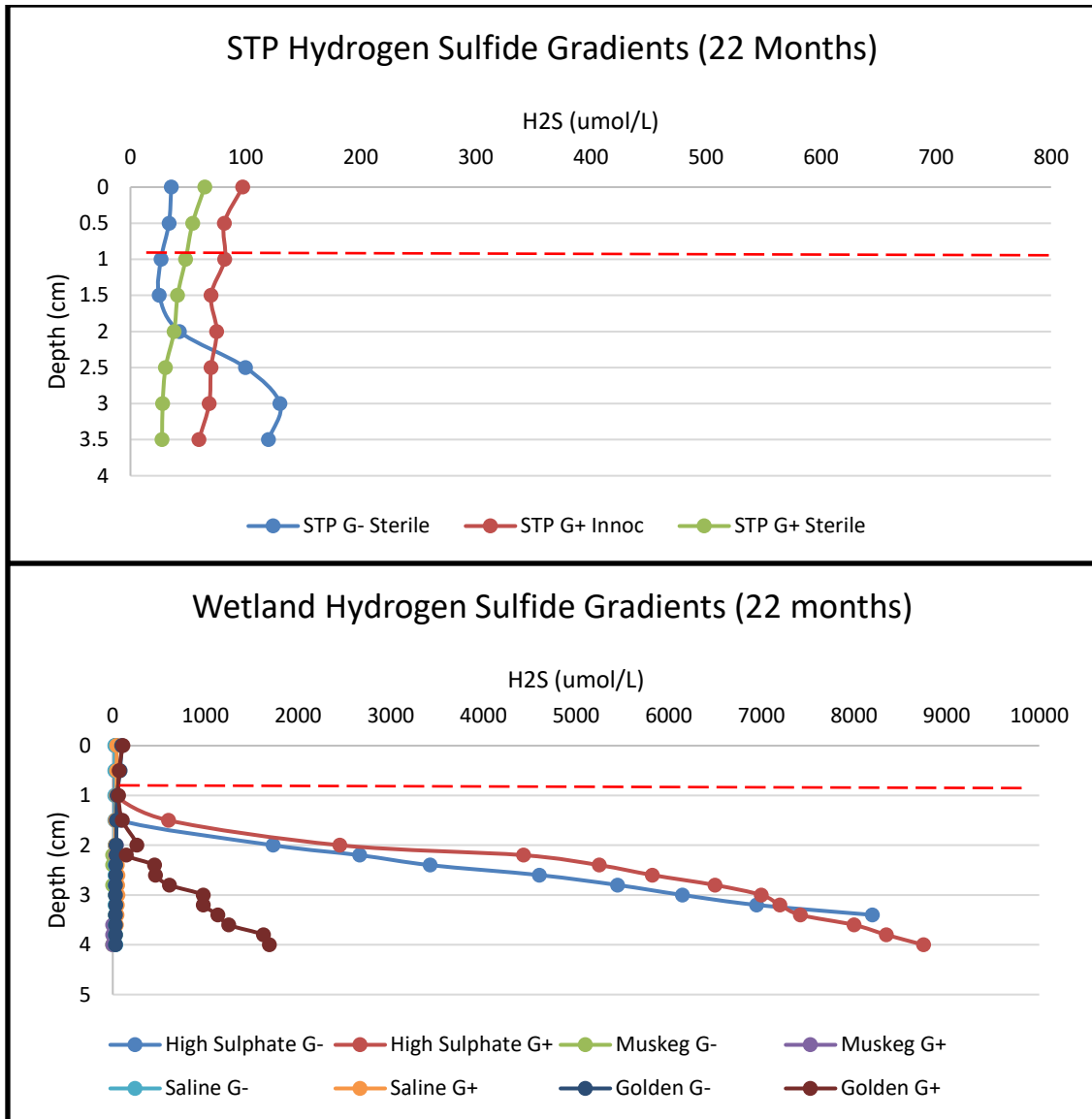
FIGURE 10 Hydrogen Sulfide gradients measured at the 22-month sampling period. Note, establishment of the Shell systems were delayed therefore represent 11-month time-point. Sediment-water interface noted with red dashed line.

P1A Hydrogen Sulfide Gradients (32 Months)

Shell Hydrogen Sulfide Gradients (*21 Months)

Syncrude Hydrogen Sulfide Gradients (32 Months)

182
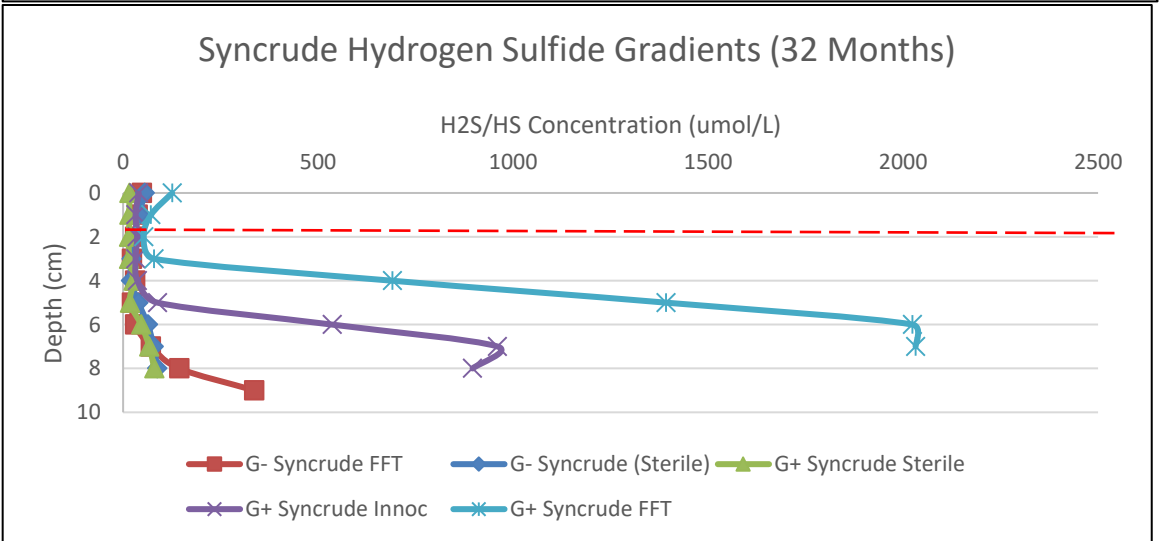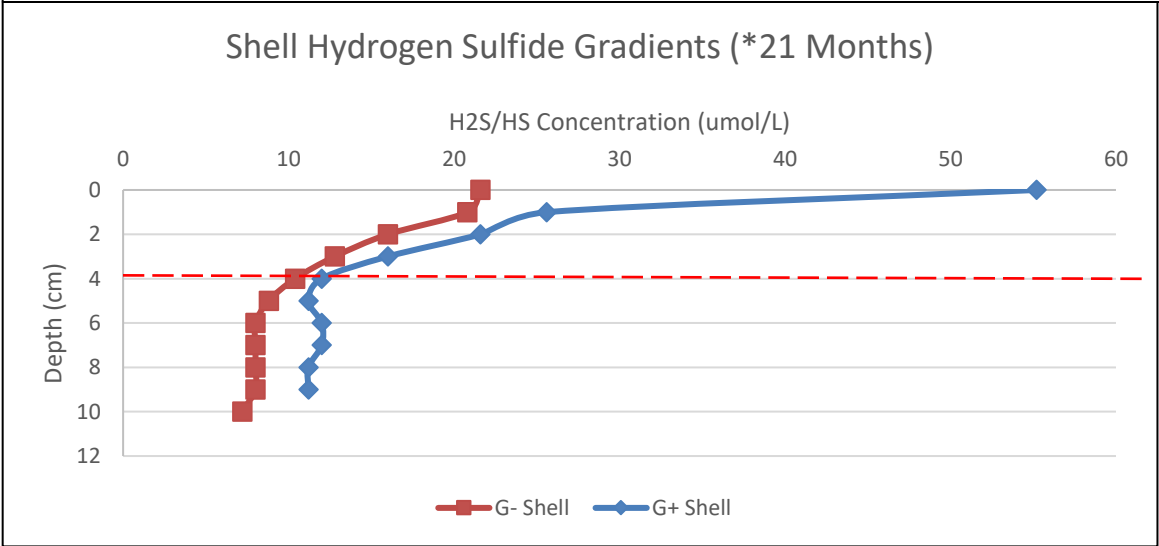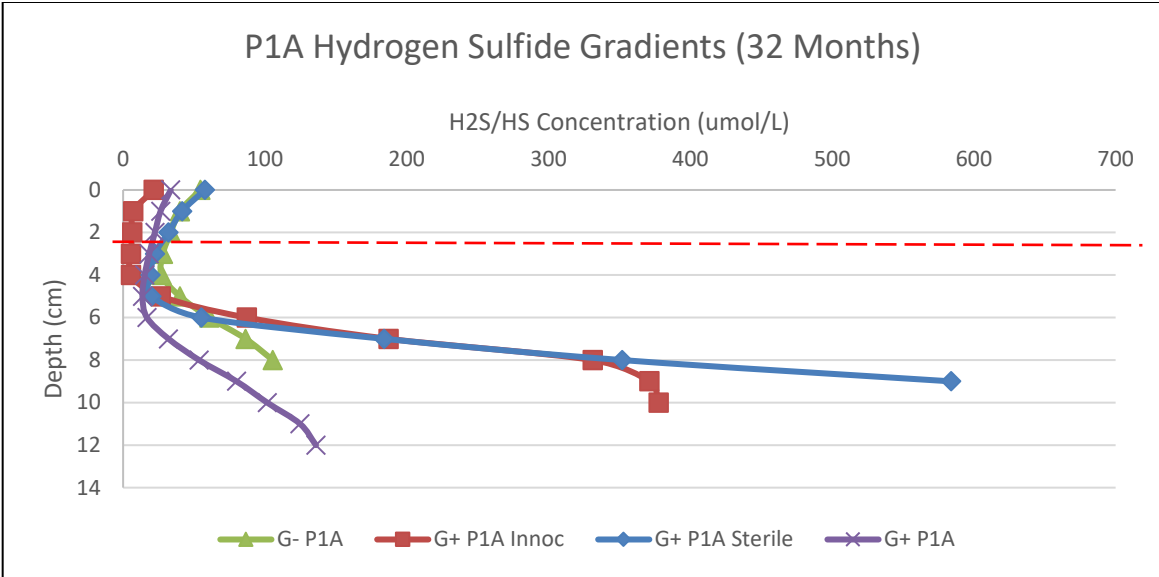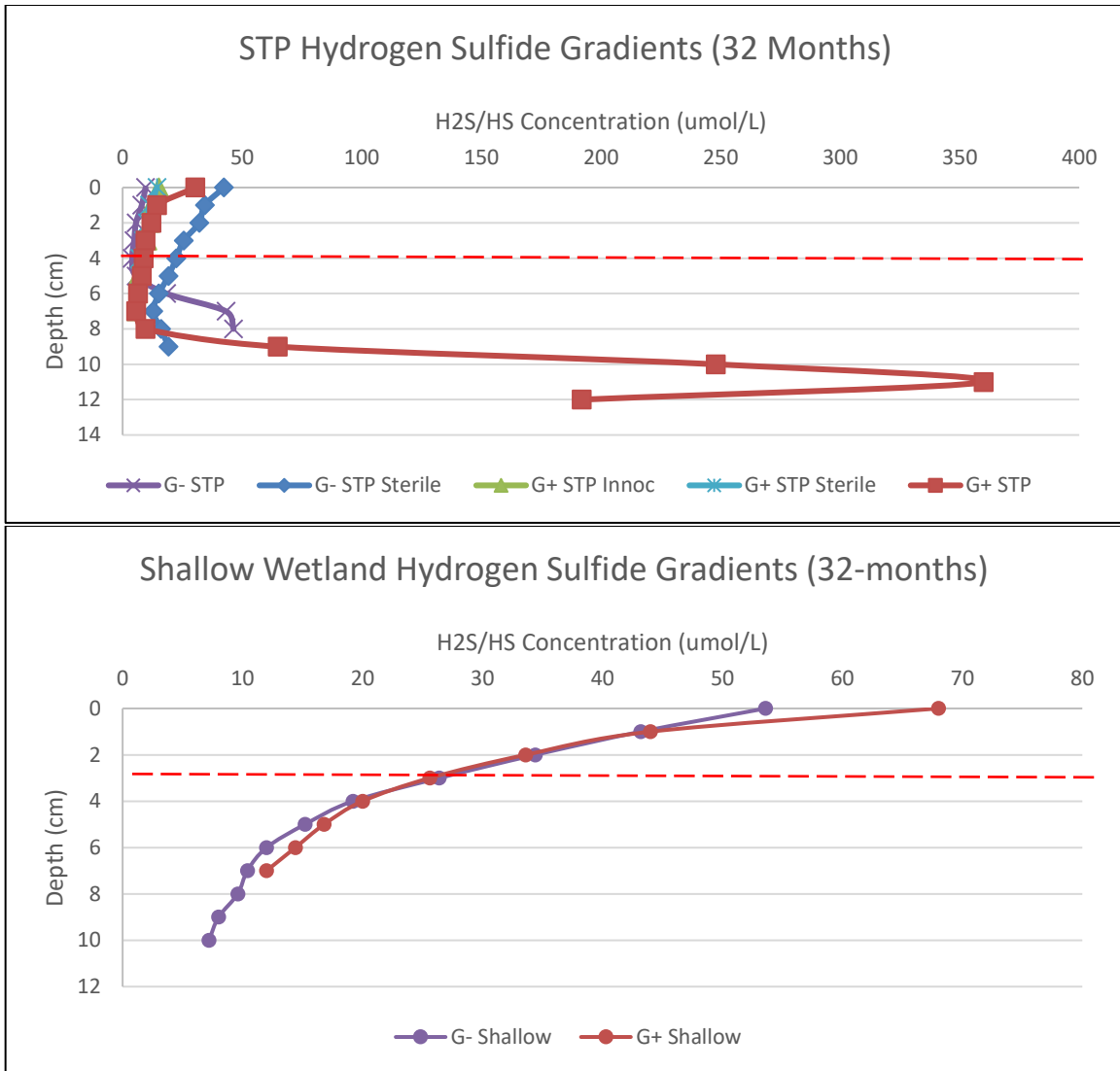
Figure 11: Hydrogen Sulfide gradients measured at the 32-month sampling period. Note, establishment of the Shell systems were delayed therefore represent 21-month time-point. Sediment-water interface noted with red dashed line.

Phylum Distribution G- vs G+

Legend:
- Unassigned
- p__Acidobacteria
- p__Actinobacteria
- p__Bacteroidetes
- p__Caldiserica
- p__Chlorobi
- p__Chloroflexi
- p__Cyanobacteria
- p__Firmicutes
- p__NKB19
- p__Nitrospirae
- p__OP8
- p__Planctomycetes
- p__Proteobacteria
- p__Spirochaetes
- p__Tenericutes
- p__Verrucomicrobia
- p__WS3
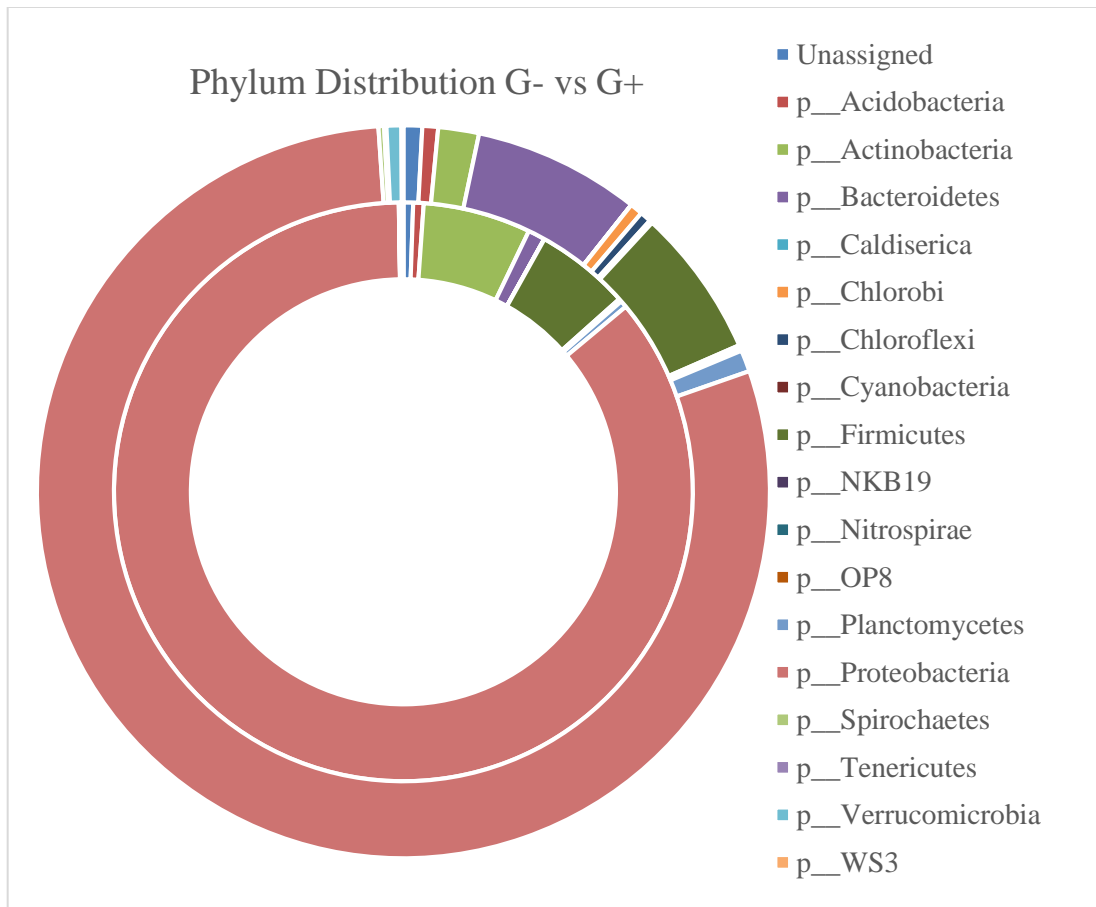
G- top abundances	G+ top abundances	Greatest FC for G+
f__Enterobacteriaceae	f__Comamonadaceae	f__Desulfobacteraceae
f__Pseudomonadaceae	f__Enterobacteriaceae	f__Geobacteraceae
f__Rubrobacteraceae	f__Pseudomonadaceae	f__Moraxellaceae
f__Paenibacillaceae	f__Flavobacteriaceae	f__Comamonadaceae
f__Rhizobiaceae	f__Hydrogenophilaceae	f__Alteromonadaceae
f__Sphingomonadaceae	f__Rhodocyclaceae	f__Sinobacteraceae
f__Corynebacteriaceae	f__Clostridiaceae	f__Hydrogenophilaceae
f__Propionibacteriaceae	f__Geobacteraceae	p__Actinobacteria
f__Phyllobacteriaceae	f__Moraxellaceae	f__Syntrophaceae
f__Streptococcaceae	p__Actinobacteria	f__Flavobacteriaceae
Other	Other	f__Rhodocyclaceae
f__Comamonadaceae	f__[Acidaminobacteraceae]	f__Spirochaetaceae
f__Caulobacteraceae	f__Desulfobacteraceae	f__Microbacteriaceae

FIGURE 12 a) Bacterial community structure at the onset of the experiment, noting broad scale differences between the G+ and G- (untreated) tailings sediments at a phylum level. B) Most highly abundance organisms (family level) observed in both the G- and G+ tailings, alongside the greatest fold change increases in the G+ treatments.

Table 1 List of source materials and mesocosm configurations with treated (G+) vs untreated (G-) differentiated. Note: Condition "sterile" indicates not re-inoculated; "inoculated" indicates only tailings inoculate. All others represent sediment amendments.

Environment	Treatment	Source	Condition
Tailings	G-	STP	
	G-	Shell	
	G-	P1A	
	G-	Syncrude	
Wetlands	G-	Golden	
	G-	High Sulphate	
	G-	Shallow	
	G-	Muskeg	
	G-	Saline	
	G-	Crescent	
Tailings	G+	P1A	
	G+	P1A	Sterile
	G+	P1A	Inoculated
	G+	STP	
	G+	STP	Sterile
	G+	STP	Inoculated
	G+	Shell	
	G+	Syncrude	
	G+	Syncrude	Sterile
	G+	Syncrude	Inoculated
Wetlands	G+	Golden	
	G+	High Sulphate	
	G+	Shallow	
	G+	Muskeg	
	G+	Saline	
	G+	Crescent	

Table 2 Elemental Analysis results of tailings and wetlands sediments over the course of the study. Elements below detection levels were omitted.

Time Point (months)	Sample Type (water or sediment/fft)	Treatment (G+ or G-)	Sample ID	Elemental Analysis (mg/L)										
				B	Ca	Fe	K	Mg	Mn	Mo	Na	Si	Th	Zr
0	water	G-	Shallow	0.19	19.95	0.05	4.06	16.46	0.00	0.00	81.70	0.57	0.01	0.00
0	water	G-	High Sulphate	0.86	151.20	1.05	14.19	104.00	0.00	0.00	278.50	2.65	0.01	0.00
0	water	G-	Syncrude	2.80	6.10	0.03	14.04	12.14	0.01	0.14	901.90	1.65	0.00	0.00
0	water	G-	Crescent	0.11	26.69	0.09	2.84	9.65	0.00	0.00	8.01	0.13	0.00	0.00
0	water	G-	Golden	0.26	84.87	0.50	5.82	66.10	0.00	0.01	325.40	0.50	0.00	0.00
0	water	G-	STP	3.76	3.61	0.02	12.20	7.13	0.01	0.33	899.80	1.34	0.00	0.01
0	water	G-	Muskeg	0.14	30.44	0.11	2.50	11.34	0.00	0.00	14.88	4.19	0.00	0.00
0	water	G-	Pond 1A	3.63	6.55	0.03	12.72	10.06	0.00	0.25	845.80	2.43	0.00	0.00
0	water	G-	Saline	0.52	66.09	0.36	10.63	47.82	0.00	0.00	150.40	1.05	0.00	0.00
0	sed	G-	Crescent	0.37	117.20	3.58	16.70	23.69	1.35	0.01	26.71	7.36	0.00	0.00
0	sed	G-	STP	2.02	41.24	0.53	10.66	10.15	0.21	0.24	425.70	3.26	0.01	0.00
0	sed	G-	Pond 1A	4.52	25.96	0.13	18.86	10.28	0.06	1.43	714.80	2.80	0.01	0.01
0	sed	G-	High Sulphate	1.26	97.14	0.80	17.76	62.38	0.09	0.01	260.80	8.22	0.00	0.00
0	sed	G-	Golden	0.38	90.11	0.77	9.19	52.53	0.19	0.00	337.60	19.87	0.00	0.00
0	sed	G-	Saline	0.75	147.60	1.07	9.83	43.81	0.67	0.00	102.20	1.36	0.00	0.00
0	sed	G-	Shallow	0.23	59.06	1.87	6.39	16.86	0.43	0.01	45.67	4.09	0.00	0.00
0	sed	G-	Syncrude	3.57	21.45	0.44	14.84	13.29	0.07	0.24	1028.00	2.97	0.00	0.02
0	sed	G-	Muskeg	0.31	150.00	27.77	5.90	25.59	0.92	0.00	33.76	25.16	0.00	0.00
0	water	G+*	Shallow	0.20	28.96	0.29	4.21	18.17	0.00	0.00	88.43	1.01	0.00	0.00
0	water	G-*	Inoculum (2014 Set up)	0.32	62.13	0.35	9.69	50.61	0.00	0.00	154.50	0.88	0.00	0.00
0	water	G+	Pond 1A	3.51	7.26	0.05	13.16	12.07	0.02	0.23	847.20	2.49	0.01	0.00
0	water	G+	Syncrude	2.68	9.84	0.08	13.72	12.31	0.02	0.13	872.70	1.91	0.00	0.01
0	water	G+	Saline	0.62	77.43	0.51	14.12	58.23	0.34	0.00	176.10	1.60	0.00	0.00

0	water	G+	Muskeg	0.14	29.47	0.11	2.57	13.04	0.04	0.00	15.69	4.57	0.00	0.00
0	water	G+	Crescent	0.08	20.64	0.05	1.62	6.06	0.01	0.00	5.36	0.26	0.00	0.00
0	water	G+	STP	0.67	0.84	0.01	2.46	1.11	0.01	0.04	146.10	0.30	0.00	0.00
0	water	G+	Golden	0.08	37.77	0.20	2.08	24.21	0.02	0.00	112.50	0.27	0.00	0.00
0	water	G+	High Sulphate	0.48	55.98	0.29	9.20	60.79	0.06	0.00	136.60	1.62	0.00	0.00
0	sed	G+	Muskeg	0.24	148.30	37.65	10.05	28.46	1.33	0.00	20.26	27.00	0.00	0.00
0	sed	G+	High Sulphate	1.48	198.40	1.65	27.64	113.80	0.12	0.00	373.50	20.41	0.00	0.00
0	sed	G+	Crescent	0.27	123.30	8.55	13.89	24.62	1.53	0.00	18.99	7.59	0.01	0.00
0	sed	G+	STP	4.38	6.11	0.03	12.72	8.53	0.03	0.27	941.50	2.28	0.01	0.01
0	sed	G+	Saline	1.28	119.50	18.45	20.46	67.16	0.63	0.00	307.40	8.15	0.00	0.00
0	sed	G+	Golden	0.26	142.50	1.70	10.68	80.91	0.32	0.00	384.50	27.11	0.00	0.00
0	sed	G+	Pond 1A	3.98	26.39	0.62	20.65	14.18	0.06	0.88	630.70	3.74	0.00	0.01
0	sed	G+	Shallow	0.39	149.70	28.99	13.00	46.97	1.96	0.01	122.40	19.19	0.00	0.00
0	sed	G+	Syncrude	3.15	7.46	0.33	12.12	9.72	0.05	0.14	863.50	2.55	0.00	0.01
0	sed		INOCULUM (Shell Totes)	1.77	57.06	5.51	14.08	26.81	0.38	0.00	462.50	6.41	0.00	0.00
0	water		INOCULUM (Shell Totes)	0.37	67.87	0.40	10.91	48.30	0.04	0.00	147.40	0.57	0.00	0.00
9	water	G+	Pond 1A sterile	2.86	3.39	0.02	12.11	8.98	0.00	0.20	615.10	0.23	0.00	0.00
9	water	G-	Crescent	0.23	23.32	0.05	6.05	13.88	0.00	0.00	28.48	0.16	0.01	0.00
9	water	G-	Pond 1A	2.92	4.26	0.02	10.40	12.04	0.00	0.13	586.60	2.32	0.01	0.00
9	water	G+	Shallow	0.28	4.68	0.02	3.85	11.05	0.00	0.00	84.49	0.21	0.00	0.00
9	water	G+	Golden	0.15	45.37	0.25	5.83	43.63	0.00	0.00	279.70	0.21	0.00	0.00
9	water	G+	STP sterile	2.72	3.07	0.02	10.11	6.62	0.01	0.24	779.00	0.68	0.00	0.01
9	water	*	Blank 1	0.08	8.13	0.03	2.20	12.64	0.00	0.00	24.66	0.12	0.00	0.00
9	water	G+	High Sulphate	0.70	68.66	0.42	11.11	58.85	0.00	0.00	192.10	0.19	0.00	0.00
9	water	G+	STP	2.85	3.98	0.02	10.08	8.49	0.00	0.21	772.10	1.49	0.00	0.01
9	water	G+	Pond 1A	2.72	3.45	0.02	11.24	10.18	0.00	0.14	541.40	2.10	0.00	0.00
9	water	G-	Golden	0.15	31.21	0.12	2.97	29.62	0.00	0.00	154.40	0.21	0.00	0.00
9	water	G-	High Sulphate	0.66	81.51	0.54	10.89	52.50	0.00	0.00	175.00	1.16	0.00	0.00

9	water	G+	Saline	0.58	9.29	0.12	10.61	33.94	0.00	0.00	149.20	0.23	0.00	0.00
9	water	G+	Muskeg	0.21	31.23	0.22	4.31	11.51	0.00	0.00	29.06	3.06	0.00	0.00
9	water	G+	Crescent	0.22	32.55	0.20	7.28	11.98	0.00	0.00	24.65	0.31	0.00	0.00
9	water	G-	Syncrude	1.94	3.33	0.02	8.78	7.66	0.00	0.02	678.10	0.35	0.00	0.00
9	water	G+	Pond 1A inoculate	3.08	4.08	0.02	10.67	9.34	0.00	0.19	578.40	2.32	0.00	0.00
9	water	*	Blank 3	0.11	18.48	0.05	2.25	11.98	0.00	0.00	24.07	0.16	0.00	0.00
9	water	G+	Syncrude Sterile	2.04	3.65	0.02	9.70	7.12	0.00	0.05	715.60	1.50	0.00	0.00
9	water	G-	Shallow	0.29	4.50	0.03	2.98	12.00	0.00	0.00	82.80	0.82	0.00	0.00
9	water	G-	Muskeg	0.15	18.63	0.15	0.66	7.29	0.00	0.00	16.93	1.09	0.00	0.00
9	water	G-	Saline	0.61	163.60	1.29	8.13	55.31	0.00	0.00	142.40	0.93	0.01	0.00
9	water	*	Blank 2	0.04	18.99	0.05	2.20	11.83	0.00	0.00	23.69	0.17	0.00	0.00
9	water	G-	STP	2.77	2.83	0.02	9.52	6.73	0.00	0.23	741.70	1.50	0.00	0.01
9	water	G+	STP inoculate	2.98	3.90	0.02	10.57	6.28	0.00	0.30	798.60	1.11	0.00	0.01
9	water	G+	Syncrude	2.02	4.01	0.02	9.74	8.34	0.00	0.03	685.00	1.63	0.00	0.00
9	water	G+	Syncrude Inoculate	1.68	2.78	0.01	7.87	6.03	0.00	0.03	573.20	1.21	0.00	0.00
11	water	G+	Shallow	0.25	5.01	0.02	3.05	8.54	0.00	0.00	53.16	1.59	0.00	0.00
11	water	*	Blank 1	0.04	9.42	0.04	1.57	7.50	0.00	0.00	19.89	0.21	0.00	0.00
11	water	G+	Pond 1A	2.31	2.97	0.02	7.98	4.99	0.00	0.04	394.30	0.34	0.00	0.00
11	water	*	Blank 2	0.04	4.65	0.02	1.46	4.90	0.00	0.00	20.30	0.35	0.00	0.00
11	water	G-	Muskeg	0.20	5.49	0.03	0.07	6.68	0.00	0.00	22.10	1.99	0.00	0.00
11	water	G+	Syncrude Sterile	1.86	2.97	0.02	7.50	6.02	0.00	0.04	579.00	0.31	0.00	0.00
11	water	G-	High Sulphate	0.74	64.43	0.41	9.26	43.71	0.00	0.00	182.30	1.45	0.00	0.00
11	water	G-	STP	2.56	3.05	0.02	7.23	5.30	0.00	0.20	585.90	0.38	0.00	0.00
11	water	G+	Saline	0.57	6.88	0.03	5.45	16.01	0.00	0.00	113.90	0.33	0.00	0.00
11	water	G+	Crescent	0.23	7.41	0.04	1.29	7.62	0.00	0.00	18.74	1.34	0.00	0.00
11	water	G-	Crescent	0.23	33.16	0.20	2.15	11.82	0.00	0.00	21.00	0.29	0.00	0.00
11	water	G+	STP inoculate	0.10	0.56	0.01	0.33	0.21	0.00	0.00	7.06	0.30	0.00	0.00
11	water	G+	Muskeg	0.18	7.32	0.04	0.97	8.27	0.00	0.00	20.25	0.31	0.00	0.00

11	water	G-	Shallow	0.24	9.94	0.10	5.83	11.24	0.00	0.00	67.33	1.47	0.00	0.00
11	water	G+	STP sterile	1.78	2.30	0.01	5.87	3.62	0.00	0.22	470.30	0.34	0.01	0.00
11	water	G+	STP	2.83	3.27	0.02	8.62	5.93	0.00	0.23	672.60	0.76	0.01	0.00
11	water	G+	Pond 1A inoculate	2.55	3.18	0.02	8.46	5.59	0.00	0.14	421.10	0.40	0.00	0.00
11	water	G-	Pond 1A	2.54	3.73	0.02	8.30	6.56	0.00	0.05	427.70	1.26	0.00	0.00
11	water	G-	Golden	0.23	35.30	0.20	1.35	33.21	0.00	0.00	225.90	2.37	0.00	0.00
11	water	*	Blank 3	0.05	9.58	0.11	2.14	10.16	0.00	0.00	21.92	0.24	0.00	0.00
11	water	G-	Syncrude	2.11	3.55	0.02	7.60	6.60	0.00	0.01	606.50	0.47	0.00	0.00
11	water	G+	Syncrude	1.81	3.30	0.02	7.02	5.87	0.00	0.02	537.80	0.33	0.00	0.00
11	water	G+	Golden	0.16	34.36	0.23	1.13	30.37	0.00	0.00	242.60	3.03	0.00	0.00
11	water	G+	High Sulphate	0.68	59.31	0.37	6.56	44.13	0.00	0.00	180.70	2.80	0.00	0.00
11	water	G+	Syncrude Inoculate	1.83	3.63	0.02	6.99	5.46	0.00	0.02	558.40	1.46	0.01	0.00
11	water	G+	Pond 1A sterile	2.64	2.92	0.02	8.50	4.03	0.00	0.18	456.00	0.36	0.01	0.00
11	water	G-	Saline	0.64	182.70	1.48	6.90	55.66	0.00	0.00	140.90	0.33	0.00	0.00
0	water	G+	Shell	ISS	ISS	ISS	ISS	ISS	ISS	ISS	ISS	ISS	ISS	ISS
0	sed	G+	Shell	3.37	37.64	0.90	22.08	22.11	0.13	0.14	460.90	3.53	0.00	0.01
0	sed	G-	Shell	3.47	41.36	0.96	23.83	24.28	0.13	0.13	474.00	3.93	0.00	0.01
0	water	G-	Shell	3.30	33.58	0.20	22.79	17.44	0.00	0.16	444.90	2.32	0.00	0.00
22	water	*	Blank 1	0.05	14.50	0.01	1.46	8.09	0.00	0.01	17.47	0.05	0.00	
22	water	G-	Crescent	0.15	20.42	0.01	3.45	8.10	0.00	0.01	18.90	0.12	0.00	
22	water	G-	Pond 1A	2.16	7.13	0.01	13.36	7.11	0.00	0.07	323.16	2.18	0.00	
22	water	G-	Golden	0.15	28.47	0.01	4.20	29.87	0.00	0.00	160.72	0.19	0.00	
22	water	G-	High Sulphate	0.55	58.04	0.01	12.21	41.34	0.00	0.01	151.12	0.97	0.00	
22	water	G-	Syncrude	1.48	4.42	0.01	10.12	5.28	0.00	0.02	382.27	0.31	0.00	
22	water	G-	Shallow	0.21	6.70	0.01	2.32	8.12	0.00	0.01	62.67	0.56	0.00	
22	water	G-	Muskeg	0.12	22.65	0.01	0.82	7.60	0.00	0.00	19.23	1.11	0.00	
22	water	G-	Saline	0.42	106.40	0.01	6.88	36.80	0.00	0.00	106.45	0.67	0.00	
22	water	G-	STP	1.90	3.90	0.01	9.74	4.17	0.00	0.12	375.06	1.26	0.00	
22	water	G-	Pond 1A Sterile	2.04	3.96	0.01	12.09	5.00	0.00	0.13	320.01	0.31	0.00	

22	water	G-	Syncrude Sterile										
22	water	G-	Shell										
22	water	G-	STP Sterile										
22	water	G+	Pond 1A sterile										
22	water	G+	Shallow	0.21	7.44	0.01	2.62	8.84	0.00	0.01	57.92	0.18	0.00
22	water	G+	Golden	0.11	32.50	0.01	4.88	27.36	0.00	0.00	157.67	0.23	0.00
22	water	G+	High Sulphate	0.51	56.94	0.01	11.42	38.13	0.00	0.00	134.44	0.14	0.00
22	water	G+	STP	1.70	3.55	0.01	11.59	3.82	0.00	0.12	610.16	1.01	0.00
22	water	G+	Pond 1A	1.60	3.30	0.01	11.73	4.42	0.00	0.06	412.47	1.57	0.00
22	water	G+	Saline	0.35	11.13	0.01	10.45	18.45	0.00	0.00	128.75	0.10	0.00
22	water	G+	Muskeg	0.11	26.55	0.01	3.06	6.58	0.00	0.00	21.77	2.45	0.00
22	water	G+	Crescent	0.12	29.28	0.01	5.20	6.96	0.00	0.00	18.35	0.09	0.00
22	water	G+	Pond 1A inoculate	1.95	4.34	0.01	14.55	5.05	0.00	0.08	501.58	1.86	0.00
22	water	G+	Syncrude Sterile	1.18	4.05	0.01	10.52	3.72	0.00	0.03	568.69	1.21	0.00
22	water	G+	STP inoculate	1.81	3.90	0.01	12.63	3.30	0.00	0.15	673.03	0.76	0.00
22	water	G+	Syncrude	1.26	4.48	0.01	11.32	4.59	0.00	0.02	587.32	1.17	0.00
22	water	G+	STP sterile	1.77	3.58	0.01	12.62	3.34	0.00	0.15	655.73	0.77	0.00
22	water	G+	Syncrude Inoculate	1.22	3.80	0.01	10.59	3.73	0.00	0.02	570.66	0.98	0.00
22	water	G+	Shell										
32	water	*	Blank 1	0.06	11.25	0.01	2.44	5.16	0.00	0.00	13.82	0.28	0.00
32	water	G-	Crescent	0.03	24.10	0.01	2.13	6.67	0.00	0.00	11.35	0.31	0.00
32	water	G-	Pond 1A	0.62	3.10	0.01	3.24	1.48	0.00	0.00	153.76	0.39	0.00
32	water	G-	Golden	0.05	35.64	0.01	1.63	15.71	0.00	0.01	81.51	0.10	0.00
32	water	G-	High Sulphate	0.19	17.15	0.01	5.73	12.58	0.00	0.00	68.83	0.27	0.00
32	water	G-	Syncrude	0.36	3.86	0.01	2.38	1.33	0.00	0.00	164.24	0.28	0.00
32	water	G-	Shallow	0.05	13.25	0.01	2.15	5.69	0.00	0.00	26.12	0.23	0.00
32	water	G-	Muskeg	0.05	28.30	0.01	2.38	9.41	0.00	0.00	15.75	0.12	0.00
32	water	G-	Saline	0.10	72.03	0.01	2.79	11.28	0.00	0.00	41.32	0.09	0.00
32	water	G-	STP	0.83	2.75	0.01	4.06	1.78	0.00	0.00	284.95	0.44	0.00

32	water	G-	Pond 1A Sterile	2.07	2.92	0.40	7.87	2.06	0.01	0.04	293.60	3.59	0.00	
32	water	G-	Syncrude Sterile	0.28	2.40	0.01	1.45	0.66	0.00	0.00	93.83	0.29	0.00	
32	water	G-	Shell	0.55	5.14	0.01	5.69	3.02	0.00	0.00	123.84	0.19	0.00	
32	water	G-	STP Sterile	0.54	2.26	0.01	2.67	1.08	0.00	0.01	184.02	0.40	0.00	
32	water	G+	Pond 1A sterile	0.44	2.90	0.01	2.03	1.19	0.00	0.00	102.94	0.46	0.00	
32	water	G+	Shallow	0.08	17.05	0.01	4.27	8.52	0.00	0.00	38.99	0.14	0.00	
32	water	G+	Golden	0.03	7.59	0.01	2.45	6.05	0.00	0.00	83.25	2.09	0.00	
32	water	G+	High Sulphate											
32	water	G+	STP	0.94	3.84	0.01	6.43	2.39	0.01	0.01	355.51	0.28	0.00	
32	water	G+	Pond 1A	0.61	4.49	0.01	2.95	1.29	0.00	0.01	132.46	0.23	0.00	
32	water	G+	Saline	0.20	8.32	0.01	5.88	11.90	0.00	0.00	89.41	0.15	0.00	
32	water	G+	Muskeg	0.03	31.90	0.01	1.83	4.68	0.00	0.00	7.51	0.23	0.00	
32	water	G+	Crescent	0.03	31.40	0.01	3.90	11.56	0.00	0.00	12.26	0.32	0.00	
32	water	G+	Pond 1A inoculate	0.50	2.81	0.01	2.87	1.27	0.00	0.00	115.75	0.46	0.00	
32	water	G+	Syncrude Sterile	0.52	2.60	0.01	4.49	1.78	0.00	0.00	309.85	0.29	0.00	
32	water	G+	STP inoculate	0.39	3.62	0.01	3.14	1.83	0.00	0.03	147.53	0.16	0.00	
32	water	G+	Syncrude	0.36	3.23	0.01	2.49	1.54	0.00	0.00	160.49	0.21	0.00	
32	water	G+	STP sterile	0.75	2.97	0.01	5.58	1.90	0.00	0.07	349.01	0.16	0.00	
32	water	G+	Syncrude Inoculate	0.44	2.83	0.01	3.69	1.41	0.00	0.00	207.33	0.23	0.00	
32	water	G+	Shell	0.29	6.87	0.01	3.30	2.25	0.00	0.00	61.77	0.07	0.00	
32	water	*	PRECIPITATION	0.01	10.32	0.01	0.32	0.68	0.00	0.00	2.39	0.09	0.00	

References

Boudens, R., Reid, T., VanMensel, D., Sabari Prakasan, M. R., Ciborowski, J. J. H., & Weisener, C. G. (2016). Bio-physicochemical effects of gamma irradiation treatment for naphthenic acids in oil sands fluid fine tailings. Science of the Total Environment, 539, 114–124. https://doi.org/10.1016/j.scitotenv.2015.08.125

Brüchert, V., Jørgensen, B. B., Neumann, K., Riechmann, D., Schlösser, M., & Schulz, H. (2003). Regulation of bacterial sulfate reduction and hydrogen sulfide fluxes in the central Namibian coastal upwelling zone. Geochimica et Cosmochimica Acta, 67(23), 4505–4518. https://doi.org/10.1016/S0016-7037(03)00275-8

Caporaso, J. G., Kuczynski, J., Stombaugh, J., Bittinger, K., Bushman, F. D., Costello, E. K., … Knight, R. (2010). QIIME allows analysis of high-throughput community sequencing data. Nature Methods, 7, 335. Retrieved from https://doi.org/10.1038/nmeth.f.303

Chen, M., Walshe, G., Chi Fru, E., Ciborowski, J. J. H., & Weisener, C. G. (2013). Microcosm assessment of the biogeochemical development of sulfur and oxygen in oil sands fluid fine tailings. Applied Geochemistry, 37, 1–11. https://doi.org/10.1016/j.apgeochem.2013.06.007

Foght, J. M., & Fedorak, P. (2015). Microbial metagenomics of oil sands tailings ponds: small bugs, big data. Genome, 58(November), 507–510. https://doi.org/10.1139/gen-2015-0146

Fru, E. C., Chen, M., Walshe, G., Penner, T., Weisener, C., Chi Fru, E., … Weisener, C. (2013). Bioreactor studies predict whole microbial population dynamics in oil sands

tailings ponds. Applied Microbiology and Biotechnology, 97(7), 3215–3224.

https://doi.org/10.1007/s00253-012-4137-6

Kuwabara, J. S., Van Geen, A., McCorkle, D. C., & Bernhard, J. M. (1999). Dissolved

sulfide distributions in the water column and sediment pore waters of the Santa

Barbara Basin. Geochimica et Cosmochimica Acta, 63(15), 2199–2209.

https://doi.org/10.1016/S0016-7037(99)00084-8

Liang, J., Tumpa, F., Estrada, L. P., El-din, M. G., & Liu, Y. (2014). Ozone-Assisted

Settling of Diluted Oil Sands Mature Fine Tailings : A Mechanistic Study, (March).

Reid, Thomas, Boudens, R., Ciborowski, J. J. H., & Weisener, C. G. (2016).

Physicochemical gradients, diffusive flux, and sediment oxygen demand within oil

sands tailings materials from Alberta, Canada. Applied Geochemistry, 75, 90–99.

https://doi.org/10.1016/j.apgeochem.2016.10.004

Reid, T., VanMensel, D., Droppo, I. G., & Weisener, C. G. (2016). The symbiotic

relationship of sediment and biofilm dynamics at the sediment water interface of oil

sands industrial tailings ponds. Water Research, 100, 337–347.

https://doi.org/10.1016/j.watres.2016.05.025

Reid, Thomas, Droppo, I. G., Chaganti, S. R., & Weisener, C. G. (2019). Microbial

metabolic strategies for overcoming low-oxygen in naturalized freshwater reservoirs

surrounding the Athabasca Oil Sands: A proxy for End-Pit Lakes? Science of The

Total Environment, 665, 113–124. https://doi.org/10.1016/j.scitotenv.2019.02.032

Risacher, F. F., Morris, P. K., Arriaga, D., Goad, C., Nelson, T. C., Slater, G. F., & Warren, L. A. (2018). The interplay of methane and ammonia as key oxygen consuming constituents in early stage development of Base Mine Lake, the first demonstration oil sands pit lake. Applied Geochemistry, 93(August 2017), 49–59. https://doi.org/10.1016/j.apgeochem.2018.03.013

Siddique, T., Kuznetsov, P., Kuznetsova, A., Arkell, N., Young, R., Li, C., … Foght, J. M. (2014). Microbially-accelerated consolidation of oil sands tailings. Pathway I: changes in porewater chemistry. Frontiers in Microbiology, 5(March), 1–11. https://doi.org/10.3389/fmicb.2014.00106

VanMensel, D., Chaganti, S. R., Boudens, R., Reid, T., Ciborowski, J., & Weisener, C. (2017). Investigating the Microbial Degradation Potential in Oil Sands Fluid Fine Tailings Using Gamma Irradiation: A Metagenomic Perspective. Microbial Ecology, 74(2), 362–372. https://doi.org/10.1007/s00248-017-0953-7

Wilson, S. L., Li, C., Ramos-Padrón, E., Nesbø, C., Soh, J., Sensen, C. W., … Gieg, L. M. (2016). Oil sands tailings ponds harbour a small core prokaryotic microbiome and diverse accessory communities. Journal of Biotechnology, 235, 187–196. https://doi.org/10.1016/j.jbiotec.2016.06.030

Yergeau, E., Lawrence, J. R., Sanschagrin, S., Waiser, M. J., Darren, R., Korber, D. R., … Darren, R. (2012). Next-generation sequencing of microbial communities in the athabasca river and its tributaries in relation to oil sands mining activities. Applied and Environmental Microbiology, 78(21), 7626–7637. https://doi.org/10.1128/AEM.02036-12

Yu, X., Lee, K., Ma, B., Asiedu, E., & Ulrich, A. C. (2018). Indigenous microorganisms residing in oil sands tailings biodegrade residual bitumen. Chemosphere, 209, 551–559. https://doi.org/10.1016/j.chemosphere.2018.06.126

CHAPTER 6: **DISSERTATION CONCLUSIONS, DISCUSSION AND FUTURE DIRECTIONS**

6.1 Summary

The systematic characterization of both natural and anthropogenically-made tailings ecosystems within the Athabasca Oil Sands region of Alberta, Canada has provided much needed insight into the biogeochemical nature of these respective systems. There has been a significant lack of understanding of the natural processes governing the microbial ecology of this region, therefore this research significantly improves upon our understanding of reclamation end-points for effective reclamation practices. This research is the first to identify in-situ microbial function in this naturally hydrocarbon-rich environment, void of additional anthropogenic influence. The unique study system of the MF provides an in-situ field-scale laboratory from which to unravel likely fate of EPL establishment and long-term maturation of oil sands tailings well into the future.

Determination of the baseline biogeochemical signature governing the natural ecosystems surrounding the industrial mine sites was completed and explained with Chapter 2-4. In particular the noted syntrophy of activity observed in both tributary sediments alongside deep, freshwater reservoirs were some of the most significant observations made within the research presented here, corroborating research hypotheses 1 & 2 (RH1 & RH2). The complex interplay of metabolic processes (i.e. photosynthesis, nitrogen, sulfur, methane and noted biodegradation genes) governed by the natural microbial consortia, indicate a uniquely tailored lifestyle adapted for life within the MF. Enhancements in sulfide production appear to be offset by an enhanced anaerobic phototrophic consortium, all too eager to consume the sulfides produced. A significant shift towards methanogenesis in relation to complex aromatic degradation has allowed the microbial communities to not only thrive in this region but work at metabolizing potentially toxic hydrocarbons under sometimes limiting thermodynamic conditions. This too is seemingly offset by unique

methanotrophic organisms capable of dual reduction-oxidation roles. This cooperative relationship across phylogenetic groups of taxa are perhaps representative of an ecosystem adapted and equilibrated to its biogeochemical niche. The microbial consortia present within these natural sediments are not working in isolation, but perhaps in a mutually beneficial, inter-species network. Though constrained by the thermodynamic limitations within the low-oxygen zones of these deeper reservoirs, these bacteria appear to maintain metabolic efficiency through adaptive metabolic routes indicative of these sub-oxic to anoxic locations. It is these processes that are likely to govern the depths of future EPLs, and as such should be studied and characterized in further detail.

Exploring the genetic response to the MF down a river continuum was also completed and presented in Chapter 5. Here, the hypothesis (RH3) was partially accepted, since there was an immediate genetic response to the MF, clearly indicative of a metabolic shift to the elevated hydrocarbons of the MF substrate. Results presented within this chapter, reveal the co-occurrence of both increased and suppressed clusters of metabolic genes pointing towards the greater syntrophy of microbial activity responding to the unique biogeochemistry of the MF. Insights gained here provide significant insights into the tracking of compounds in hydrodynamic environments utilizing novel genetic approaches. It is clear that these shotgun metatranscriptomics surveys were provided the sensitivity required to track exposure to the MF, with the genetic response readily responding in both suspended and bed sediments. Additionally, though it is easy to attribute the noted expression of perhaps alkB, badB or bbsBD genes as appropriate biomarkers for the onset of the MF, correlating trends in broader/multi gene clusters provides more robust and meaningful insight into how the biological *ecosystem* responds. It is this repeated observation of similar changes to several

genes within energy metabolism pathways that suggest using a series of genes as biomarkers, and not being reliant on single genes as implemented so frequently within the literature. This has already given rise to the use of functional gene arrays to identify changes at a primary productivity level, which is clearly the appropriate research direction moving forward.

Characterizing the long-term evolution of tailings and natural wetland sediments in field-scale mesocosms, provided a proof of concept to the use of GI treatment for the detoxification and advancement of tailings towards reclaimed environments. This study proved to partially validate the hypothesis (RH4), in that the biogeochemical signature of the various tailings systems trended towards a more natural state indicative of the natural wetlands studied. However, after 32-months of study, even the NA and salinity variations were nearly negligible as measured within the overlying water column, suggesting the feasibility of natural reclamation given sufficient time-lines. This field validation of the previously studied GI treatment proves the effectiveness of this treatment in reducing the concentration of NAs, though long-term characterization showed natural breakdown of NAs in untreated systems as well. This suggests that GI treatment may be a viable option to shorten reclamation timelines, despite the natural progression noted here.

6.2 Significance

Insight gathered here into the natural biogeochemical signature of the MF, and the genetic responses to hydrocarbon exposure extend far beyond the reaches of the MF itself. These advanced -omics techniques to track and identify the actual biological impact of exposure to an increasing chemical gradient lends to the notion that these sensitive gene expression surveys can be implemented as novel approaches to track contaminant plumes around the world. What's advantageous about such an approach, is that it presents an

effective means by which to identify true biological response to compound exposure, providing insight into exposure effects at a primary productivity level. Understanding these primary ecological shifts resulting from these environmental gradients effectively characterizes the extent to which the propagation of a given compound impacts biological activity. Furthermore, being able to isolate gene expression in both the suspended and bed sediment compartments provides an increased level of sensitivity in tracking the dynamic response under hydrodynamic conditions.

Our daily lives put immense pressures on our local and regional ecosystems, as waste products enter our local waterways, and road-runoff washes a variety of xenobiotic compounds into both surface and groundwaters at any given time. Complex erosion processes erode, transport and deposit foreign matter at alarming rates, taking with it the contaminants once deposited within it. These compounds are inevitably met by a consortium of microorganisms eager to metabolize these products for their energetic requirements. Understanding these front-line operators within any given ecosystem is the first step in addressing remedial action if necessary. Microbes are uniquely adapted to live in every environment known to man, as such, their phenotypic plasticity should not be underestimated. Our once theoretically understood understanding of the functional abilities of cultured microbes has long been outdated practice. Characterizing in-situ environments, as performed here, in both natural and contaminated ecosystems provides novel insight into the similarities and differences in the systems ecology at a microscopic level. What's more, is that these findings go well beyond their unique study systems. The cooperative framework of metabolisms observed in any one environment, only lends itself to explore those not yet understood. Results discovered here, within the uniquely complex MF, can provide

invaluable insight into other freshwater ecosystems, both lotic and lentic, where hydrocarbons or other complex organics may be present. The mechanistic adaptation techniques employed by these microbes is insight into how truly adept they are at dealing with complex environmental gradients and utilizing their functional plasticity to their advantage. Insights gathered here further indicate how dynamic and interconnected these aquatic environments are, wreaking havoc on our conventional, theoretical understandings of redox processes. Microbes do not function in isolation, and as such, their cooperative metabolic processes are able to bridge thermodynamic barriers once thought improbable prior to high-throughput sequencing technologies.

Overall the extensive use of metatranscriptomics approaches within these research chapters advances our understanding of microbial processes governing natural ecosystems. For the first time in the Athabasca Oil Sands region, these active gene expression surveys provided insights into the processes driving the alteration of various nutrients and compounds within the environment, going beyond what strict geochemical or microbiology studies alone could uncover. This methodology is still relatively new to environmental science, and as such is quickly adapting, as evidenced by the progression and refinement of the methodology exemplified in Chapters 2-4. Nonetheless, aside from the scientific discoveries presented herein, the advancements in our abilities to utilize metatranscriptomics approaches in other freshwater and marine environments is perhaps of equal importance, given its ability to reveal active microbial activity in even the most complex ecosystems.

6.3 Recommendations and Future Directions

The ability to effectively characterize biogeochemical processes governing any ecosystem is invaluable in overcoming biases associated with targeted approaches or even

taxonomic assessments reliant on theoretical functional traits. These processes actively dictating the dynamics associated with both suspended and bed sediments provides a holistic framework from which to understand the interplay and diffusive dynamics across sediment-water boundaries. Future studies would benefit even more from augmentation with geochemical approaches such as stable isotope probing, providing additional supportive evidence for microbially mediated transformations of various compounds. Additionally, carefully monitored laboratory studies could be beneficial in quantifying specific genetic responses to specific metabolites, as such correlations remain understudied in functional microbial studies. Overall these approaches utilized here alongside these aforementioned geochemical approaches would be ideal methodologies in determining environmental and ecosystem response to both acute and chronic exposures to any compound of interest. Here in the McMurray Formation, more specifically the oil sands tailings environments, these types of in-situ genomic studies remain lacking at best. Taxonomic surveys need to be augmented with functional profiles that given true insight into *what* these microbes are doing in these heterogeneous tailings ecosystems. Insights gathered here suggest a slow shift towards a naturalized ecosystem given sufficient time, though further insight into actual microbial expression would be ideal in teasing out the true biogeochemical trends over time.

Dating back to the mid-1900's, Sergei Winogradsky introduced to the world the notion of chemolithotrophy, and the cooperative metabolism of several nitrogen and sulfur metabolizing organisms. It is his work that began our understanding of microbial ecology, and the coexistence of microorganisms in infinitely small redox zones within waters, sediments and soils. This discovery of environmental microbiomes began to shape our understanding of environmental biogeochemistry, and the truly complex nature in which it

operates. He also discovered how differently microbes grew and evolved in controlled laboratory studies compared to their natural environment:

"…a microbe cultivated sheltered from any living competitors and luxuriously fed becomes a hot-house culture, and is induced to become in a short period of time a new race that could not be identified with its prototype without special study."

(Windogradsky, 1949)

It is this fundamental understanding put forth years ago, that we must strive to follow as environmental scientists, microbial ecologists and geochemists. Targeted approaches have become technologically advanced, though are often considered in absence of a holistic mindset needed to unravel the complexities of environmental systems. There is a need to develop methodologies more adept at unravelling in-situ, holistic biogeochemical signatures of aquatic ecosystems, going beyond short-circuited approaches in characterizing single/isolated metabolic pathways. In isolation, even the most advanced -omics or geochemical approaches are unable to provide the entire biogeochemical picture. The studies presented here attempt to follow these fundamental ideas put forth by Windogradsky almost 70 years ago, largely relying on in-situ observations in the attempt to better understand the natural ecology of this truly unique regional ecosystem. Studies in recent years have unfortunately been reliant on cultured observations, and thus we must be careful in how much knowledge can be truly gained from studies providing this "sheltered" and "luxuriously fed" environment in which to thrive. Isolating a complex system in an attempt to understand finite processes can never be performed in absolute parallel to its in-situ setting, as such

203

conclusions drawn from such studies must be cognizant of this inherent bias. Thus, moving forward, researchers must go back to the fundamental insights provided by Windogradsky, and implement truly multi-disciplinary, holistic approaches to accurately characterize the biogeochemical signature governing the world's most diverse pristine and contaminated ecosystems.

Appendix A (Chapter 2)
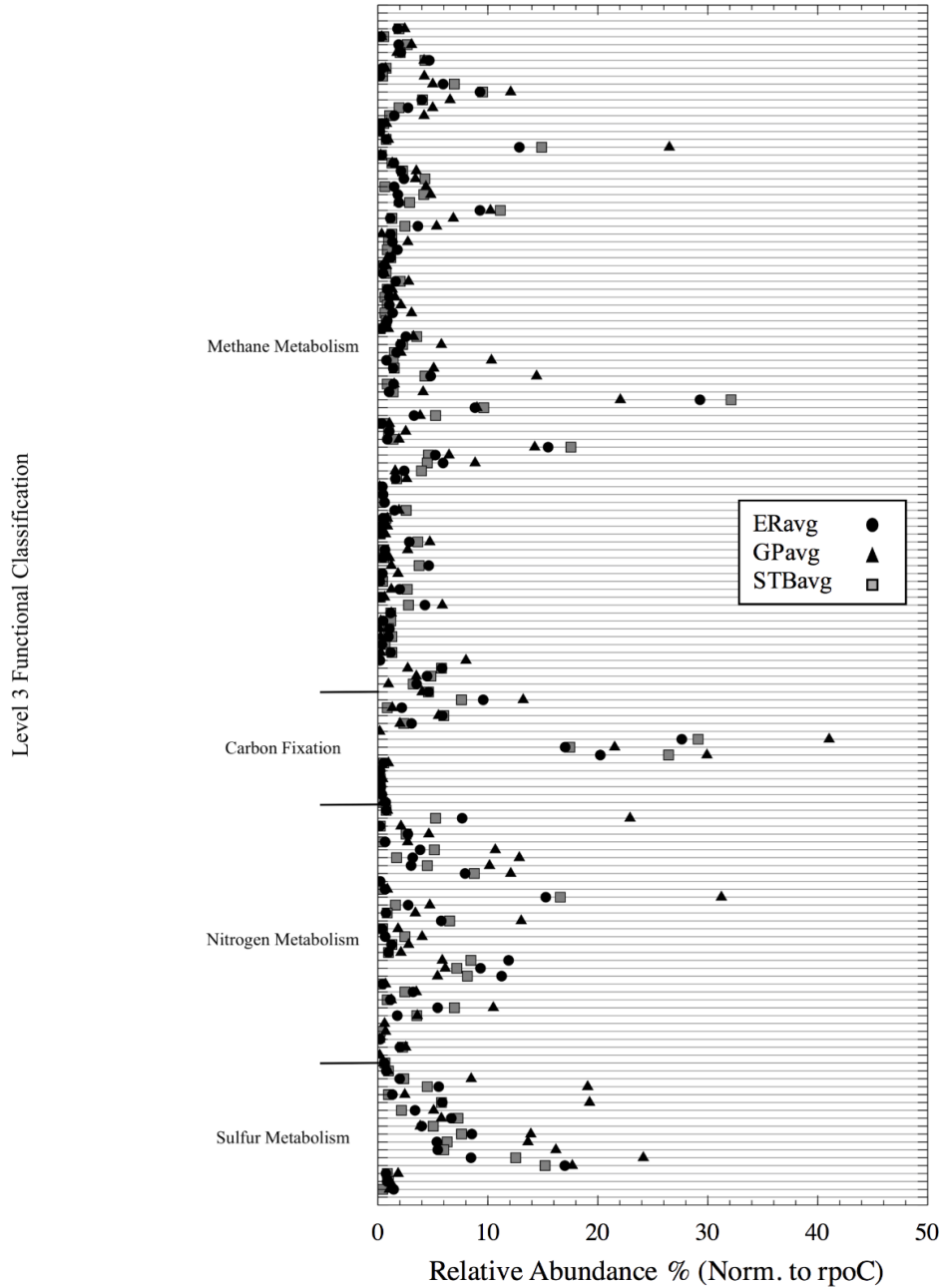
Figure S1: Energy Metabolism transcripts plotted to reveal dominant expression within level 3 categories of methane metabolism, carbon fixation, nitrogen metabolism and sulfur metabolism. The y-axis is made up of individual enzymes/genes within each functional category, with their relative abundances along the x-axis. Differential expression between sites is visualized according to the embedded legend.
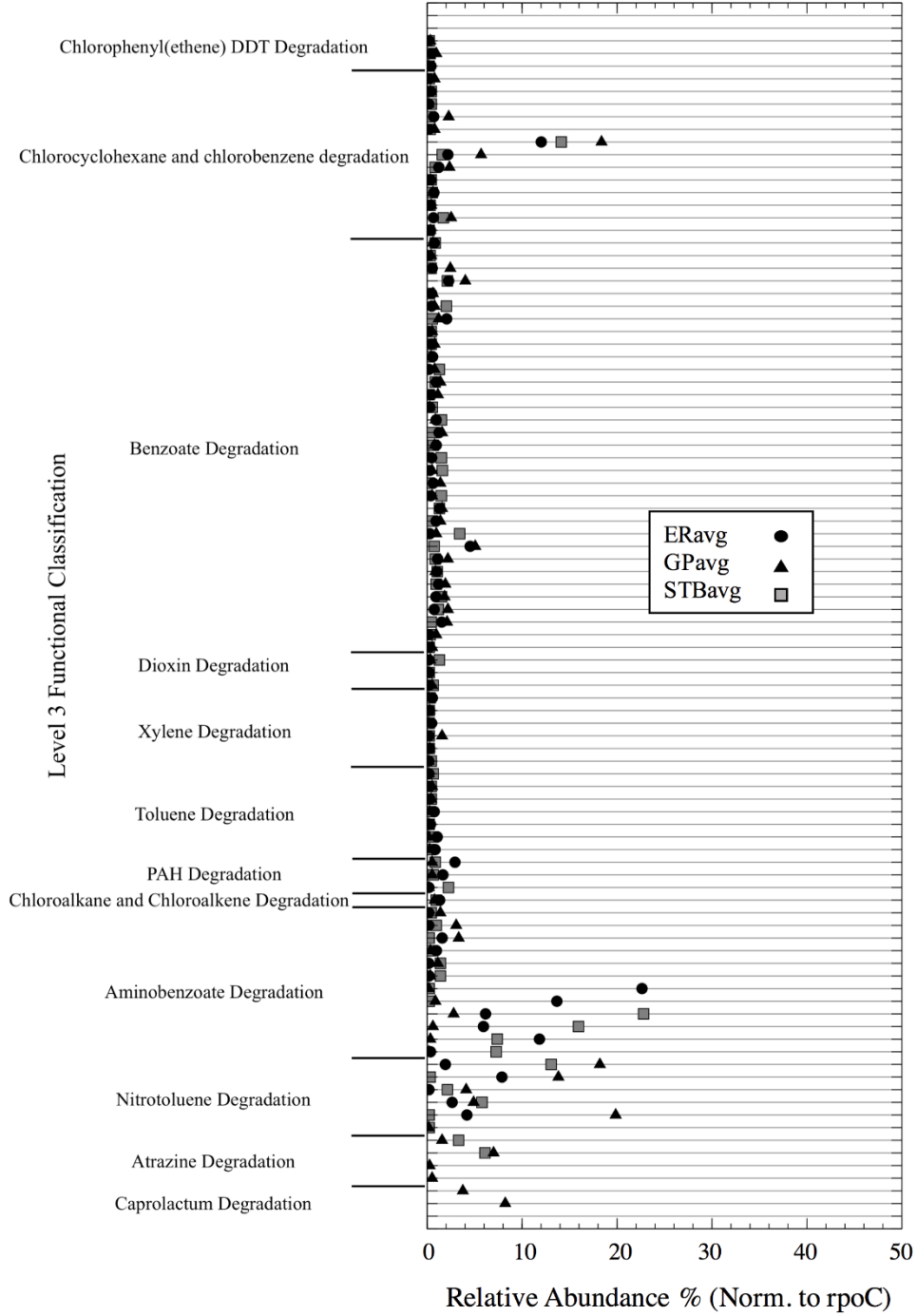
Figure S2: Hydrocarbon and Xenobiotic biodegradation transcripts plotted to reveal dominant expression within level 3 categories (i.e. PAH, Toluene, Chloroalkane etc.). The y-axis is made up of individual enzymes/genes within each functional category, with their relative abundances along the x-axis. Differential expression between sites is visualized according to the embedded legend.

Table S1: Sequencing results from the Illumina HiSeq 2000, identifying bp counts, and identified features and mean GC %.

Metagenome Name	Ells River (ER)	Groundwater Plume (GP)	Steepbank River (STB)
bp Count	7 980 387 131	6 494 536 006	3 432 270 576
Sequence Count	67 626 392	53 880 774	29 185 998
Identified Protein Features	800 797	1 993 714	684 482
Identified rRNA Features	352 347	215 547	144 269
Identified Functional Categories	579 894	1 574 505	510 407
Mean GC%	52	48.5	51

Appendix B (Chapter 3)
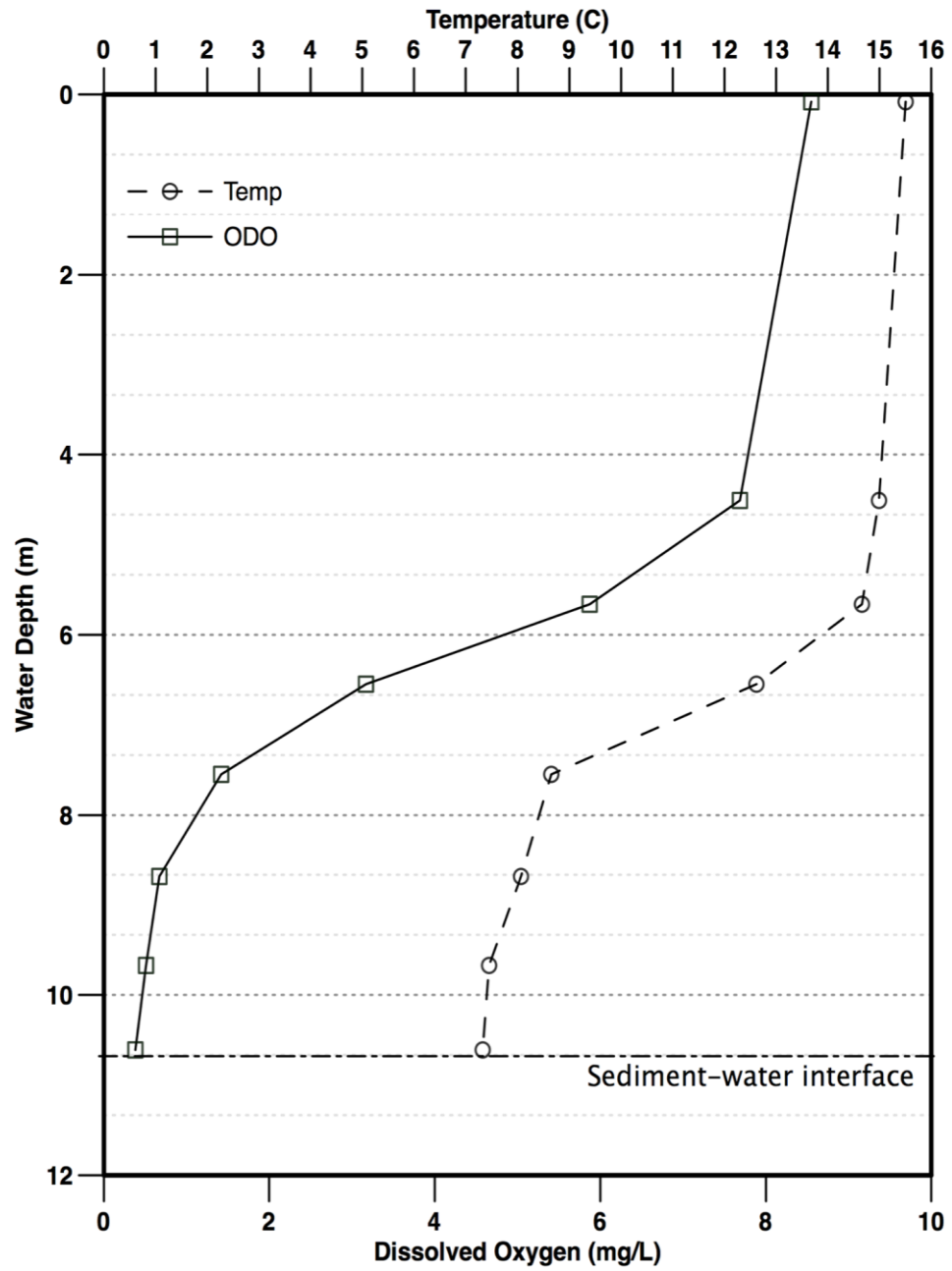
FIGURE S1 Limnological profile of Poplar Creek Reservoir South - the only location deeper than 2m measured in both PCR and RL, and only site to contain a thermocline.
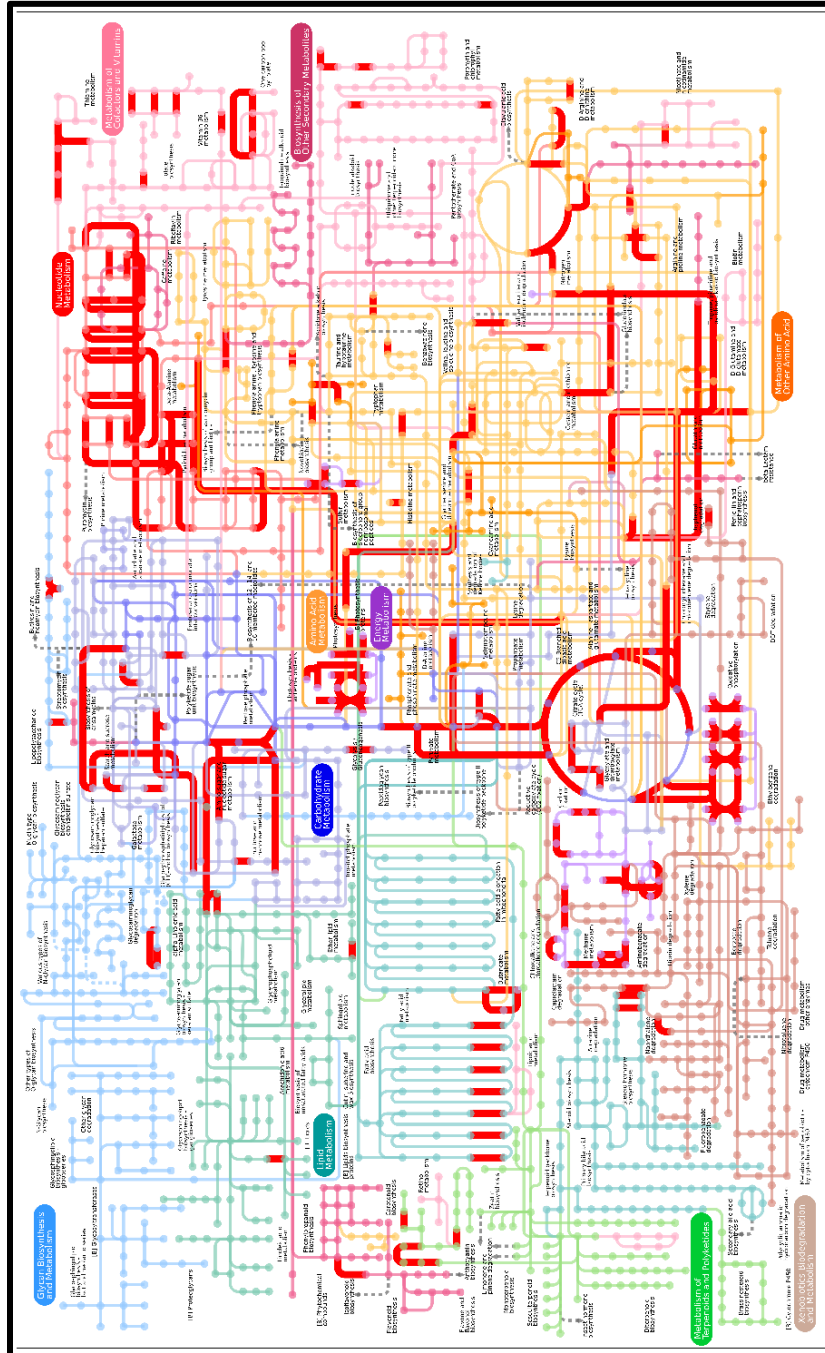
FIGURE S2 Differentially expressed transcripts mapped to the KEGG Atlas, identifying significantly overexpressed genes in PCR South compared to the more oxygenated sites of PCR Shallow and RL. Areas of significantly higher expression include photosynthesis, xenobiotic degradation, fatty acid metabolism, carbon fixation, nitrogen, sulfur and methane metabolism. Figure plotted using The Interactive Pathways Explorer v2 (iPath2) (Yamada et al., 2011).

Table S1 Lists of all differentially expressed genes (COG Annotations provided), significantly differentially expressed between noted sites, p<0.05. (Referenced from Figure 4 caption)

PCR Shallow vs Ruth Lake	PCR Shallow vs PCR Deep	PCR Deep vs Ruth Lake
COG0004	COG0003	COG0005
COG0021	COG0005	COG0019
COG0033	COG0019	COG0023
COG0050	COG0023	COG0035
COG0055	COG0035	COG0037
COG0056	COG0037	COG0039
COG0088	COG0051	COG0048
COG0089	COG0076	COG0050
COG0091	COG0078	COG0051
COG0092	COG0080	COG0052
COG0093	COG0086	COG0055
COG0155	COG0101	COG0056
COG0158	COG0148	COG0076
COG0191	COG0162	COG0078
COG0199	COG0177	COG0080
COG0200	COG0193	COG0081
COG0208	COG0206	COG0086
COG0219	COG0235	COG0088
COG0221	COG0242	COG0089
COG0222	COG0244	COG0090
COG0224	COG0274	COG0091
COG0227	COG0280	COG0092
COG0230	COG0295	COG0093
COG0234	COG0297	COG0094

COG0236	COG0311	COG0096
COG0238	COG0312	COG0097
COG0244	COG0334	COG0098
COG0255	COG0342	COG0099
COG0260	COG0343	COG0100
COG0261	COG0344	COG0148
COG0268	COG0351	COG0155
COG0269	COG0366	COG0162
COG0288	COG0371	COG0177
COG0291	COG0395	COG0190
COG0296	COG0402	COG0191
COG0316	COG0403	COG0192
COG0326	COG0404	COG0193
COG0333	COG0420	COG0197
COG0339	COG0423	COG0198
COG0347	COG0428	COG0200
COG0348	COG0438	COG0201
COG0356	COG0444	COG0202
COG0360	COG0455	COG0203
COG0369	COG0456	COG0211
COG0372	COG0464	COG0222
COG0377	COG0470	COG0224
COG0400	COG0475	COG0234
COG0408	COG0477	COG0236
COG0448	COG0478	COG0238
COG0450	COG0481	COG0242
COG0479	COG0482	COG0244
COG0488	COG0490	COG0250
COG0506	COG0495	COG0274

COG0508	COG0496	COG0280
COG0523	COG0498	COG0282
COG0526	COG0503	COG0291
COG0539	COG0513	COG0292
COG0545	COG0522	COG0297
COG0563	COG0525	COG0326
COG0567	COG0534	COG0333
COG0572	COG0549	COG0334
COG0583	COG0552	COG0342
COG0589	COG0561	COG0343
COG0604	COG0562	COG0344
COG0623	COG0574	COG0351
COG0625	COG0579	COG0356
COG0633	COG0594	COG0366
COG0635	COG0595	COG0369
COG0636	COG0597	COG0371
COG0637	COG0599	COG0372
COG0643	COG0601	COG0395
COG0649	COG0606	COG0404
COG0652	COG0608	COG0420
COG0654	COG0621	COG0425
COG0659	COG0630	COG0428
COG0664	COG0638	COG0443
COG0670	COG0643	COG0450
COG0676	COG0647	COG0456
COG0678	COG0648	COG0465
COG0699	COG0656	COG0469
COG0702	COG0674	COG0475
COG0711	COG0675	COG0477

COG0712	COG0677	COG0480
COG0722	COG0680	COG0481
COG0723	COG0688	COG0482
COG0783	COG0724	COG0488
COG0790	COG0737	COG0496
COG0791	COG0745	COG0503
COG0826	COG0747	COG0513
COG0835	COG0752	COG0522
COG0839	COG0756	COG0534
COG0840	COG0765	COG0539
COG0843	COG0784	COG0542
COG0853	COG0833	COG0545
COG0861	COG0835	COG0549
COG1007	COG1014	COG0553
COG1034	COG1029	COG0554
COG1038	COG1031	COG0557
COG1049	COG1035	COG0572
COG1053	COG1058	COG0574
COG1146	COG1078	COG0580
COG1161	COG1079	COG0594
COG1162	COG1084	COG0595
COG1274	COG1093	COG0597
COG1282	COG1095	COG0599
COG1290	COG1100	COG0606
COG1309	COG1102	COG0621
COG1383	COG1103	COG0625
COG1398	COG1107	COG0629
COG1448	COG1123	COG0633
COG1485	COG1129	COG0636

COG1544	COG1145	COG0642
COG1553	COG1153	COG0643
COG1554	COG1155	COG0652
COG1622	COG1156	COG0656
COG1629	COG1157	COG0659
COG1651	COG1167	COG0674
COG1652	COG1172	COG0675
COG1678	COG1173	COG0678
COG1686	COG1175	COG0680
COG1734	COG1178	COG0697
COG1740	COG1190	COG0712
COG1802	COG1202	COG0715
COG1816	COG1203	COG0723
COG1825	COG1206	COG0724
COG1845	COG1208	COG0730
COG1850	COG1222	COG0737
COG1866	COG1229	COG0745
COG1875	COG1242	COG0756
COG1926	COG1243	COG0760
COG1952	COG1251	COG0762
COG1969	COG1256	COG0765
COG1981	COG1258	COG0776
COG2010	COG1269	COG0784
COG2015	COG1278	COG0804
COG2030	COG1287	COG0835
COG2046	COG1291	COG0840
COG2072	COG1293	COG0843
COG2077	COG1307	COG1031
COG2124	COG1311	COG1034

COG2127	COG1315	COG1035
COG2142	COG1323	COG1047
COG2168	COG1328	COG1049
COG2171	COG1334	COG1079
COG2175	COG1338	COG1089
COG2181	COG1340	COG1100
COG2183	COG1344	COG1129
COG2210	COG1348	COG1145
COG2221	COG1352	COG1160
COG2223	COG1356	COG1161
COG2224	COG1357	COG1162
COG2225	COG1360	COG1172
COG2227	COG1361	COG1175
COG2308	COG1363	COG1178
COG2326	COG1366	COG1185
COG2346	COG1377	COG1256
COG2352	COG1387	COG1269
COG2358	COG1395	COG1278
COG2514	COG1397	COG1290
COG2609	COG1404	COG1291
COG2703	COG1405	COG1307
COG2823	COG1406	COG1315
COG2825	COG1410	COG1334
COG2838	COG1413	COG1340
COG2844	COG1419	COG1344
COG2847	COG1422	COG1352
COG2857	COG1432	COG1357
COG2863	COG1434	COG1363
COG2885	COG1449	COG1366

COG2916	COG1459	COG1392
COG2920	COG1461	COG1394
COG2923	COG1479	COG1397
COG2993	COG1482	COG1403
COG3005	COG1483	COG1406
COG3012	COG1484	COG1410
COG3043	COG1491	COG1413
COG3047	COG1494	COG1419
COG3090	COG1497	COG1422
COG3108	COG1500	COG1429
COG3123	COG1516	COG1432
COG3162	COG1518	COG1434
COG3166	COG1523	COG1436
COG3168	COG1526	COG1449
COG3170	COG1527	COG1459
COG3203	COG1536	COG1460
COG3215	COG1537	COG1479
COG3221	COG1543	COG1482
COG3237	COG1549	COG1484
COG3239	COG1552	COG1494
COG3243	COG1571	COG1516
COG3245	COG1577	COG1523
COG3278	COG1585	COG1527
COG3303	COG1586	COG1543
COG3317	COG1598	COG1544
COG3338	COG1599	COG1554
COG3349	COG1602	COG1585
COG3396	COG1606	COG1586
COG3439	COG1609	COG1609

COG3664	COG1614	COG1653
COG3685	COG1634	COG1670
COG3729	COG1644	COG1677
COG3730	COG1646	COG1699
COG3781	COG1647	COG1704
COG3808	COG1650	COG1706
COG3853	COG1653	COG1728
COG3909	COG1655	COG1744
COG3954	COG1670	COG1749
COG4102	COG1672	COG1766
COG4108	COG1675	COG1776
COG4117	COG1677	COG1788
COG4133	COG1681	COG1799
COG4147	COG1693	COG1801
COG4196	COG1699	COG1825
COG4213	COG1704	COG1840
COG4242	COG1706	COG1843
COG4263	COG1712	COG1855
COG4391	COG1724	COG1868
COG4548	COG1727	COG1871
COG4553	COG1728	COG1873
COG4564	COG1731	COG1879
COG4575	COG1739	COG1894
COG4582	COG1744	COG1905
COG4636	COG1746	COG1922
COG4638	COG1749	COG1926
COG4654	COG1751	COG1927
COG4663	COG1766	COG1932
COG4678	COG1767	COG1941

COG4770	COG1775	COG1957
COG4775	COG1776	COG1962
COG4803	COG1779	COG1976
COG4902	COG1782	COG1982
COG4957	COG1788	COG2007
COG4969	COG1799	COG2010
COG4993	COG1801	COG2015
COG5008	COG1805	COG2018
COG5013	COG1812	COG2046
COG5023	COG1813	COG2048
COG5044	COG1821	COG2057
COG5059	COG1829	COG2058
COG5064	COG1831	COG2059
COG5078	COG1832	COG2063
COG5126	COG1843	COG2072
COG5169	COG1847	COG2089
COG5190	COG1853	COG2092
COG5245	COG1855	COG2101
COG5262	COG1857	COG2115
COG5265	COG1868	COG2116
COG5267	COG1871	COG2117
COG5272	COG1873	COG2124
COG5274	COG1883	COG2141
COG5276	COG1884	COG2165
COG5322	COG1885	COG2170
COG5394	COG1906	COG2172
COG5464	COG1922	COG2179
COG5501	COG1927	COG2181
COG5557	COG1933	COG2182

COG5640	COG1938	COG2201
	COG1941	COG2202
	COG1945	COG2209
	COG1953	COG2221
	COG1955	COG2274
	COG1957	COG2310
	COG1958	COG2319
	COG1962	COG2340
	COG1973	COG2353
	COG1976	COG2376
	COG1987	COG2403
	COG2018	COG2469
	COG2019	COG2604
	COG2024	COG2703
	COG2036	COG2738
	COG2037	COG2759
	COG2048	COG2770
	COG2051	COG2838
	COG2057	COG2864
	COG2058	COG2871
	COG2064	COG2908
	COG2089	COG2987
	COG2092	COG3239
	COG2101	COG3252
	COG2103	COG3259
	COG2116	COG3307
	COG2117	COG3330
	COG2118	COG3341
	COG2140	COG3345

COG2141	COG3349
COG2144	COG3383
COG2150	**COG3396**
COG2170	COG3424
COG2172	COG3426
COG2179	COG3437
COG2182	COG3457
COG2201	COG3481
COG2202	COG3670
COG2209	COG3673
COG2218	COG3678
COG2231	COG3808
COG2237	COG3833
COG2238	COG3842
COG2268	COG3845
COG2272	COG3853
COG2274	COG3876
COG2340	COG3882
COG2353	COG3920
COG2376	COG3934
COG2403	COG3937
COG2404	COG3968
COG2431	COG4054
COG2445	COG4055
COG2450	COG4056
COG2452	COG4057
COG2469	COG4059
COG2524	COG4060
COG2604	COG4061

COG2710	COG4063
COG2723	COG4065
COG2738	COG4120
COG2759	COG4198
COG2770	COG4213
COG2813	COG4371
COG2820	COG4403
COG2856	COG4577
COG2864	COG4581
COG2865	COG4603
COG2874	COG4624
COG2886	COG4636
COG2894	COG4659
COG2908	COG4678
COG2987	COG4786
COG3072	COG4870
COG3199	COG4902
COG3227	COG5052
COG3246	COG5064
COG3252	COG5069
COG3259	COG5078
COG3261	COG5147
COG3291	COG5245
COG3307	COG5262
COG3330	COG5265
COG3341	COG5271
COG3345	COG5272
COG3356	COG5276
COG3364	COG5322

COG3390	COG5421
COG3408	COG5464
COG3426	COG5550
COG3457	COG5563
COG3467	COG5607
COG3481	COG5662
COG3527	
COG3576	
COG3584	
COG3649	
COG3673	
COG3678	
COG3682	
COG3829	
COG3833	
COG3839	
COG3842	
COG3845	
COG3872	
COG3876	
COG3877	
COG3882	
COG3920	
COG3934	
COG3937	
COG3961	
COG4008	
COG4021	
COG4022	

COG4041

COG4048

COG4051

COG4054

COG4055

COG4056

COG4057

COG4058

COG4059

COG4060

COG4061

COG4062

COG4063

COG4065

COG4070

COG4081

COG4120

COG4198

COG4213

COG4403

COG4529

COG4577

COG4581

COG4603

COG4608

COG4624

COG4636

COG4659

COG4675

COG4738

COG4786

COG4907

COG4995

COG5052

COG5119

COG5250

COG5256

COG5257

COG5270

COG5271

COG5421

COG5550

COG5563

COG5607

Appendix C (Chapter 4)
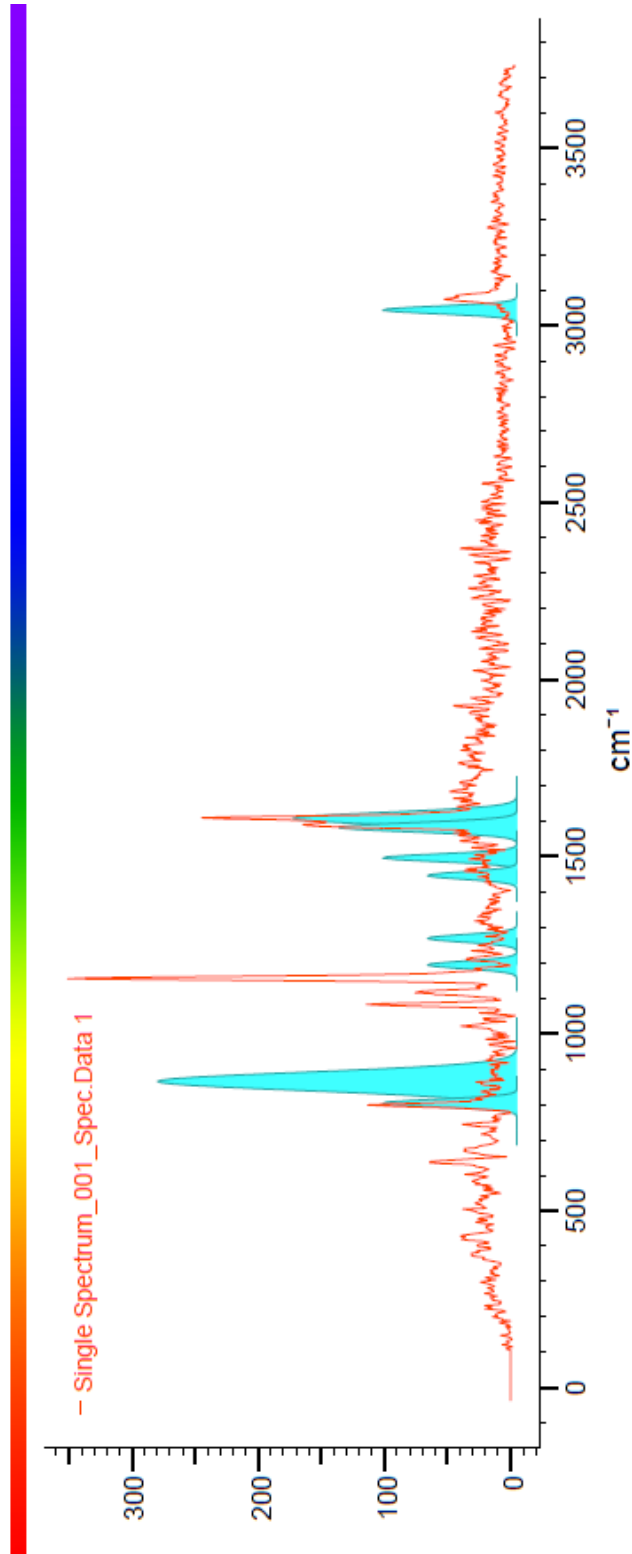
Appendix D (Chapter 5)

Table D-1 OWS Determination for initial sediments prior to experimental setup.

Treatment (G+ or G-)	Sample ID	OWS- Oil/Water/Solids Determination				
		MASS BAL.	% BITUMEN	% WATER	% SOLIDS	SAMPLE WT.
G-	Crescent	99.23	0.58	50.89	47.76	129.25
G-	STP	99.34	2.71	45.01	51.62	118.658
G-	Pond 1A	99.75	8.9	52.56	38.29	111.666
G-	High Sulphate	99.98	0.65	53.77	45.55	132.828
G-	Golden	100.25	0.24	75.72	24.29	121.168
G-	Saline	100.24	0.85	24.02	75.37	103.424
G-	Shallow	100.67	0.08	23.75	76.83	124.127
G-	Syncrude	98.6	3.76	52.66	42.18	107.269
G-	Muskeg	100.62	0.07	50.83	49.72	115.949
G+	Muskeg	100.13	0.12	65.63	34.39	132.071
G+	High Sulphate	99.78	0.59	53.27	45.92	119.665
G+	Crescent	100.08	0.74	53.09	46.25	130.8
G+	STP	99.67	2.05	68.23	29.38	125.219
G+	Saline	100.26	1.43	57.76	41.06	135.037
G+	Golden	99.99	0.15	78.5	21.35	126.954
G+	Pond 1A	100.52	1.89	76.93	21.7	130.579
G+	Shallow	99.65	0.21	36.59	62.85	124.517
G+	Syncrude	99.95	2.57	70.87	26.51	121.44

	INOCULUM (Shell Totes)	99.44	1.64	56.17	41.63	123.877
G+	Shell	99.27	7.61	42.97	48.69	118.191
G-	Shell	99.5	7.31	45.85	46.34	115.429

Table D-2 Anion concentrations measured over the duration of the GI study.

Time Point (months)	Sample Type	Treatment (G+ or G-)	Sample ID	ANI (Anions determination by IC) [mg/L]						
				F	Cl	NO2	NO3	PO4	SO4	Br
0	water	G-	Shallow	0.11	9.59	0.81	0.66	<0.1	2.54	<0.2
0	water	G-	High Sulphate	0.25	7.01	0.38	0.64	<0.1	1040	<0.2
0	water	G-	Syncrude	1.76	354	<0.1	<0.2	<0.1	295	<0.2
0	water	G-	Crescent	<0.05	0.95	0.77	0.82	<0.1	7.09	<0.2
0	water	G-	Golden	0.16	60	<0.1	1.29	<0.1	820	<0.2
0	water	G-	STP	2.97	641	2.79	4.47	<0.1	222	0.53
0	water	G-	Muskeg	<0.05	10.7	0.75	1.68	<0.1	8.64	<0.2
0	water	G-	Pond 1A	2.07	475	<0.1	<0.2	<0.1	165	0.42
0	water	G-	Saline	0.14	2.77	0.51	<0.2	<0.1	409	<0.2
0	sed	G-	Crescent	0.19	8.01	<0.1	<0.2	0.38	72	<0.2
0	sed	G-	STP	1.63	255	<0.1	<0.2	<0.1	110	<0.2
0	sed	G-	Pond 1A	3.42	273	<0.1	<0.2	2.13	204	<0.2
0	sed	G-	High Sulphate	0.29	12.4	<0.1	<0.2	7.52	43.5	0.23
0	sed	G-	Golden	0.34	72.2	<0.1	<0.2	4.49	211	<0.2
0	sed	G-	Saline	0.57	2.01	0.53	<0.2	<0.1	553	<0.2
0	sed	G-	Shallow	0.41	2.82	0.98	<0.2	<0.1	57.5	<0.2
0	sed	G-	Syncrude	2.44	565	<0.1	<0.2	0.18	74.3	0.3
0	sed	G-	Muskeg	0.17	30.3	0.53	<0.2	<0.1	66.7	<0.2
0	water	G+*	Shallow	0.15	10.6	0.95	<0.2	<0.1	4.21	<0.2
0	water	G-*	Inoculum (2014 Set up)	0.15	19.4	0.48	<0.2	<0.1	453	<0.2
0	water	G+	Pond 1A	1.19	494	<0.1	<0.2	0.24	171	0.21
0	water	G+	Syncrude	2.55	462	<0.1	<0.2	<0.1	414	1.25

0	water	G+	Saline	0.16	3.78	0.6	<0.2	<0.1	574	<0.2
0	water	G+	Muskeg	<0.05	10.6	0.74	<0.2	<0.1	8.52	<0.2
0	water	G+	Crescent	<0.05	0.61	0.73	<0.2	<0.1	3.59	<0.2
0	water	G+	STP	0.97	99.3	<0.1	<0.2	<0.1	41.5	<0.2
0	water	G+	Golden	0.07	21.5	0.17	<0.2	<0.1	309	<0.2
0	water	G+	High Sulphate	0.14	4.24	0.53	<0.2	<0.1	517	<0.2
0	sed	G+	Muskeg	0.18	23.2	<0.1	<0.2	<0.1	6.36	<0.2
0	sed	G+	High Sulphate	0.27	10.8	<0.1	<0.2	6.38	148	0.55
0	sed	G+	Crescent	0.18	5.54	<0.1	<0.2	0.55	27.9	<0.2
0	sed	G+	STP	1.95	635	<0.1	<0.2	<0.1	167	0.23
0	sed	G+	Saline	0.31	5.73	<0.1	<0.2	<0.1	7.17	<0.2
0	sed	G+	Golden	0.28	71.1	<0.1	<0.2	3.09	267	0.22
0	sed	G+	Pond 1A	1.99	140	<0.1	<0.2	0.88	73.4	<0.2
0	sed	G+	Shallow	0.35	16.4	<0.1	<0.2	<0.1	67.8	<0.2
0	sed	G+	Syncrude	2.44	498	<0.1	<0.2	0.18	29.8	0.27
0	sed		INOCULUM (Shell Totes)	0.85	193	<0.1	<0.2	0.43	6.57	<0.2
0	water		INOCULUM (Shell Totes)	0.15	22.8	0.49	<0.2	<0.1	431	<0.2
9	water	G+	Pond 1A sterile	2.31	355	<0.1	<0.2	0.13	143	0.29
9	water	G-	Crescent	0.09	6.4	0.64	<0.2	<0.1	55	<0.2
9	water	G-	Pond 1A	2.19	315	<0.1	<0.2	<0.1	155	0.24
9	water	G+	Shallow	0.22	13.4	0.69	<0.2	<0.1	58.8	<0.2
9	water	G+	Golden	0.17	57.6	<0.1	<0.2	<0.1	520	<0.2
9	water	G+	STP sterile	2.16	495	<0.1	0.4	<0.1	171	0.37
9	water	*	Blank 1	<0.05	21.6	0.34	<0.2	<0.1	34.6	<0.2

9	water	G+	High Sulphate	0.2	9.68	0.29	<0.2	<0.1	605	<0.2
9	water	G+	STP	1.94	495	<0.1	<0.2	<0.1	200	0.39
9	water	G+	Pond 1A	2.05	296	<0.1	<0.2	<0.1	145	0.23
9	water	G-	Golden	0.08	30	<0.1	<0.2	<0.1	325	<0.2
9	water	G-	High Sulphate	0.27	8.88	0.12	<0.2	<0.1	650	<0.2
9	water	G+	Saline	0.18	7.48	0.5	<0.2	<0.1	356	<0.2
9	water	G+	Muskeg	0.06	15.1	<0.1	<0.2	<0.1	21.5	<0.2
9	water	G+	Crescent	0.09	6.51	<0.1	<0.2	<0.1	44.2	<0.2
9	water	G-	Syncrude	1.11	274	<0.1	<0.2	<0.1	157	<0.2
9	water	G+	Pond 1A inoculate	2.46	351	<0.1	<0.2	<0.1	140	0.28
9	water	*	Blank 3	0.05	24	0.47	<0.2	<0.1	40.6	<0.2
9	water	G+	Syncrude Sterile	2.03	441	<0.1	0.2	<0.1	266	<0.2
9	water	G-	Shallow	0.29	10.8	0.79	<0.2	<0.1	58.4	<0.2
9	water	G-	Muskeg	0.06	5.73	0.55	<0.2	<0.1	51.9	<0.2
9	water	G-	Saline	0.22	6.42	0.45	<0.2	<0.1	780	<0.2
9	water	*	Blank 2	<0.05	23.9	0.45	<0.2	<0.1	40.9	<0.2
9	water	G-	STP	1.98	514	<0.1	0.56	<0.1	201	0.4
9	water	G+	STP inoculate	2.42	562	<0.1	4.11	<0.1	200	0.44
9	water	G+	Syncrude	1.82	415	<0.1	<0.2	<0.1	276	<0.2
9	water	G+	Syncrude Inoculate	1.38	304	<0.1	<0.2	<0.1	161	<0.2
11	water	G+	Shallow	0.17	3.14	0.76	<0.2	<0.1	51.1	<0.2
11	water	*	Blank 1	<0.05	18.7	0.17	0.31	<0.1	29	<0.2
11	water	G+	Pond 1A	1.82	234	<0.1	<0.2	<0.1	87.5	<0.2

11	wat er	*	Blank 2	<0.0 5	20.2	0.33	0.34	<0.1	4.09	<0.2
11	wat er	G-	Muskeg	0.1	2.3	0.57	<0.2	<0.1	40	<0.2
11	wat er	G+	Syncrude Sterile	1.71	344	<0.1	<0.2	<0.1	227	<0.2
11	wat er	G-	High Sulphate	0.23	5.8	0.31	0.24	<0.1	586	<0.2
11	wat er	G-	STP	1.75	414	<0.1	<0.2	<0.1	162	0.3
11	wat er	G+	Saline	0.17	0.53	0.64	<0.2	<0.1	206	<0.2
11	wat er	G+	Crescent	0.06	0.2	0.66	<0.2	<0.1	21.5	<0.2
11	wat er	G-	Crescent	0.06	2.05	0.66	<0.2	<0.1	91.6	<0.2
11	wat er	G+	STP inoculate	0.31	3.95	0.29	<0.2	<0.1	1.02	<0.2
11	wat er	G+	Muskeg	0.07	2.68	0.68	<0.2	<0.1	34.5	<0.2
11	wat er	G-	Shallow	0.13	8.42	0.74	<0.2	<0.1	95.6	<0.2
11	wat er	G+	STP sterile	1.87	308	<0.1	<0.2	<0.1	156	0.21
11	wat er	G+	STP	1.46	330	<0.1	<0.2	<0.1	126	0.21
11	wat er	G+	Pond 1A inoculate	1.95	242	<0.1	<0.2	<0.1	89.4	<0.2
11	wat er	G-	Pond 1A	2.06	248	<0.1	<0.2	<0.1	110	<0.2
11	wat er	G-	Golden	0.11	42.5	<0.1	<0.2	<0.1	466	<0.2
11	wat er	*	Blank 3	<0.0 5	21.2	0.37	0.41	<0.1	34.8	<0.2
11	wat er	G-	Syncrude	1.62	348	<0.1	<0.2	<0.1	172	<0.2
11	wat er	G+	Syncrude	1.54	306	<0.1	<0.2	<0.1	204	<0.2
11	wat er	G+	Golden	0.27	45.6	<0.1	<0.2	<0.1	467	<0.2
11	wat er	G+	High Sulphate	0.25	0.17	0.26	<0.2	<0.1	447	<0.2
11	wat er	G+	Syncrude Inoculate	1.83	331	<0.1	<0.2	<0.1	184	<0.2
11	wat er	G+	Pond 1A sterile	2.02	275	<0.1	<0.2	<0.1	115	0.23

11	water	G-	Saline	0.21	4.36	0.32	<0.2	<0.1	835	<0.2
0	water	G+	Shell	3.38	147	<0.1	<0.2	<0.1	237	2.23
0	sed	G+	Shell	1.6	268	<0.1	<0.2	<0.1	115	0.24
0	sed	G-	Shell	1.58	279	<0.1	0.25	<0.1	171	<0.2
0	water	G-	Shell	3.48	146	<0.1	0.83	<0.1	225	<0.2
22	water	*	Blank 1	<0.05	16.6	0.17	<0.2		31.9	<0.2
22	water	G-	Crescent	0.060	0.46	0.29	<0.2		32.9	<0.2
22	water	G-	Pond 1A	1.880	208	<0.1	<0.2		23.4	<0.2
22	water	G-	Golden	0.090	25.3	0.23	<0.2		272	<0.2
22	water	G-	High Sulphate	0.250	7.39	0.18	0.26		382	<0.2
22	water	G-	Syncrude	1.680	249	<0.1	<0.2		96.1	<0.2
22	water	G-	Shallow	0.170	6.61	0.4	<0.2		15	<0.2
22	water	G-	Muskeg	0.070	1.06	0.28	<0.2		26.8	<0.2
22	water	G-	Saline	0.200	4.77	0.2	<0.2		639	<0.2
22	water	G-	STP	1.840	375	<0.1	<0.2		87	0.28
22	water	G-	Pond 1A Sterile	2.090	21.2	0.34	<0.2		9.46	<0.2
22	water	G-	Syncrude Sterile	1.320	276	<0.1	<0.2		30.6	<0.2
22	water	G-	Shell	1.360	99.2	<0.1	<0.2		24.9	<0.2
22	water	G-	STP Sterile	2.050	483	<0.1	<0.2		146	0.39
22	water	G+	Pond 1A sterile	1.970	303	<0.1	<0.2		57.8	0.25
22	water	G+	Shallow	0.180	6.82	0.28	<0.2		4.48	<0.2
22	water	G+	Golden	0.300	34.5	0.12	<0.2		310	<0.2
22	water	G+	High Sulphate	0.230	1.14	0.22	0.43		364	<0.2

22	water	G+	STP	1.960	356	<0.1	<0.2		130	0.26
22	water	G+	Pond 1A	2.060	213	<0.1	<0.2		29.2	<0.2
22	water	G+	Saline	0.130	0.42	0.44	<0.2		37.8	<0.2
22	water	G+	Muskeg	<0.05	3.22	0.29	<0.2		95.4	<0.2
22	water	G+	Crescent	0.060	<0.1	0.16	<0.2		136	<0.2
22	water	G+	Pond 1A inoculate	2.090	255	<0.1	<0.2		44	0.22
22	water	G+	Syncrude Sterile	2.240	445	<0.1	0.21		248	<0.2
22	water	G+	STP inoculate	1.840	405	<0.1	<0.2		150	0.3
22	water	G+	Syncrude	1.240	216	<0.1	<0.2		76.2	<0.2
22	water	G+	STP sterile	2.030	493	<0.1	<0.2		185	0.36
22	water	G+	Syncrude Inoculate	2.120	399	<0.1	<0.2		151	<0.2
22	water	G+	Shell	1.080	104	<0.1	<0.2		75.4	<0.2
32	water	*	Blank 1	<0.05	11.4	0.13	<0.2		23.8	<0.2
32	water	G-	Crescent	0.070	3.72	0.33	<0.2		30.6	<0.2
32	water	G-	Pond 1A	0.930	82.5	<0.1	<0.2		7.82	<0.2
32	water	G-	Golden	0.100	38.6	0.27	<0.2		375	<0.2
32	water	G-	High Sulphate	0.240	7.94	0.27	<0.2		195	<0.2
32	water	G-	Syncrude	0.960	150	<0.1	<0.2		52.5	<0.2
32	water	G-	Shallow	0.190	13.6	0.41	<0.2		5.6	<0.2
32	water	G-	Muskeg	0.060	4.12	0.26	0.3		13.2	<0.2
32	water	G-	Saline	0.160	4.4	0.24	<0.2		430	<0.2
32	water	G-	STP	0.990	165	<0.1	<0.2		35.5	<0.2
32	water	G-	Pond 1A Sterile						SAMPLE	

32	water	G-	Syncrude Sterile	0.680	91.5	<0.1	<0.2		12.3	<0.2
32	water	G-	Shell	1.420	89.4	<0.1	<0.2		15.6	<0.2
32	water	G-	STP Sterile	1.320	335	<0.1	0.29		87.3	0.25
32	water	G+	Pond 1A sterile	1.020	175	<0.1	0.24		24.9	<0.2
32	water	G+	Shallow	0.220	8.02	0.36	<0.2		1.13	<0.2
32	water	G+	Golden	0.180	15.1	0.11	<0.2		104	<0.2
32	water	G+	High Sulphate	0.220	6.57	0.25	<0.2		188	<0.2
32	water	G+	STP	1.560	364	<0.1	<0.2		98.3	0.27
32	water	G+	Pond 1A	1.290	106	<0.1	<0.2		10.6	<0.2
32	water	G+	Saline	0.220	5.55	0.3	<0.2		28.6	<0.2
32	water	G+	Muskeg	<0.05	3.99	0.21	<0.2		55.4	<0.2
32	water	G+	Crescent	0.060	5.77	0.3	<0.2		99.2	<0.2
32	water	G+	Pond 1A inoculate	0.960	105	<0.1	<0.2		14	<0.2
32	water	G+	Syncrude Sterile	0.800	178	<0.1	<0.2		93.1	<0.2
32	water	G+	STP inoculate	0.880	159	<0.1	<0.2		66.6	<0.2
32	water	G+	Syncrude	0.490	67.3	<0.1	0.22		19.2	<0.2
32	water	G+	STP sterile	0.960	216	<0.1	<0.2		78.5	<0.2
32	water	G+	Syncrude Inoculate	1.290	324	<0.1	<0.2		95.7	<0.2
32	water	G+	Shell	0.620	43.4	0.11	<0.2		22.9	<0.2
32	water	*	PRECIPITATION							

Table D-3 Naphthenic acid concentrations of tailings mescosms for the duration of the study. See Ch. 6 Figure 3 for linear regression of NA concentrations over time

Time Point (months)	Treatment (G+ or G-)	Sample ID	NAPH_WT_PPM
0	G-	Shallow	2
0	G-	High Sulphate	8
0	G-	Syncrude	57
0	G-	Crescent	4
0	G-	Golden	2
0	G-	STP	69
0	G-	Muskeg	1
0	G-	Pond 1A	64
0	G-	Saline	5
0	G-	Shell	59
0	G-*	Inoculum (2014 Set up)	3
0	G+	Pond 1A	29
0	G+	Syncrude	5
0	G+	Saline	1
0	G+	Muskeg	1
0	G+	Crescent	1
0	G+	STP	6
0	G+	Golden	1
0	G+	High Sulphate	1
0	G+	Shell	1
0	G+*	Shallow	1
0		INOCULUM (Shell Totes)	2
9	*	Blank 1	1
9	*	Blank 3	1
9	*	Blank 2	1
9	G-	Crescent	4
9	G-	Pond 1A	50
9	G-	Golden	1
9	G-	High Sulphate	7
9	G-	Syncrude	39
9	G-	Shallow	3
9	G-	Muskeg	1
9	G-	Saline	5
9	G-	STP	40
9	G+	Pond 1A sterile	29

9	G+	Shallow	1
9	G+	Golden	2
9	G+	High Sulphate	4
9	G+	STP	13
9	G+	Pond 1A	25
9	G+	Saline	4
9	G+	Muskeg	2
9	G+	Crescent	2
9	G+	Pond 1A inoculate	39
9	G+	Syncrude Sterile	19
9	G+	STP inoculate	22
9	G+	Syncrude	35
9	G+	STP sterile	19
9	G+	Syncrude Inoculate	23
11	*	Blank 1	1
11	*	Blank 2	1
11	*	Blank 3	4
11	G-	Muskeg	1
11	G-	High Sulphate	7
11	G-	STP	29
11	G-	Crescent	3
11	G-	Shallow	2
11	G-	Pond 1A	42
11	G-	Golden	3
11	G-	Syncrude	25
11	G-	Saline	5
11	G+	Shallow	2
11	G+	Pond 1A	24
11	G+	Syncrude Sterile	19
11	G+	Saline	4
11	G+	Crescent	2
11	G+	STP inoculate	3
11	G+	Muskeg	1
11	G+	STP sterile	12
11	G+	STP	16
11	G+	Pond 1A inoculate	36
11	G+	Syncrude	25
11	G+	Golden	4
11	G+	High Sulphate	8

11	G+	Syncrude Inoculate	21
11	G+	Pond 1A sterile	23
22	*	Blank 1	2
22	G-	Crescent	2
22	G-	Pond 1A	27.5
22	G-	Golden	1.2
22	G-	High Sulphate	4.9
22	G-	Syncrude	23.5
22	G-	Shallow	1.7
22	G-	Muskeg	1.1
22	G-	Saline	3.3
22	G-	STP	37.4
22	G-	Pond 1A Sterile	44.8
22	G-	Syncrude Sterile	25.8
22	G-	Shell	14.1
22	G-	STP Sterile	31
22	G+	Pond 1A sterile	22.8
22	G+	Shallow	1.6
22	G+	Golden	2.8
22	G+	High Sulphate	3.5
22	G+	STP	14
22	G+	Pond 1A	21.1
22	G+	Saline	1.7
22	G+	Muskeg	1
22	G+	Crescent	1.3
22	G+	Pond 1A inoculate	28.4
22	G+	Syncrude Sterile	21.9
22	G+	STP inoculate	12.8
22	G+	Syncrude	15.2
22	G+	STP sterile	12.9
22	G+	Syncrude Inoculate	22.6
22	G+	Shell	5.7
31	*	Blank 1	1.2
31	*	PRECIPITATION	
31	G-	Crescent	1.5
31	G-	Pond 1A	12.9
31	G-	Golden	1.6
31	G-	High Sulphate	3.4
31	G-	Syncrude	14.3

31	G-	Shallow	2.1
31	G-	Muskeg	0.7
31	G-	Saline	1.6
31	G-	STP	11.4
31	G-	Pond 1A Sterile	
31	G-	Syncrude Sterile	9
31	G-	Shell	11.1
31	G-	STP Sterile	17.5
31	G+	Pond 1A sterile	10.8
31	G+	Shallow	1.4
31	G+	Golden	1.2
31	G+	High Sulphate	2.3
31	G+	STP	9.9
31	G+	Pond 1A	23.2
31	G+	Saline	3.7
31	G+	Muskeg	1
31	G+	Crescent	2.1
31	G+	Pond 1A inoculate	12.7
31	G+	Syncrude Sterile	8.4
31	G+	STP inoculate	5.3
31	G+	Syncrude	4.5
31	G+	STP sterile	5.6
31	G+	Syncrude Inoculate	14
31	G+	Shell	1.9

VITA AUCTORIS

NAME: Thomas Reid

PLACE OF BIRTH: Barrie, ON

YEAR OF BIRTH: 1989

EDUCATION: St. Joseph's High School, Barrie, ON, 2007

                         Western University, Honors B.Sc., London, ON, 2011

                         University of Windsor, M.Sc., Windsor, ON, 2014